

DISSERTATION

MECHANICS OF SEDIMENT PLUG FORMATION
IN THE MIDDLE RIO GRANDE, NM

Submitted by

Kiyoung Park

Department of Civil and Environmental Engineering

In partial fulfillment of the requirements

For the Degree of Doctor of Philosophy

Colorado State University

Fort Collins, Colorado

Fall 2013

Doctoral Committee:

Advisor: Pierre Y. Julien

Christopher I. Thornton

Subhas K. Venayagamoorthy

Ellen E. Wohl

Copyright by Kiyoung Park 2013

All Rights Reserved

ABSTRACT

MECHANICS OF SEDIMENT PLUG FORMATION IN THE MIDDLE RIO GRANDE, NM

The Rio Grande is a dynamic river system which has experienced significant hydraulic and geomorphic changes through recorded history from the early 1900's to the present. These changes stem, for the most part, from natural and human interventions to the river system, which experienced channel bed elevation changes, lateral migration, straightening, channel realignment, etc. Sediment plugs have formed in the Tiffany area near San Marcial in 1991, 1995, and 2005, and in the Bosque Reach 14 miles upstream from the Tiffany plug location in 2008. Many authors have investigated the cause of sediment plugs in the Middle Rio Grande but the previous studies do not provide a complete criteria for sediment plug formation. Better understanding of the complex mechanics of plug formation on the Middle Rio Grande is therefore pursued.

Based on the historic flow and geometric characteristics of plug areas, seven parameters were identified as major causing factors of sediment plug formation in the Middle Rio Grande: (1) two geometric factors: variability of channel widths and roughness; (2) two water and sediment loss factors: perching/overbanking and sediment concentration distribution profiles; and (3) three backwater effect factors: backwater effects from a reservoir, a bridge, and sharp bends. The purpose of this research is to analyze possible sediment plug parameters and to assess the primary causing factors. The specific objectives are to: (1) investigate the mechanics of sedimentation effect due to each factor; (2) simulate the historic sediment plugs using a numerical aggradation/degradation program; and (3) determine which factors contribute the most to the formation of sediment plugs.

Geometric factors show that the channel has narrowed 40% between 1962 and 2002 and channel capacity has 77% decreased over time. The representative composite roughness increased 50 % between 1992 and 2002. Accordingly sediment transport capacity has decreased 45%. The narrowing (40%) with increase in roughness (50%) causes considerable loss of sediment transport capacity (45%). Therefore geometric factors induce more overbank flows and channel bed aggradation.

Sedimentation factors show that the perching ratio increased from 13% to 87% between 1992 and 2002. Bank depth has decreased 51% between 1992 and 2002. The perching and lower bank depth facilitated more overbank flows and 13 ~ 20% loss of water. As particle sizes have coarsened (0.2mm in 1992 → 0.25mm in 2002) and width/depth ratios have increased (129 in 1992 → 229 in 2002), leading to higher Rouse numbers and more near-bed concentration profiles. High Rouse number ($R_o > 1.2$) and near-bed sediment concentration profile speed up the aggradation rates (4 ~ 7 times faster) than for a uniform-concentration profile. The high near-bed concentrations shorten the plug formation time from 90 to 20 days. Since snowmelt floods exceed bankfull discharges less than 2 months, the acceleration factors are essential for sediment plugs to form.

Backwater effects from the Elephant Butte Reservoir influenced the upstream channel bed elevation over time. At an average flow discharge (1,550cfs), the aggradation (up to 7ft) time to fill the 25.5 mile long channel is roughly 10 years. The historic Tiffany plug area has been influenced by the reservoir levels, but with a lag time of several years. Around the San Marcial Railroad Bridge, channel bed elevation has aggraded consistently (12ft increased between 1979 and 1987). The pier contraction and congested abutments generate about a 1ft high backwater propagating to the Tiffany plug area. Sharp bends caused a 1.6ft high backwater which

propagates roughly 1 mile upstream. As the beginning point of the Bosque plug is located 0.6 mile upstream of the sharp bends, backwater does influence the channel aggradation of the Bosque plug. The time to fill the main channel up to the bank crest was estimated as approximately 17 days.

In terms of significance, perching/overbank flow and sediment concentration profiles can be evaluated as the primary causing factors of sediment plugs, followed by the backwater effects from bridge and sharp bends. Backwater effect from the reservoir has influenced the upstream channel elevation on a long-term basis (7 ft / 10 years). Channel narrowing and higher roughness promote overbank flows and decrease of sediment transport capacity. Owing to the increase of overbank flows, sediment concentration profiles speed up the rate of channel aggradation, causing a sediment plug within a matter of weeks, thus these two factors are the most significant factors (1.2 ft / 20 days). Two other factors, the backwater effect from the railroad bridge and sharp bends, explain why the historic sediment plugs formed at particular areas, therefore these two parameters can be classified as local triggering factors (1~1.6 ft / 20 days).

On the other hand, causal factors can be divided into two groups depending on the plug location. The Tiffany plugs have been more affected by the backwater effect from the reservoir and railroad bridge. On the other hand, the Bosque plug was more influenced by the decrease of channel width/channel capacity, roughness, and sharp bends.

ACKNOWLEDGEMENT

I am very thankful to my advisor, Dr. Pierre Julien for his great guidance, warm encouragement, and excellent suggestions. I would also like to thank to my committee members: Dr. Christopher Thornton, Dr. Subhas Venayagamoorthy, and Dr. Ellen Wohl for their helpful comments and assistance during my studies at Colorado State University.

I am also grateful to the U.S. Bureau of Reclamation in Albuquerque for the incredible amount of data. I would especially like to thank Jonathan Aubuchon, of the Albuquerque office, and Dr. Drew Baird, of the Denver office, for their insights and comments. I also thank all members of Dr. Julien's Rising Stars : Christopher Shrimpton, Jaehoon Kim, Jazuri Abdullah, Jonathan Rainwater, Katharine Anderson, Nur Shazwani Muhammad, Tracy Owen, Theodore Bender, especially to Sangdo An. I also thank CSU staffs including, Laurie Alburn, Linda Hinshaw, and Karleene Schindler for their kindness and help.

I also would like to thank the K-water (Korea Water Resources Corporation) for supporting and providing the opportunity to study at CSU. Special thanks to Phyl-sun Hwang, Kee-uk Cha for their support and life-time mentoring. I am grateful to my own teachers and professors at Kyoungpook national university, and particular to my undergraduate and graduate advisor Kun-yeon Han.

Finally, my deepest thanks extend to all my family members including my mother, parents-in-law, and my siblings (Kyoung-hee, Youn-kyoung, Youn-joo), and especially my wife Daejoong, my daughter Sieun, and sons (Jiwon and Jihoo) for their support, encouragement, and unconditional love. I intensively miss my deceased father and grandmother at this moment.

TABLE OF CONTENTS

ABSTRACT	ii
ACKNOWLEDGEMENTS	v
TABLE OF CONTENTS	vi
LIST OF TABLES	x
LIST OF FIGURES	xi
LIST OF SYMBOLS	xv
1. INTRODUCTION AND OBJECTIVES	1
1.1 SEDIMENT PLUGS	1
1.2 PROBLEM STATEMENT	1
1.3 PREVIOUS STUDIES	2
1.4 DISSERTATION OBJECTIVES	5
1.5 RESEARCH APPROACH AND METHODOLOGY	6
2. LITERATURE REVIEW	8
2.1 SEDIMENT PLUGS	8
2.1.1 Historic Occurrences	8
2.1.2 River Maintenance in the Middle Rio Grande	10
2.1.3 Possible Causing Factors	13
2.1.4 Reclamation's Endeavors	13
2.1.5 Cooperative Project of CSU with Reclamation	14
2.2 MECHANICS OF SEDIMENT PLUG FORMATION	15
2.2.1 Sediment Transport Capacity	15
2.2.2 Analytical Descriptions of River Response	18
2.2.3 Sediment Concentration Profiles	20
2.2.4 Numerical Simulation	24
2.3 SUMMARY	26

3.	SITE DESCRIPTION	28
3.1	RIO GRANDE	28
3.2	CLIMATE	29
3.3	GEOMORPHIC CHANGES	31
3.4	SEDIMENT PLUGS	33
3.5	STUDY REACH AND SUBREACHES	34
4.	AVAILABLE DATA AND PLUG CAUSING FACTORS	36
4.1	GEOMETRIC DATA	36
4.1.1	Channel Widths	36
4.1.2	Channel Depths and Perching	39
4.1.3	Longitudinal Profiles	42
4.1.4	Roughness	43
4.2	FLOW DATA	44
4.3	SEDIMENT DATA	46
4.3.1	Particle Size	46
4.3.2	Settling Velocity	49
4.3.3	Sediment Transport Capacity	50
4.4	PLUG CAUSING FACTORS	53
5.	GEOMETRIC FACTORS	54
5.1	CHANNEL WIDTHS	54
5.1.1	Relationship Between Width and Sediment Discharge	55
5.1.2	Relationship Between Width/depth ratio and Sediment Discharge	55
5.1.3	Application to the Middle Rio Grande	56
5.1.3.1	Sediment Transport Capacity for the Bosque Reach	56
5.1.3.2	Sediment Transport Capacity for the Elephant Butte Reach	57
5.1.3.3	Sediment Transport Capacity for cross sections	58

5.2	ROUGHNESS	60
5.2.1	Increase in Roughness.....	60
5.2.2	Vegetation Encroachment without Channel Narrowing.....	61
5.2.3	Vegetation Encroachment with Channel Narrowing.....	62
5.2.4	Temporal Change in Channel Roughness	64
5.2.5	Composite Channel Roughness and Sediment Transport Capacity	66
6.	OVERBANK FLOWS AND CONCENTRATION PROFILES	67
6.1	PERCHING AND OVERBANK FLOWS	67
6.1.1	Perching.....	67
6.1.2	Overbank Flows and Sediment Transport Capacity	67
6.1.3	Sedimentation due to Perching.....	69
6.1.4	Application to the Middle Rio Grande	70
6.1.4.1	Channel Conveyance Capacity	70
6.1.4.2	Overbank Flows	71
6.1.4.3	Historic Overbank Flows and Perching	72
6.2	VERTICAL SEDIMENT CONCENTRATION PROFILES	74
6.2.1	Overbank Flow In Case Of Uniform Sediment Concentration Profile	74
6.2.2	Overbank Flow In Case Of Non-uniform Sediment Concentration Profile.....	76
6.2.3	Sediment Concentration Distribution Effect on the MRG bed elevation.....	78
6.2.4	Concentration Profiles at Historic Sediment Plug Locations.....	80
6.2.4.1	Concentration Profiles at Agg/Deg 1683 (Tiffany Plug location)	80
6.2.4.2	Concentration Profiles at Agg/Deg 1550 (Bosque Plug location)	81
6.2.4.3	Comparison of the Concentration Profiles.....	83
7.	BACKWATER EFFECTS ON BED AGGRADATION.....	84
7.1	BACKWATER EFFECTS FROM REERVOIR	84
7.1.1	Temporal Changes in Channel Bed Elevations	86
7.1.2	Mechanics of Backwater Effects on Channel Bed Aggradation	87
7.1.3	Aggradation Time due to Reservoir Backwater	90

7.2	BACKWATER EFFECTS FROM A BRIDGE	91
7.2.1	The San Marcial Railroad Bridge.....	91
7.2.2	Backwater Effect due to the San Marcial Railroad Bridge	92
7.2.2.1	Backwater Effect on Water Depth.....	92
7.2.2.2	Backwater Effect on Sedimentation.....	93
7.3	BACKWATER EFFECTS FROM SHARP BENDS	95
7.3.1	Sinuosity in the Middle Rio Grande.....	95
7.3.2	Sharp Bends	96
7.3.3	Backwater Effect on Water Depth.....	97
7.3.4	Backwater Effect on Sediment Deposits.....	99
8.	NUMERICAL SIMULATIONS	100
8.1	INTRODUCTION	100
8.2	HYDRODYNAMICS	100
8.3	SEDIMENTATION	103
8.4	STABILITY	104
8.5	PROGRAM LIMITATIONS	105
8.6	APPLICATION TO THE MIDDLE RIO GRANDE	106
8.6.1	Geometric Factors	106
8.6.2	Overbank Flows and Concentration Distribution Profiles	107
8.6.3	Backwater Effects From the Reservoir, the Bridge, and Sharp Bends.....	109
8.6.4	Application to the Middle Rio Grande Sediment Plugs	110
9.	SUMMARY AND CONCLUSIONS	112
	RECOMMENDATIONS FOR FUTURE STUDY.....	116
	BIBLIOGRAPHY.....	118

LIST OF TABLES

Table 3.1: Sediment plug formations in the Middle Rio Grande (Reclamation 2010).....	33
Table 4.1: Settling velocity (m/s).....	50
Table 5.1: Energy loss due to sharp bends.....	97
Table 9.1: Significance of causing factors	115

LIST OF FIGURES

Figure 1.1: Criteria for plug formation (Boroughs, 2005).....	3
Figure 1.2: Fractional loss of flow of main channel per unit length of river.....	4
Figure 1.3: Duration of overbank flows (days).....	4
Figure 1.4: Incoming total sediment load per available channel area.....	4
Figure 1.5: PLGNUM for the 2008 Bosque plug	5
Figure 1.6: Research approach to proceed this study	6
Figure 2.1: Temporal change in channel bed elevation (Reclamation, 2011)	11
Figure 2.2: Vertical sediment concentration profile (Park and Julien, 2011).....	15
Figure 2.3: Sediment transport capacity and supply (Julien, 2010).....	15
Figure 2.4: Sediment transport capacity versus sediment discharge in the MRG (León, 2002) ..	18
Figure 2.5: Dimensionless plot of suspended-load distribution (Rouse, 1938).....	22
Figure 2.6: Ratio of suspended to total load versus ratio of shear to fall velocity (Julien, 2010)	23
Figure 2.7: Procedure of river bed analysis (modified from Woo, 2002).....	25
Figure 3.1: The Middle Rio Grande and hydraulic structures (US. Fish and wildlife service)	28
Figure 3.2: Rio Grande floods and droughts (Modified after Makar 2011, Pers. Comm.).....	30
Figure 3.3: Morphological changes around the Bosque plug (a) 1935 (b) 2008	32
Figure 3.4: Morphological changes around the Tiffany plugs (a) 1935 (b) 2008.....	32
Figure 3.5: (a) 2008 Bosque Reach sediment plug (b) pilot channel excavation (Reclamation) .	33
Figure 3.6: Delineation of sub-reaches and location of sediment plugs	35
Figure 4.1: Cross section geometry obtained from HEC-RAS model.....	37
Figure 4.2: Active channel width and channel width in a cross section	37
Figure 4.3: Changes in bankfull widths between 1992 and 2002	38
Figure 4.4: Changes in channel widths at the Tiffany plug location (Agg/Deg 1683).....	38
Figure 4.5: Hydraulic mean depth (USBR, 2001)	39
Figure 4.6: Changes in bank depths between 1992 and 2002.....	39
Figure 4.7: Changes in channel bed elevations between 1992 and 2002.....	40
Figure 4.8: Channel bed elevation and perching in 1992	41

Figure 4.9: Channel bed elevation and perching in 2002	41
Figure 4.10: Longitudinal channel profile (Modified after Baird 2011, Pers. Comm.).....	42
Figure 4.11: Composite channel roughness for various discharges (Park et al., 2011)	43
Figure 4.12: Flow discharges in 1999.....	44
Figure 4.13: Flow discharges in 1995.....	45
Figure 4.14: Flow discharges in 2008.....	45
Figure 4.15: Sediment particle size distribution at San Acacia and San Marcial Guages	46
Figure 4.16: Median grain diameter (mm).....	47
Figure 4.17: Seasonal changes in sediment sizes in 1991	48
Figure 4.18: Seasonal changes in sediment sizes in 1995	48
Figure 4.19: Water temperature and viscosity	49
Figure 4.20: Sediment transport capacity of sub-reaches in the Bosque Reach	51
Figure 4.21: Sediment transport capacity of sub-reaches in the Elephant Butte Reach	52
Figure 4.22: Seven major possible factors causing sediment plug formation	53
Figure 5.1: Water and sediment balance for different widths.....	54
Figure 5.2: Sediment transport capacity for various widths of the Bosque Reach	57
Figure 5.3: Sediment transport capacity for various width/depth ratios of the Bosque Reach.....	57
Figure 5.4: Sediment transport capacity for various widths of the Elephant Butte Reach	58
Figure 5.5: Changes in bed elevation and in active channel widths between 1992 and 2002	59
Figure 5.6: Changes in bed elevation and width/depth ratio between 1992 and 2002	59
Figure 5.7: A cross section with different roughness coefficients (at Agg/Deg 1531).....	60
Figure 5.8: Roughness effects on water depth and flow discharge.....	61
Figure 5.9: Changes in water depths and flow discharge with vegetation encroachment	62
Figure 5.10: Changes in water depth and flow discharge with channel narrowing (a) without roughness effect and (b) with roughness effect	63
Figure 5.11: Changes in active channel roughness (1962-2002).....	64
Figure 5.12: Changes in floodplain roughness (1962-2002)	64
Figure 5.13: Channel widths at the Bosque plug location (a) 1992, (b) 2001, (c) 2006, (d) 2008, (e) 1962-2002, and (f) 2002-2009.....	65
Figure 5.14: Channel widths at the Tiffany plug location (a) 1992, (b) 2001, (c) 2006, (d) 2008, (e) 1962-2009and (f) 2002-2009.....	66

Figure 5.15: Sediment transport capacity in the main channel (5,000 cfs, HEC-RAS data).....	66
Figure 6.1: Overbank flows (a) without perching (b) with perching.....	68
Figure 6.2: Flooded areas (a) in 2005 (Tiffany plug) and (b) in 2008 (Bosque plug).....	68
Figure 6.3: Temporal change in channel conveyance (1992, 2002).....	70
Figure 6.4: The ratio of the overbank flow to the total flow in 1992.....	71
Figure 6.5: The ratio of the overbank flow to the total flow in 2002.....	72
Figure 6.6: Overbank flows, return flows, and floodmarks.....	73
Figure 6.7: Flow and sediment discharges with uniform concentration distribution.....	74
Figure 6.8: Flow and sediment discharges with non-uniform concentration distribution.....	76
Figure 6.9: Changes in shear velocity and Rouse number due to overbank flows.....	78
Figure 6.10: Aggradation due to overbank flows (a) with uniform concentration distribution, (b) with non-uniform concentration distribution, and (c) comparison of two cases.....	79
Figure 6.11: Water surface profiles for various flow discharges at the Tiffany plug location.....	80
Figure 6.12: Sediment concentration profiles at the Tiffany plug location.....	81
Figure 6.13: Water surface profiles for various flow discharges at the Bosque plug location.....	82
Figure 6.14: Sediment concentration profiles at the Bosque plug location.....	82
Figure 6.15: Comparison of sediment concentration profiles at plug locations.....	83
Figure 6.16: Comparison of sediment concentration profiles at sub-reaches.....	83
Figure 7.1: Channel bed changes due to reservoir stage (a) aggradation (b) head-cut.....	84
Figure 7.2: Elephant Butte Reservoir and sediment plug location.....	85
Figure 7.3: Elephant Butte Reservoir level time series (Owen, 2012).....	85
Figure 7.4: Changes in thalweg elevations at Range lines from 1980 to 2010 (Owen, 2012).....	86
Figure 7.5: Channel bed aggradation due to reservoir backwater.....	87
Figure 7.6: Bed elevation change due to backwater effect from reservoir.....	88
Figure 7.7: Bed elevation change due to the increase of channel widths.....	89
Figure 7.8: Bed elevation changes due to channel width expansion.....	89
Figure 7.9: Backwater effect on bed elevation change at the river mouth.....	90
Figure 7.10: Time to fill the channel (7 ft).....	90
Figure 7.11: Location of the Tiffany plugs and the San Marcial Railroad Bridge.....	91
Figure 7.12: Sketch of backwater at bridge contraction.....	92

Figure 7.13: Location of the Tiffany plugs and sedimentation due to backwater effect	93
Figure 7.14: Inundated area with 2005 flood (CSU database).....	94
Figure 7.15: Sinuosity of channel thalweg (1962-2002)	95
Figure 7.16: Progress of sinuosity (Agg/Deg 1555~1557) (a) 1996, (b) 2005, (c) 2006 and (d) 2009.....	96
Figure 7.17: Sharp bends at Agg/Deg 1555~1557.....	98
Figure 7.18: Time to fill active channel with sediments.....	99
Figure 8.1: Procedure to compute the sediment discharge Q_s	103
Figure 8.2: Channel aggradation/degradation model.....	104
Figure 8.3: Program structure and modeling procedure	105
Figure 8.4: Distribution of friction slope and bed slope depending on channel widths	106
Figure 8.5: Bed elevation changes depending on channel widths	107
Figure 8.6: Simulation results with uniform concentration profile at the Bosque plug location	108
Figure 8.7: Simulation results with non-uniform concentration profile at the Bosque plug location.....	108
Figure 8.8: Channel bed aggradation due to reservoir backwater	109
Figure 8.9: Backwater effect from the bridge on bed elevation	110
Figure 8.10: Backwater effect from sharp bends on bed elevation.....	110
Figure 8.11: Simulation of the 1995 Tiffany plug	111
Figure 8.12: Simulation of the 2008 Bosque plug	111

LIST OF SYMBOLS

a	reference elevation
A	cross sectional area
C	Chezy coefficient
C_a	near-bed sediment concentration
C_b	broad weir crest coefficient
C_{ppm}	sediment concentration in parts per million
CR	conveyance ratio
C_v	volumetric sediment concentration
C_w	concentration by weight
d^*	dimensionless sediment diameter
d_s	sediment size
F_r	Froude number
G	specific gravity
g	gravitational acceleration
h	flow depth
H	bank height
h_1, h_2	upstream and downstream water depths
K	Yarnell's pier shape coefficients
K_c	channel conveyance
K_b	energy loss coefficient
L	length of pier
n	Manning's roughness coefficient
P	wetted perimeter
p_o	porosity
Q	water discharge
q_l	lateral inflow
Q_o	overbank flow discharge
q_s	unit sediment discharge
Q_s	sediment discharge
Q_{so}	overbank sediment discharge
r_c	radius of curvature
R_o	Rouse number

R_h	hydraulic radius
S_f	friction slope
S_o, S	bed slope
t	time
T	top width
u^*	shear velocity
V_c	average flow velocity at incipient motion
W	channel width
W_p, w_p	projected and actual width of pier
x	distance
z	bed elevation

Greek symbols

α	ratio obstructed area to total unobstructed area of bridge piers
β_s	ratio of sediment to momentum exchange coefficient
ΔE	energy loss
Δt	time step
$\Delta z, \Delta z_b$	change in channel elevation
ε	dispersion coefficient
ε_m	momentum exchange coefficient
θ	meandering angle
κ	von Kármán constant
ν_m, ν	kinematic viscosity
ξ	width-depth ratio
τ	shear stress
τ^*	Shields parameter
ω	settling velocity
Φ	1.49 for English units and 1 for metric units

Subscripts

$j, j+1$	subscripts to indicate upstream and downstream nodes
----------	--

CHAPTER 1 INTRODUCTION AND OBJECTIVES

1.1 SEDIMENT PLUGS

The Rio Grande is a dynamic river system which has experienced significant hydraulic and geomorphic changes through recorded history from the early 1900's to the present. Reclamation has actively maintained the Middle Rio Grande from Cochiti Dam to Elephant Butte Reservoir, including temporary channels and other maintenance activities. As a result, the river has been changed through: channel bed elevation changes, lateral migration, straightening, channel realignment, etc. In addition, several sediment plugs have formed in the Middle Rio Grande at various locations over the last two decades. After a series of plugs in the Tiffany area in 1991, 1995, and 2005, a sediment plug occurred in the Bosque Reach located 14 mile upstream from the Tiffany plug location in 2008. The sediment plugs have become one of the primary concerns for the river management agencies.

1.2 PROBLEM STATEMENT

A sediment plug is defined as an excessive sediment aggradation in a river which completely blocks the original channel and grows upstream by accretion (Diehl 1994, 2000). The river blockage, or sediment plug, has various possible negative effects on the river system: (1) the increase of water loss due to evaporation and difficulty of water delivery downstream to Elephant Butte Reservoir; (2) the decrease of bank stability on the west side of the river by erosion or sand boiling; and (3) the decrease of wildlife habitat and native vegetation (Tetra Tech 2010). Sediment plug can be removed by excavation of a pilot channel through the plug to encourage water to re-channelize through the sediment deposits.

Reclamation has investigated historic sediment plug formations and geomorphologic and environmental changes, but the mechanics of sediment plug development are still mostly unknown. Thus, in this research, a step forward is being taken to better understand plug formation mechanics by focusing on the seven major causal factors.

1.3 PREVIOUS STUDIES

Earlier research on sediment plug formation in the Middle Rio Grande was performed by Boroughs (2011). In his dissertation (2005), technical report for Reclamation (2005) and papers (2011), four major processes in sediment plug formation were examined for the 1991 and 1995 Tiffany plugs: (1) abrupt and significant loss of flow to overbank areas; (2) overbank flows that continue for several days or weeks; (3) upstream sediment supply exceeds the local sediment transport capacity; and (4) non-uniform vertical distribution of the total sediment load. Through his investigation regarding why the Tiffany plugs formed, criteria for sediment plug formation in alluvial rivers have been suggested:

$$PLGNUM = FO * ND * QA * b * Ro^{1/3} \quad (1.1)$$

where, FO = loss of main channel conveyance ($Q_{ob}/Q_{in}/L_{ob}$, Q_{ob} = overbank flow, Q_{in} = inflow, L_{ob} =overbank length), ND = the duration that flow is lost to the overbank areas, QA = the ratio of the available sediment supply to the available depositional area of the channel ($Q_{savg}/A/(1-p_o)$, A: cross sectional area, p_o : porosity), b = exponent of sediment load and flow, Ro = Rouse number.

The PLGNUM is a dimensionless variable to provide an estimate of whether a channel would plug. A greater PLGNUM value indicates higher confidence of sediment plug development (Figure 1.1).

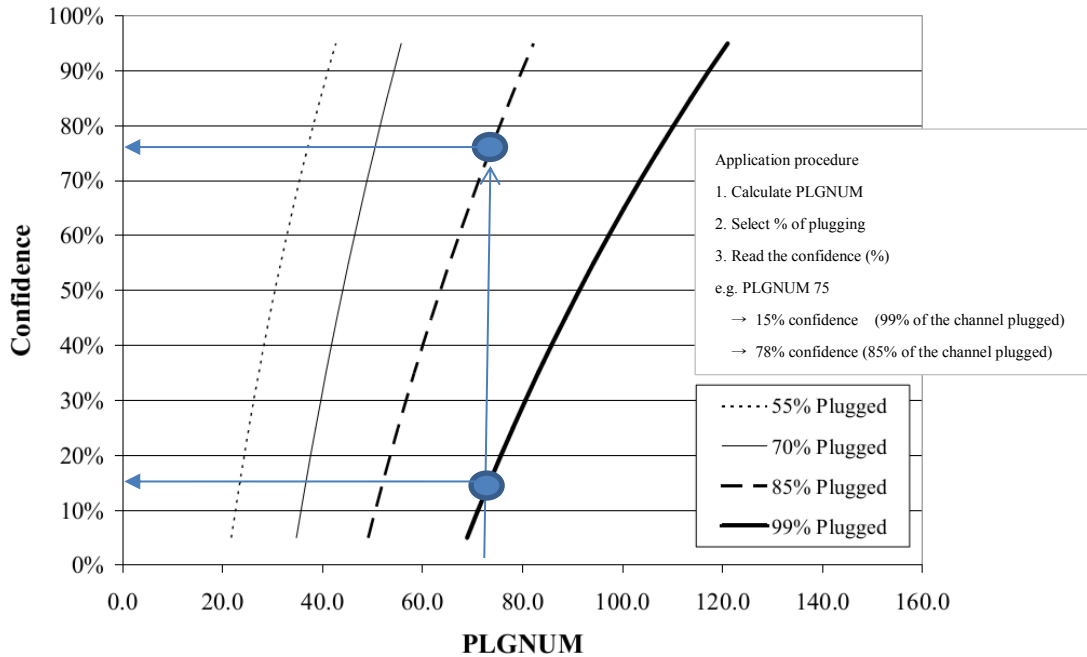


Figure 1.1. Criteria for plug formation (Boroughs, 2005)

After the criteria were suggested based on the Tiffany plugs in 1991 and 1995, two more sediment plugs occurred in the Middle Rio Grande: the 2005 Tiffany plug and the 2008 Bosque plug. When applying these criteria to the Bosque plug in 2008, the parameters, FO, ND, QA, and PLGNUM (Figure 1.2-1.5, respectively) for the Bosque Reach can be determined using $b = 1.24$ and $R_o = 1.15$, as used in Boroughs' research.

The resulting PLGNUM values (Figure 1.5) showed that the criteria can be indicative of sediment plug formation as a necessary condition. However, the criteria could not show the location of the Bosque plug in 2008. Other places (black dotted) showed bigger PLGNUM than the Bosque Plug location. Therefore, more investigation is needed to better understand why another sediment plug formed in the Bosque area.

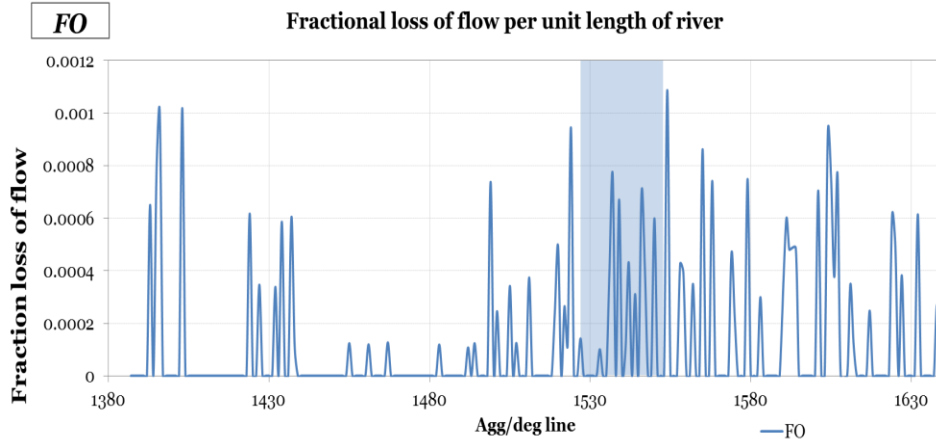


Figure 1.2. Fractional loss of flow of main channel per unit length of river

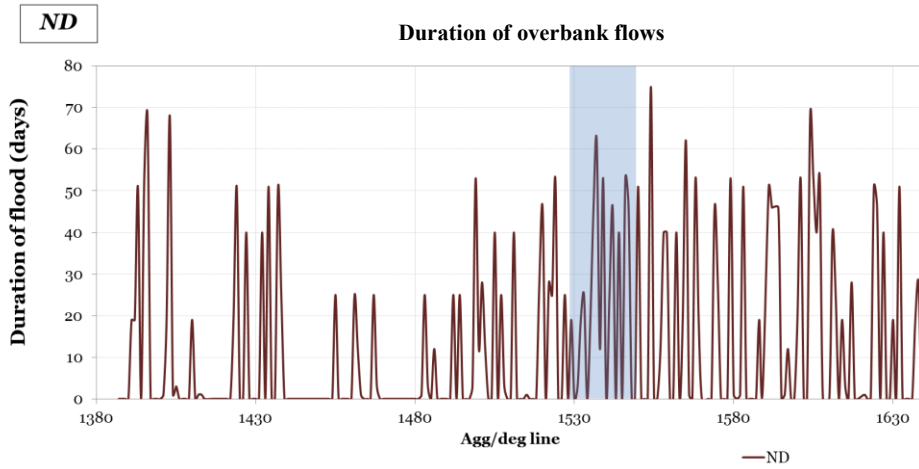


Figure 1.3. Duration of overbank flows (days)

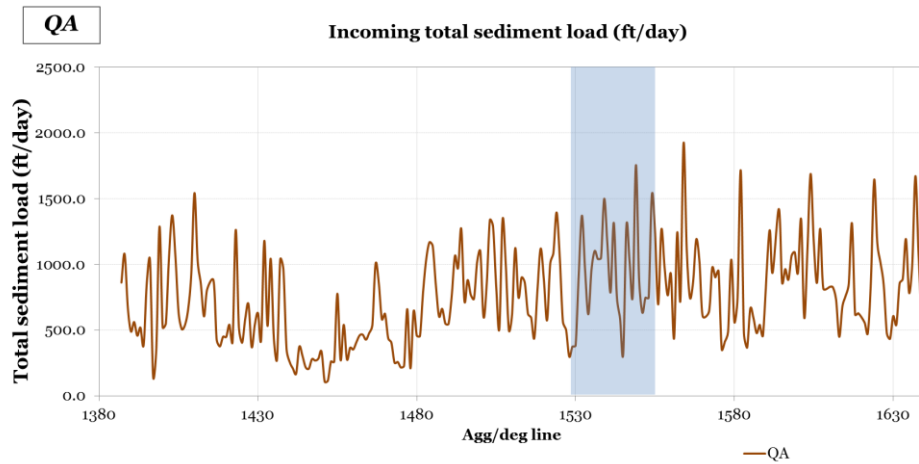


Figure 1.4. Incoming total sediment load per available channel area (ft/day)

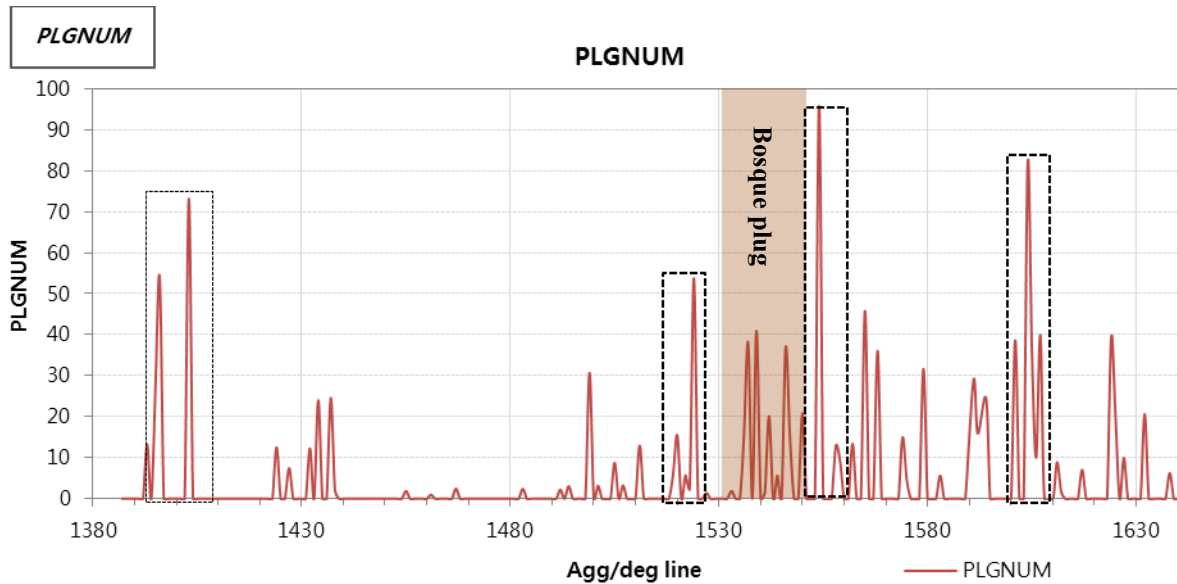


Figure 1.5. PLGNUM for the 2008 Bosque plug

1.4 DISSERTATION OBJECTIVES

The objectives of this research are to analyze the seven sediment plug parameters and to assess the primary causing factors. To accomplish this study, the following analyses are performed:

- Analysis of sedimentation effect due to two geometric factors: (1) channel width/capacity; and (2) roughness
- Analysis of sedimentation effect due to two flow and sediment loss factors: (1) perched channel and overbank flows; and (2) vertical sediment concentration profile
- Analysis of sedimentation effect due to three backwater factors: (1) reservoir; (2) bridge; and (3) sharp bends
- Determination of which factors contribute the most to the formation of sediment plugs

1.5 RESEARCH APPROACH AND METHODOLOGY

Sediment plug causing factors which can be identified by investigating spatial and temporal changes in the Middle Rio Grande were verified through (Figure 1.6): (1) understanding and analyzing the basic characteristics of flow and geometry; (2) an analytical approach to determine the effect of each causal factor on sediment plug formation; and (3) a numerical simulation using practical detailed cross sections and flow-rates.

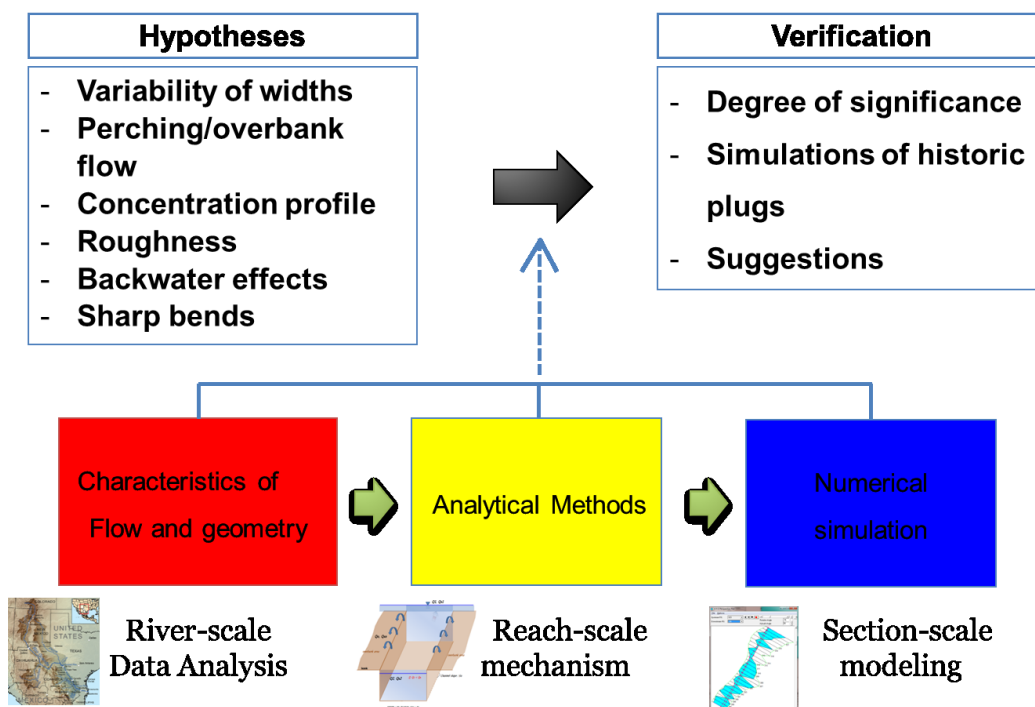


Figure 1.6. Research approach to proceed this study

The detailed procedures of this research are to:

- (1) **Determine flow and geometric characteristics of plug areas:** The cross section geometry, levee, elevation, particle size distribution, channel roughness, slope, width, depth, overbank height, longitudinal profile, and water and sediment transport capacity are determined based on field data provided by Reclamation.

- (2) **Identify major parameters to cause sediment plug formation** based on spatial and temporal changes in the river system as well as hydrodynamic and sedimentation conditions.
- (3) **Analytically investigate the mechanics of sediment plug formation** in terms of seven causing factors based on channel width, depth, particle size, slope, concentration, discharge and sediment discharge, reservoir stage, bridge dimensions, flow and sediment discharge, and Rouse's sediment concentration distribution equation.
- (4) **Develop a numerical aggradation/degradation model** to replicate the historic sediment plugs. The model includes seven major causal factors and combines Exner's sediment continuity equation with Yang's sediment transport equation. The numerical model is calibrated and validated with available plug data.

This dissertation consists of nine chapters. An introduction is presented in Chapter 1. Chapter 2 is the literature review for the historic sediment plugs and effects, sediment transport capacity, and sedimentation modeling. The site description and the river characteristics are described in Chapter 3. Chapter 4 describes the available data and defines possible plug causing factors for understanding the mechanics of sediment plug development. In Chapters 5, 6, and 7, analytical approaches to investigate the mechanics of sediment plug formation are stated in the dissertation objectives. Chapter 8 includes the 1-D aggradation-degradation numerical model development and application to the Middle Rio Grande. The summary and conclusions are addressed in Chapter 9.

CHAPTER 2 LITERATURE REVIEW

2.1 SEDIMENT PLUGS

2.1.1 Historic occurrences

A sediment plug, originally defined as a valley plug or channel block, is a channel blockage which occurs at sites where the sediment transport capacity of the stream is less than the sediment load carried from upstream (Diehl 1994). The major causes of sediment plug formation were historically channel bed aggradation and driftwood accumulation (Diehl 1994; Shields 2000; Borough 2005). After the occurrence of a sediment plug, flow tends to shift to a single alternative channel or multiple distributary channels. As a result, sediment transport capacity decreases and sediment deposition accelerates, eventually migrating upstream in the main channel.

Historically, sediment plugs have occurred at several different locations around the country. Diehl (1994) studied valley plug cases caused by river bed aggradation and congestion of trees and woody debris. He investigated the plug formation in the Hatchie River basin and attributed the plug development to low-gradient alluvial system and sediment-laden tributary system. Thus valley plugs were typically considered to form where the slope of a sand-laden tributary decreases downstream, or where the tributary joins its parent stream (Diehl 1994). Along the Yalobusha River in northern Mississippi, a sediment plug occurred after river channelization due to the shrinkage of bank-full discharge and the decreased channel slope (Shields et al. 2000). Woody vegetation, previously growing on these channel banks, delivered to the flow was transported downstream to form a large debris plug. The debris plugs function as

dams, causing higher water levels and reduced flow velocities. This, in turn, causes even greater rates of deposition, further reducing channel capacity, and blocking the flow of the river.

Below Canyon Dam on the Guadalupe River in Texas, a sediment plug formed during the summer of 2002 (Gergens 2003). A flood with a 0.4 percent annual exceedance probability (250-year return period) caused the overtopping of the emergency spillway and subsequent significant spillway channel erosion. The transported sediments and debris deposited in the main channel of the Guadalupe River eventually plugged the channel and made a cutoff swale.

Shields et al. (2000) studied numerous historic cases of human perturbations of lowland river channels and occurrences of valley plugs. According to his research, despite the advances in river management, the removal of blocks of plugs triggers a new type of erosion with excessive sediment transport. Thus, consideration to escape from the cycle should be taken by adapting land use objectives and policies to the hydrologic regime or by a variety of structural approaches.

Clear Branch Creek of the Middle Fork of the Hood River in Oregon experienced a sediment plug during flood in 1996 (Hickman 2001). The cause of the plug was attributed to flooding and other human activities, but, the specific river mechanics processes resulting in sediment plugs have not been developed.

Sediment plugs in the Middle Rio Grande occurred four times over the last two decades and various authors have studied the plug formation. The cause of the plugs has been known as the decrease of sediment transport capacity with significant loss of water to overbank areas. The observed sediment plugs developed within a matter of weeks and the main channel aggraded up to the bank crest, causing water delivery stoppage through the main channel. Water delivery to downstream states (e.g., Texas) and Mexico is an international issue, thus the understanding of the plug occurrence and sustainable river management became a top priority for river engineers.

Boroughs (2005) studied the sediment plugs in the Tiffany area and suggested PLGNM as the criteria for plug development based on a function of the independent variables.

Reclamation (2011) studied the sediment plug formation in the Bosque Reach located 14 miles upstream from the Tiffany area and prepared various river maintenance plans including the Bosque del Apache Sediment Plug Management.

2.1.2 River maintenance in the Middle Rio Grande

Alluvial rivers tend to adjust their gradient, planform, and cross-sectional geometry toward a state of dynamic equilibrium (Schumm 1977). The Rio Grande has a complex geomorphic and geologic history (Belcher 1975) and one of the highest sediment loads of any river in the world (Baird 1998). The Middle Rio Grande (MRG) consistently tends to move forward to cause changes in channel morphology, including width, thalweg elevation and slope, attaining long-term river equilibrium (Lagasse 1980; León 1998; Bauer 2000; Richard 2001). The river channel has been drastically changed, both vertically and laterally, due to man-made river infrastructure, reservoir water level variations, and ensuing upstream delta sediment deposits (Makar et al. 2012). Sediment plugs need to be investigated by understanding historic changes in this river. Reclamation maintenance programs for the Middle Rio Grande have focused on providing effective transport of water and sediment to Elephant Butte Reservoir, reducing channel aggradation and degradation, protecting riverside structures and facilities, and providing improved habitat for the endangered species (Reclamation 2007).

The channel bed has aggraded and degraded depending on the relative magnitude of the upstream sediment supply and sediment transport. While most of the reach of interest has been gradually aggrading since the 1930s (Reclamation 2007), degradation associated with the low

levels of the Elephant Butte Reservoir caused upstream head-cutting at low water stages (USACE 1989; Reclamation 1998).

Channel aggradation causes the reduction of overall hydraulic capacity. During the high reservoir storage period from 1979 to the late 1990's, sediment deposited upstream of the reservoir pool (Figure 2.1). Due to the channel bed rising during this period, the hydraulic capacity of the Atchison, Topeka, and Santa Fe railroad bridge (the San Marcial Railroad Bridge) was drastically decreased. The bed accretion restricted releases from the Cochiti Dam upstream (Reclamation 2007).

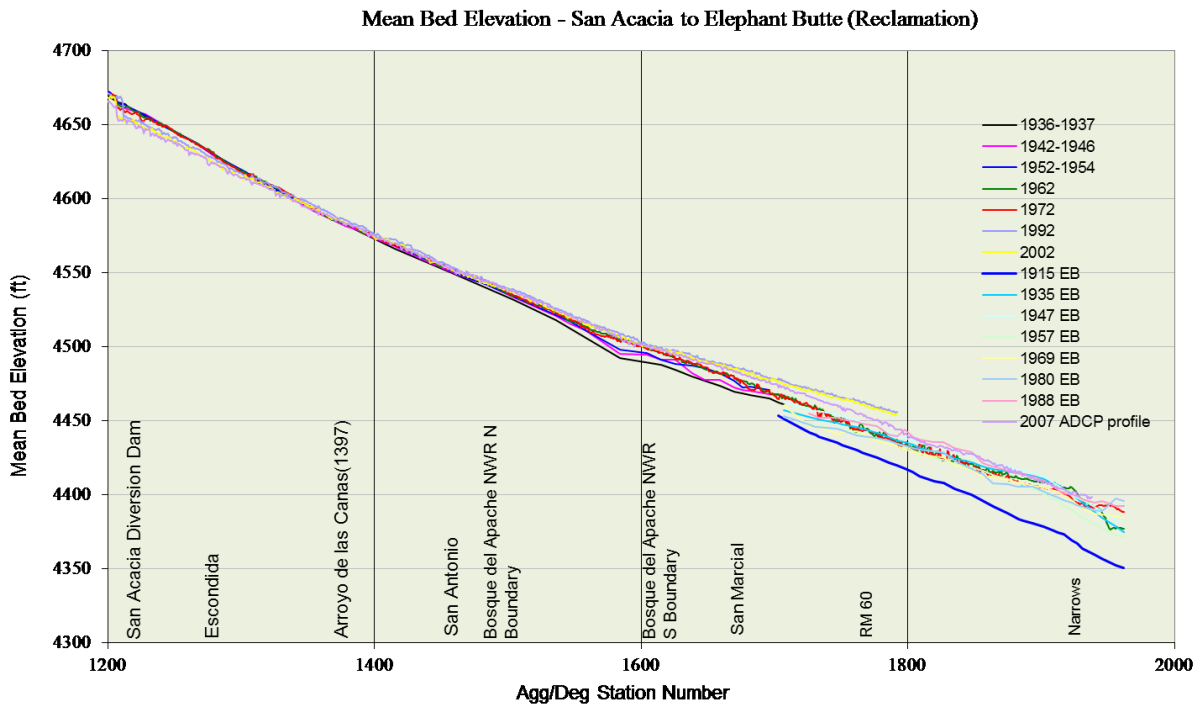


Figure 2.1. Temporal change in channel bed elevation (Reclamation, 2011)

Conversely, there have been cases of increased hydraulic capacity. A bankfull discharge at the San Acacia diversion dam (Agg/Deg 1,207) increases from 3,600 to 9,100 cfs (Mussetter

Engineering Inc. 2002). The increased hydraulic capacity resulted from the channel degradation by the operation of San Acacia Dam.

The downstream reach, which is under the influence of backwater effects from Elephant Butte reservoir, has had greater hydraulic capacity at low reservoir levels and ensuing upstream directional incision than at high levels.

As the river has been confined to the west side of the floodplain by the levee to protect the low-flow conveyance channel, the aggradation of the river bed in the San Marcial area has perched in a narrow strip along the floodplain. The head difference between the perched river bed and the low-flow channel caused cracking and occasional water piping through the embankment (Gorbach 1999).

Amongst the geomorphological changes in this river, sediment plugs and delta deposits have caused severe water delivery issues. The MRG was clogged by a sediment plug in 1991, 1995 and 2005 in the Tiffany area and in 2008 in the Bosque Reach. These sediment plugs caused water to spread over large areas and significantly diminished flow to the downstream reservoir. Although the maintenance activities were not cost effective, mechanical removal of sediment deposits was necessary on a continuing basis to maintain channel capacity (Reclamation 2007).

In and around the alluvial delta just upstream of the Elephant Butte Reservoir, temporary channel maintenance has continued to promote effective water delivery (Padilla et al. 2010). Presently, without continual maintenance, sediment will deposit in the main channel and at the upstream end of the reservoir, which causes the river not to reach the reservoir pool.

A varying water table affects the riparian vegetation; stress and mortality of the riparian vegetation has obvious negative implications for endangered species habitat.

2.1.3 Possible causing factors

Diehl (1994) demonstrated that valley plugs typically form at locations where the sediment transport capacity of the stream decreases in the downstream direction to the point that the stream cannot deliver the sediment load. Shields (2000) reported that a sediment plug forms whenever there is a discontinuity in sediment or woody conveyance. Boroughs (2005) investigated historic sediment plugs including the Tiffany plugs and identified that the main cause of sediment plugs in the Middle Rio Grande was the constriction and expansion of the river channel that caused flow to overtop the banks during flood events. Shrimpton and Julien (2012) framed hypotheses that vertical sediment distribution, backwater effects from bridges, low bank height, local variation in channel width, channel perching, reservoir levels, changes in channel slope, cycles of droughts and floods, duration and magnitude of spring runoff, and coarsening of bed material might cause plugs to form. In spite of these investigations, the mechanics of sediment plug formation in the Middle Rio Grande have not been fully examined.

2.1.4 Reclamation's endeavors

Reclamation (2007) established the Middle Rio Grande River Maintenance Plan to assess the current maintenance strategies and to seek potential new strategies. In this voluminous plan, a sediment plug was selected as one of four major maintenance problems of priority.

Tetra Tech (2010) studied the recurring conditions of plug formation and indicated that the physical characteristics of the Bosque Reach are in place for future sediment plugs.

Reclamation (2011) carried out Bosque del Apache Sediment Plug Baseline Studies and prepared Bosque del Apache Sediment Plug Management: Alternatives Analysis. The analysis classified alternatives into five types of river maintenance activities.

Lai (2012) at the Technical Service Center of the Bureau of Reclamation predicted a sediment plug on the Rio Grande with the SRH-2D Model. In addition to these river management planning and researches, various monitoring and inter-agency cooperation are being executed to alleviate the future sediment plug.

2.1.5 Cooperative project of CSU with Reclamation

This has led the Bureau of Reclamation (Reclamation), in conjunction with Colorado State University (CSU), to undertake studies, including: (1) overbank analysis modeling (Bender et al. 2011); (2) sustainable width analysis (Park et al. 2011); (3) literature review and conceptual assessment (Park et al. 2011); and (4) mechanics of sediment plugs (Park et al. 2012).

Bender et al. (2011) evaluated the channel conveyance in the Bosque del Apache Reach and suggested that generally the bank-full discharge has been decreased and the channel width of bank-full discharge has widened over time.

Park et al. (2011) estimated the sediment transport capacity of the reaches where sediment plugs occurred and described that the widening of the reaches decreased the sediment transport capacity and accelerated sediment plug formation in the river. In order to investigate the mechanics of sediment plug formation, Park et al. (2012) developed a 1-D numerical model that incorporates the sediment concentration profile as well as aggradation/degradation in the main channel and overbank areas (Figure 2.2). There is still a need to investigate the mechanics of sediment plugs associated with the relationship between various suspended sediment concentrations and accelerated aggradation of the main channel profile.

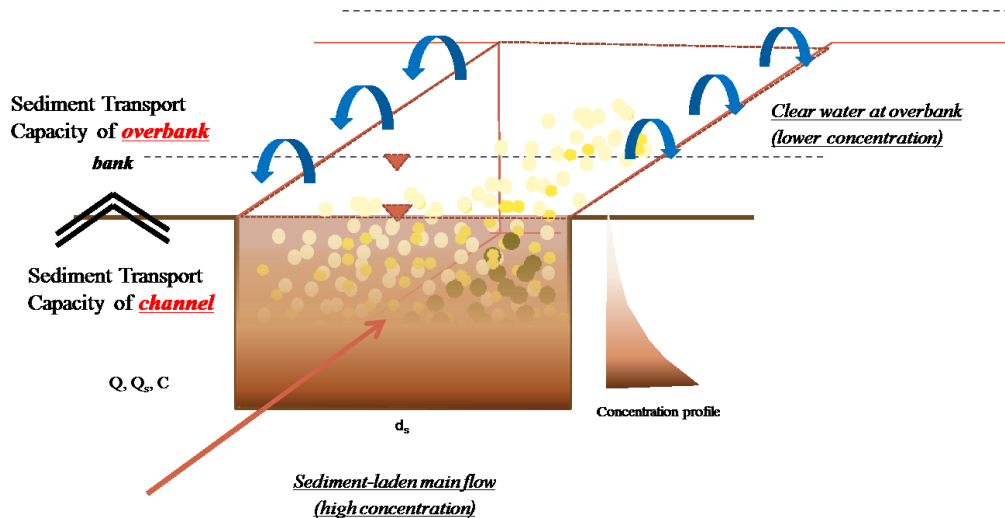


Figure 2.2. Vertical sediment concentration profile (Park and Julien, 2012)

2.2 MECHANICS OF SEDIMENT PLUG FORMATION

2.2.1 Sediment Transport Capacity

The natural processes of erosion, transport, and sedimentation of solid particles can lead to significant engineering and environmental problems. Sediment particles at a given stream cross section must have been eroded somewhere in the watershed and transported by flow from the place of erosion to the cross section (Knighton 1988). The fundamental cause of most channel and floodplain adjustments is an imbalance between sediment supply and transport capacity (Reclamation 2006).

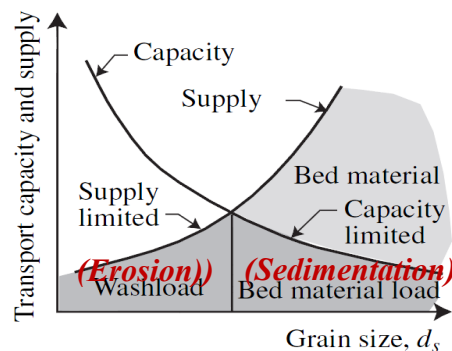


Figure 2.3. Sediment transport capacity and supply (Julien, 2010)

Sediment transport capacity, which is defined as the maximum load of sediment that a determined flow rate can carry by the river under a given flow, sediment, and channel conditions, is the basic concept in determining detachment and deposition processes in the current process-based erosion model framework (Huang et al. 2011; Reclamation 2012).

Specific parameters that control the transport capacity of the stream include channel geometry, width, depth, shape, wetted perimeter, alignment, slope, vegetation, roughness, velocity distribution, tractive force, turbulence, and uniformity of discharge. The sediment transport capacity under unlimited sediment supply can be determined as a function of hydraulic variables and the shape of the stream cross-section (Julien 2010).

In practice, there are two approaches to determine the sediment transport capacity. The first is to develop a sediment rating curve (relationship between flow and sediment discharge) based on sediment transport measurements in the field. The second, which was utilized in this study, is to compute the sediment transport capacity using published sediment transport equations.

For the first approach, León (2003) evaluated the applicability of a rating curve method by computing the incoming sediment load to the channel with the bed material rating curves developed at San Acacia and San Marcial gages. The incoming sediment loads from the rating curves and the potential transport rates from Yang's (1973) equation were not in balance, thus this approach is not applicable to this reach of interest.

For the second approach, numerous sediment transport formulas have been proposed, but none of the published transport equations can determine the total load. For a practical purpose, comparison of the results from several formulas with field observations leads to choosing the most appropriate equation at a given location (Julien 2010).

The formulas can be classified into several categories depending on the fundamental approaches: equations based on advection, equations based on the energy concept, and graphical and empirical methods based on regression analysis (Julien 2010).

Most research with respect to sedimentation modeling in the Middle Rio Grande used the Engelund-Hansen equation (1972) and Yang's equation (1973). Huang et al. (2010) used Engelund-Hansen's 1972 equation and Yang's 1973 sand equation for 2009 historical bed elevation trends and hydraulic modeling from San Antonio to Elephant Butte Reservoir. Lai (2012) used the Engelund-Hansen capacity equation for predicting channel morphology upstream of Elephant Butte Reservoir on the Middle Rio Grande. León (2002) and Borough (2005) used Yang's equation for their dissertation research. Yang's (1973) sediment transport equation has been used in sediment transport modelling in the upper end of Elephant Butte Reservoir. Its results are in good agreement with field measured transport rates (León 2003; Borough 2005).

León (2003) compared existing sediment transport equations with field sediment discharge measurement in the Middle Rio Grande (Figure 2.4), and showed that most of the equations are in reasonable agreement with sediment discharge at high flows when the sediment plugs occurred. Among these equations, Yang's equation (1973) and Julien's equation were used in León's research. Firstly, Yang's equation has been developed based on the MRG sedimentation data set and Reclamation has used this equation for river maintenance planning and future river bed simulations in the MRG. Therefore, this equation was used in analytical calculation and numerical simulations to investigate the mechanics of sediment plug development. On the other hand, Julien's equation provides dimensionless sediment discharge based on the Shield's parameter, and the bed load equation was used in the analytical derivation owing to its simplicity and meaningfulness in terms of river bed sedimentation.

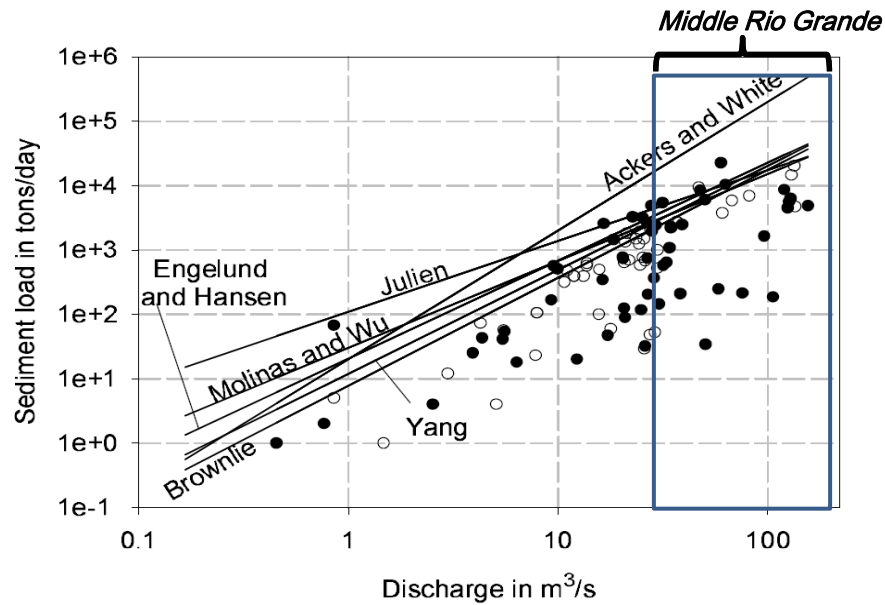


Figure 2.4. Sediment transport capacity versus sediment discharge in the MRG (León, 2002)

2.2.2 Analytical descriptions of river response

Numerous researches have been conducted to characterize channel response to changes in water and sediment discharge and to obtain a unique channel configuration, based on the extremal hypothesis that a channel adjusts to convey the maximum possible bed-load, given the slope, water discharge and sediment size, or to carry the sediment load with the available discharge on the lowest possible slope (Ferguson 1986).

Kirkby (1977) pioneered a quantitative approach with the hypothesis of maximum sediment efficiency, which indicates that rivers will adjust to carry the sediment load imposed upon them as efficiently as possible in the medium term. Kirkby (1977) used the Meyer-Peter and Müller equation for bed-load transport, the Darcy-Weisbach resistance equation and the continuity equation to develop a set of curves that represent the relationship between sediment concentration and channel slope, depth, and grain size.

Chang (1979) introduced the hypothesis of minimum stream power in alluvial channels based on the theorem of least work. An alluvial channel with given water discharge and sediment inflow tends to establish its width, depth, and slope such that the stream power or slope is a minimum. Chang (1979) also pointed out that possible multiple channel geometries with identical water discharge and sediment load must be associated with different flow regimes, stream-bed roughness, velocity, etc. He used the Engelund-Hansen resistance formula, the Lacey resistance equation, and three different sediment transport equations (DuBoys, Engelund-Hansen, and Einstein-Brown), and developed slope-width curves for different water discharge and sediment load values that reflect two minimum slopes: one for the lower regime and another for the upper regime.

White et al. (1982) analytically demonstrated that extreme values of the sediment concentration lead to extreme values for the slope. White et al. (1982) used Ackers and White sediment transport theory, and the frictional characteristics were computed using the White, Paris, and Bettess linear relationship between mobility factors related to total shear stress and to effective shear stress.

Huang and Nanson (2000) solved the problem of indeterminacy of channel adjustment by reducing the number of dependent variables to three (width to depth ratio, slope, and velocity) and using three basic equations ; continuity, Lacey's resistance equation, and DuBoys' sediment transport formula. Huang and Nanson (2000) identified an optimum condition for sediment transport by adjusting the width/depth ratio for given flow discharge, channel slope and sediment size. The optimum condition is maintained in the range of 2.5 to 30 for the width to depth ratio. Julien and Wargadalam (1995) and Huang and Nanson (1995) developed the optimum condition for sediment transport, revealing high levels of consistency with the downstream hydraulic geometry equations.

Carson and Griffiths (1987) noticed that the existence of a peak in the sediment load-width relationship is due to the inclusion of a threshold shear stress in the transport equations. Carson and Griffiths (1987) also noticed that different researchers have used different sediment transport and resistance equations, and all of the equations include a threshold shear stress. Carson and Griffiths (1987) found that the optimum width for maximum sediment transport will emerge if the three equations developed by Einstein-Brown are used, because these equations represent the curvilinear nature of the data. Furthermore, Carson and Griffiths (1987) show that an optimum width for a maximum sediment transport exists in all cases when $c > m$, assuming wide channels ($R_h = D$), where c is the exponent of the flow depth factor in the resistance equation ($BD^c = nQ/S^{0.5}$) and m is the exponent of the excess shear stress factor in the sediment transport equation. The width is B , the flow depth is D , the friction factor is n , the water discharge is Q , and the slope is S .

Chitale (2003) and León (2003) developed an analytical description of the slope versus width and width-depth ratio of channels in equilibrium under steady state input water and sediment discharges. These relationships indicate that an increase in channel width will require an increase in channel slope to satisfy continuity of sediment transport. The analytical solution of the width ratio versus the slope ratio for large widths is in good agreement with the laboratory flume data and field measurements of the Middle Rio Grande (León et al., 2009).

2.2.3 Sediment concentration profiles

If flows of an alluvial river exit the main channel and spill into the overbank areas, the vertical sediment distribution determines the fraction of sediment load lost to the overbank areas, which has a significant impact on erosion and deposition in the main channel (Boroughs 2005, Reclamation 2011).

If a significant amount of the flow is lost to the overbank but less sediment is being carried at the top of the water column, the sediment load is not reduced by the same proportion as the loss to the sediment transport capacity. As a result, deposition is induced. While the link between deposition in the main channel and the loss of flow to the overbank areas has not been well documented, there has been extensive study of the vertical distribution of suspended sediment.

One of the more commonly used relationships is the Rouse equation (Julien 1995). Considering upward and downward flux, the diffusion-dispersion equation can be simplified as:

$$\frac{\partial C}{\partial t} + v_x \frac{\partial C}{\partial x} + v_y \frac{\partial C}{\partial y} + v_z \frac{\partial C}{\partial z} = \dot{C} + (D + \epsilon_x) \frac{\partial^2 C}{\partial x^2} + (D + \epsilon_y) \frac{\partial^2 C}{\partial y^2} + (D + \epsilon_z) \frac{\partial^2 C}{\partial z^2} \quad (2.1)$$

If a state of equilibrium is to obtain, this rate of settling must exactly equal the rate at which the material is lifted by the turbulence; thus,

$$wC = \epsilon_z \frac{\partial C}{\partial z} \quad (2.2)$$

Integrating Equation 2.2 leads to the general expression.

$$c = c_o e^{-\omega z / \epsilon_z} \quad (2.3)$$

Vanoni (1946, 1975) and Ismail (1952) proposed that the vertical dispersion coefficient (ϵ_z) can be expressed as a function of the momentum exchange coefficient (ϵ_m) and the factor of proportionality β ($=\epsilon_z/\epsilon_m$).

$$\epsilon_z = \beta_x \epsilon_m = \beta_s \frac{\tau dz}{\rho_m dv_x} \quad (2.4)$$

The stress resulting from the momentum transport will vary with the gradient of both density and velocity,

$$\tau = \rho v \frac{\partial v_x}{\partial z} + \rho \epsilon_z \frac{\partial v_x}{\partial z} \approx \rho \epsilon_z \frac{\partial v_x}{\partial z} \quad (2.5)$$

Therefore, substitution of Equation 2.4 and 2.5 to Equation 2.3 leads to the following concentration profile formula:

$$\frac{C}{C_a} = \left(\frac{h-z}{z} \frac{a}{h-a} \right)^{R_o = \frac{\omega}{\beta_s \kappa u_*}} \quad (2.6)$$

$$R_o = \frac{\omega}{\beta_s \kappa u_*} \quad (2.7)$$

where C is the concentration at elevation z , C_a represents the reference sediment concentration at a reference elevation “ a (η in original Rouse equation)” above the bed elevation, z is the elevation above a reference elevation, h is the flow depth, R_o is the Rouse number, ω is the particle fall velocity, β_s is the ratio of the turbulent mixing coefficient of sediment to the momentum exchange coefficient, κ is the von Kármán constant, and u_* is the shear velocity.

This equation is referred to as the Rouse equation (1938). As a Rouse number increases, a greater fraction of the sediment will be transported on the bed (Figures 2.5-2.6). Conversely, as the Rouse number decreases, suspended load would be dominant (Julien 2010; Woo 2001).

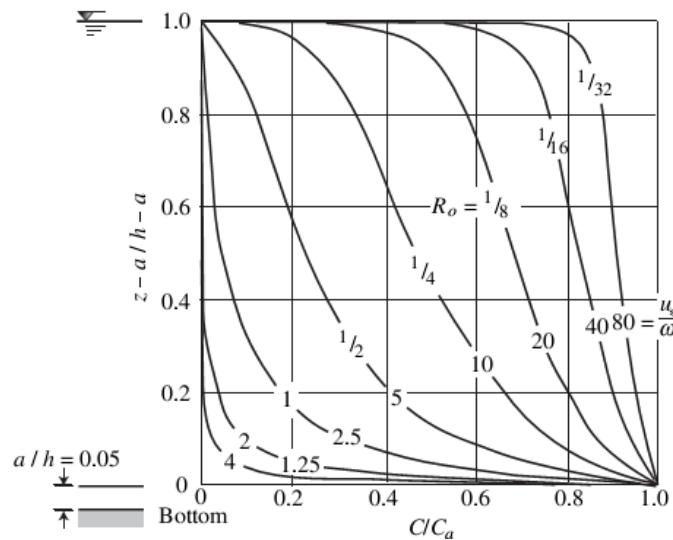


Figure 2.5. Dimensionless plot of suspended-load distribution (Rouse, 1938)

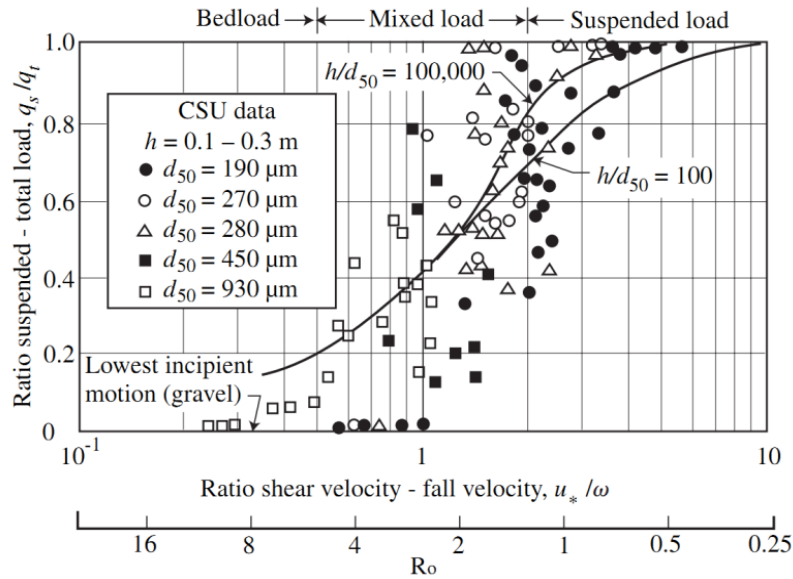


Figure 2.6. Ratio of suspended to total load versus ratio of shear to fall velocities (Julien, 2010)

Vanoni (1946) and Vanoni et al. (1957) derived the vertical distribution of relative concentration C/C_a compared with results from the Rouse equation for wide range of stream size and Rouse numbers. Einstein and Chien (1954) compared measured and calculated Rouse number and found that for low Rouse number, calculated values show good agreement with measured Rouse number, while for large Ro number greater than 1, calculation tends to be greater than measurement. Nordin and Dempster (1963) used samples of suspended sediment and measurements of 3 points in a vertical and defined sediment concentration profiles for cross sections of Rio Grande. They found that the suspended sediment is distributed more uniformly than conventional theory predicts due to flow regime, size of bed material, and the effect of concentration of suspended fine materials. Also, they derived values for the Middle Rio Grande: a value of 1.15 corresponds with a mean particle size of 0.25 mm.

Mofjeld and Lavelle(1988), Woo and Julien (1988), Williams (1989), Hay and Sheng (1992), Homes and Garcia (2002), Kim (2003), Nagy et al. (2002), and Liu et al. (2007) also applied various technologies to investigate the vertical concentration profiles in rivers.

Research with respect to sediment concentration has been focused on vertical and lateral concentration distribution, but vertical sediment concentration profiles on overbank areas have not been investigated so far.

2.2.4 Numerical simulation

Most of the sediment transport models used in river engineering are one dimensional, especially those used for a long-term simulation of a long river reach. One-dimensional models are usually based on the same conservation principles as the multi-dimensional models; the conservation of mass and momentum (Simões and Yang 2006).

Conservation of mass and momentum can be respectively expressed as:

$$\frac{\partial A}{\partial t} + \frac{\partial Q}{\partial x} = q_l \quad (2.8)$$

$$\frac{\partial Q}{\partial t} + \frac{\partial}{\partial x} \left(\beta \frac{Q^2}{A} \right) + gA \frac{\partial h}{\partial x} + gA(S_f - S_o) = 0 \quad (2.9)$$

where A = cross-sectional area of the flow, Q = water discharge, q_l = lateral inflow per unit length, g = gravitational acceleration, S_f = friction slope, S_o = bed slope, β = momentum correction coefficient, h = water depth, t = time, and x = spatial distance.

The continuity equation for sediment mass (Exner equation) can be expressed as

$$\frac{\partial Z}{\partial t} = \frac{-1}{(1-p_o)} \frac{\Delta q_s}{\Delta x} \quad (2.10)$$

where q_s = sediment discharge in the x direction, Z = bed elevation, and p_o = porosity.

With these governing equations, numerical techniques, and proper boundary conditions, numerical solutions will be determined. Figure 2.7 shows a general analysis procedure for uncoupled sedimentation modeling.

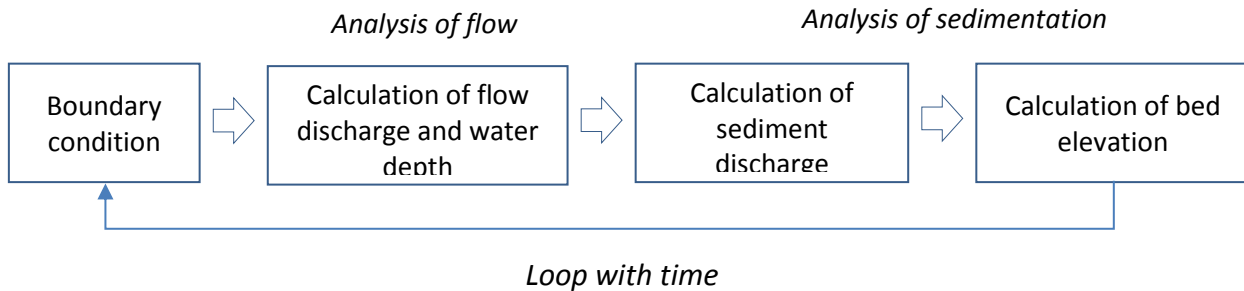


Figure 2.7. Procedure of river bed analysis (modified from Woo, 2002)

Numerous recent studies have developed or applied various numerical models to simulate river bed changes. Recent studies (Boroughs et al. 2005, 2011; Lai 2009, 2012; Tetra Tech 2010) have investigated the parameters associated with sediment plug formation on the Rio Grande.

Yang et al. (2005) developed the Generalized Stream Tube model for Alluvial River Simulation (GSTARS 1.0) and Huang et al. (2003) applied this numerical model to the stretch of the Rio Grande from San Acacia Diversion Dam to Elephant Butte Reservoir, predicting transport and bed evolution in the river. To predict the erosion and deposition in the same cross section, the river was divided into three sub-channels; main channel and left and right floodplains.

Boroughs (2005) developed a 1-D numerical model, the Sediment Plug formation in Alluvial Rivers (SPAR), to evaluate his plug formation theory. A criterion for sediment plug formation, PLGNUM, was suggested as a function of slope, porosity, the exponent in total sediment load power function, the Rouse number, and the change to main channel cross-sectional area. Boroughs (2005) applied the SPAR model to the Tiffany Junction Reach to simulate the

sediment plugs in 1991 and 1995 and found that the total sediment load exceeded the historical average daily load with significant overbank flow. The prolonged high flow periods caused sediment deposition and led to sediment plug development.

Huang et. al (2003) used the 1-D sediment transport model (SRH-1D) to simulate the future channel bed response to river geometry with and without channelization. Huang and Makar (2010) applied the SRH-1D model to simulate the historic degradation in the Bosque del Apache National Wildlife Refuge that is due to base level lowering from the drop in pool elevation of Elephant Butte Reservoir combined with the high flows since 2004. The study also provided the potential future degradation at several locations of the Refuge.

Lai (2012) carried out sedimentation simulations to evaluate the channel morphology of the river reach upstream of the Elephant Butte Reservoir on the Rio Grande using a two dimensional mobile-bed simulation model, SRH-2D.

However, there are concerns that a number of important plug formation processes were overly simplified or ignored, thus limiting the model to a specific site with minimal predictive capabilities (Lai 2009). The ability to spatially and temporally predict future plug formation is of low resolution due to changes in channel and floodplain morphology over time and the uncertain nature of hydrology (Tetra Tech 2010).

2.3 SUMMARY

Sediment plugs in the Middle Rio Grande occurred 4 times over the last 20 years in spite of continuous river maintenance by Reclamation. These plugs are possibly caused by the changes in channel width, but the mechanics of sediment plug formation are not fully understood. Thus, understanding plug formation mechanics by deriving analytical relationships and by

developing a 1-D numerical model that incorporates various causing factors including the sediment concentration profile and the aggradation/degradation in the main channel and overbank areas, is pursued.

Various sediment transport capacity equations have been published, but Yang's (1973) equation has been qualified for sedimentation modeling in the Middle Rio Grande. This equation was used to calculate the total sediment discharge at cross sections in the reach of interest.

Analytical approaches to characterize channel response have been conducted over time. In order to understand the river response to flow and sedimentation changes, an analytical description with respect to width, width/depth ratio, sediment discharge, and sediment concentration needs to be determined. Concentration profiles can be determined by the Rouse equation, which has been validated as a physically reasonable formula to represent vertical sediment distribution.

Numerous studies have developed and applied numerical models, but sedimentation simulations have been focused on river bed changes in the main channel. Since there is no proper numerical model to calculate the sediment concentration, overbank flow, and other factors, a numerical model needs to be developed to prove the effect of each causing factor on sediment plug formation and to simulate historic sediment plugs. For calibration and verification of the model, sediment plug data on the Middle Rio Grande will be used.

CHAPTER 3 SITE DESCRIPTION

3.1 RIO GRANDE

The Rio Grande is about 1900 miles long, making it one of the longest rivers in the United States (Kammerer 1990). It forms high in the Rocky Mountains of southern Colorado and flows southeast toward the Gulf of Mexico, passing through New Mexico and along the border between Texas and Mexico on its way to the Gulf of Mexico (USGS Geographic Name Information System). The entire Middle Rio Grande extends from Cochiti Dam to Elephant Butte Reservoir, which is 180 miles long. Figure 3.1 shows a map of the Rio Grande and the Middle Rio Grande.

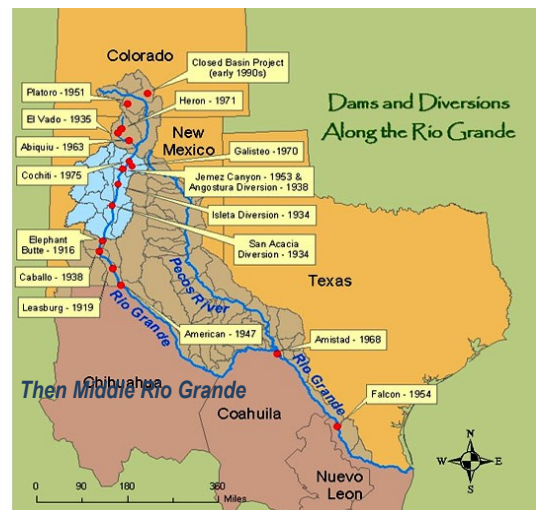


Figure 3.1. The Middle Rio Grande and hydraulic structures (US. Fish and wildlife Service)

Human activities such as farming, hunting, ranching, mining, logging, stream impoundment, and recreation, have had an impact on ecosystem's structure, including the river system, for thousands of years, especially after European settlement from the late 15th century (Finch 1995).

The reach of interest, the Middle Rio Grande, has experienced dramatic geomorphological and river mechanical changes. As part of the Middle Rio Grande Project, the San Acacia Diversion Dam was constructed in 1934. The dam caused rapid channel incision downstream of the dam (Bauer 2006). While the reach spanning from Arroyo de las Cañas to the city of San Antonio is mostly stable, the riverbed downstream of this reach has aggraded, maintaining a wide, braided, shallow channel planform with a sand bed. In locations where significant construction efforts exist, such as channelization, Low Flow Conveyance Channel (LFCC), and pilot channels through the floodplains, the channel widths are significantly narrower and floodplains are vegetated (Reclamation 2007). The Elephant Butte temporary channel has been maintained to ensure continuous surface water flow to the Elephant Butte Reservoir. Without the maintenance activities, the upstream end of the reservoir would see significant deposition repeatedly (Tetra tech 2003).

3.2 CLIMATE

Weather records dating from the late 19th century to the present indicate that most of the region is a continental plateau with arid to semi-arid climate. Salient characteristics include an average annual precipitation below 15 inches; high solar radiation; low relative humidity; moderate, but wide ranges of diurnal/nocturnal and seasonal temperatures; and high evaporation and transpiration rates (Finch et al. 1995). Precipitation fluctuates widely about the mean, and most summer rain is of high intensity and associated with thunderstorms. Average annual precipitation ranges from 7.25 inches at Pena Blanca to 8.31 inches at Las Cruces (Gabin and Lesperance 1977). Mean monthly (July) high temperatures for the Rio Abajo range from 76.2° F at Pena Blanca to 82.2° F at Las Cruces.

Mean lows (December) for these two locations are 31.1° F and 37.6° F. Floods, due either to spring runoff resulting from the melting mountain snowpack or from intense summer rains, have played a significant environmental role in the Rio Grande's hydrology and associated land-use activities during the historic period. Before the construction of major flood control structures on the upper Rio Grande and major tributaries in the 1930s, late spring and summer flooding of stream valleys was common (Figure 3.2). Historic droughts damaged or destroyed crops and rangelands, devastated wildlife populations, and depleted water supplies. Historical documentation from the mid-seventeenth century to the late 19th century corroborates analyses of more recent detailed weather records, which suggest the occurrence of a major drought in the region every 20 to 25 years (Tuan et al. 1973). These periodic droughts, increasing use of surface and ground waters, and intensive grazing have generally resulted in dramatic changes in the flora.

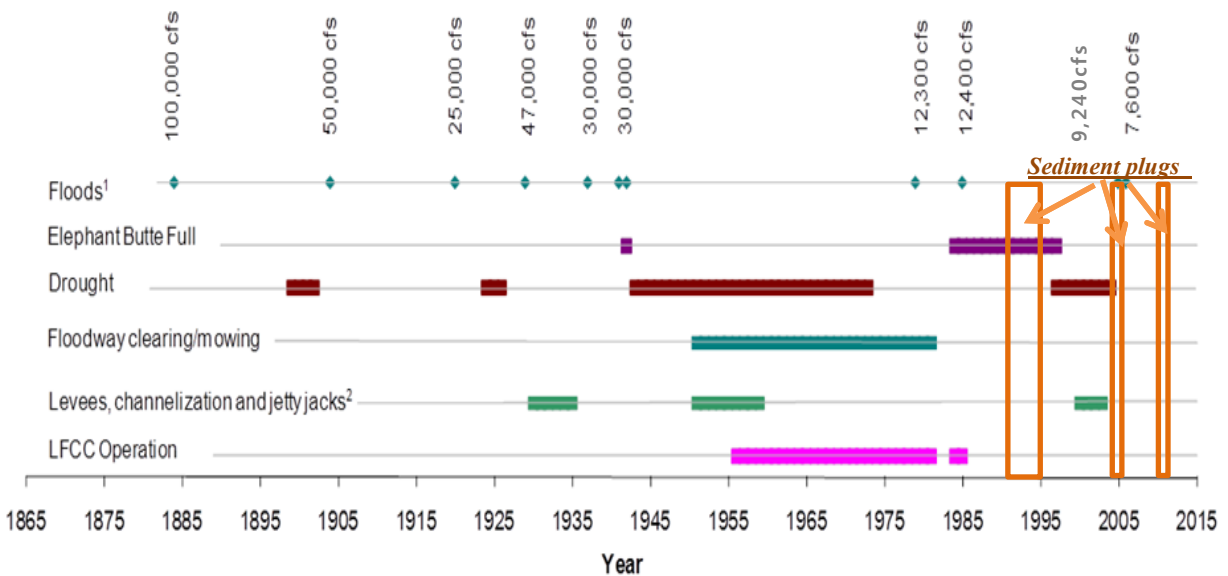


Figure 3.2. Rio Grande floods and droughts (Modified After Makar 2011, Pers. Comm.)

3.3 GEOMORPHIC CHANGES

Changes in hydrology and sediment supply, as well as man-made modifications have caused significant changes in the morphology of the Middle Rio Grande between Cochiti Dam and Elephant Butte Reservoir. Man-made interventions including, importations of water, the water-supply and flood-control reservoirs, diversion structures on the river, the flood-control project and the water conveyance project, have been to cause changes in channel width, thalweg elevation, the ability of the river to migrate laterally, the capacity of the channel, and hence the frequency of overbank flooding, local sediment storage and bar morphology, and bed-material composition reported (Lagasse 1980; León 1998; Bauer 2000; Richard 2001; Smith et al. 2001).

The channel of the Middle Rio Grande has narrowed. The narrowing began prior to the closure of Cochiti Dam, and may be the result of reduced sediment delivery from tributaries, as well as water diversions and engineering structures (Carter 1955; Dewey et al. 1979; Graf 1994; Lagasse 1994).

The channel of the Middle Rio Grande has deepened (Reclamation 1998). Degradation is probably the result of reduced sediment loads and channel narrowing (Lagasse 1994). The Middle Rio Grande has changed from a braided channel to a single channel as a result of reduced bed load (Culbertson and Dawdy 1964; Graf 1994; Lagasse 1994). Sediment characteristics vary from reach to reach of the Middle Rio Grande as a result of tributary influences (Culbertson et al. 1972; Graf 1994; Nordin and Beverage 1963; Rittenhouse 1944).

Figure 3.3 shows that the channel of the MRG around the Bosque plug location has narrowed between 1935 and 2008. And the channel around the Tiffany plug location has been realigned to the current channel and narrowed drastically during the same period (Figure 3.4).

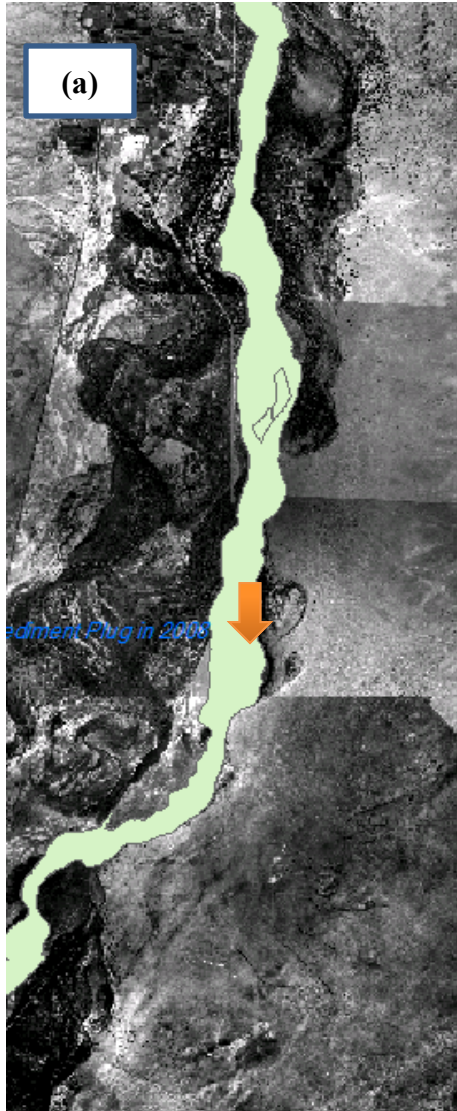


Figure 3.3 Morphological changes around Bosque plug (a) 1935 (b) 2008

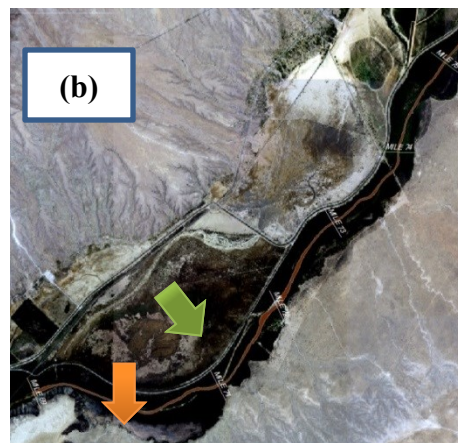
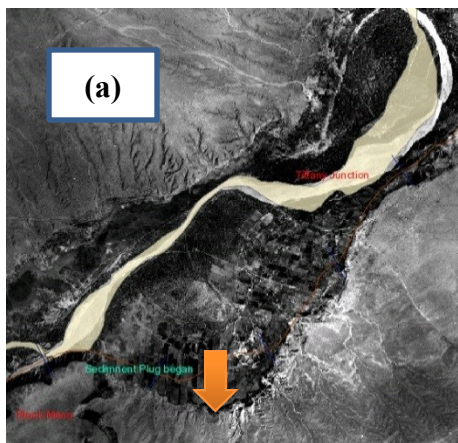


Figure 3.4 Morphological changes around Tiffany plugs (a) 1935 (b) 2008

3.4 SEDIMENT PLUGS

The river channel spanning from the Bosque del Apache Wildlife Refuge to the Elephant Butte Reservoir has been drastically changed, both vertically and laterally, due to man-made river infrastructure, reservoir water level variations, and ensuing upstream delta sediment deposits. Amongst them, sediment plugs and delta deposits must have caused severe water delivery issues. The MRG was clogged by sediment plugs in 1991, 1995, and 2005 in the Tiffany area and in 2008 in the Bosque Reach (Table 3.1).

Table 3.1. Sediment plug formations in the Middle Rio Grande (Reclamation, 2010)

Data Plug First Observed	Location	Length of Plug (miles)	Remarks
June 17, 1991	Tiffany Junction ~RM 70	1.0	Agg/Deg 1683
July 1, 1995	Tiffany Junction ~RM 70	5.0	Agg/Deg 1683
May 15, 2005	Tiffany Junction ~RM 70	5.0	Agg/Deg 1683
May 17, 2008	BDANWR ~RM 81-82	1.7	Agg/Deg 1531~1550

These sediment plugs (Figure 3.5a) caused water to spread over large areas and significantly diminished flow to the downstream reservoir. Mechanical removals of sediment deposits (Figure 3.5b) were necessary on a continuing basis to maintain channel capacity (Reclamation 2007). Without continual maintenance, sediment will deposit in the main channel and at the upstream end of the reservoir, which causes the river not to reach the reservoir pool.

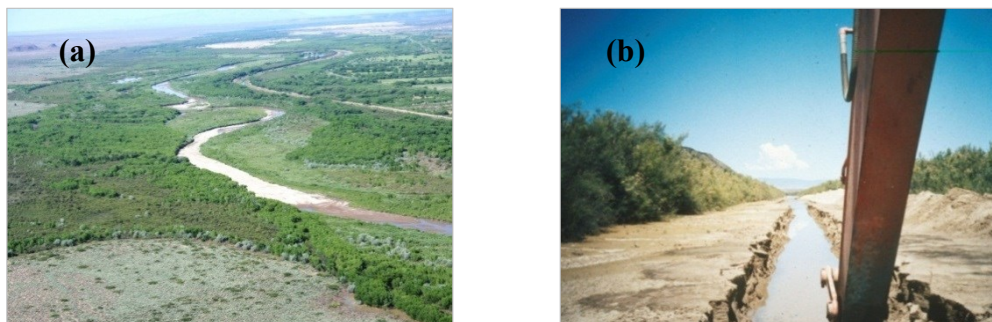


Figure 3.5. (a) 2008 Bosque Reach sediment plug (b) pilot channel excavation (Reclamation)

3.5 STUDY REACH AND SUBREACHES

The sections of the Middle Rio Grande examined in this study include the Bosque del Apache Reach (for Bosque plug) and Elephant Butte Reach (for Tiffany plugs), which are identified officially by Reclamation based on the presence of geologic and geomorphic controls.

The Bosque Reach spans 22.9 miles on the Middle Rio Grande, extending from Arroyo de las Canas (River Mile 95.3), which lies 8.2 river miles north of the US Highway 380 Bridge, to the south boundary of the Bosque del Apache National Wildlife Refuge (Refuge). Based on the assessment of channel elevations, channel slope, channel widths, and planform, the reach was divided into four sub-reaches. There is a USGS stream-flow gauge, San Acacia Gauge (USGS 08354900), just downstream from the San Acacia Diversion Dam. Flow discharge data are available from 1958 to present on real time basis. Within this reach, a sediment plug formed in 2008 around the Refuge, which is in the sub-reach 3, from Agg/Deg line 1531 to 1550.

Elephant Butte Reach stretches about 30 miles, the beginning from the south boundary of the Bosque del Apache National Wildlife Refuge (River Mile 73.9) to Elephant Butte Reservoir (River Mile 44.65). Based on the same conditions with those of Bosque sub-reaches, this reach was divided into six sub-reaches with same criteria. There is another stream-flow gauge, San Marcial Floodway Gauge (USGS 08358400), 2 miles downstream from the starting location of the historic Tiffany sediment plugs. Discharge data from 1949 to present are available, and San Acacia and San Marcial gauges provide this research with the flow discharges and sedimentation data. Sediment plugs occurred in 1991 just downstream Agg/Deg 1683 in the sub-reach 6 and extended 5 miles upstream to around Tiffany junction. Figure 3.6 shows the location of the project area, major gauging stations, historic sediment plugs and sub-reach delineation in New Mexico.



Figure 3.6. Delineation of sub-reaches and location of sediment plugs

CHAPTER 4 AVAILABLE DATA AND PLUG CAUSING FACTORS

In this chapter, available data for analytical derivations and numerical simulations are described. Section 4.1 describes the geometric characteristics in terms of width, depth, perching, longitudinal profile, and slope. Flow characteristics, flow discharge and resistance to flow are described in section 4.2. Sediment characteristics are presented in Section 4.3.

4.1 GEOMETRIC DATA

Cross section geometry data were obtained from the overbank flow analysis (Bender et al. 2011) and Elephant Butte Reach report (Owen et al. 2011). Cross sections were prepared using HEC-RAS 4.1.0 models developed by the U.S. Army Corps of Engineers. For sediment plug simulation, the 1992 and 2002 channel geometry files provided by Reclamation were used. Cross sections based on Agg/Deg line are spaced approximately 500 ft apart for most cross sections and 2,000-9,000 ft for cross sections in the reservoir area. The HEC-RAS model for 1992 does not contain geometry data at every Agg/Deg line, whereas the 2002 HEC-RAS model contains geometry data at nearly every Agg/Deg line. The thalweg was delineated in ArcGIS using aerial photographs for each year. Cross section data from the Bosque Reach and the Elephant Butte Reach were combined together into one HEC-RAS model by importing Elephant Butte Reach data and attaching downstream to the Bosque Reach data. The resulting 266 cross sections in 1992 and 404 cross sections in 2002 are available to this study.

4.1.1 Channel widths

Two types of channel width definition were used in this study: (1) active channel widths, which were determined by measuring the distance between the vegetation growths on each riverbank; and (2) channel width, which includes active channel and flood plains.

The left and right bank-lines in Figure 4.1 were delineated along vegetation boundaries. The active channel width was determined from the width within the main channel at the bankfull discharge. The channel width was determined from the top width of the HEC-RAS model at various flow discharges above the bankfull discharge (Figure 4.2).

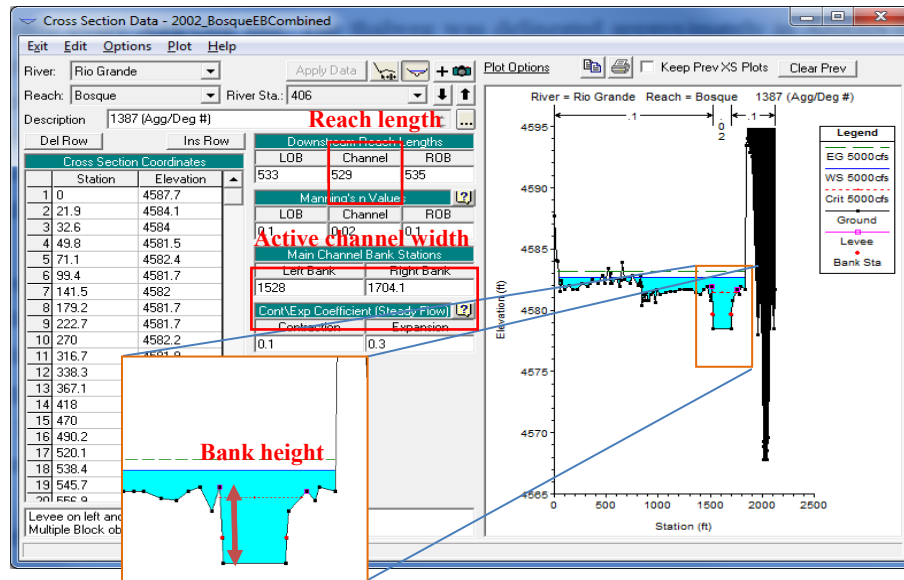


Figure 4.1. Cross section geometry obtained from HEC-RAS model

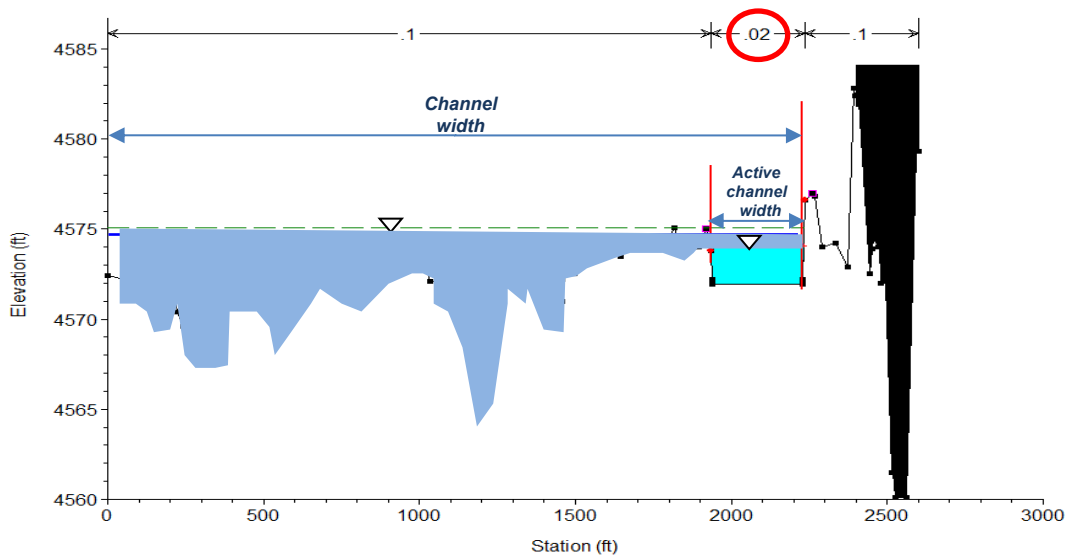


Figure 4.2. Active channel width and channel width in a cross section

With consistent river maintenance and nature's adjustment, the main channel width has narrowed over time (Figure 4.3). Compared with 1992 channel widths, 2002 channel widths decreased 11% on average. The channel width around the historic Bosque plug location decreased 77%, which was greatest in the study reach. Figure 4.4 shows the narrowing trend at the Tiffany plug location.

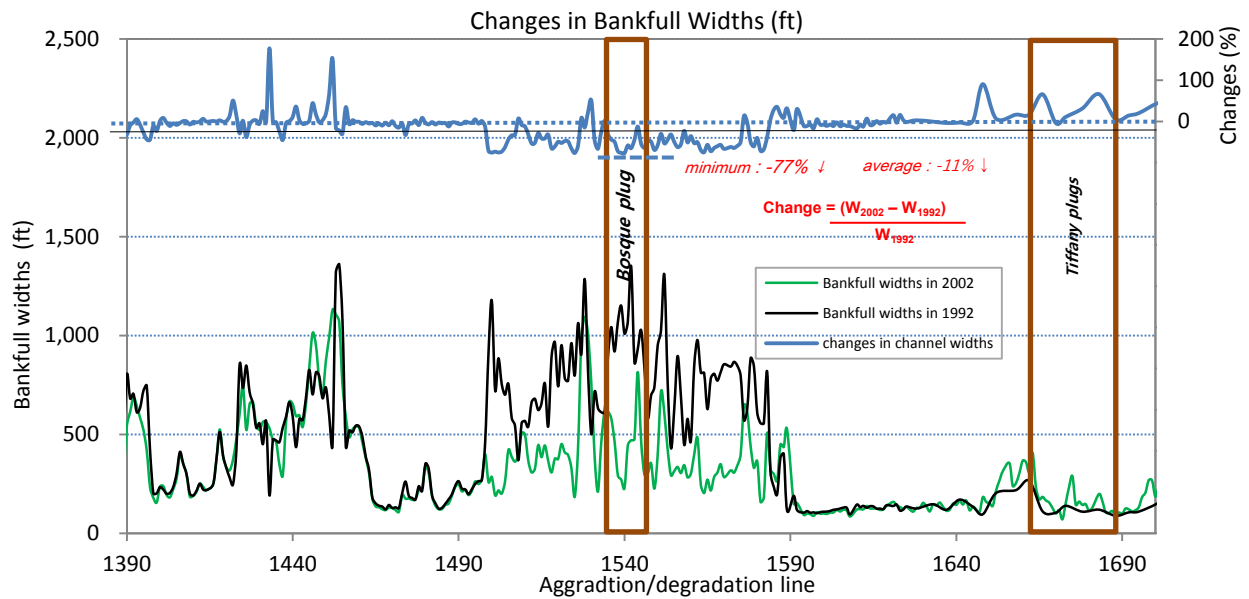


Figure 4.3. Changes in bankfull widths between 1992 and 2002

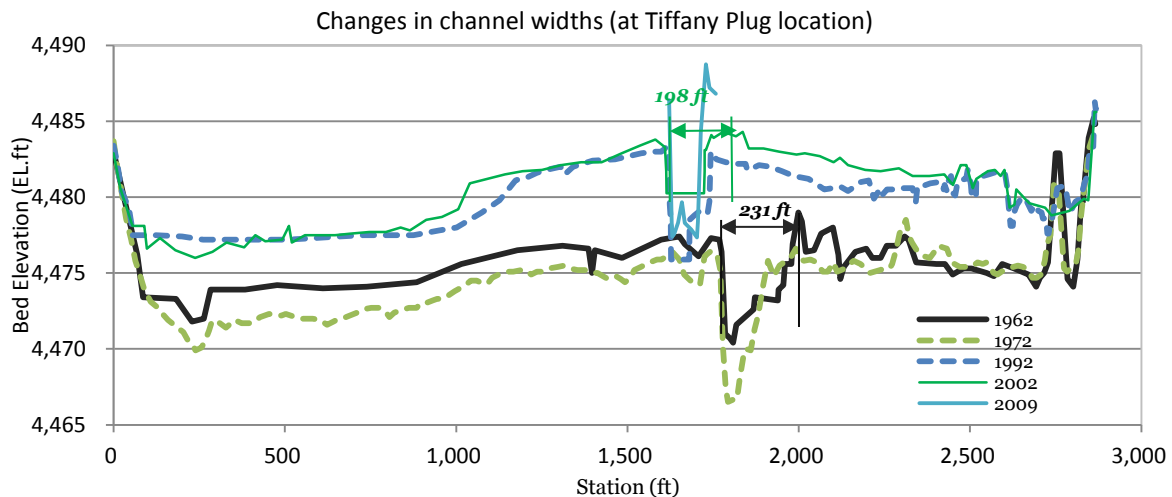


Figure 4.4. Changes in channel widths at the Tiffany plug location (Agg/Deg 1683)

4.1.2 Channel depths and perching

Channel depth is the height between the main channel bottom and bank crest. As the cross sections in the main channel were assumed to be rectangular in HEC-RAS model, the channel depth in this study was the hydraulic mean depth, which is defined by the area of the flow section divided by top width of the flow surface (Figure 4.5).

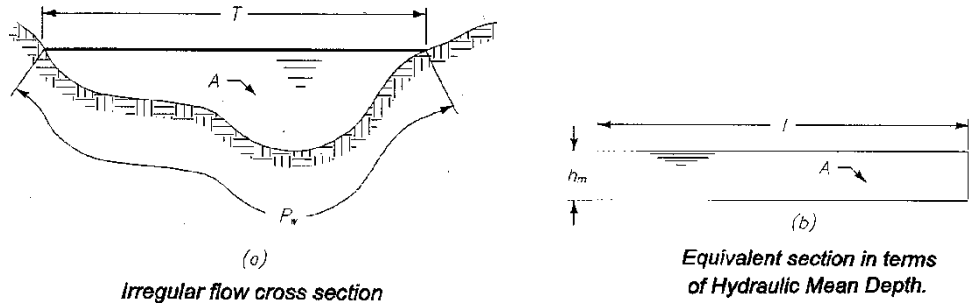


Figure 4.5. Hydraulic mean depth (USBR, 2001)

The channel depth has decreased 51% (Figure 4.6). The channel width also decreased 11% on average. Around the Bosque sediment plug location, average depths decreased 64%. On the other hand, the bank depths at the Tiffany plug location have increased over time.

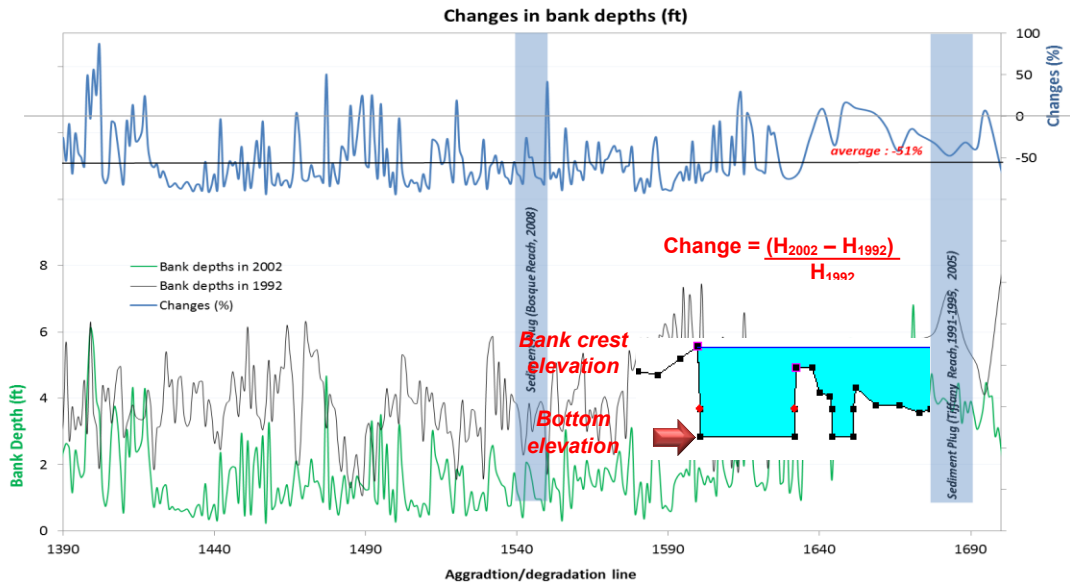


Figure 4.6. Changes in Bank Depths between 1992 and 2002

The changes in bed elevations between 1992 and 2002 (Figure 4.7) show that the average bed elevation has increased 3.7 ft and the bed elevation aggradation around the Bosque plug location was significant. Between Agg/Deg 1590 and Agg/Deg 1640, the aggradation was less.

This channel bed aggradation has resulted in a perched river in this downstream reaches of the Middle Rio Grande. A perched channel is obtained when the main channel bed elevation is higher than the floodplain elevation, thus leading to poor connectivity of flow and discharge. The difference between the channel bed elevation and the lowest elevation of the floodplain ranges from 0 to 2.5 ft in 1992 and from 0 to 8 ft in 2002. Figures 4.8 and 4.9 show that the perching ratios in the Bosque and Tiffany area were 13% in 1992 and 87% (a 74% increase) in 2002, respectively. The downstream sub-reaches have been perched more than the upstream sub-reaches. The Bosque Reach was perched by 1.5 ft, while the Tiffany plug reach was perched by 5 ft. From the observation of temporal changes of perching and channel aggradation, the relationship between the perching and sediment plug formation needs to be derived for application to the MRG plug formation.

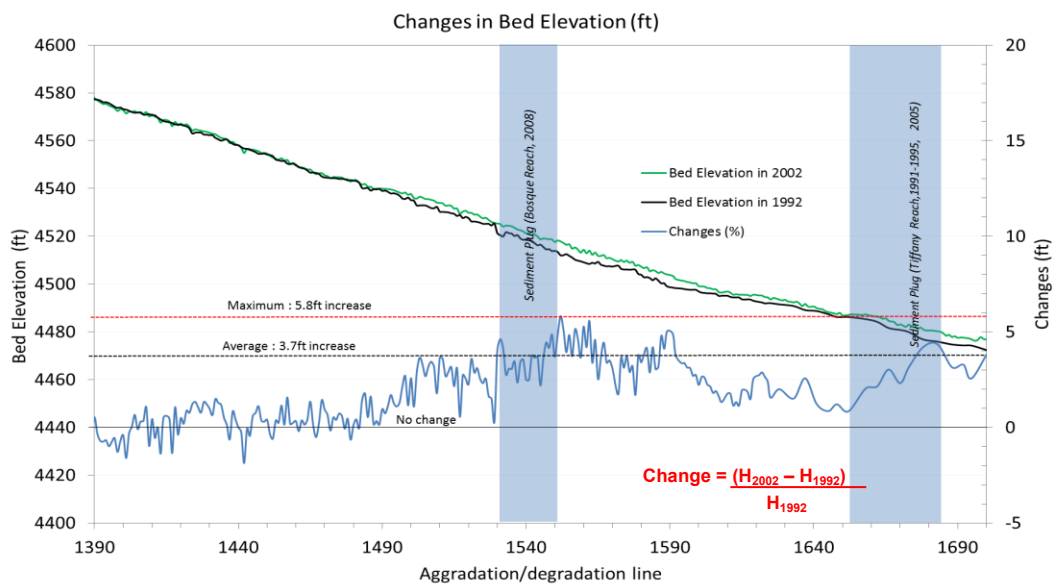


Figure 4.7. Changes in channel bed elevations between 1992 and 2002

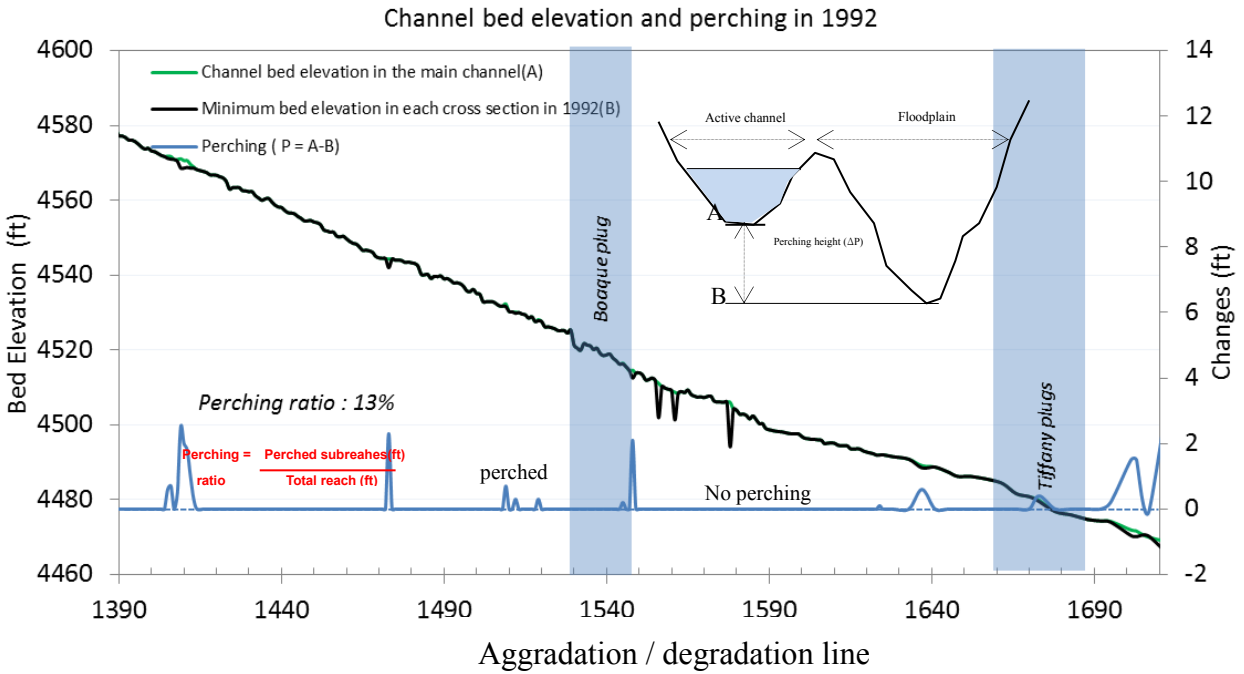


Figure 4.8. Channel bed elevation and perching in 1992

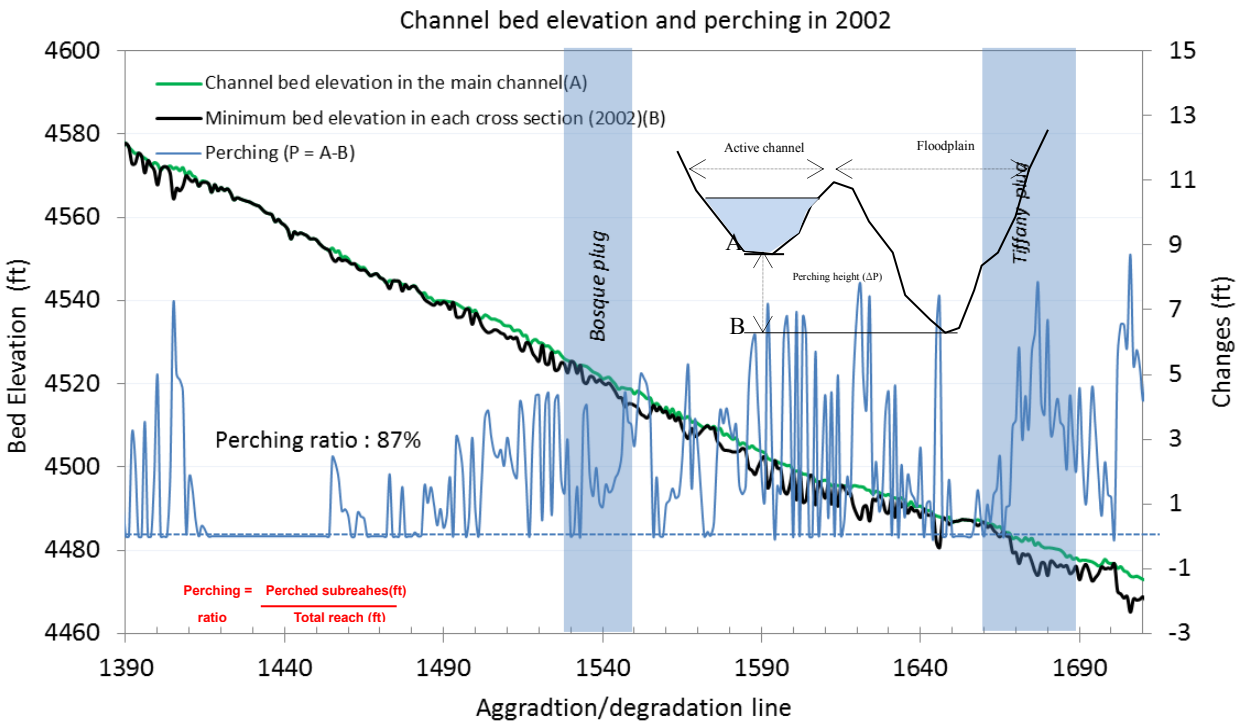


Figure 4.9. Channel bed elevation and perching in 2002

4.1.3 Longitudinal profiles

Figure 4.10 shows the historical sediment survey longitudinal profile, with reservoir sediment surveys completed in 1915, 1988, 1999, and 2007. There has been significant channel adjustment along the study reach. The downstream portion of this reach, including the reservoir area, generally has aggraded over time except for degradation during drought periods. The San Marcial Railroad Bridge (the Atchison, Topeka, and Santa Fe railroad) had to be raised three times after more than 25 ft of channel bed aggradation. In contrast, the upstream portion of the reach, especially just downstream of the San Acacia Diversion Dam, has degraded systematically due to impoverished sediment flows from upstream dams. The locations downstream from the dam have been degraded about 12 ft over the past three decades (Reclamation 2007). Meanwhile, the bed elevation around Arroyo de Las Canas has remained relatively stable at this point; thus, this location, which is a hinge point for this study reach, can be used as the upstream geometric boundary condition for the numerical simulation, which is described in Chapter 8.

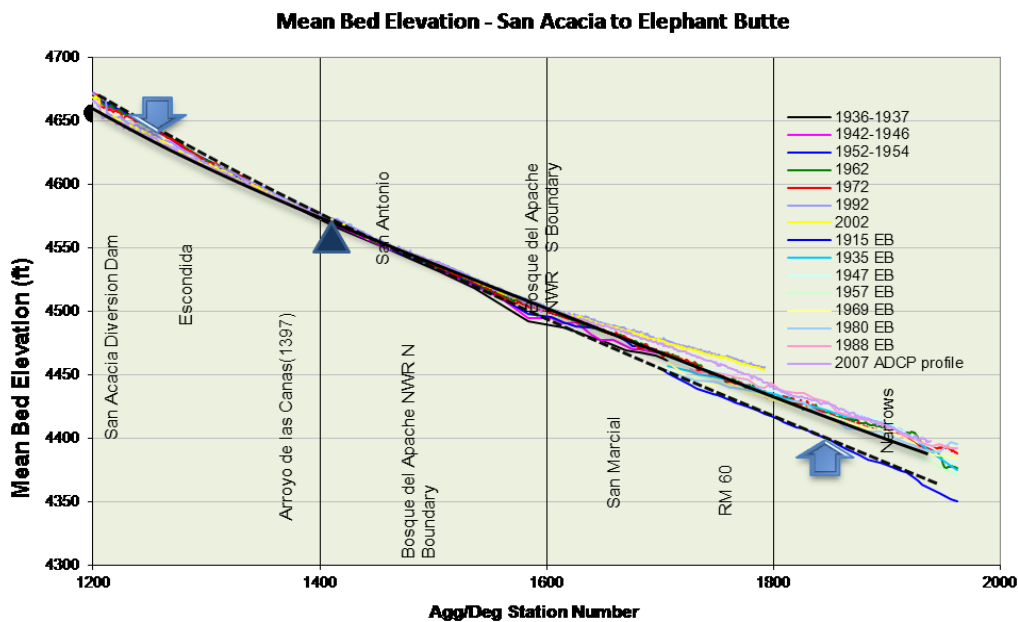


Figure 4.10. Longitudinal channel profile (Modified after Baird 2011, pers. Comm.)

4.1.4 Roughness

Channel roughness contributes to the highest uncertainty in hydraulic modeling results. In this study, a single roughness coefficient was used, representing the flow characteristics of the main channel and floodplain areas. For the evaluation of alternatives for the Rio Grande, a Manning n value of 0.017 was used for the main channel along the entire Tiffany Junction Reach based on previous estimates (Reclamation 2000). FLO Engineering (1995) computed a Manning n of 0.015-0.017 for cross-sections at the upstream portion of the Tiffany Junction Reach with data from 1993 and 1994 for flows ranging from 2,700 cfs to 5,400 cfs. In this study, the Manning n value provided by Reclamation was 0.017 ~ 0.024 in the main channel and 0.1 in floodplain areas (left and right overbank areas). Based on HEC-RAS data from combined cross section geometry, composite Manning n values for various flow-rates and flow years were computed (see Figure 4.11). The active channel width has not changed over time, but the representative Manning roughness has increased over time. Compared with 1992, channel roughness in 2002 increased 50%. For numerical simulation in Chapter 8, representative roughness of 0.027 was used.

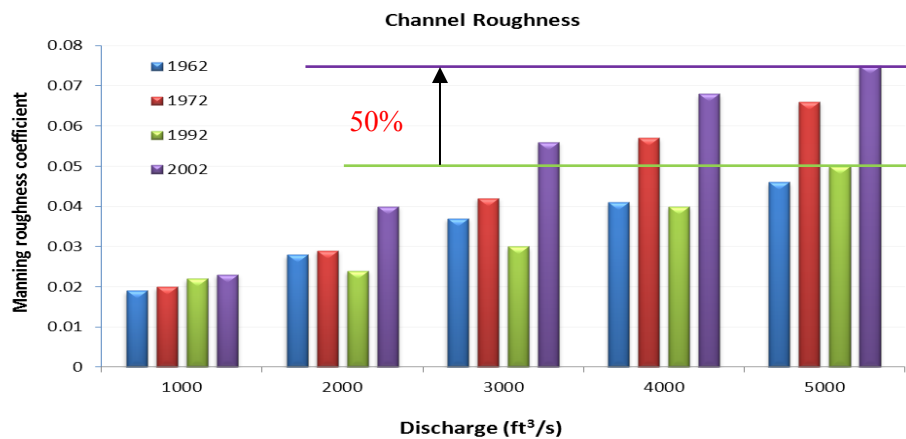


Figure 4.11. Composite channel roughness for various discharges (Park et al. 2011)

4.2 FLOW DATA

Mean daily discharges from the San Marcial gauge (USGS 08358400) and the San Acacia gauge (USGS 08354900) were used for flow discharges in 1995 and 2008 when sediment plugs occurred. Figure 4.12 shows an example hydrograph for the San Acacia and San Marcial gauges for the year 1999 to demonstrate typical double peaks of flow discharge on the Middle Rio Grande: The first peak occurs during snow melt periods between mid-May and the end of June, and the second peak occurs in August during the rainfall season. The four sediment plugs all occur from May to July, which is during the snowmelt season.

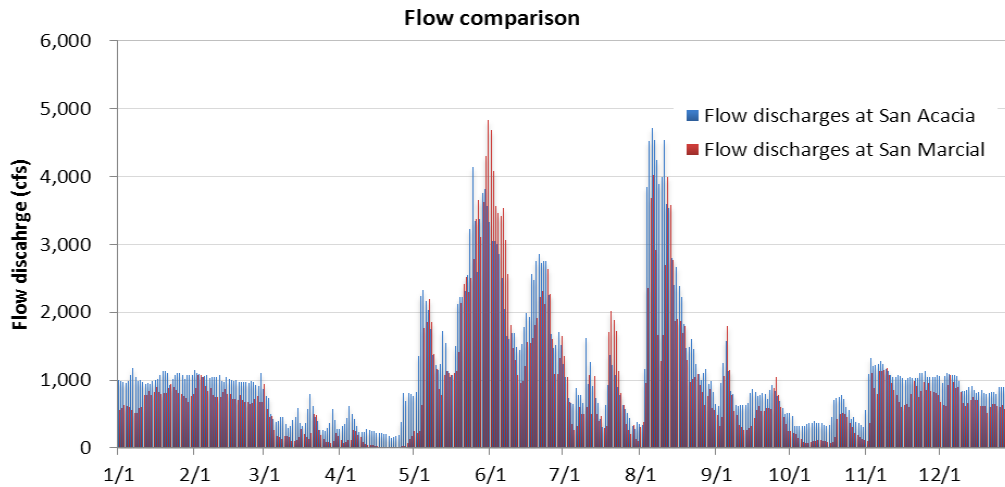


Figure 4.12. Flow discharges in 1999

Figures 4.13 and 4.14 show flow discharges of San Acacia and San Marcial gauges in 1995 and 2008. Although there is no specific information associated with the timing of sediment plugs, reference documents showed that the channel was clogged over only several weeks. Therefore, based on the time when the sediment plugs were detected, about 1 month may be the duration of sedimentation. Comparison between San Acacia and San Marcial flow discharges showed a 13-20% water loss.

This average monthly flow loss was used to determine the weir coefficients of the broad-crested weir equation when considering water losses to overbank areas during floods.

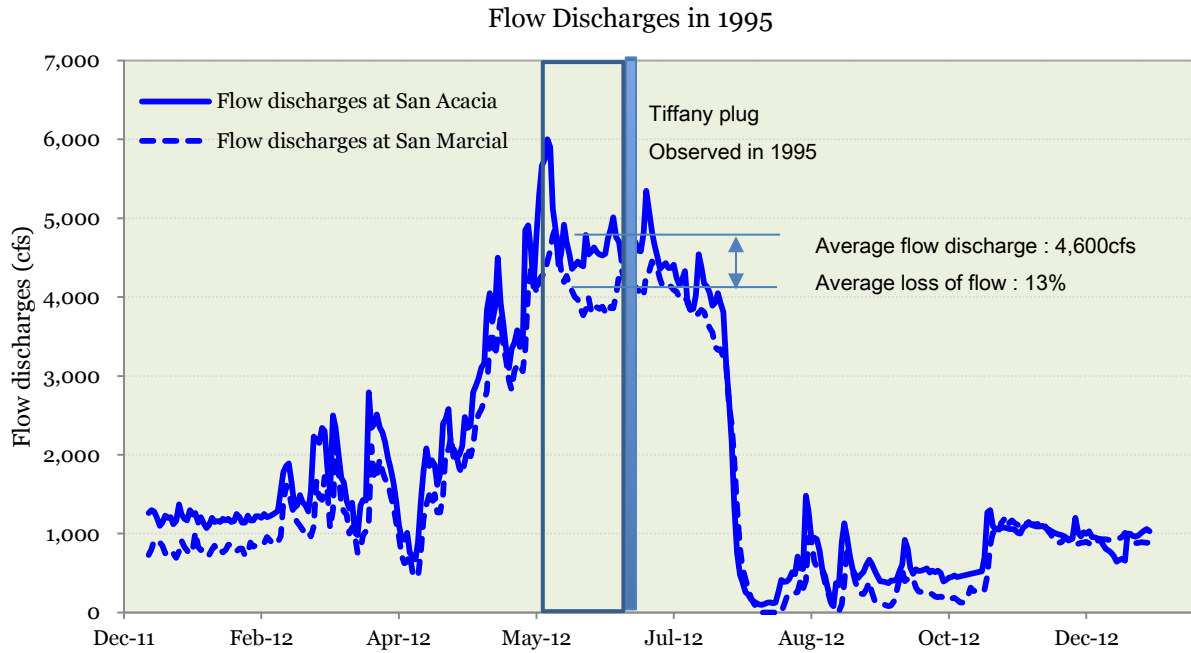


Figure 4.13. Flow discharges in 1995

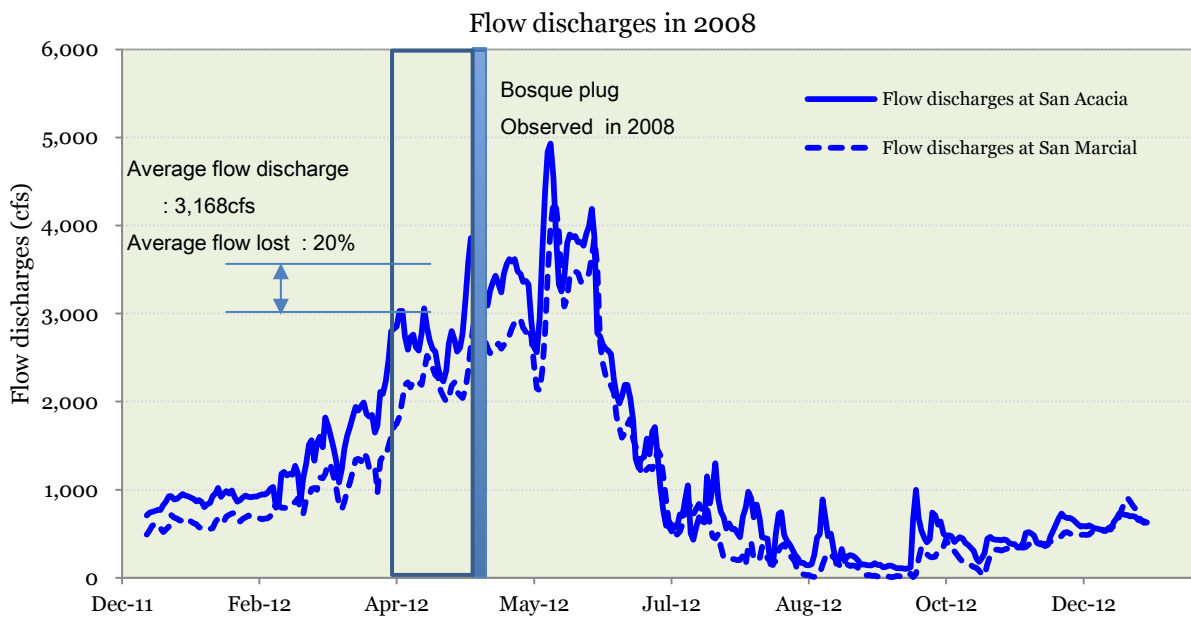


Figure 4.14. Flow discharges in 2008

4.3 SEDIMENT DATA

4.3.1 Particle size

The bed material grain size distributions at San Acacia and San Marcial gauges were plotted to study general trends in bed material grain size along the channel and over time. Figure 4.15 shows the grain size analyses from the Bosque Reach report (Paris et al. 2011) and Elephant Butte Reach report (Owen et al. 2011). Grain size distributions were plotted and median diameters of the bed material were determined for each sub-reach. Moving in the downstream direction, sediment tends to be finer (Figure 4.15). With time, the bed sediment has coarsened (Figure 4.16). The overall median diameter was 0.2 mm in 1992 to 0.23 mm in 2002.

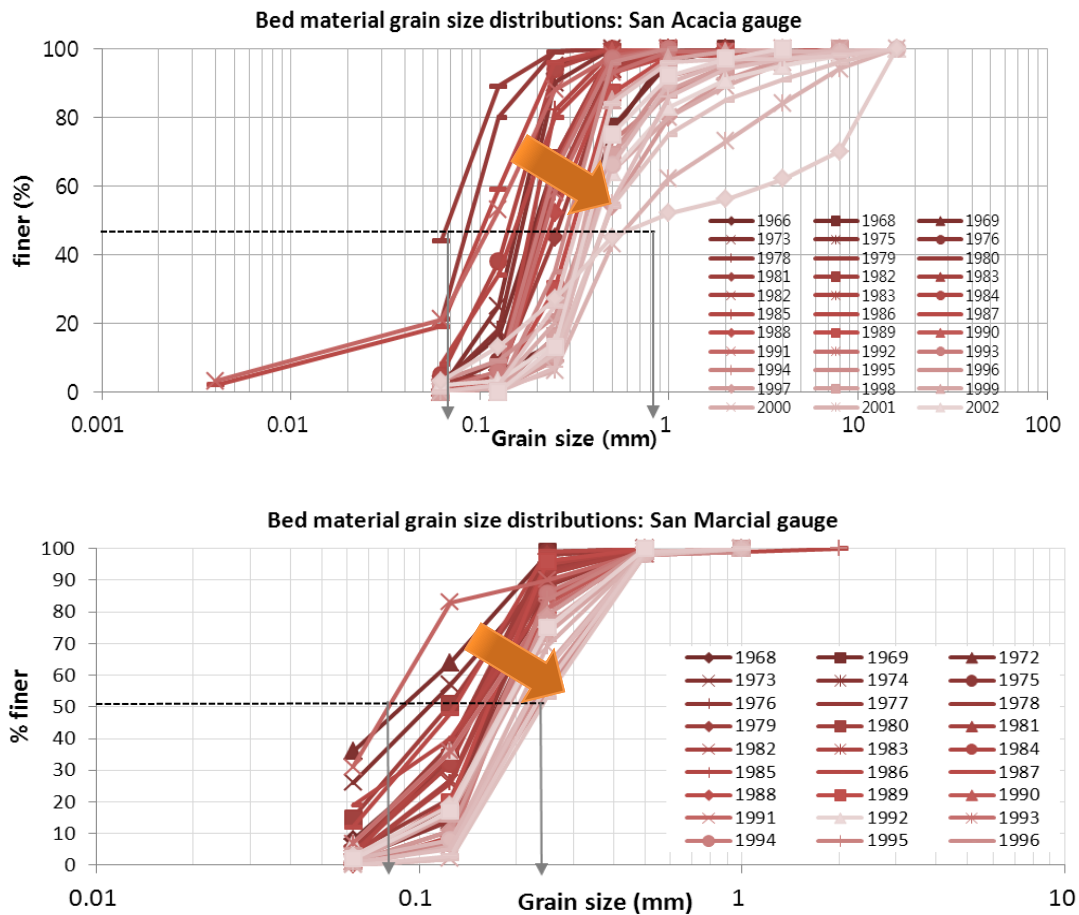


Figure 4.15. Sediment particle size distribution at San Acacia and San Marcial

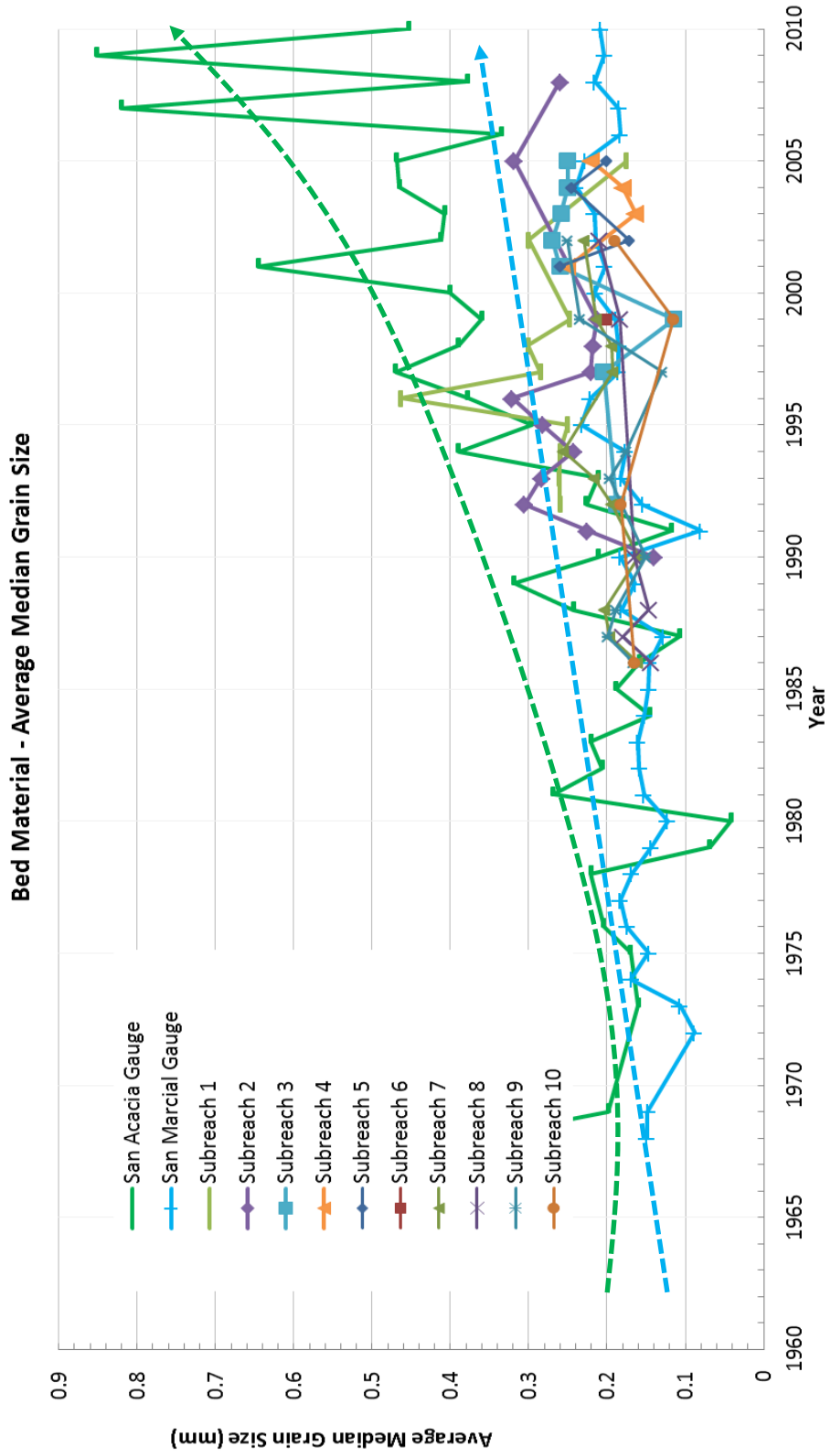


Figure 4.16. Median grain diameter

Figures 4.17 and 4.18 show the sediment size distributions at various times in a year in order to investigate the seasonal changes in sediment size. There is a clear difference between San Acacia and San Marcial in sediment size, but no significant relations between the seasonal sediment size and sediment plug formation.

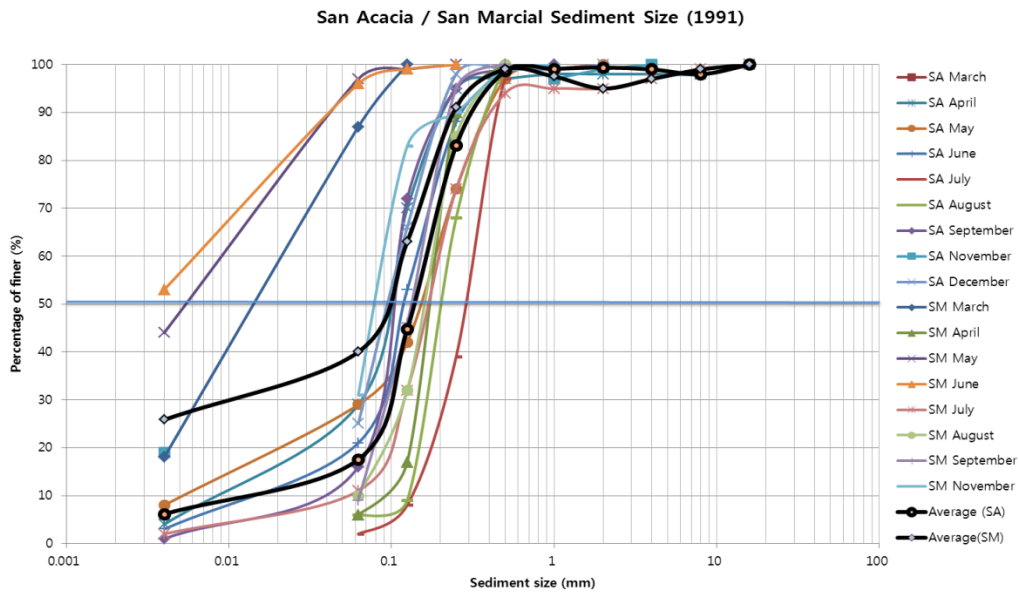


Figure 4.17. Seasonal changes in sediment sizes in 1991

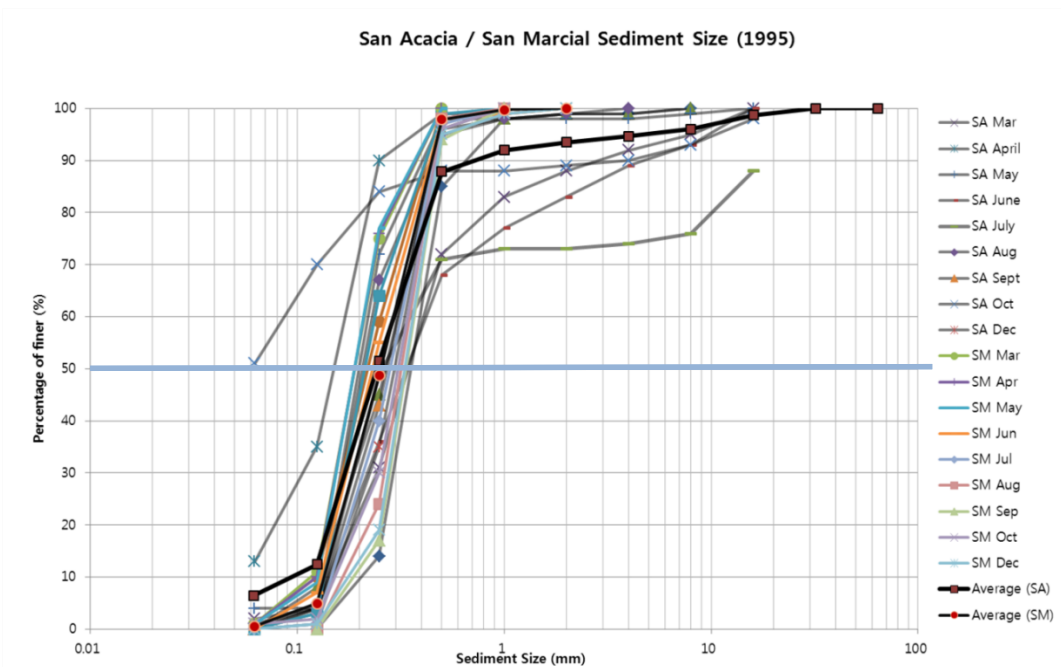


Figure 4.18. Seasonal changes in sediment sizes in 1995

4.3.2 Settling velocity

Settling velocity is the one of key parameters to decide the sediment concentration and transport capacity, thus settling velocity for each grain size was determined using the following equation (Julien 2010).

$$\text{Settling velocity } \omega = \frac{8v_m}{d_s} [(1 + 0.0139d_*^3)^{0.5} - 1]$$

where v_m is the kinematic viscosity of sediment mixture (m^2/s), d_s is the median sediment diameter, $d_* = d_s \left[\frac{(G-1)g}{v^2} \right]^{1/3}$ is the dimensionless sediment diameter.

The kinematic viscosity can be expressed as a function of temperature as:

$$v = \frac{1.78 \times 10^{-6} m^2/s}{[1 + 0.0337T_c^o + 0.0002217T_c^{o2}]}$$

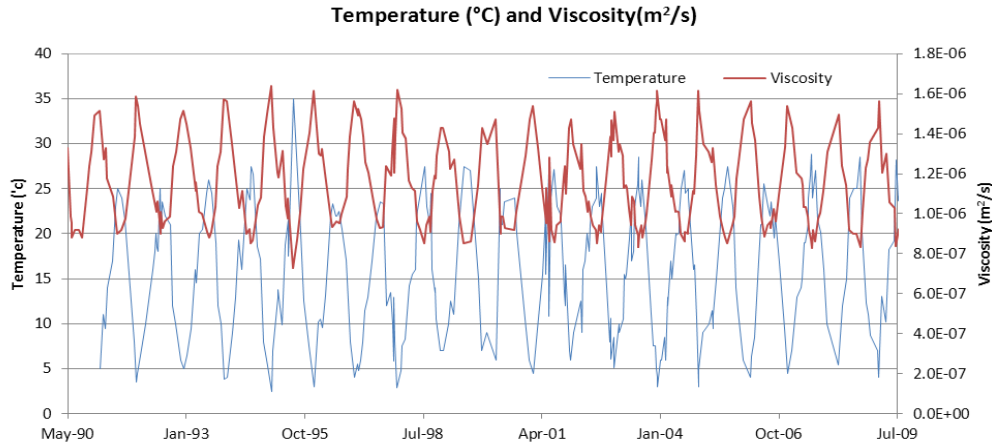


Figure 4.19. Water temperature and viscosity

Water temperature ranges 3 to 35 degrees Celsius around a year: 25 degrees Celsius during Tiffany plug and 23 degrees Celsius during Bosque plug (Figure 4.19). Settling velocity ranges 0.01m/s to 0.05 m/s and average value 0.027m/s and 0.034m/s were used for Tiffany plug and Bosque plug simulations, respectively (Table 4.1).

Table 4.1. Settling velocity (m/s)

Sub-reach	1992	2002
1 (SO 1414)	0.040	0.046
2 (SO 1471)	0.034	0.040
3 (SO 1573)	0.018	0.034
4 (SO 1613)	0.015	0.024
5 (SO 1641)	0.046	0.037
6 (SO 1683)	0.027	0.027
7 (EB-10)	0.034	0.040
8 (EB-13)	0.027	0.034
9 (EB-18)	0.009	0.015
10 (EB-24)	0.024	0.030
Overall	0.027	0.034

4.3.3 Sediment transport capacity

In practice, there are two approaches for determining sediment transport capacity. The first is to develop a sediment rating curve (relationship between flow and sediment discharge) based on sediment transport measurements in the field. The second, which was utilized in this study, is to compute sediment transport capacity using published sediment transport equations. Sediment transport capacity was calculated using Yang's equation (2005, 2007) and Julien's equations based on hydraulic characteristics for the two major reaches (Bosque, Elephant Butte), and 10 sub-reaches. Yang's and Julien's equations are as follows:

- Yang's method (for sand)

$$\begin{aligned} \log C_{ppm} = & 5.435 - 0.286 \log \frac{\omega d_s}{v} - 0.457 \log \frac{u^*}{\omega} + (1.799 - 0.409 \log \frac{\omega d_s}{v} \\ & - 0.314 \log \frac{u^*}{\omega}) \log \left(\frac{V_c}{\omega} - \frac{V_c S}{\omega} \right) \end{aligned} \quad (4.1)$$

$$\text{Where } \frac{V_c}{\omega} = \frac{2.5}{[\log(\frac{u^* d_s}{v}) - 0.06]} + 0.66 \text{ for } 1.2 < \frac{u^* d_s}{v} < 70 \quad (4.2a)$$

$$\frac{V_c}{\omega} = 2.05 \text{ for } \frac{u^* d_s}{v} \geq 70 \quad (4.2b)$$

- Julien's method

$$Q_{bv} = 18W \sqrt{gd_s^3 \tau_*^2} \quad \text{for } 0.1 < \tau_* < 1 \quad (4.3)$$

where V, V_c : mean and critical velocity (m/s)
 Ω : settling velocity (m/s)
 d_s : sediment median diameter (m)
 ν : kinematic viscosity (m^2/s)
 u_* : shear velocity ($=\sqrt{gR_hS}$, ft/s)
 R_h : hydraulic radius (m)
 S : channel slope (m/m)
 G : specific gravity ($=2.65$)
 τ_* : Shields parameter ($=\frac{R_h S}{(G-1)d_s}$)

Sediment Transport Capacity for Sub-reaches

Sediment transport capacity was computed for ten sub-reaches (four sub-reaches for the Bosque Reach and six sub-reaches for the Elephant Butte Reach). In the Bosque Reach, 5,000 cfs ($141 m^3/s$) was used as a bank-full discharge. Sub-reach 3, where the sediment plug formed, had the lowest sediment transport capacity among the four sub-reaches in Bosque Reach (Figure 4.20). This means that the sediment supply from the upstream sub-reach exceeds the transport capacity downstream, leading to sediment deposits at sub-reach 3.

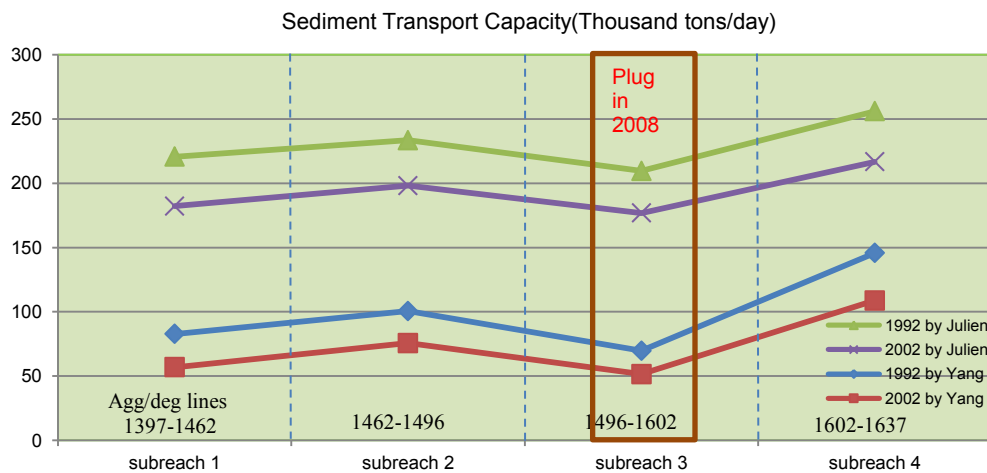


Figure 4.20. Sediment transport capacity of sub-reaches in the Bosque Reach

Similarly, the sediment transport capacity was calculated for Elephant Butte Reach using 2,000 cfs as bank-full discharge. Compared with the Bosque Reach, overall sediment transport capacity was lower due to the milder slope, and lower discharge (Figure 4.21). The trend of low transport capacity in the location where sediment plugs formed is not as significant as in the Bosque Reach. While the location of the Bosque plug relates highly to the change in sediment transport capacity, the location of the Tiffany plugs may be related to other factors, such as fluctuations in reservoir levels. The decrease in sediment transport capacity over time is likely due to an increase in bank-full width.

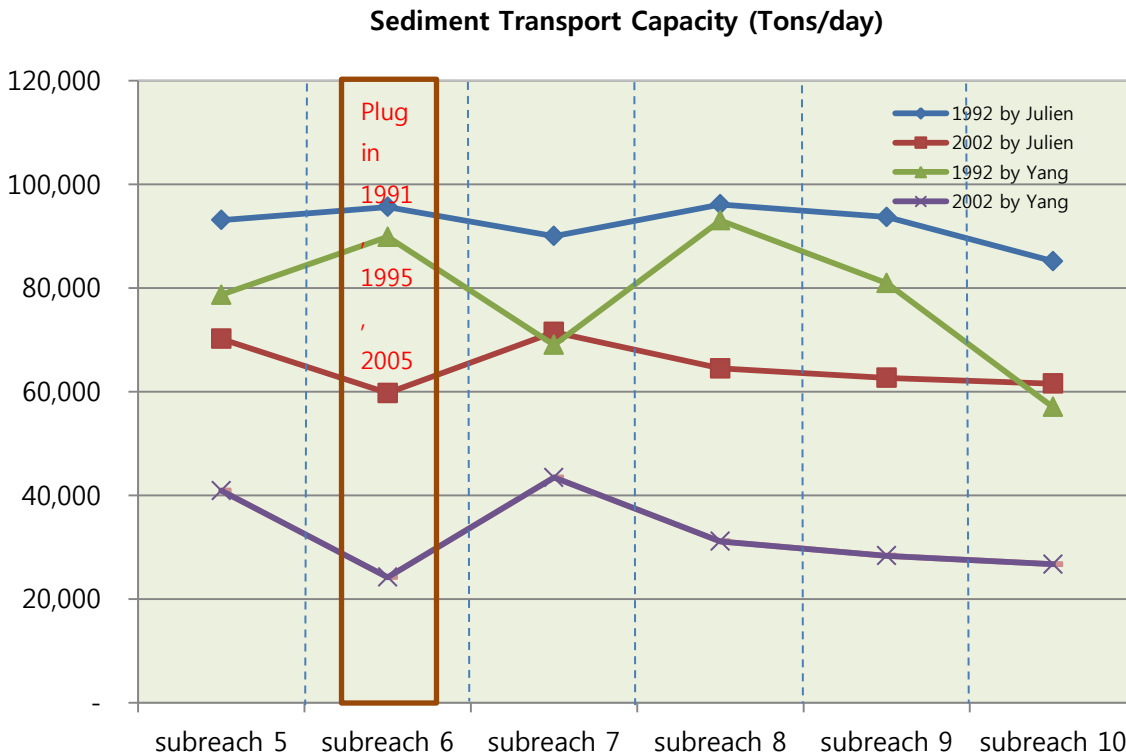


Figure 4.21. Sediment transport capacity of sub-reaches in the Elephant Butte Reach

4.4 PLUG CAUSING FACTORS

Numerous parameters can be identified based on the sediment plug observations. Possibly a theory may be proposed to describe the sediment plug development. Based on understanding of the basic characteristics of the MRG with respect to erosion and sedimentation, seven dominant factors sketched in Figure 4.22 are proposed and investigated in chapters 5, 6, and 7: (1) variability of channel widths; (2) roughness; (3) perching / overbank flows; (4) concentration profiles; (5) backwater effect from reservoir; (6) backwater effect from bridge; and (7) backwater from sharp bends. Basic equations and conceptual modeling provide the information as to whether the channel characteristic has effect on the channel bed aggradation and plug formation as the worst case.

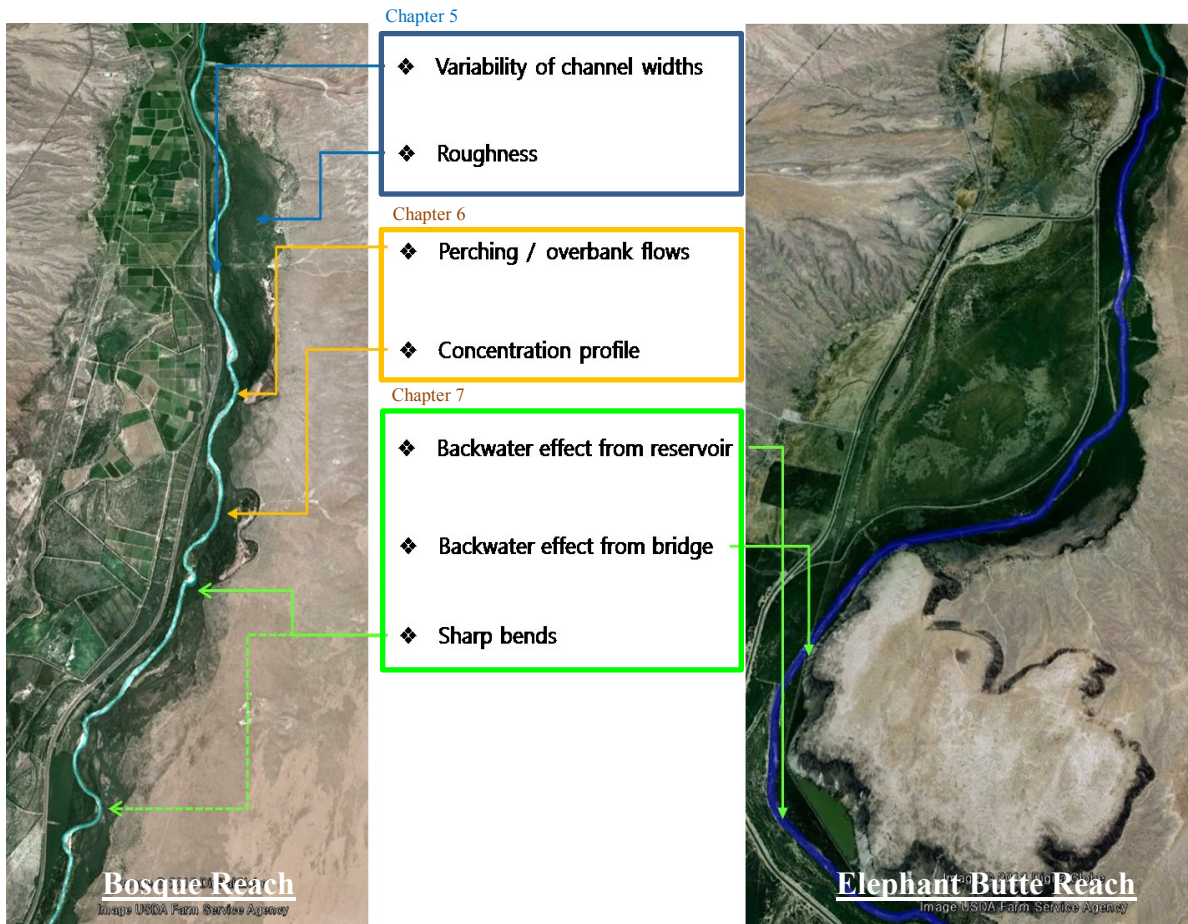


Figure 4.22. Seven major possible factors causing sediment plug formation

CHAPTER 5 GEOMETRIC FACTORS

In this chapter, geometric factors causing a sediment plug are presented. Two analytical relationships with respect to the variability in channel width and application to the MRG are described in Section 5.1. The resistance to flow (Section 5.2) includes various changes in roughness resulting from channel narrowing and vegetation encroachment.

5.1 CHANNEL WIDTHS

The relationships of active channel width, and width-depth ratio with sediment transport capacity were derived and applied to the Bosque and Elephant Butte Reaches. Two connected channel reaches with different widths and different sediment discharges are depicted in Figure 5.1.

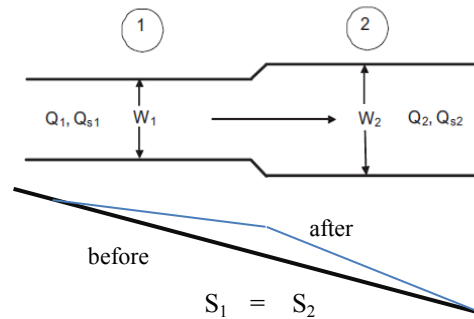


Figure 5.1. Water and sediment balance for different widths

In order to derive the relationship between the change in channel width and sediment discharge, three equations were used: continuity, roughness, and sediment transport equations.

- Continuity equation : $Q = V A$ (5.1)

- Flow resistance equation : $V = 1.49/n R_h^{2/3} S^{1/2}$ (5.2)

- Sediment discharge equation : $Q_s = 18Wg^{0.5} d_s^{3/2} \tau_*^2$, $\tau_* = \frac{R_h S}{(G-1)d_s}$ (5.3)

5.1.1 Relationship between width and sediment discharge

A simplified analytical solution can be found if the hydraulic radius is approximate to the flow depth (i.e., only for large widths, $R_h \approx h$). Replacing the resistance equation with the discharge equation and approximating R_h to the flow depth h gives

$$Q = Wh \frac{1}{n} h^{\frac{2}{3}} S^{\frac{1}{2}} = W \frac{1}{n} h^{\frac{5}{3}} S^{\frac{1}{2}} \quad (5.4)$$

To satisfy the mass balance between 1 and 2 sections,

$$\frac{Q_2}{Q_1} = \frac{W_2 n_1 h_2^{\frac{5}{3}} S_2^{\frac{1}{2}}}{W_1 n_2 h_1^{\frac{5}{3}} S_1^{\frac{1}{2}}} = W_r h_r^{\frac{5}{3}} = 1, \quad h_r = W_r^{-\frac{3}{5}} \quad (5.5)$$

where W_r = ratio of the widths, h_r = ratio of the flow depths

Repeating the procedure for sediment load with $R_h \approx h$, a fixed grain size, and specific gravity, the sediment discharge ratio can be described as

$$\frac{Q_{s2}}{Q_{s1}} = \frac{W_2 h_2^2 S_2^2}{W_1 h_1^2 S_1^2} = W_r h_r^2 = Q_{sr} \quad (5.6)$$

Substituting equation 5.5 for equation 5.6,

$$Q_{sr} = W_r \times \left(W_r^{-\frac{3}{5}} \right)^2 = W_r^{-0.2} \quad (5.7)$$

Therefore, from this simplified relationship, the increase of a channel width causes the decrease of sediment transport with power of -0.2.

5.1.2 Relationship between width/depth ratio and sediment discharge

When the hydraulic radius is not approximated to the flow depth ($R_h = \frac{Wh}{W+2h}$), from León (2003), the sediment discharge can be expressed as

$$Q_s = 18g^{\frac{1}{2}}d_s^{\frac{3}{2}} \left[\frac{Q^{\frac{3}{8}}n^{\frac{3}{8}}}{S^{\frac{3}{16}}\phi^{\frac{3}{8}}} (\xi + 2)^{\frac{1}{4}\xi^{\frac{3}{8}}} \right] \frac{S^2}{(G - 1)^2 d_s^2} \frac{\xi^2}{(\xi + 2)^2} \left[\frac{Q^{\frac{6}{8}}n^{\frac{6}{8}} (\xi + 2)^{\frac{1}{2}}}{S^{\frac{6}{16}}\phi^{\frac{6}{8}} \xi^{\frac{5}{4}}} \right] \quad (5.8)$$

Where ξ : width-depth ratio, ϕ : 1.49 for English units and 1 for metric units.

Assuming gravitational acceleration, sediment size, discharge, and channel slope are constant at two cross sections, Equation 5.8 can be simplified as

$$Q_s \sim \left[(\xi + 2)^{1/4} \xi^{3/8} \right] \frac{\xi^2}{(\xi + 2)^2} \left[\frac{(\xi + 2)^{1/2}}{\xi^{5/4}} \right] = (\xi + 2)^{\frac{1}{4}-2+\frac{1}{2}} \xi^{\frac{3}{8}+2-\frac{5}{4}} = \frac{\xi^{9/8}}{(\xi + 2)^{5/4}} \quad (5.9)$$

Taking the derivative of this equation with respect to ξ and equating it to zero,

$$\frac{dQ_s}{d\xi} \sim \frac{\frac{9}{8} \xi^{1/8} (\xi + 2)^{5/4} - \xi^{9/8} (\frac{5}{4}) (\xi + 2)^{1/4}}{(\xi + 2)^{10/4}} = 0 \quad \rightarrow \quad \xi = 18 \quad (5.10)$$

Therefore, the maximum sediment transport capacity from Equation 5.8 is at a width-depth ratio $\xi = 18$, and decreases with the power of -0.125 when ξ is much larger than 18.

5.1.3 Application to the Middle Rio Grande

5.1.3.1 Sediment Transport Capacity for the Bosque Reach

Applying the two analytical relationships to the MRG, sediment transport capacity decreases as width or width/depth ratio increases for the range of practical widths within the reach (see Figures 5.2 and 5.3). Sediment transport capacity decreases below the optimum width at a slope of -0.2. Although the values of the transport capacity are different, the transport capacity in 2002 was lower than in 1992, commonly in Yang's and Julien's equations.

This decrease of sediment transport capacity may have contributed to sediment plug formation in 2008.

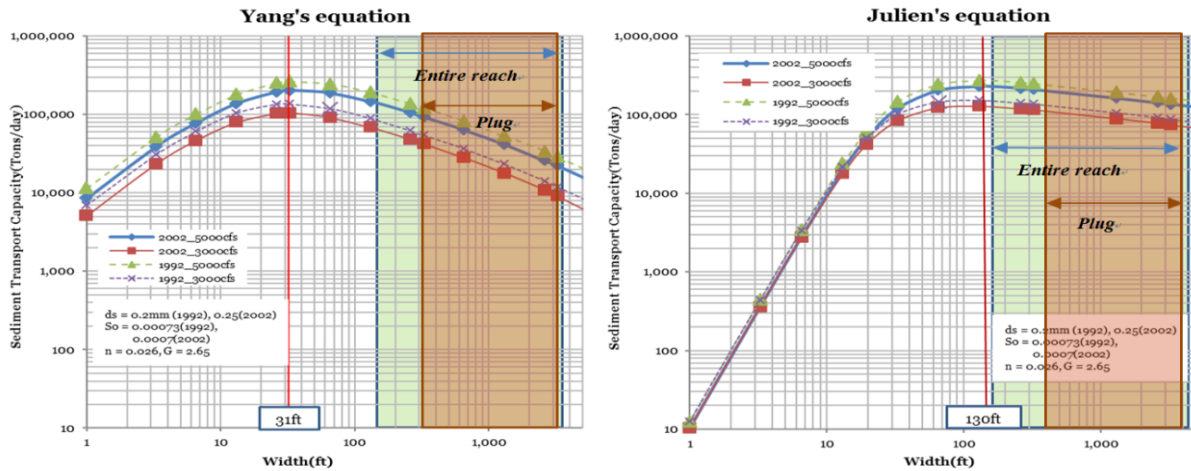


Figure 5.2. Sediment transport capacity for various widths of the Bosque Reach

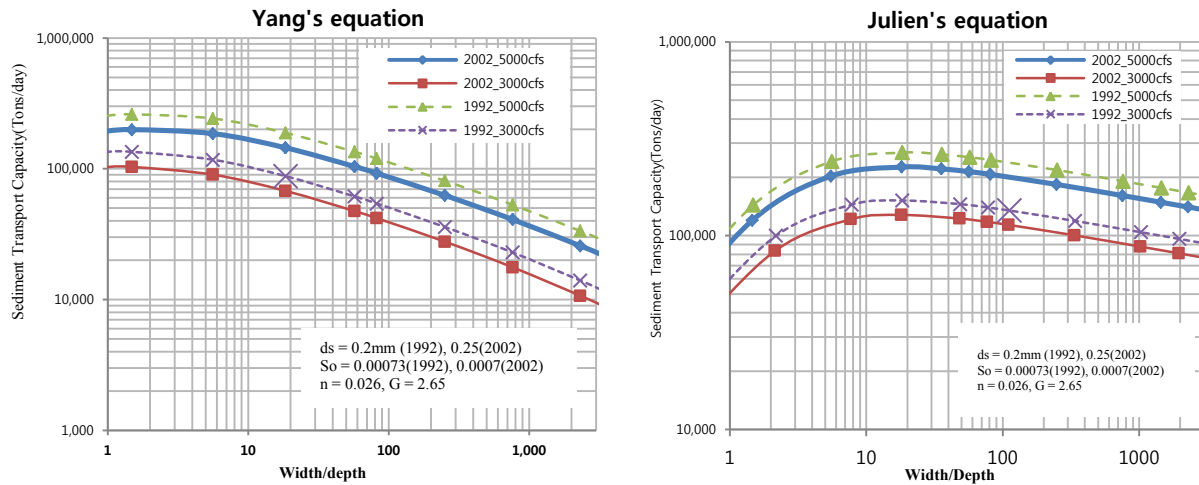


Figure 5.3. Sediment transport capacity for various width/depth ratios of Bosque Reach

5.1.3.2 Sediment Transport Capacity for the Elephant Butte Reach

Although the magnitude of sediment transport is slightly lower than that of the Bosque Reach due to a milder slope and lower flow velocity, the trend of the sediment transport capacity curve is similar. In both cases, sediment transport capacity decreases as width increases for the range of practical channel widths, which are in the green shadowed area for the entire reach and in the orange shadowed area for the historic plug location. Also, transport capacity was greater in 1992 than in 2002 for both reaches as a result of having milder slope.

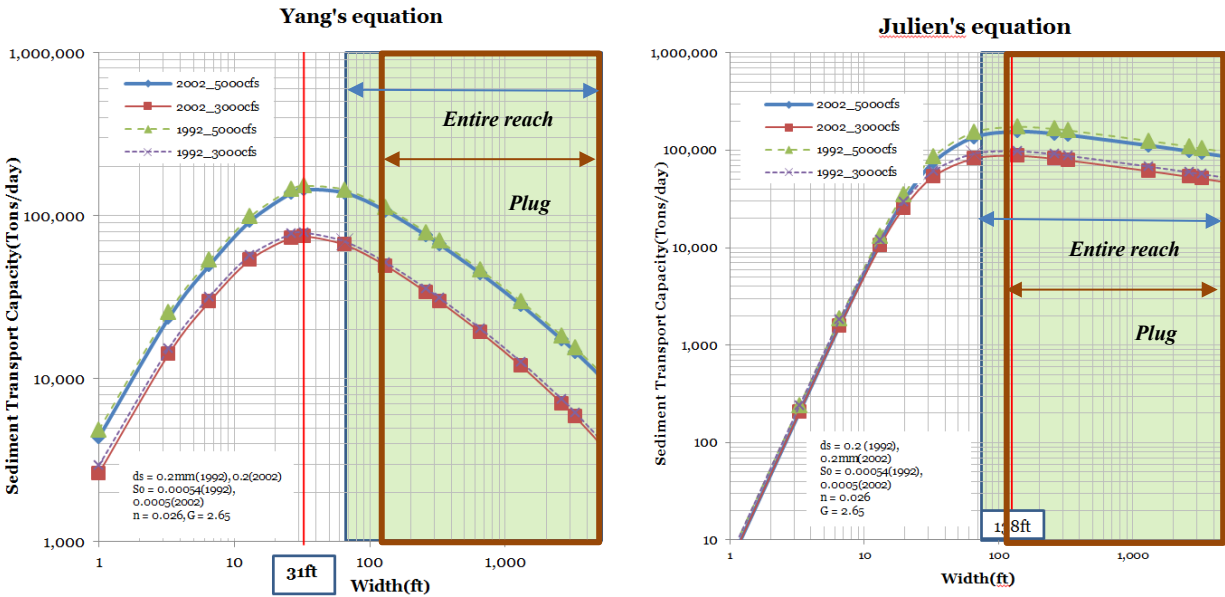


Figure 5.4. Sediment transport capacity of the Elephant Butte Reach

5.1.3.3 Sediment Transport Capacity for cross sections

In order to evaluate the effect of variability of channel widths for practical channel widths on channel bed elevation, 1992 and 2002 channel widths and bed elevation were compared in Figure 5.5. This comparison shows that a wider section causes the decrease of channel bed elevation, which is opposite to expectations. However, width/depth ratio and change in channel bed elevation (Figure 5.6) have reasonable relationships. Therefore, even though the change in channel bed depends on the variability of channel widths at a given moment, temporal changes in bed elevation have a closer association with width/depth ratio in the downstream river in the Middle Rio Grande. At the cross section with higher width/depth ratio, sediments tend to deposit on the channel bed. The variability of channel widths is a major causal factor of the change in channel bed elevation at low flows below bankfull discharges. But, at high discharges, the change in the channel bed elevation is influenced by other parameters.

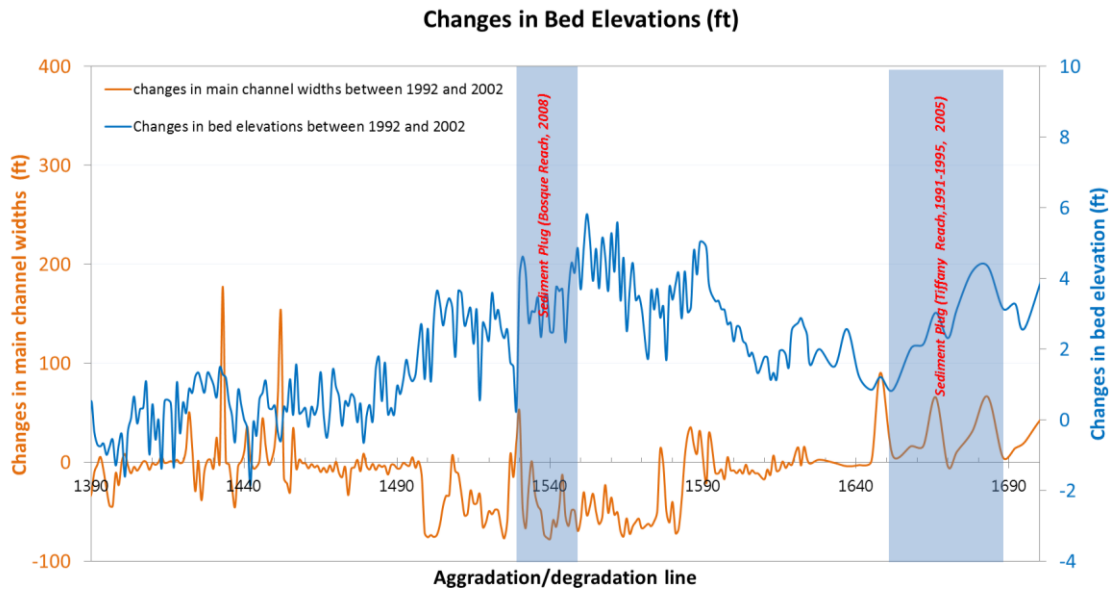


Figure 5.5. Changes in bed elevations and in active channel widths between 1992 and 2002

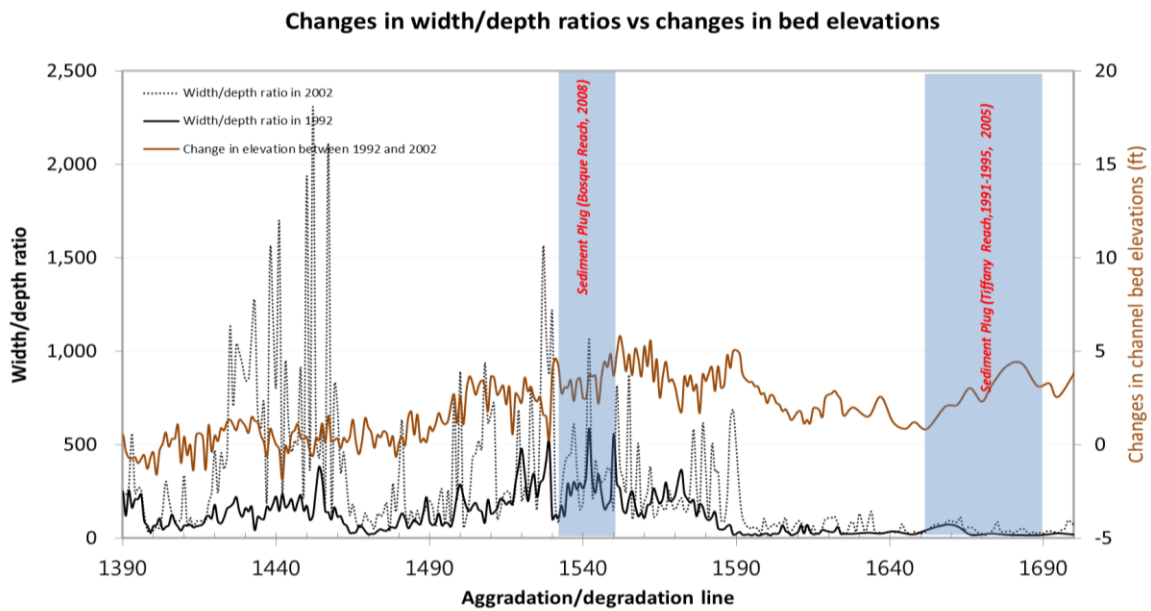


Figure 5.6. Changes in bed elevation and width/depth ratios between 1992 and 2002

5.2 ROUGHNESS

Roughness coefficients represent resistance to flow in a cross section for both the main channel and floodplains. An increase in the roughness causes a decrease in flow velocity, resulting in a decrease in transport capacity and sedimentation on the bed floor. A narrowing of the conveyance channel and widening of the overbank areas over time increase flow resistance and sediment deposition. Figure 5.7 shows a typical channel cross section, including a main stream and left- and right-floodplains with different roughness coefficients.

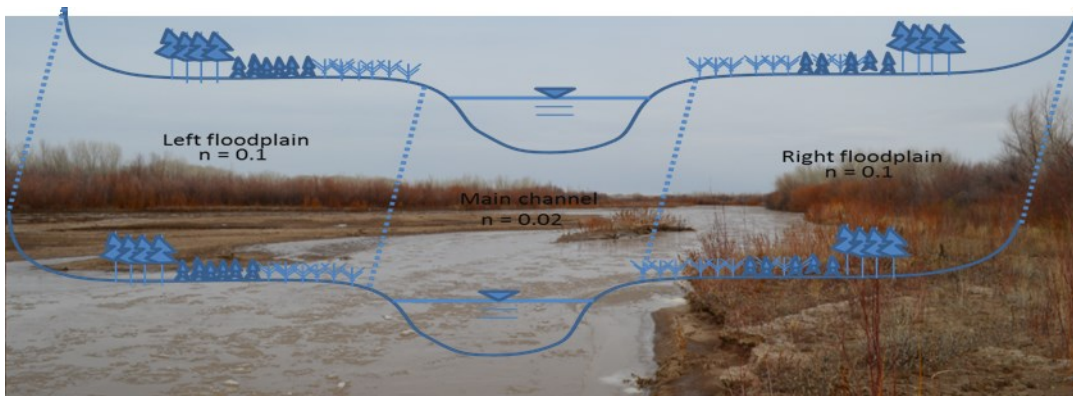


Figure 5.7. A cross section with different roughness coefficients (at Agg/Deg 1531)

In order to assess the roughness effect on sediment transport capacity, three basic conditions can be used in this analysis: (1) continuity of flow: $Q = AV = WhV$; (2) resistance

equation: $v = \frac{Q}{n} R_h^{2/3} S^{1/2}$; and (3) sediment transport capacity: $Q_s = 18W \sqrt{g} d_s^{3/2} \left(\frac{R_h S}{(G-1)d_s} \right)^2$.

5.2.1 Increase in roughness

Figure 5.8 shows the flow depth calculation based on a discharge of 5,000 cfs, a Manning's roughness coefficient of 0.02 in the main channel and 0.1 on floodplains, and a channel slope of 0.0007. The 10% roughness increase in the main channel causes an 8% increase in flow depth, while a 10% roughness increase on both floodplains causes a 1% increase in flow

depth. A 10% roughness increase in the main channel reduces the flow discharge by 2.4%, while a 10% roughness increase on the floodplains increases the flow discharge of the main channel by 1.5%.

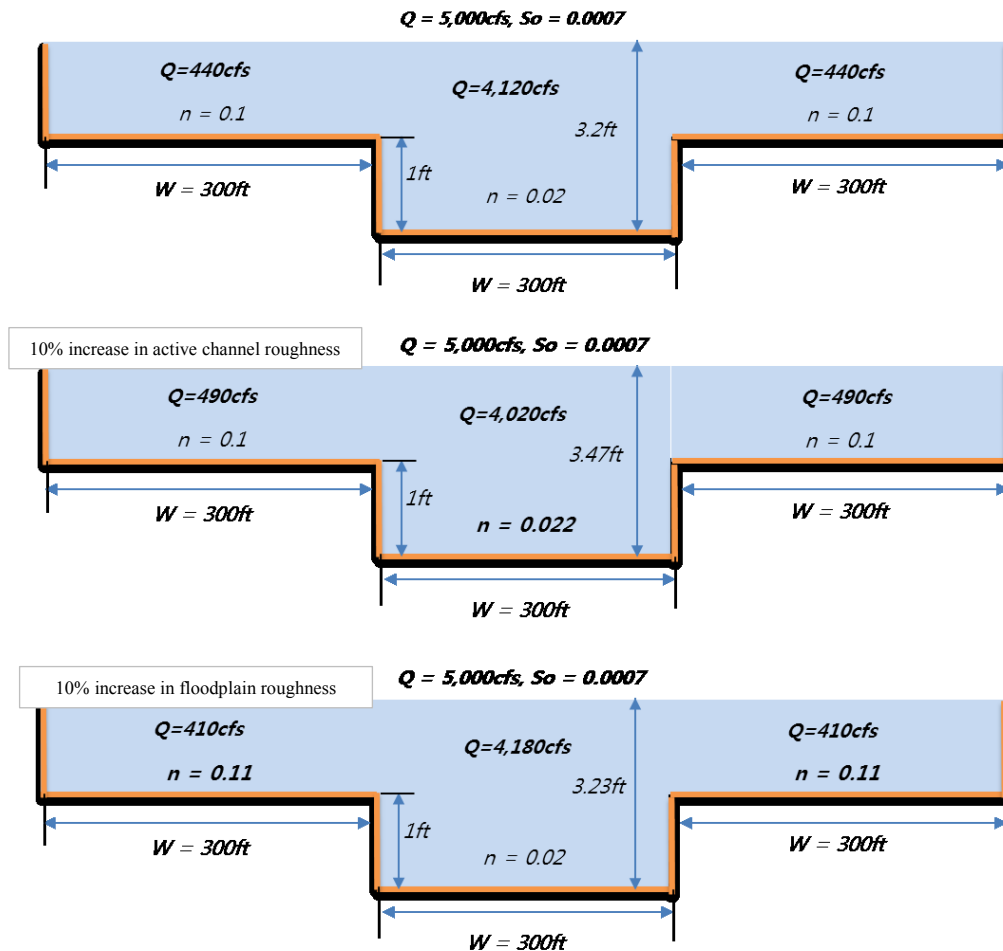


Figure 5.8. Roughness effects on water depth and flow discharge

5.2.2 Vegetation encroachment without channel narrowing

A vegetation encroachment toward the active channel without channel narrowing (e.g., non-flood season) accelerates changes in the flow depths and flow discharges. Figure 5.9 illustrates the effect of a 10% and 20% vegetation encroachment from the left- and right-overbank area toward the active channel, which cause 3% and 9% increase in water depth and 4% and 4.7% decrease of flow velocity, respectively.

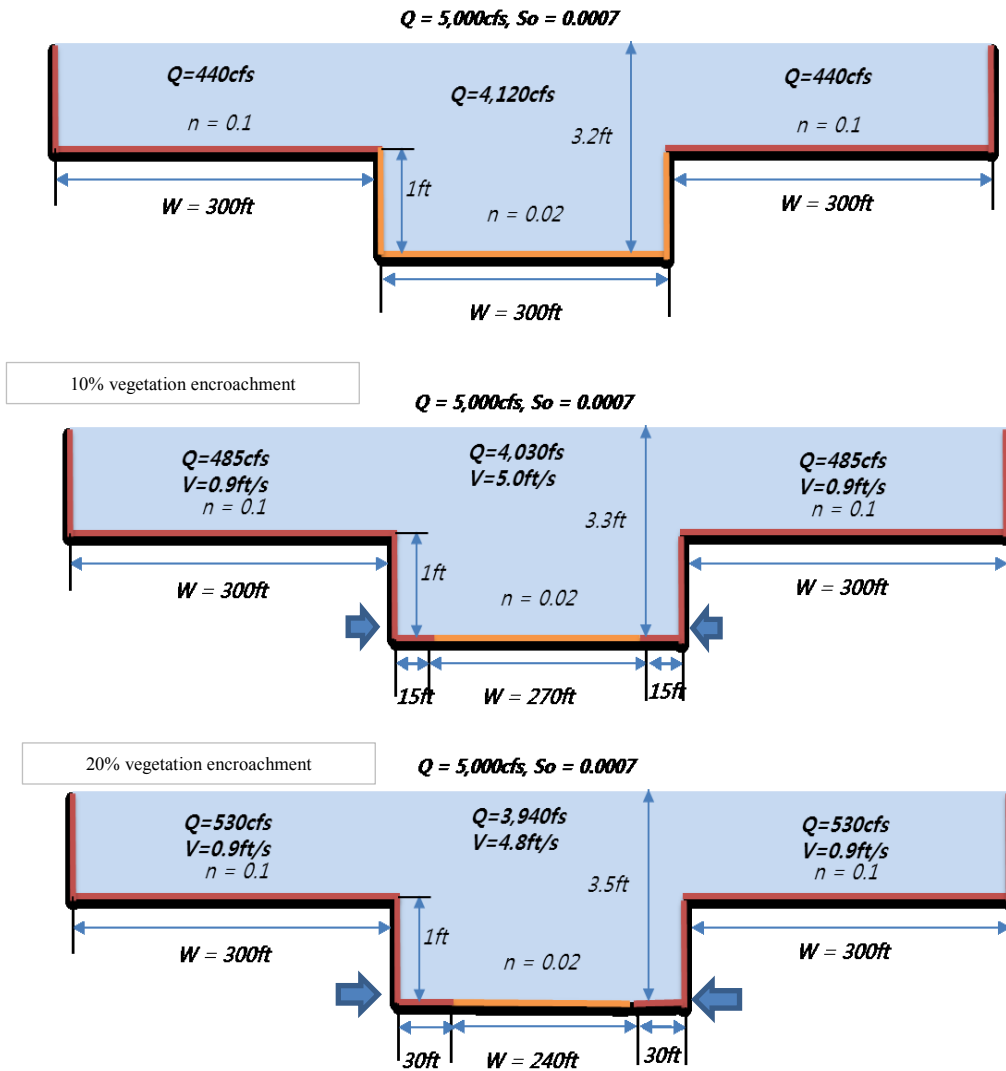


Figure 5.9. Changes in water depths and flow discharge with vegetation encroachment

5.2.3 Vegetation encroachment with channel narrowing

A 40% (narrowed from 1962 to 2002 at Bosque plug location) channel narrowing without roughness effect causes a 5% increase in flow depth and a 33% decrease in flow discharge in the main channel (Figure 5.10a). The flow velocity increases 3.6% after narrowing. On the other hand, Figure 5.10b shows that, as roughness effect is also increased, a channel narrowing of 40% causes 22% flow depth increase, an 18% decrease of flow discharge and 13% increase of flow velocity. Therefore, when the main channel has narrowed with riparian plants, the vegetation

encroachment contributes to higher flood stages which facilitate overbank flows. Channel characteristics of increased water depth and easier overbank flows also lead to a decrease of sediment transport capacity.

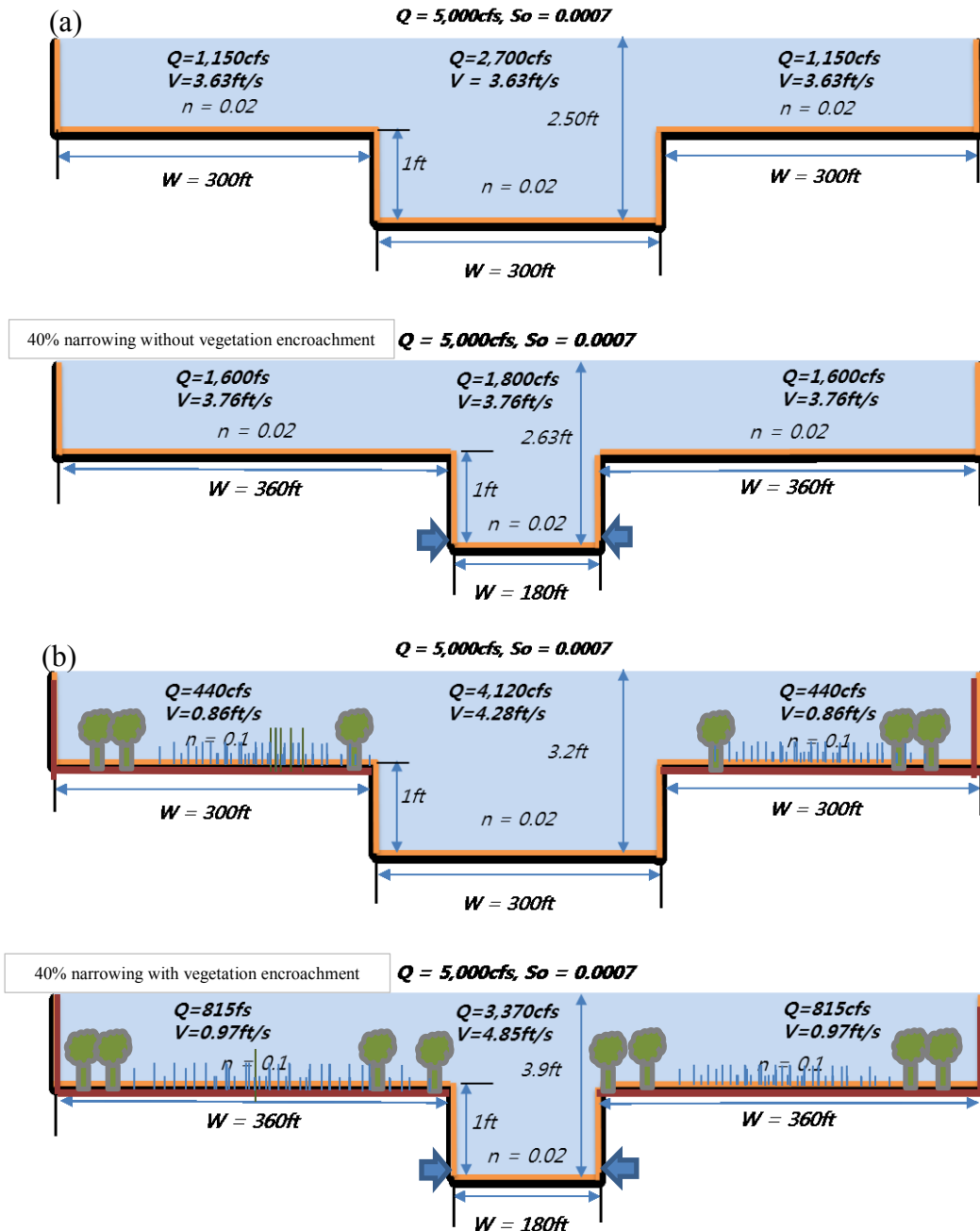


Figure 5.10. Changes in water depths and flow discharges after channel narrowing (a) without roughness effect (b) with roughness effect

5.2.4 Temporal change in channel roughness

Manning's n in the active channel ranges from 0.017 to 0.024. Although the roughness has changed, as mentioned in Section 5.2.1, the increase / decrease of active channel roughness does not cause changes in water depths and flow discharges (Figure 5.11). Likewise, the roughness in the floodplains has not changed between 1992 and 2002 when the sediment plug formed (Figure 5.12).

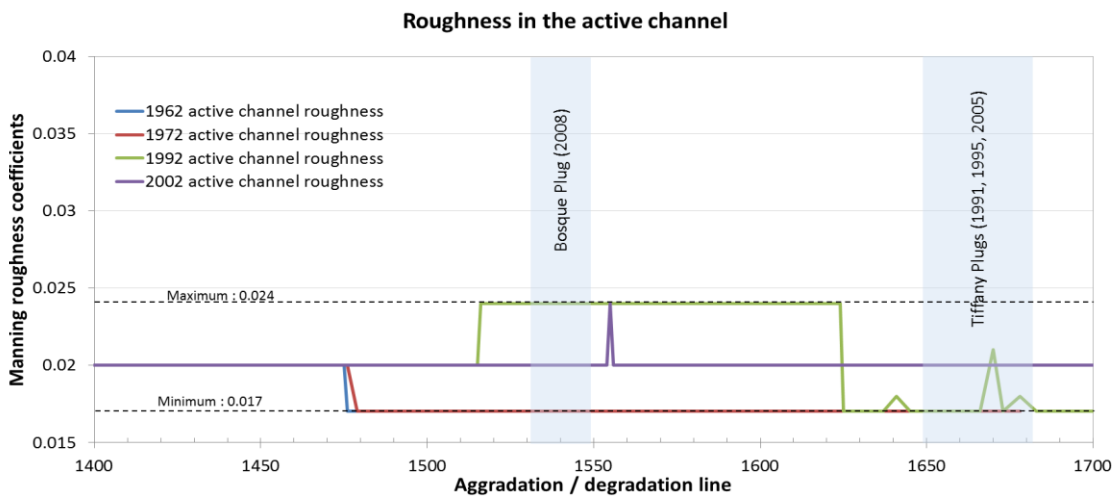


Figure 5.11. Changes in active channel roughness (1962-2002)

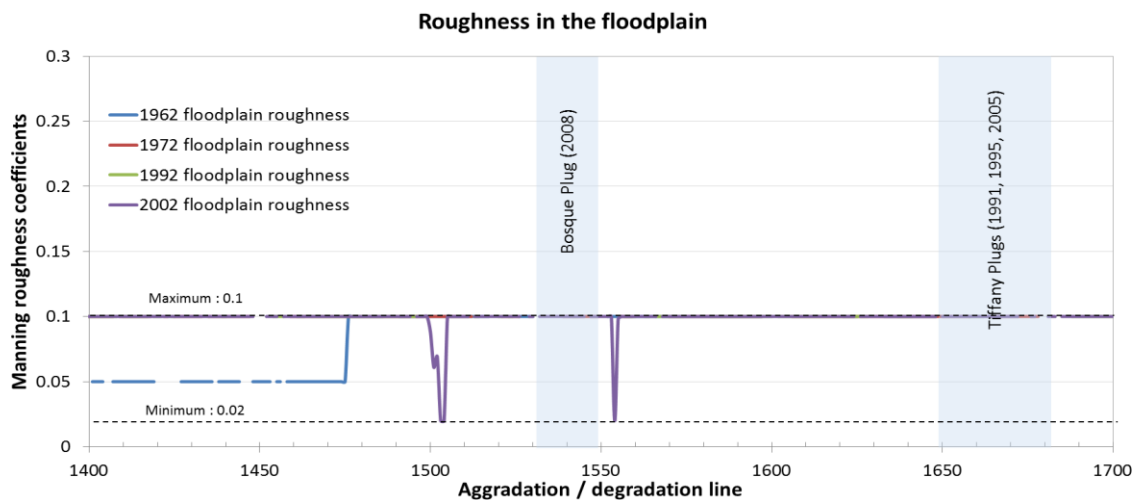


Figure 5.12. Changes in floodplain roughness (1962-2002)

However, the temporal change of channel roughness due to channel narrowing and vegetation encroachment was significant (Figure 5.13). At around Agg/Deg 1550 (Bosque plug location), the channel width shrank 40% between 1962 and 2002 and 70% again between 2002 and 2008. Low root riparian vegetation encroached toward the main channel, resulting in the increase of the resistance to flow consistently over time. As described in Section 5.2.3, vegetation encroachment with channel narrowing augments overbank flows in the main channel due to the increase of flow depth.

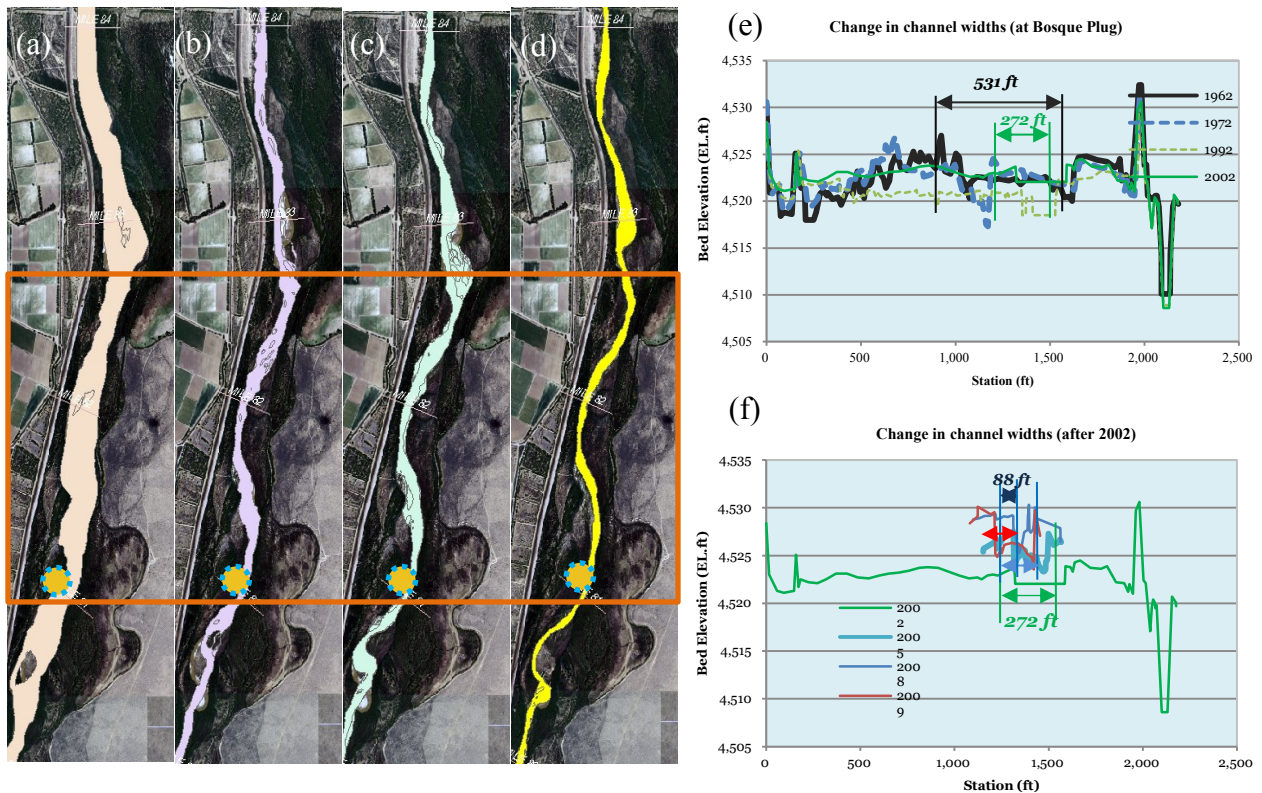


Figure 5.13 Channel widths (a) 1992 (b) 2001 (c) 2006 (d) 2008 (e) 1962 - 2002 and (f) 2002 - 2009

On the other hand, the roughness in the Tiffany area (Figure 5.14) has not changed as much as the Bosque plug area. The man-made channel which was constructed during the Rio Grande Project during the early 1950s has remained constant over time. Accordingly, vegetation and roughness remained unchanged over time.

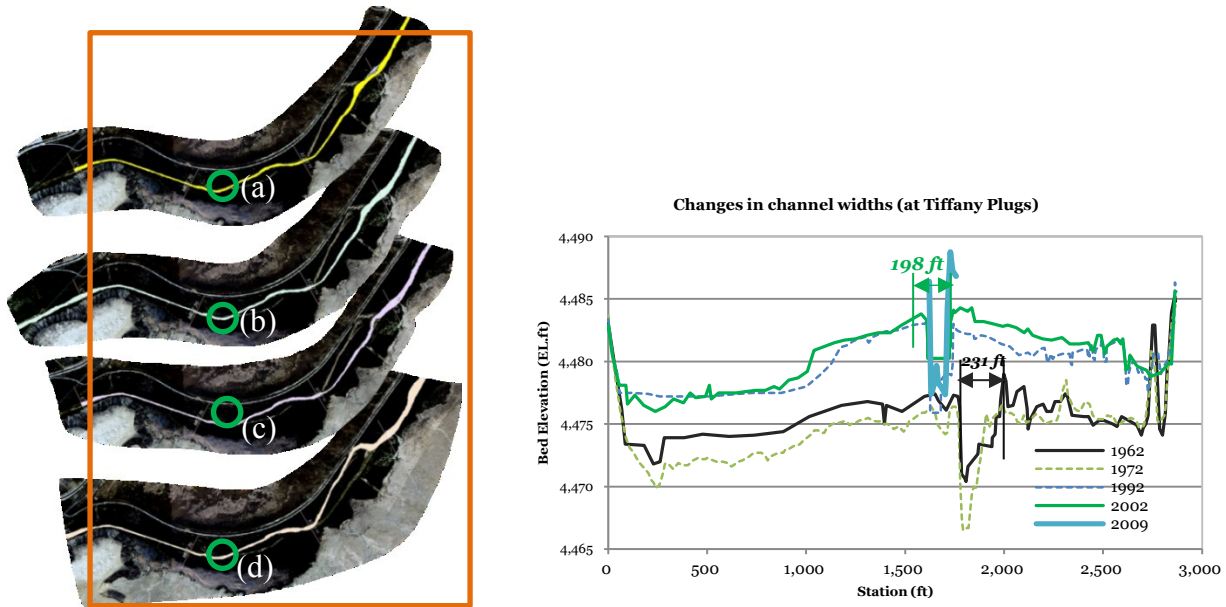


Figure 5.14 Channel widths (a) 1992 (b) 2001 (c) 2006 (d) 2008 (e) between 1962 and 2009

5.2.5 Composite channel roughness and sediment transport capacity

Sediment transport capacity in the active channel was calculated by using hydraulic depths, active channel widths, composite roughness, and channel slopes from HEC-RAS modeling (Figure 5.15). Compared with 1992, sediment transport capacity decreased 45% in 2002.

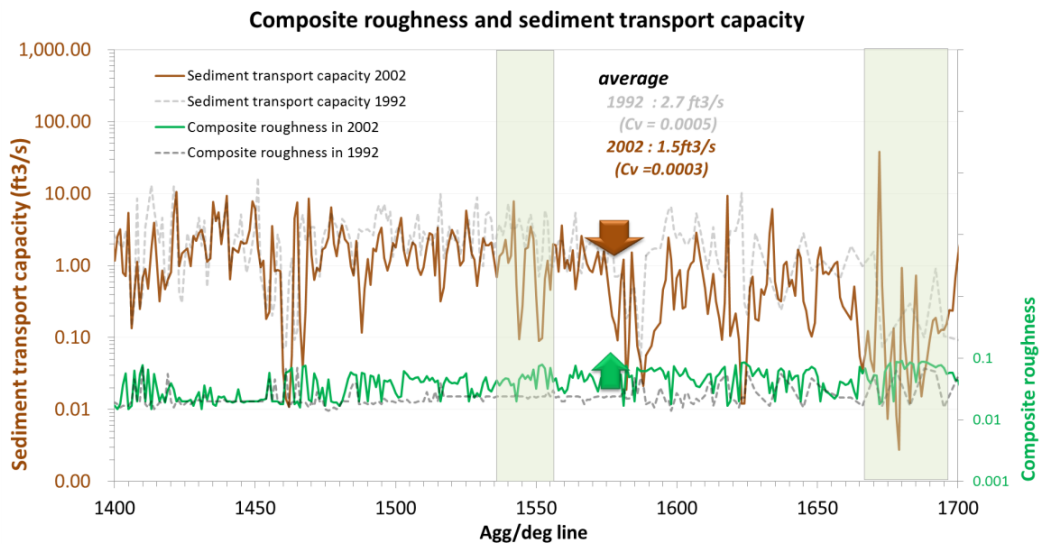


Figure 5.15. Sediment transport capacity in the main channel (5,000 cfs, HEC-RAS data)

CHAPTER 6 OVERBANK FLOWS AND CONCENTRATION PROFILES

Overbank flows and the perching phenomenon are described in Section 6.1. An analytical relationship between flow discharge and sediment transport capacity explains how the overbank flow influences the channel bed aggradation. The effect of sediment concentration profile on bed elevation changes is explained in Section 6.2.

6.1 PERCHING AND OVERBANK FLOWS

6.1.1 Perching

Perching is related to river bed aggradation so that the bed elevation of the main channel becomes higher than the bed elevation of the neighboring floodplain. When overbank flow initiates, perched channels lose surface water to the floodplains. The loss of water generates the loss of sediment transport capacity, causing sedimentation near the river banks to form natural levees. As mentioned in Section 2.1, perching has been intensified over time. In this section, quantitative evaluation is carried out to determine how much perching contributes to sediment plug formation.

6.1.2 Overbank flows and sediment transport capacity

When there is flexible connectivity between the main channel and floodplains, as shown in Figure 6.1a, overbank flows do not cause the decrease of sediment transport capacity and ensuing sedimentation as long as the channel widths do not change. On the contrary, perched channels (Figure 6.1b) lose flow and sedimentation to overbank areas, which causes sedimentation in the main channel. Figure 6.2 shows the historic inundated area, including the Tiffany and Bosque plugs. Around the plug locations, overbank flows were widely observed.

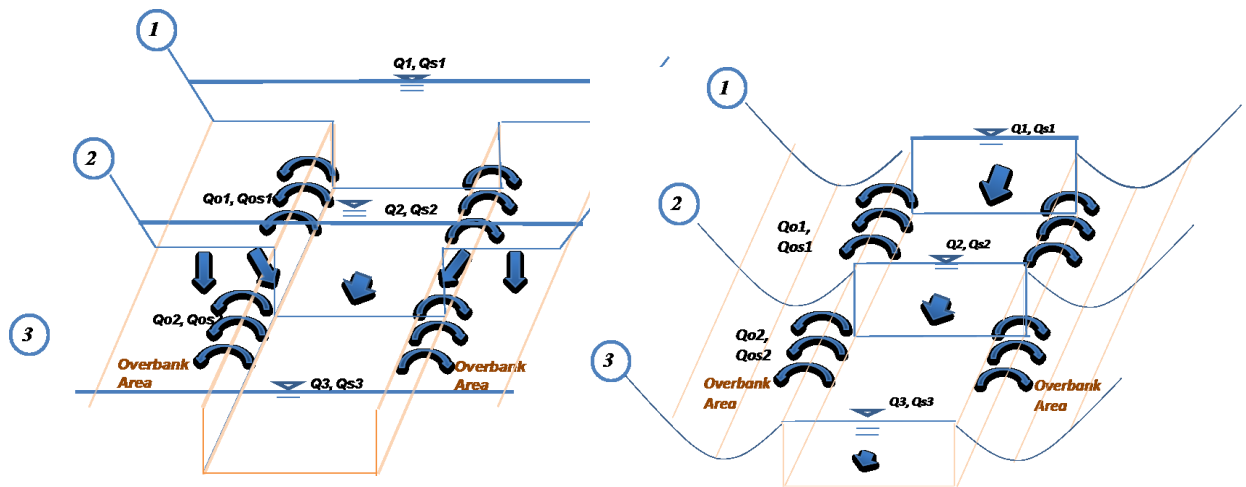


Figure 6.1. Overbank flows (a) without perching (b) with perching

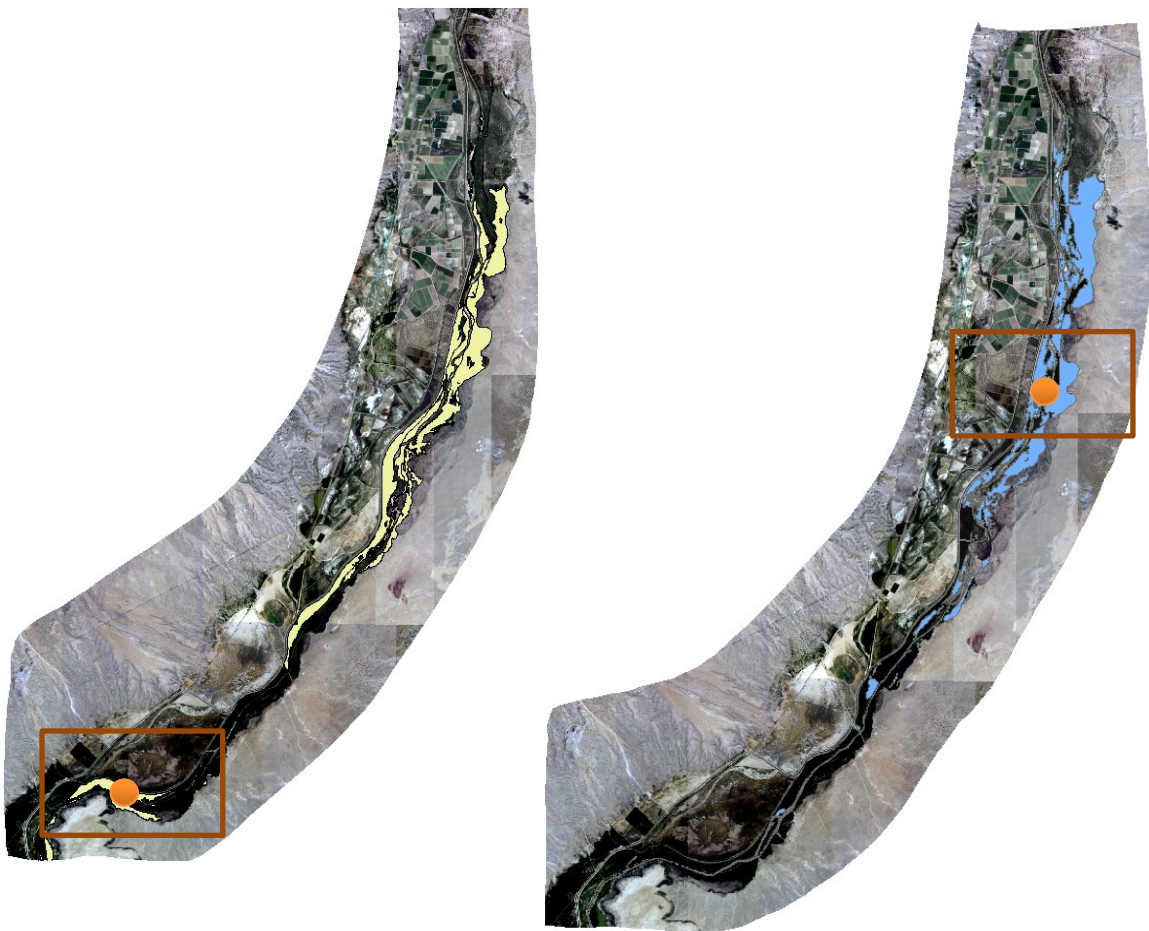


Figure 6.2. Flooded areas (a) in 2005 (Tiffany plug) and (b) in 2008 (Bosque Plug)

6.1.3 Sedimentation due to perching

In order to determine the perching effect on sedimentation, three basic equations with reference to Figure 6.1 were used, as follows:

Flow discharge

$$Q_1 = \frac{\varphi W}{n} h_1^{5/3} S_o^{1/2}, \quad Q_2 = \frac{\varphi W}{n} h_2^{5/3} S_o^{1/2}, \quad Q_3 = \frac{\varphi W}{n} h_3^{5/3} S_o^{1/2} \quad (6.1\sim 6.3)$$

Sediment discharge

$$Q_{s1} = 18W \sqrt{gd_s^3} \left(\frac{h_1 S}{(G-1)d_s} \right)^2, \quad Q_{s2} = 18W \sqrt{gd_s^3} \left(\frac{h_2 S}{(G-1)d_s} \right)^2, \quad Q_{s3} = 18W \sqrt{gd_s^3} \left(\frac{h_3 S}{(G-1)d_s} \right)^2 \quad (6.4\sim 6.6)$$

Erosion and Sedimentation

$$Q_{bed1-2} = Q_{s1} - Q_{s2} = \frac{\Delta Z}{\Delta t} [W(1 - p_o)\Delta x], \quad Q_{bed2-3} = Q_{s2} - Q_{s3} = \frac{\Delta Z}{\Delta t} [W(1 - p_o)\Delta x] \quad (6.7\sim 6.9)$$

Where Q_1, Q_2, Q_3 : flow discharges, φ is unit coefficient (SI : 1, English : 1.49), W is channel width of rectangular cross section, h_1, h_2, h_3 flow depths, S_o is the constant downstream channel slope, Δx is the longitudinal length of the control volume, g is the gravitational acceleration, d_s is the median sediment size, G is the specific gravity, ΔZ is the change in the channel elevation, p_o is the porosity, and Δt is the time step.

Overbank flow without perching is the condition that the flow depths at cross sections 1, 2, and 3 remain constant for uniform-steady flow conditions. As the flow depths do not change, sediment discharges for water bodies also do not change. There is no erosion or sedimentation as the sediment supply equals transport capacity in this case.

Conversely, in the case of perching, overbank flow leads to the decrease of flow depth and the loss of sediment transport capacity between two cross sections. Flow depth at cross sections 2 and 3 is lower than flow depth h_1 , thus the net sediment discharges either between 1 and 2 or between 2 and 3 have positive values. As a result, the channel bed aggrades.

Meanwhile, the sediment discharge can be expressed with flow discharge.

$$Q_s = 18W \sqrt{gd_s^3} \left(\frac{hS_f}{(G-1)d_s} \right)^2 = aQ^{1.2}, \quad \text{where } a = \left[\frac{18\sqrt{gn}^{6/5} S_f^{7/5}}{(G-1)^2 \varphi^{6/5} \sqrt{d_s}} \right] \quad (6.10)$$

Therefore, the loss of flow leads to further loss of sediment transport capacity. The reduced sediment transport capacity causes sedimentation in the main channel.

6.1.4 Application to the Middle Rio Grande

6.1.4.1 Channel conveyance capacity

Channel conveyance capacity relates to the likelihood of overbank flows. The channel conveyance ($K_c = \frac{\Phi}{n} AR^{2/3}$) has been drastically decreased over time (Figure 6.3). The overall conveyance decreased at the location where the 2008 sediment plug formed. The channel capacity around the Tiffany plug location has not changed during the same time period. Thus the Bosque plug conveyance seems to be related to overbank flows, while the 1995 and 2005 Tiffany plugs have been influenced by other contributing factors.

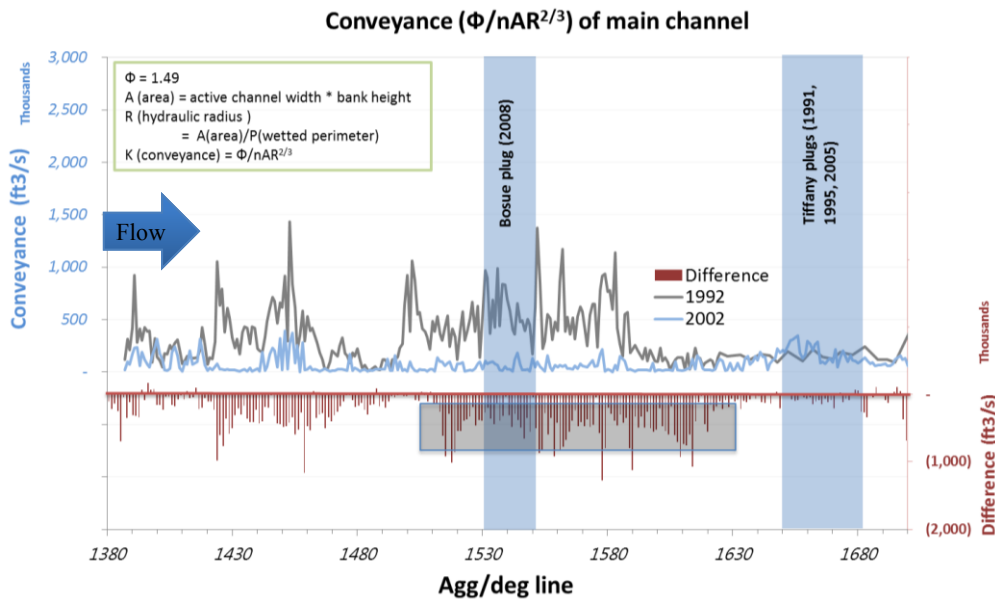


Figure 6.3. Temporal change in channel conveyance (1992 and 2002)

6.1.4.2 Overbank flows

The decrease in channel conveyance leads to easier overbank flows. Figure 6.4 shows the ratio of overbank flow to total flow in 1992 and in 2002 using the HEC-RAS geometry obtained from Reclamation. The overbank flow ratio in 1992 shows that the overbank flow at the Tiffany plug location was over 50% of the total flow. This means that at 50% of cross sections, overbank flow occurred. On the other hand, at the Bosque plug location, most of the flow was within the main channel without overbank flows.

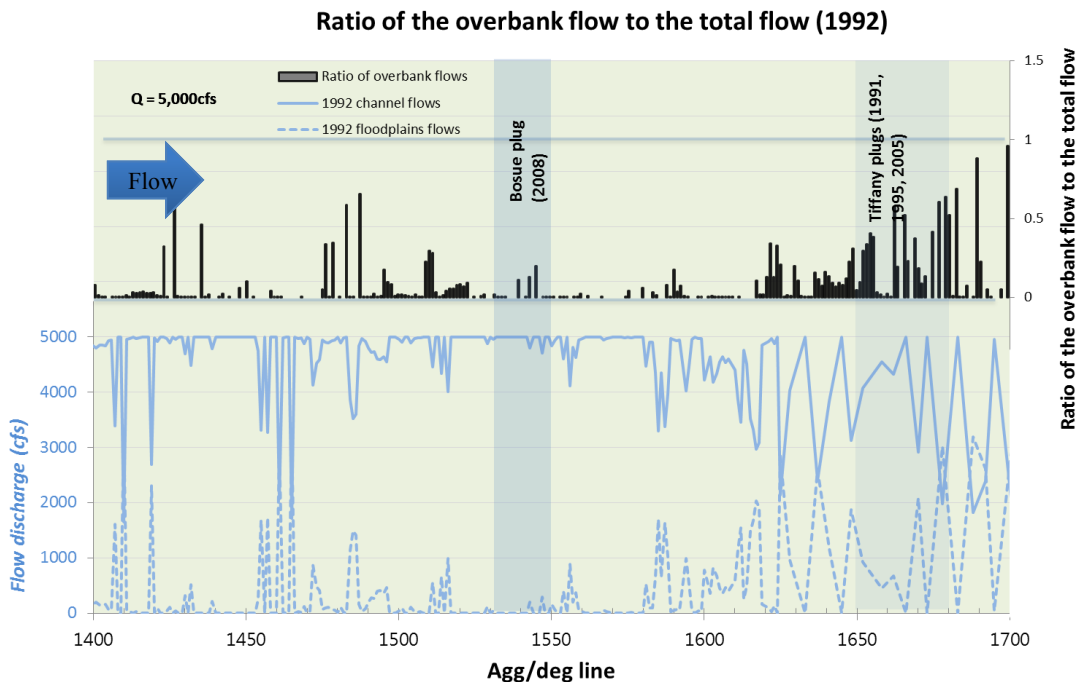


Figure 6.4. The ratio of the overbank flow to the total flow in 1992

In the meantime, in 2002 (Figure 6.5), the channel geometry reduced flow conveyance because most cross sections showed overbank flow. At only 4% of cross sections, flow discharge was within the main channel. At the Bosque location, about half of the flow discharge was lost to overbank areas. At Agg/Deg 1551 where the 2008 sediment plug started, 2/3 of flow was lost to overbank areas.

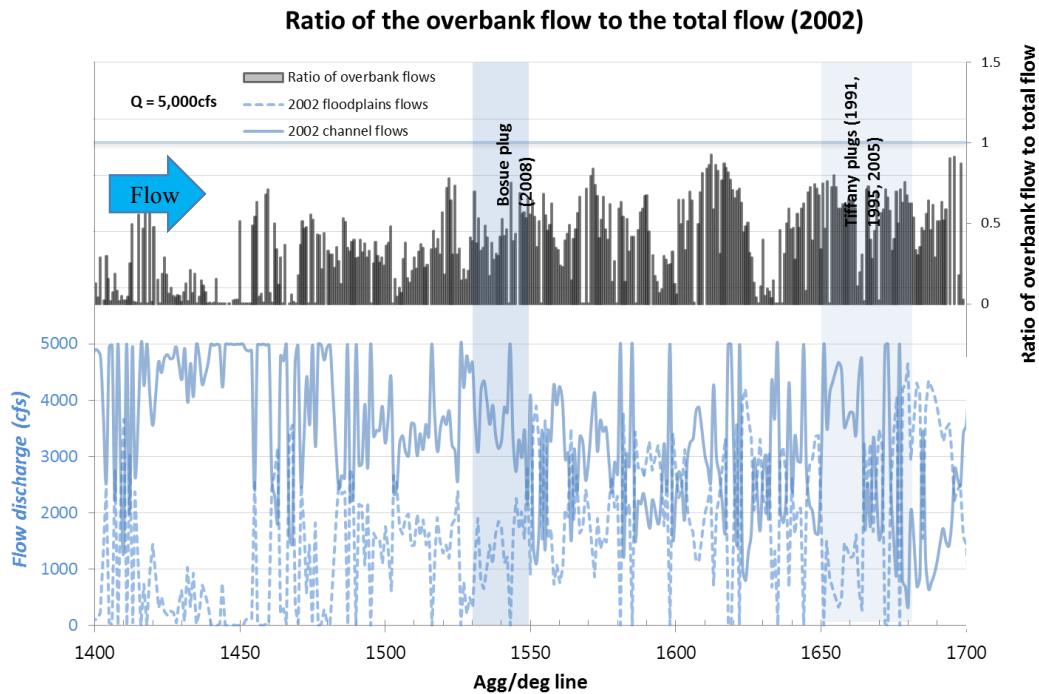


Figure 6.5. The ratio of the overbank flow to the total flow in 2002

6.1.4.3 Historic overbank flows and perching

It has been observed that the flow in some areas of the Bosque Reach spills onto the floodplain before the main channel banks are overtopped through side channels (Figure 6.6b and 6.6c). Channel aggradation, observed in the upstream portion of the reach, promotes more flow into the floodplain. Some of the floodplain flow returns into the main channel just downstream of the 2008 sediment plug (Figure 6.6a and 6.6d). In the lower portion of Bosque del Apache National Wildlife Refuge (BDANWR), the channel has degraded, lowering the channel profile and confining the flow in the main channel. When the channel was perched, the flow was lost to overbank areas without return flow. A crevasse splay was observed around Agg/Deg 1532, which is at the end of the 2008 sediment plug location. Significant decrease of sediment transport capacity can be assumed to happen around this location.

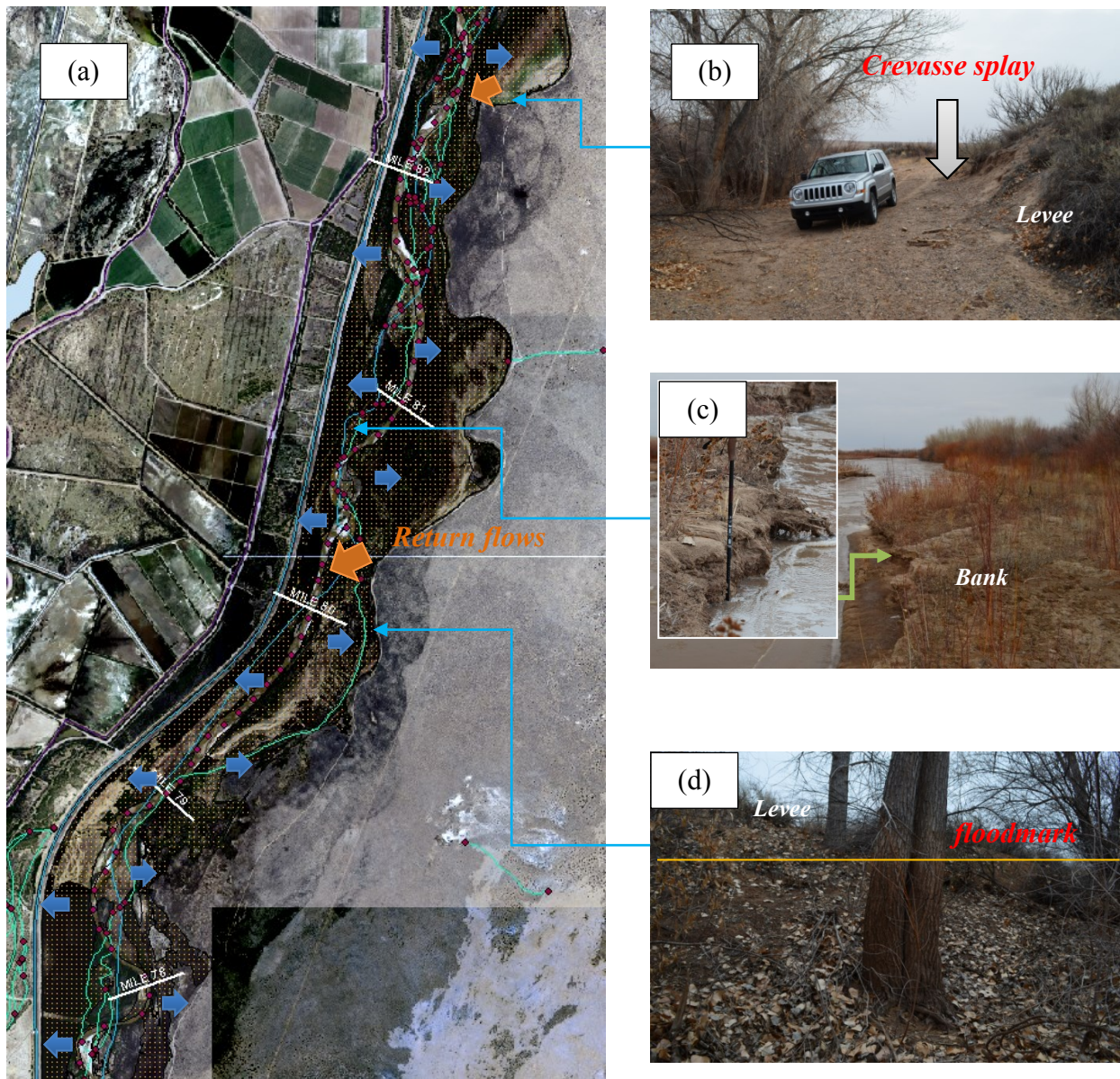


Figure 6.6. (a) Overbank flows and return flows, (b) crevasse splay, (c) bank crest, and (d) floodmarks

6.2 VERTICAL SEDIMENT CONCENTRATION PROFILES

The vertical sediment concentration profile is dependent on the relative strength between the settling velocity of sediment particles and the shear velocity describing turbulence that keeps particles in suspension. The shape of the sediment concentration profile is determined based on the Rouse parameter. Comparison of two cases provides an analysis of vertical concentration distribution on the sedimentation in the main channel.

6.2.1 Overbank flow in case of uniform sediment concentration profile

Overbank flows result in a decrease in flow depth and velocity in the main channel, and subsequently a decrease in sediment transport capacity. Aggradation occurs when the inflowing sediment transport capacity exceeds the exiting sediment due to loss to overbank areas. Figure 6.7 shows a control volume with constant channel width, W , and channel slope, S .

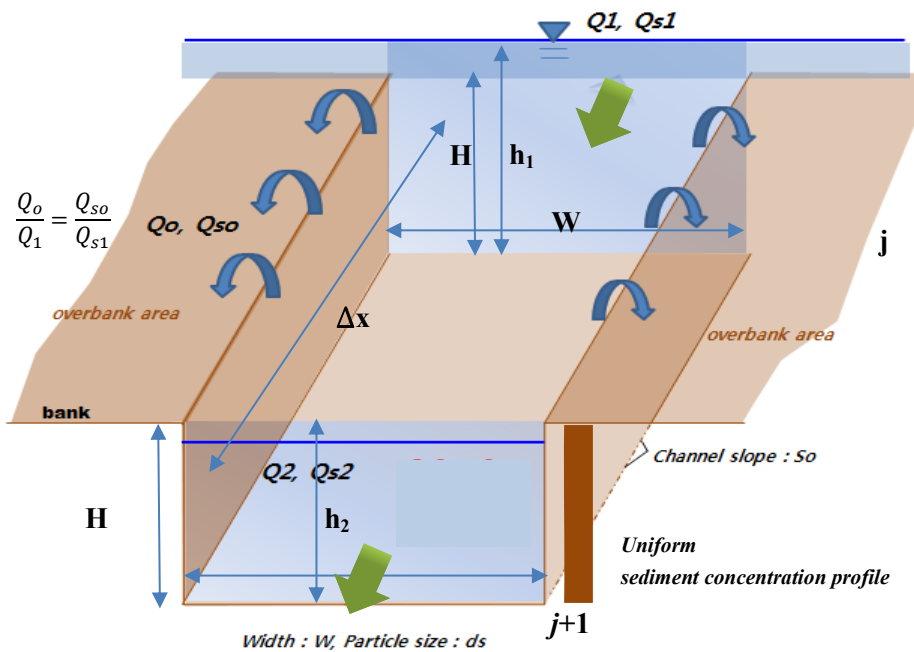


Figure 6.7. Flow and sediment discharges with uniform concentration distribution

In order to determine the concentration distribution effect on sedimentation in the main channel, continuity of water and continuity of sediment can be expressed as:

$$\mathbf{Q_1 = Q_2 + Q_o} \quad (6.11)$$

$$Q_1 = \frac{\varphi W}{n} h_1^{5/3} S_o^{1/2} \quad (6.12)$$

$$Q_2 = \frac{\varphi W}{n} h_2^{5/3} S_o^{1/2} \quad (6.13)$$

$$Q_o = C_b(\Delta x)(h_1 - H)^{3/2} \text{ (when } h_1 > H) \quad (6.14)$$

$$\mathbf{Q_{s1} = Q_{s2} + Q_{so} + Q_{bed}} \quad (6.15)$$

$$Q_{s1} = 18W \sqrt{g d_s^3} \left(\frac{h_1 S}{(G-1)d_s} \right)^2 \quad (6.16)$$

$$Q_{s2} = 18W \sqrt{g d_s^3} \left(\frac{h_2 S}{(G-1)d_s} \right)^2 \quad (6.17)$$

$$Q_{so} = C_v \times Q_o \quad (6.18)$$

$$Q_{bed} = Q_{s1} - Q_{s2} - Q_{so} = \frac{\Delta Z_b}{\Delta t} [W(1-p_o)\Delta x] \quad (6.19)$$

where Q_1 is the water inflow, Q_2 is the water outflow, Q_o is the overbank flow, φ is unit coefficient (SI : 1, English : 1.49), W is the channel width of a rectangular cross section, h_1 , is the upstream flow depth, h_2 is the downstream flow depth, S_o is the constant channel slope, C_b is the weir coefficient, Δx is the longitudinal length of the control volume, H is the bankfull depth, g is the gravitational acceleration, d_s is the median sediment size, G is the specific gravity, C_v is the volumetric sediment concentration, ΔZ is the change in the channel elevation, p_o is the porosity, and Δt is the time step.

Substituting Equations 6.12-6.14 into Equation 6.11 and Equation 6.16-6.19 into Equation 6.15 yields:

$$\frac{\varphi W}{n} h_1^{5/3} S_o^{1/2} = \frac{\varphi W}{n} h_2^{5/3} S_o^{1/2} + C_b(\Delta x)(h_1 - H)^{3/2} \quad (6.20)$$

$$18W\sqrt{gd_s^3} \left(\frac{h_1S}{(G-1)d_s}\right)^2 = 18W\sqrt{gd_s^3} \left(\frac{h_2S}{(G-1)d_s}\right)^2 + \frac{18W\sqrt{gd_s^3} \left(\frac{h_1S}{(G-1)d_s}\right)^2}{\frac{\phi W}{n} h_1^{\frac{5}{3}} S_o^{\frac{1}{2}}} \cdot C_b(\Delta x)(h_1 - H)^{\frac{3}{2}} + \frac{\partial Z_b}{\partial t} [W(1 - p_o)\Delta x] \quad (6.21)$$

Combining Equation 6.20 and Equation 6.21 and rearranging yields:

$$\Delta Z_b = \frac{\Delta t}{\Delta x} \frac{18\sqrt{g}S^2}{(1-p_o)(G-1)^2\sqrt{d_s}} \left(h_1^2 \left(\frac{h_2^{\frac{5}{3}}}{h_1^{\frac{5}{3}}} \right) - h_2^2 \right) = \frac{\Delta t}{\Delta x} \frac{18\sqrt{g}S^2 h_2^{\frac{5}{3}}}{(1-p_o)(G-1)^2\sqrt{d_s}} \left(h_1^{\frac{1}{3}} - h_2^{\frac{1}{3}} \right) \quad (6.22)$$

When h_2 decreases due to water loss to overbank areas, ΔZ_b increases, resulting in aggradation. When h_1 is less than H , there is no aggradation/degradation in the channel. A lower bank height, H , causes an increase of flow and sediment loss to overbank areas, and a decrease in sediment transport capacity at the downstream cross-section, resulting in bed aggradation.

6.2.2 Overbank flow in case of non-uniform sediment concentration profile

In case of non-uniform vertical concentration profile of sediment discharge (Figure 6.8), overbanking sediment is not proportional to loss of water discharge to overbank areas. The fraction of sediment loss to overbank areas, CR(Conveyance Ratio), can be determined using the Rouse equation:

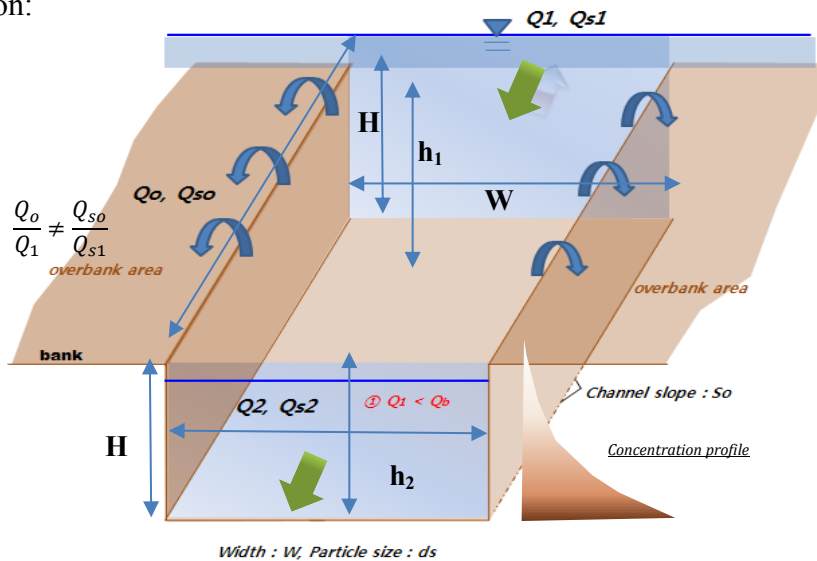


Figure 6.8. Flow and sediment discharges with non-uniform concentration distribution

$$\mathbf{Q_1 = Q_2 + Q_o} \quad (6.23)$$

$$\mathbf{Q_{s1} = Q_{s2} + Q_{so} + Q_{bed}} \quad (6.24)$$

$$Q_{so} = CR \times C_v \times Q_o \quad (6.25)$$

$$CR = \frac{C_a \int_{Z=H}^{Z=h-H} \left(\frac{h-z}{z} \frac{a}{h-a} \right)^{Ro = \frac{\omega}{\beta_s \kappa u^*}} dz}{C_a \int_{Z=a}^{Z=h1} \left(\frac{h-z}{z} \frac{a}{h-a} \right)^{Ro = \frac{\omega}{\beta_s \kappa u^*}} dz} \quad (6.26)$$

Similar to the case of a uniform concentration profile, substituting 6.12-6.14 into Equation 6.23 and Equations 6.16-6.19 and 6.25 into Equation 6.24:

$$\frac{\varphi W}{n} h_1^{\frac{5}{3}} S_o^{\frac{1}{2}} = \frac{\varphi W}{n} h_2^{\frac{5}{3}} S_o^{\frac{1}{2}} + C_b(\Delta x)(h_1 - H)^{\frac{3}{2}} \quad (6.27)$$

$$18W \sqrt{g d_s^3} \left(\frac{h_1 S}{(G-1)d_s} \right)^2 = 18W \sqrt{g d_s^3} \left(\frac{h_2 S}{(G-1)d_s} \right)^2 + CR \times C_v \times C_b(\Delta x)(h_1 - H)^{\frac{3}{2}} + \frac{\Delta Z_b}{\Delta t} [-W(1 - p_o)\Delta x] \quad (6.28)$$

Combining the equations for hydraulic continuity (Equation 6.27) and continuity of sediment (Equation 6.28) and rearranging:

$$\Delta Z_b = \frac{\Delta t 18 \sqrt{g} S^2}{\Delta x (G-1)^2 (1-p_o) \sqrt{d_s}} \left\{ (h_1^2 - h_2^2) - CR h^{0.33} (h_1^{\frac{5}{3}} - h_2^{\frac{5}{3}}) \right\} \quad (6.29)$$

When the suspended load is relatively high, CR is high and more sediment is lost overbank. This reduces the amount of channel aggradation ΔZ . When h_l is less than H , $CR = 0$, and there is no loss of flow or sediment from the main channel. In the case of a uniform sediment concentration profile, if h_l exceeds H , the proportion of sediment lost to overbank areas is equal to the proportion of flow lost. However, if the sediment concentration profile is non-uniform and sediment load is concentrated near the bed, the fraction of water loss exceeds the fraction of sediment loss, resulting in a decrease in sediment transport capacity. From Equation 6.29, when the aggradation height is known, the time to fill the channel can be determined as well.

6.2.3 Sediment concentration distribution effect on MRG channel bed elevation

From the Rouse equation, the sediment concentration profile is expressed as a function of water depth, h , fall velocity ω , and shear velocity, $u_* = \sqrt{ghS_o}$, where g is gravitational acceleration and S_o is the bed slope ($S_f = S_o$). As a single sediment particle size is used, the sediment concentration profile is dependent on the flow depth and channel slope. If channel slope is constant between two cross-sections, sediment concentration profile can be determined from the flow depth. Figure 6.9 shows the decrease of flow depth in the downstream direction as a result of overbank flow. The decrease in flow depth causes a decrease of shear velocity (Figure 6.9a) and an increase in Rouse number (Figure 6.9b). A high Rouse number generates a near-bed-concentration profile (Figure 6.9c), which generally causes accelerated channel aggradation and, in extreme cases, sediment plug formation.

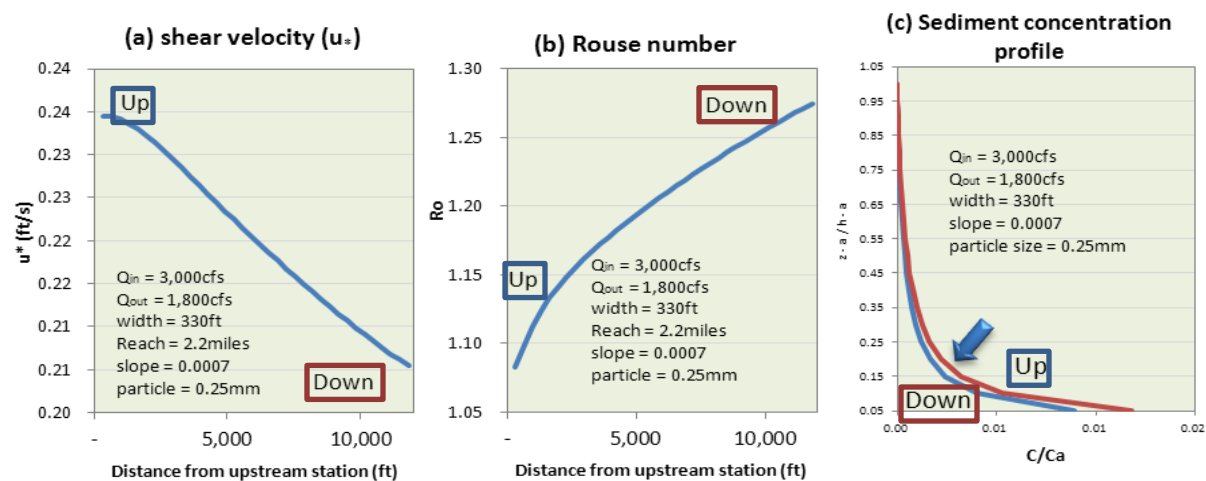


Figure 6.9. Changes in shear velocity and Rouse number due to overbank flows

Aggradation due to overbank flow with uniform sediment concentration and non-uniform sediment concentration is illustrated in Figures 6.10a and 6.10b, respectively. The comparison of two cases (Figure 6.10c) shows that non-uniform concentration profiles accelerate the channel bed aggradation 4~7 times greater than uniform concentration profiles.

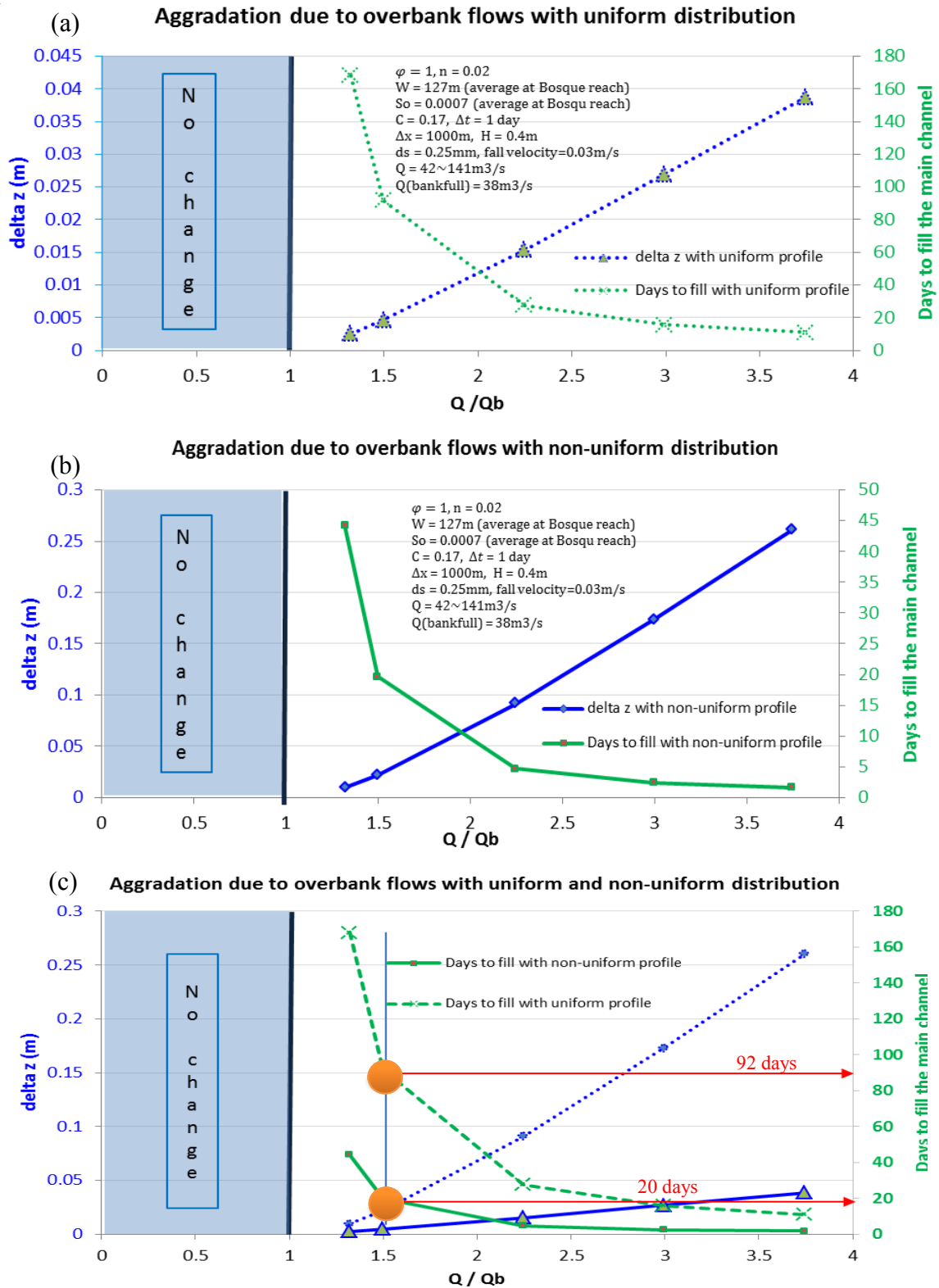


Figure 6.10. Aggradation due to overbank flows with (a) uniform concentration distribution, (b) non-uniform concentration distribution, and (c) comparison of two cases

6.2.4 Concentration profiles at historic sediment plug locations

6.2.4.1 Concentration profile at Agg/Deg 1683 (Tiffany plug location)

The cross section at the Tiffany plug location (Agg/Deg 1683) shows that the channel elevation in the main channel was higher than the floodplain elevation (perched) and the bankfull discharge was 2,000 cfs. As the flow exceeds the bankfull discharge, overbank flows are lost to overbank areas due to the channel perching (Figure 6.11).

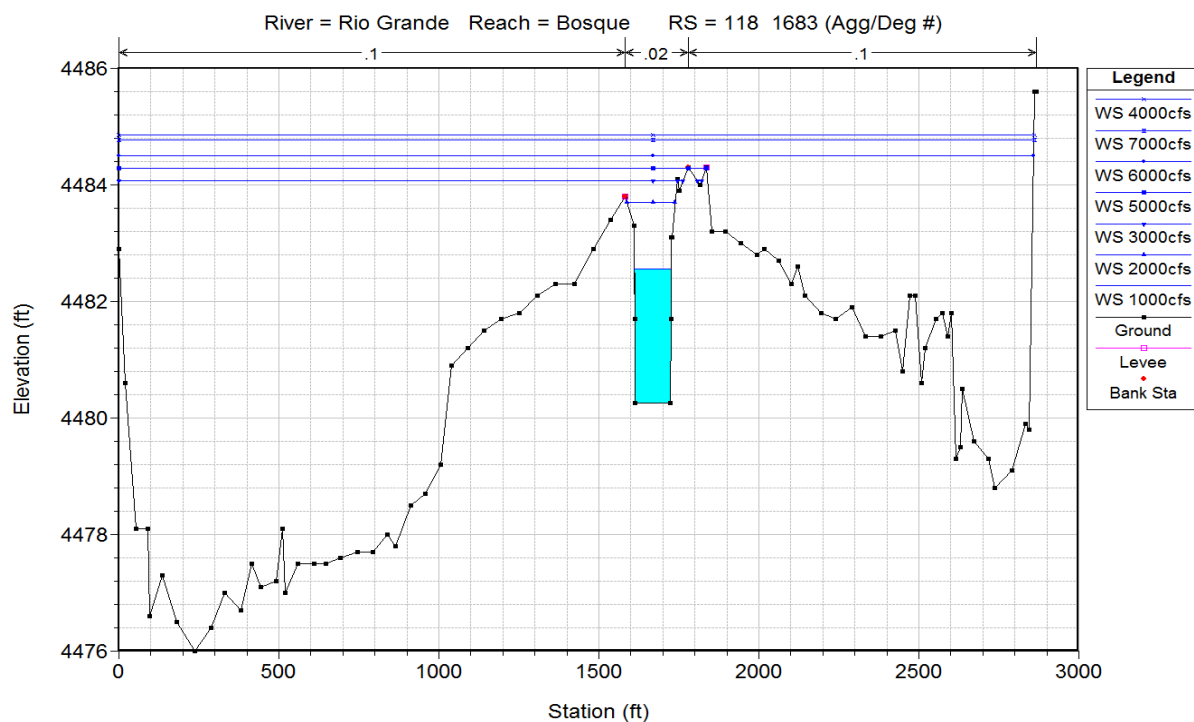


Figure 6.11. Water surface profiles for various flow discharges at the Tiffany plug location

The flow depth gradually increases with discharge prior to the overbank flow discharge of 2,000 cfs. Beyond this discharge, the flow depth does not increase before the floodplains are filled with flood waters. After that, the flow depth increases again. The Rouse number gradually decreases with increase of discharge prior to overbank flow. Once flow goes overbank, the Rouse number remains relatively constant.

With the Rouse equation and water depths from the 2002 HEC-RAS model, sediment concentration profiles at the Tiffany plug location are plotted in Figure 6.12. Sediment concentration decreases rapidly above the bed layer thickness, a ($= 2d_s$, d_s : sediment size). At mid-depth, $z = 0.5h$, sediment concentration is only 0.03% of near-bed sediment concentration. Thus, the concentration of sediment particles becomes increasingly small near the water surface and sediment is mostly transported near the bed. Accordingly, only less than 1% of sediments is lost to overbank areas during significant amounts of overbank flow at flow discharges above a bankfull discharge.

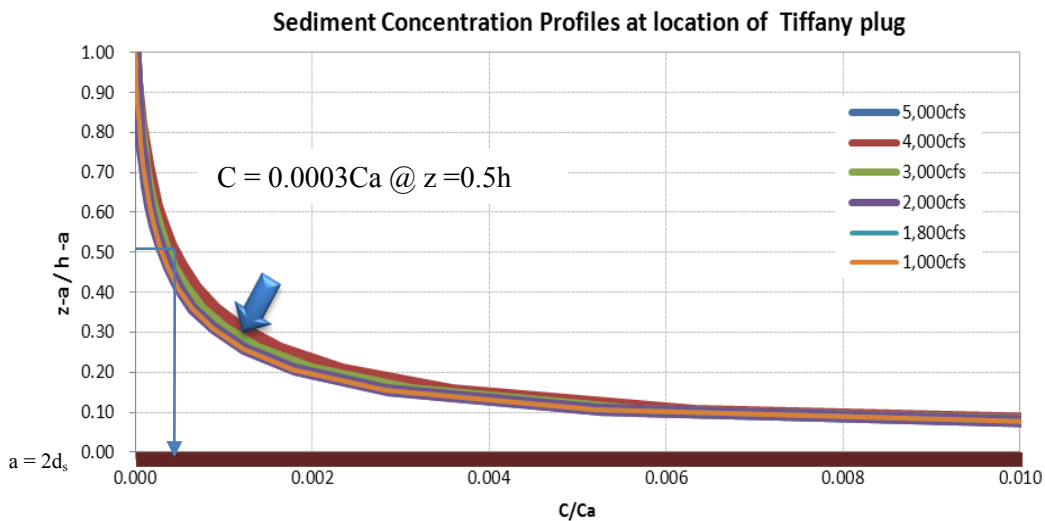


Figure 6.12. Sediment Concentration Profiles at the Tiffany plug location

6.2.4.2 Concentration profile at Agg/Deg 1550 (Bosque plug location)

Figure 6.13 depicts water surface level including the main channel and the west side floodplain at various discharges. The discharges at which overbank flow initiated were 1,800 cfs toward the right-side bank and 4,500 cfs toward the left-side bank. The left black area of the cross section is an artificial levee and the right black one is the Low Flow Conveyance Channel (LFCC), which delivers water from the San Acacia Dam to Elephant Butte Reservoir.

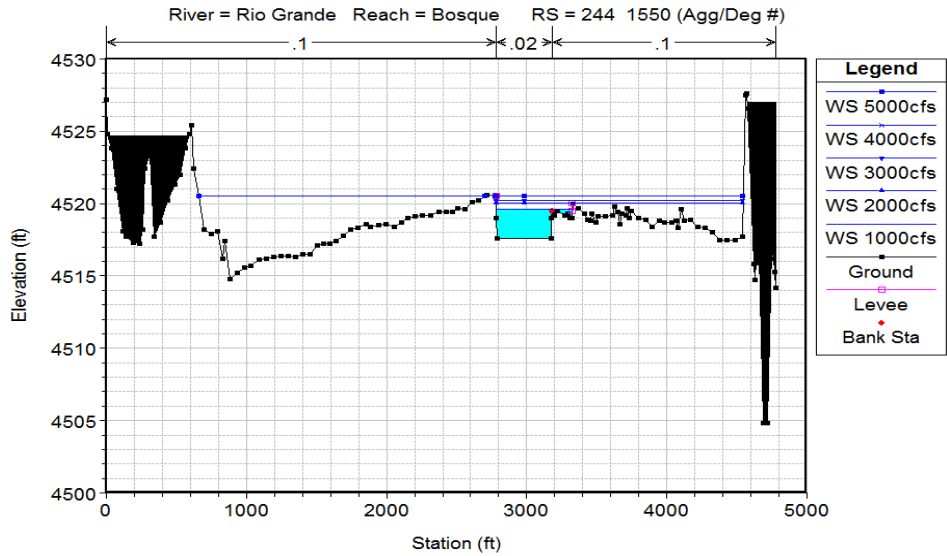


Figure 6.13. Water surface profiles for various discharges at the Bosque plug location

When the hydraulic mean depth is highest at a discharge of 1,800 cfs, the Rouse number is at a minimum and the sediment concentration profile is relatively more uniform than at higher flow discharges. Like the concentration profile at the Tiffany plug location, the concentration at mid-depth is only 0.06% of near-bed sediment concentration (Figure 6.14). Depending on the water depth, there is a tremendously large variability in sediment concentration.

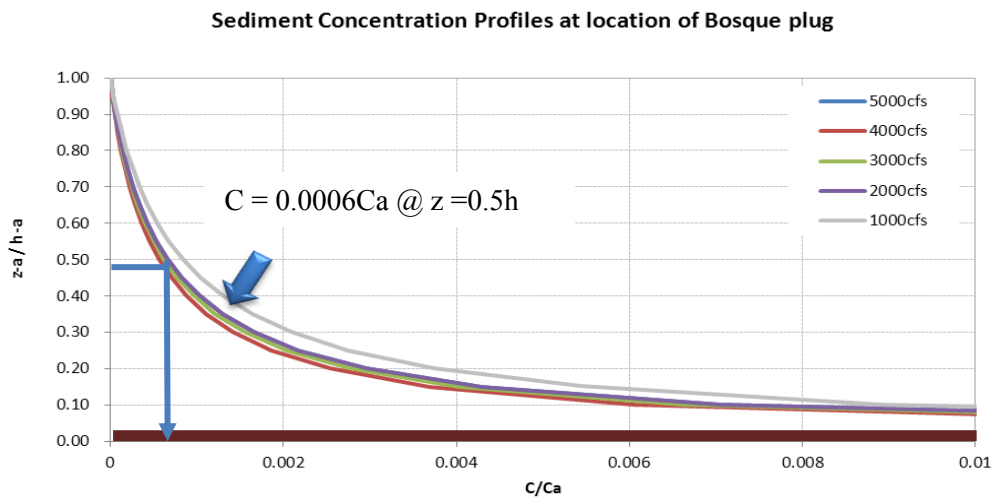


Figure 6.14. Sediment concentration profiles at the Bosque plug location

6.2.4.3 Comparison of the concentration profiles

A comparison of sediment concentration profiles between the two locations (Figure 6.15) shows that both locations have predominantly near-bed concentrations. The Rouse parameter in the Tiffany plug location is comparatively higher than the Bosque plug location and decreases as the flow discharge increases.

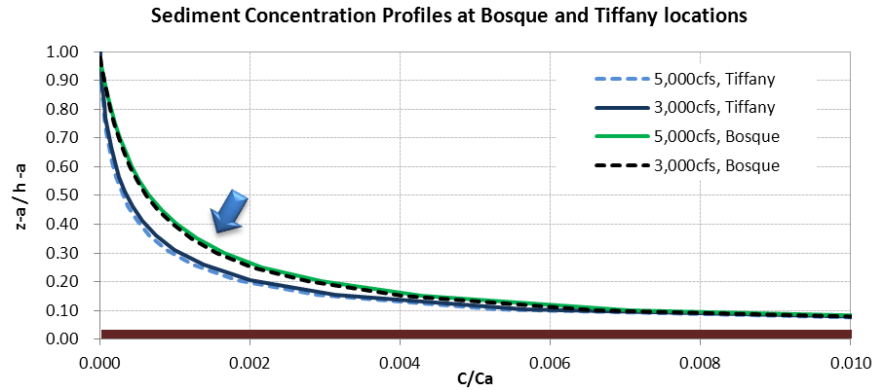


Figure 6.15. Comparison of sediment concentration profiles at plug locations

Sediment concentration profiles for sub-reaches (Figure 6.16) show that sub-reach 3, where the Bosque plug occurred in 2008, has the highest Rouse number and most near-bed sediment concentration. From this sub-reach scale analysis, Rouse number ranges from 0.7 to 1.4 and the Bosque plug sub-reach has a higher Rouse number than the Tiffany plug sub-reach.

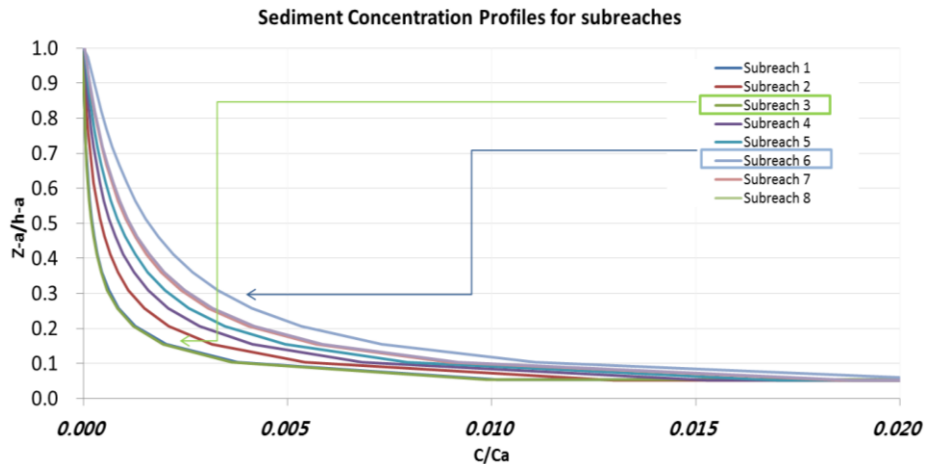


Figure 6.16. Comparison of Sediment Concentration Profiles at sub-reaches

CHAPTER 7 BACKWATER EFFECTS ON BED AGGRADATION

Backwater effects on water surface profile and channel bed elevation are examined in this chapter. The backwater effect from Elephant Butte Reservoir is covered in Section 7.1. An increase in a water stage and a subsequent aggradation at the river mouth are determined. The backwater effect from the San Marcial Railroad Bridge includes the increase of water depth and the possibility to cause the historic Tiffany plugs, which is discussed in Section 7.2. The sharp bends less than 1 mile downstream from the 2008 Bosque plug location may have increased the water stage and caused sediment deposition in the Bosque plug area. The backwater effects due to sharp bends are detailed in Section 7.3.

7.1 BACKWATER EFFECTS FROM RESERVOIR

The upstream and downstream ends of the Middle Rio Grande are confined with man-made structures: upstream Cochiti Dam, downstream Elephant Butte Reservoir, and tributary dams. The downstream Elephant Butte Reservoir, which is located 45 miles downstream from the Tiffany area, has influenced upstream aggradation and degradation (Figure 7.1). For the investigation regarding the backwater effect, the relation between bed elevation and reservoir stage was evaluated qualitatively with historic survey data.

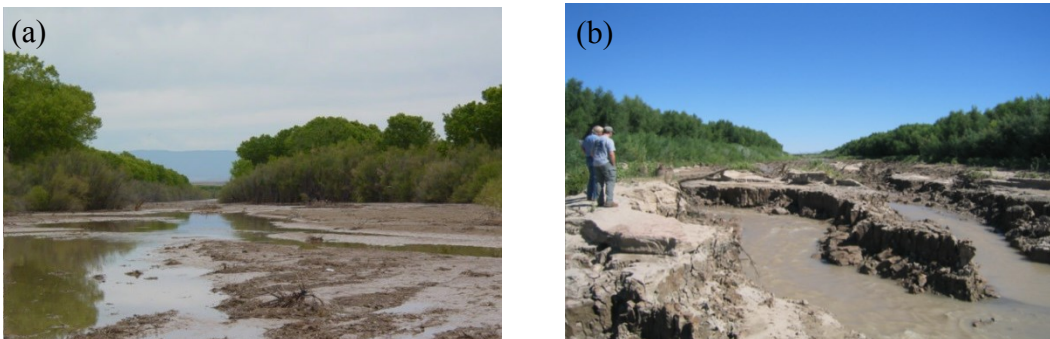


Figure 7.1. Channel bed changes due to reservoir stage (a) aggradation (b) head-cut

The water level in Elephant Butte Reservoir has fluctuated, ranging from E.L.4260 ft to E.L. 4407 ft (Figures 7.2 and 7.3). When the 1991 and 1995 sediment plugs occurred, the reservoir was full. On the other hand, when the 2005 Tiffany plug formed, the reservoir was at the end of a drought period.

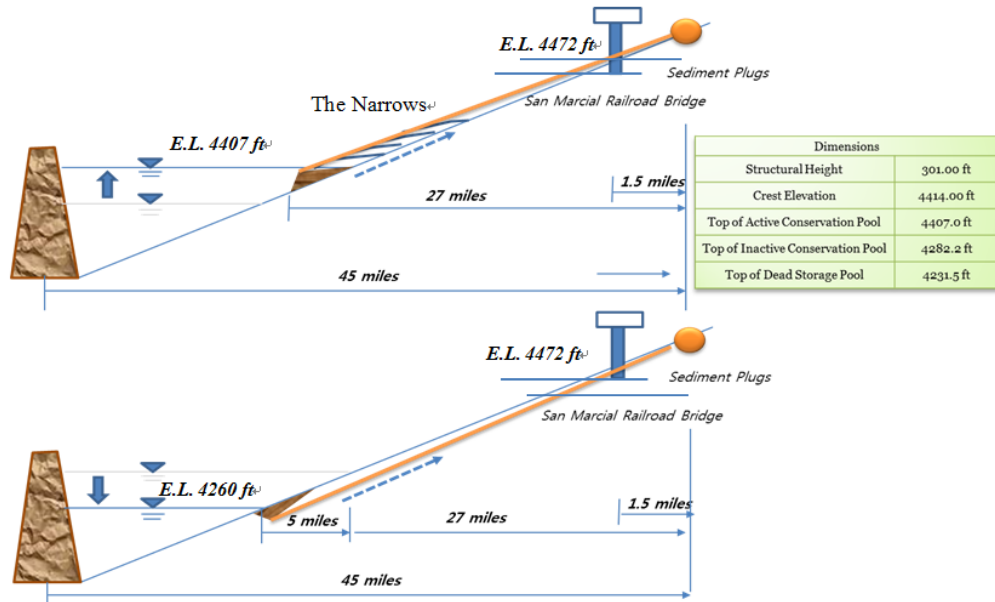


Figure 7.2. Elephant Butte Reservoir and Sediment plug location

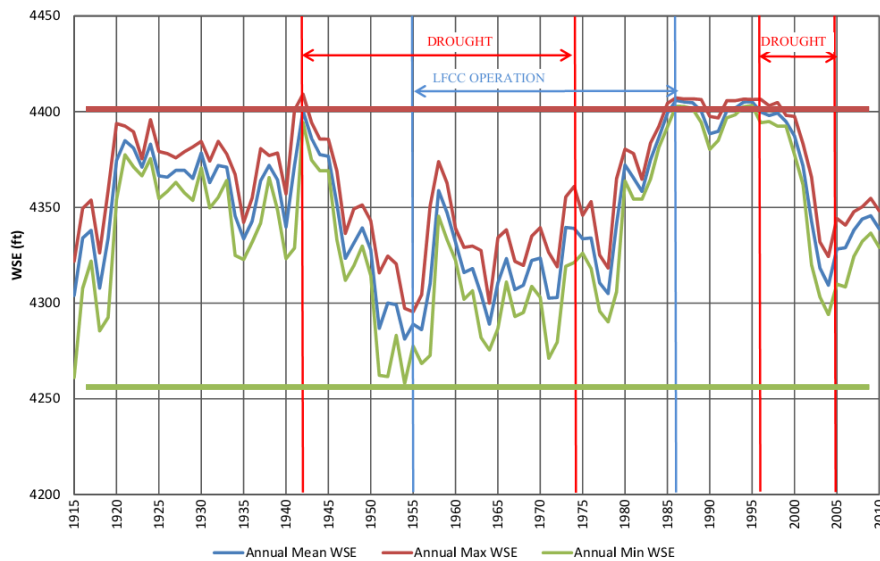


Figure 7.3. Elephant Butte Reservoir level time series (Owen, 2012)

7.1.1 Temporal changes in channel bed elevations

The temporal trends in reservoir stage and upstream bed elevation (Figure 7.4) show that channel bed elevation has responded to reservoir stage immediately at the locations within the reservoir, while the upstream bed elevation responded to the variation of water stage with some time delay. The bed elevation at the Narrows (EB-50) responds to reservoir stage fluctuation without delay. The increase of water stage by 40 ft between 2004 and 2009 caused the 7 ft increase of bed elevation at the Narrows. The reservoir effects propagated toward upstream reaches in sequence.

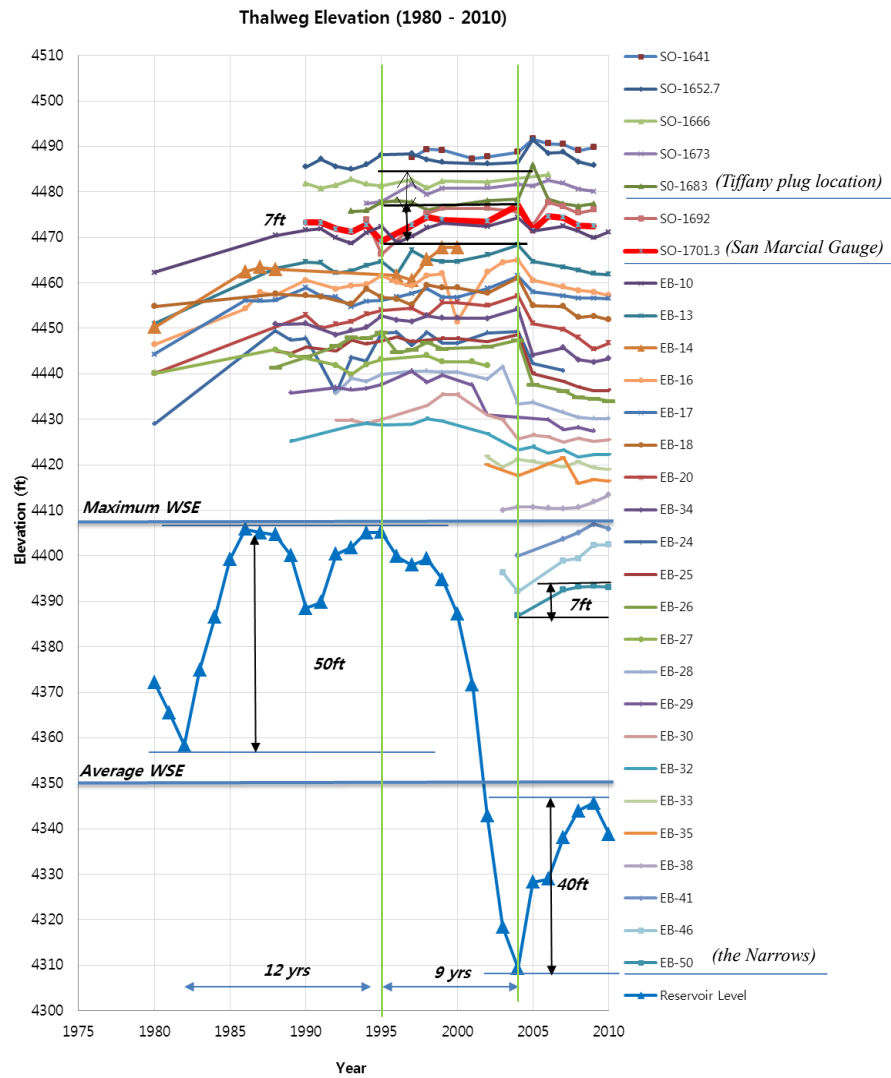


Figure 7.4. Changes in thalweg elevations from 1980 to 2010 (modified after Owen, 2012)

7.1.2 Mechanics of backwater effect on channel bed aggradation

During the sediment plugs in the Tiffany area, between 1991 and 2005, bed elevations around San Marcial Railroad Bridge (Agg/Deg 1701) continued to aggrade. Considering that the river bed elevation has been aggraded in the downstream reaches of the Middle Rio Grande, partial changes in bed elevation are attributed to reservoir effects.

Bed elevation changes due to backwater effects from the reservoir can be determined by an analytical approach using three basic equations, as mentioned in Section 5.1. To determine the backwater profile due to reservoir stages, the diffusive wave equation was used. The Exner equation was utilized to determine the magnitude of channel bed aggradation.

Figure 7.5 shows the downstream stage under the backwater effect that causes the decrease of sediment transport capacity, generating aggradation of the channel bed. The sediment transport capacity is a function of hydraulic radius (water depth for wide-rectangular channel) and friction slope. Therefore, the increase in water depth and the more significant decrease of friction slope lead to the reduction in transport capacity within the water body between cross sections 1 and 2.

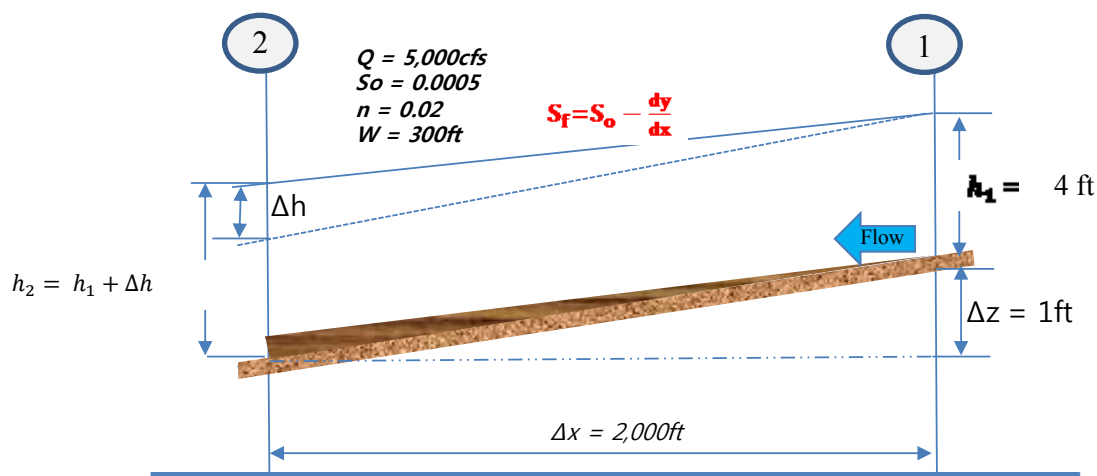


Figure 7.5. Channel bed aggradation due to reservoir backwater

The relationship between the backwater effect (Δh) and sedimentation was graphed in Figure 7.6. As the water depth increases to 1.5h at section 2, the aggradation rate is approximated as 0.17 ft per day. When discharges are maintained constant, the main channel fills up with sediments within three weeks. As the difference between the two sections increases, the days to fill the main channel decrease accordingly.

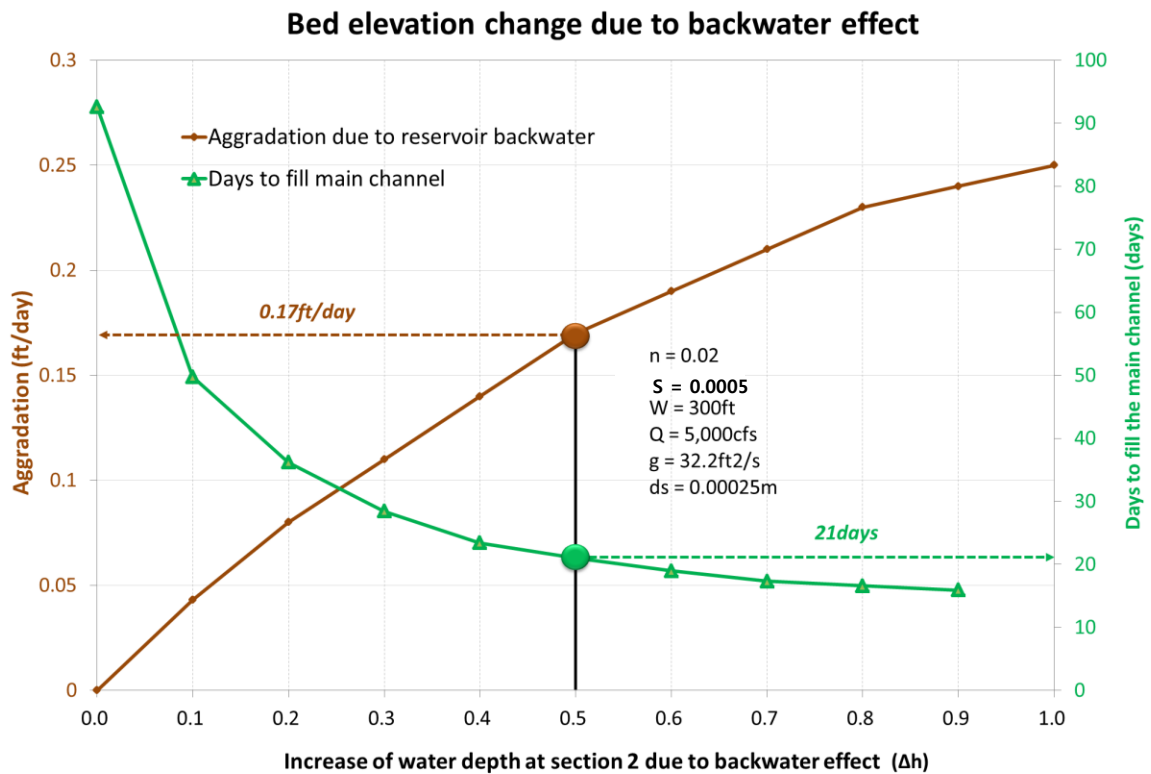


Figure 7.6. Bed elevation change due to backwater effect from reservoir

On the other hand, channel bed aggradation is dependent on the increase of channel width as well within the reservoir area. When the sediment-laden flood intrudes into the reservoir area with increasing channel widths, the magnitude of channel bed aggradation increases significantly. When the channel width at section 2 is double than at section 1, the aggradation rate becomes 0.23 ft/day, which is 50% higher than that of constant widths (Figure 7.7).

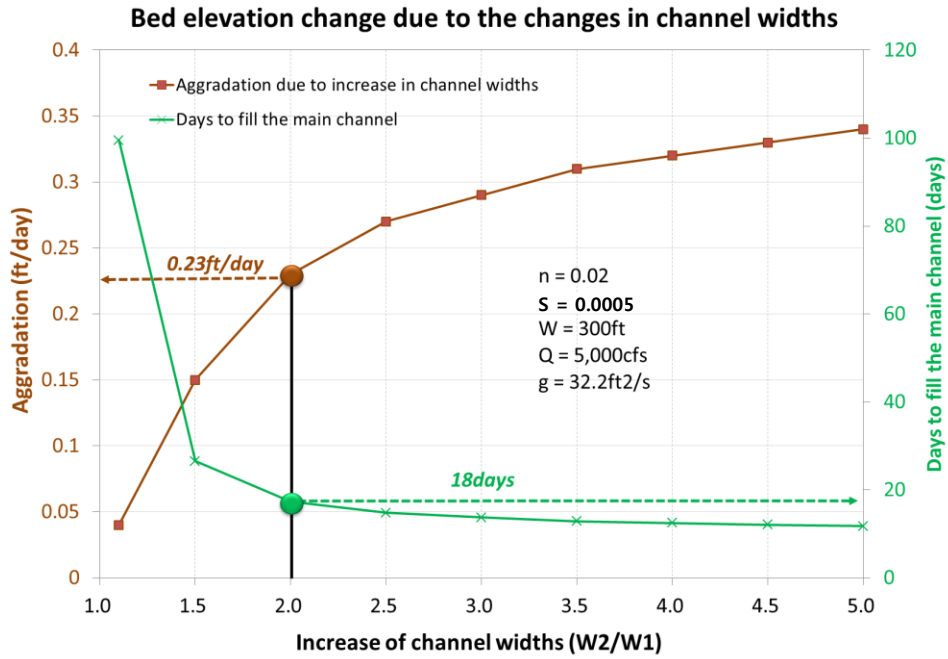


Figure 7.7. Bed elevation change due to the increase of channel widths

Therefore, the backwater effect combined with significant expansion near the Elephant Butte Reservoir (Figure 7.8), causes significant sedimentation at the river mouth.



Figure 7.8. Bed elevation change due to channel width expansion

The reservoir backwater effect on bed elevation changes along the longitudinal profile shows that, at the river mouth, the loss of energy and ensuing sedimentation is highest and decreases in the downstream direction (Figure 7.9).

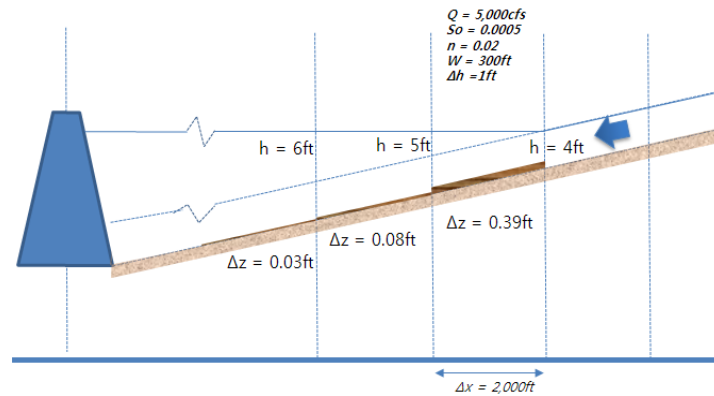


Figure 7.9. Backwater effect on bed elevation change at the river mouth

7.1.3 Aggradation time due to reservoir backwater

The aggradation time to fill the channel to 7 ft (bed elevation change between 1995 and 2005 at the Tiffany area) can be determined by using Julien's sediment transport capacity equation and Exner's equation. Assuming all sediment discharge deposits in the area, the filling time to 7 ft is 1,290 days (3.5 years) for 5,000 cfs ($141\text{m}^3/\text{s}$) and 3,864 days (10.5 years) for 1,550 cfs ($44\text{m}^3/\text{s}$), which is the average flow discharge between 1982 and 1995 (reservoir filling period).

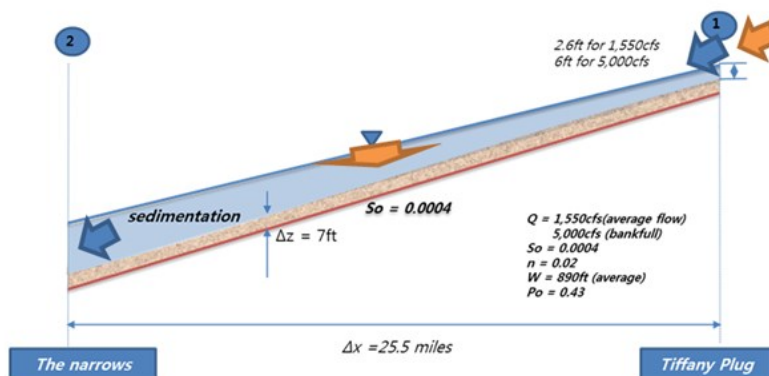


Figure 7.10. Time to fill the Channel (7 ft)

7.2 BACKWATER EFFECTS FROM A BRIDGE

The backwater from a bridge increases the water level of the upstream channel reach and decreases the sediment transport capacity, resulting in sediment deposits. Just 1.5 mile downstream from the Tiffany plug location (Figure 7.11a), the San Marcial Railroad Bridge crosses the Middle Rio Grande river.

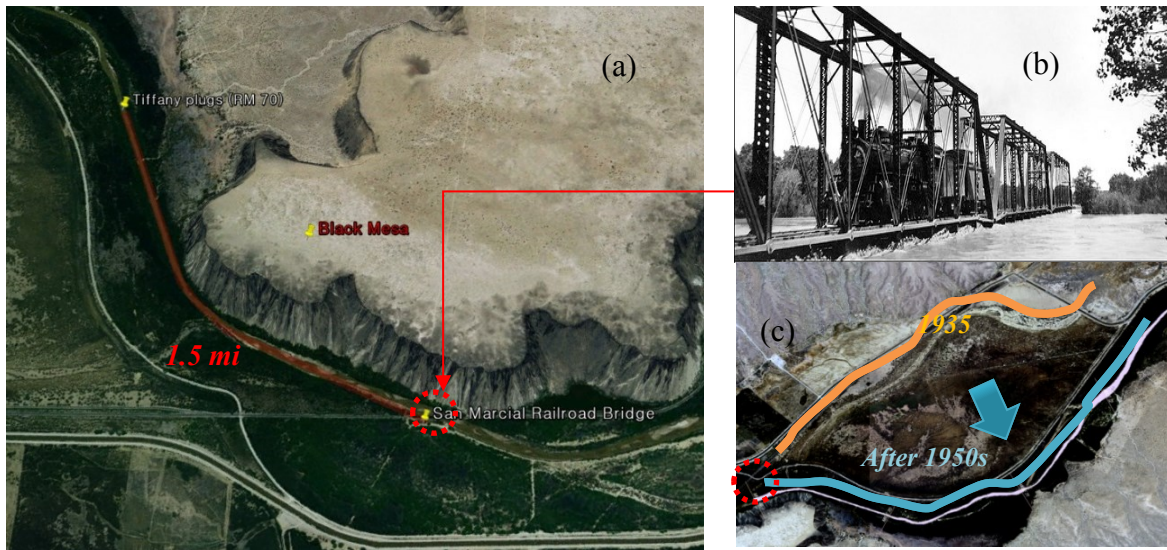


Figure 7.11. (a) Location of the Tiffany plugs, (b) the Railroad Bridge, and (c) new river route

7.2.1 The San Marcial Railroad Bridge

The steel truss-typed bridge with five spans and four piers (Figure 7.11b) was constructed in 1929. The lower cord of the bridge has been less than 5 ft above the channel bottom because of bed aggradation and reduced flow conveyance. The original channel around this area in the 1930s, which was the natural river system, has been changed to the present river route after the Rio Grande Project (Figure 7.11c), causing the bridge piers to be skewed 30° against the flow direction. The lack of channel conveyance due to the pier obstruction and skewedness induced upstream sedimentation (USACE 2010).

7.2.2 Backwater effect due to the San Marcial Railroad Bridge

7.2.2.1 Backwater effect on water depth

Although there has been an analytical approach to calculate the backwater effects from bridge piers by various authors, empirical equations are commonly used in engineering projects. The HEC-RAS manual (USACE 2010) provides four standard methods for computing the energy losses through the bridge. In this research, Yarnell's Equation was used to compute the increase of water level. Figure 7.12 shows the water level increase due to contraction of bridge piers using Yarnell's equation.

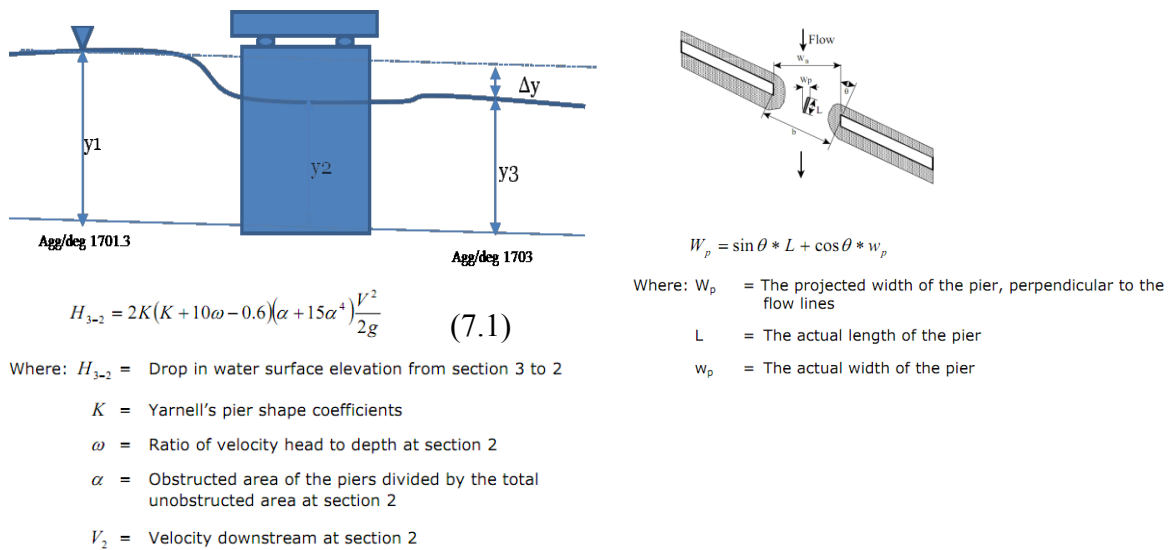


Figure 7.12. Sketch of backwater at bridge contraction

The bridge piers were rectangular, thus K , the coefficient for pier shape, is 1.25. The pier-to-pier distance is 150 ft, pier width is 5 ft, and pier length is 20 ft, thus $\alpha = \frac{\sin 60 * 20 + \cos 60 * 5}{150} = 0.13$. The flow depth in the downstream of the bridge and the Froude number are dependent on cross section geometry and flow conditions. In the case of 5,000 cfs discharge with 200 ft width, 0.0005 bed slope, and 0.02 Manning roughness, the increase of water level due to backwater effect from the bridge can be determined as 1 ft.

7.2.2.2 Backwater effect on sedimentation

The process to determine the backwater effect on channel bed elevation is the same as the backwater effect from a reservoir. The increase of water depth causes the drop of flow velocity at the plunging point and ensuing sedimentation. When the flow and sedimentation are being supplied from the upstream reach, a significant amount of sediment will be deposited at the low velocity location and a lower sediment concentration will be delivered downstream (Figure 7.13). The sediment deposits around the transitional zone between the river and the temporary reservoir. The decreased bed slope induces upstream aggradation. Based on the increase of water depth and effect on channel bed sedimentation, the backwater effect due to the railroad bridge impacts the sediment plug formation with significant probability. The historic inundated area due to the 2005 flood shows that the backwater reaches the Tiffany plug location.

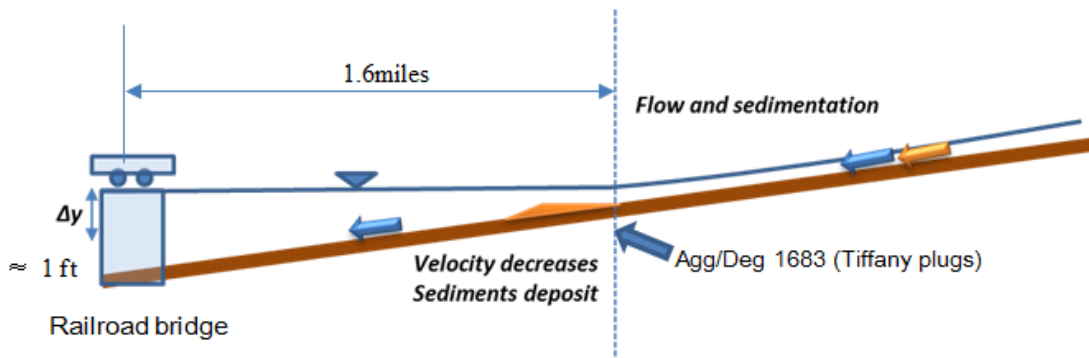


Figure 7.13. Location of Tiffany plugs and sedimentation due to backwater effect



Figure 7.14. Inundated area with 2005 Flood (CSU database)

7.3 BACKWATER EFFECTS FROM SHARP BENDS

7.3.1 Sinuosity in the Middle Rio Grande

River sinuosity can be defined as the ratio of the channel length to the valley length between two points located on the river. In general, sinuosity increases the energy loss and cross-sectional area and decreases the flow velocity and sediment transport capacity (Julien 2002). The energy loss of sinuosity results from additional turbulence due to secondary flow, additional bed shear, distortion of flow velocity, and separation of flow (Woo 2002). The increase in centrifugal acceleration due to sinuosity also has an influence on the super-elevation at the concave outer bank and additional stress on the bank slope. Historically, the channel of interest in this research has been straightened with time (Figure 7.15). Sinuosity for sub-reaches ranges from 1 to 1.2 and average sinuosity has been generally decreased in the river sections (sub-reach 1 to 4), while the reservoir sections (sub-reach 5 to 9) have varied depending on the reservoir levels.

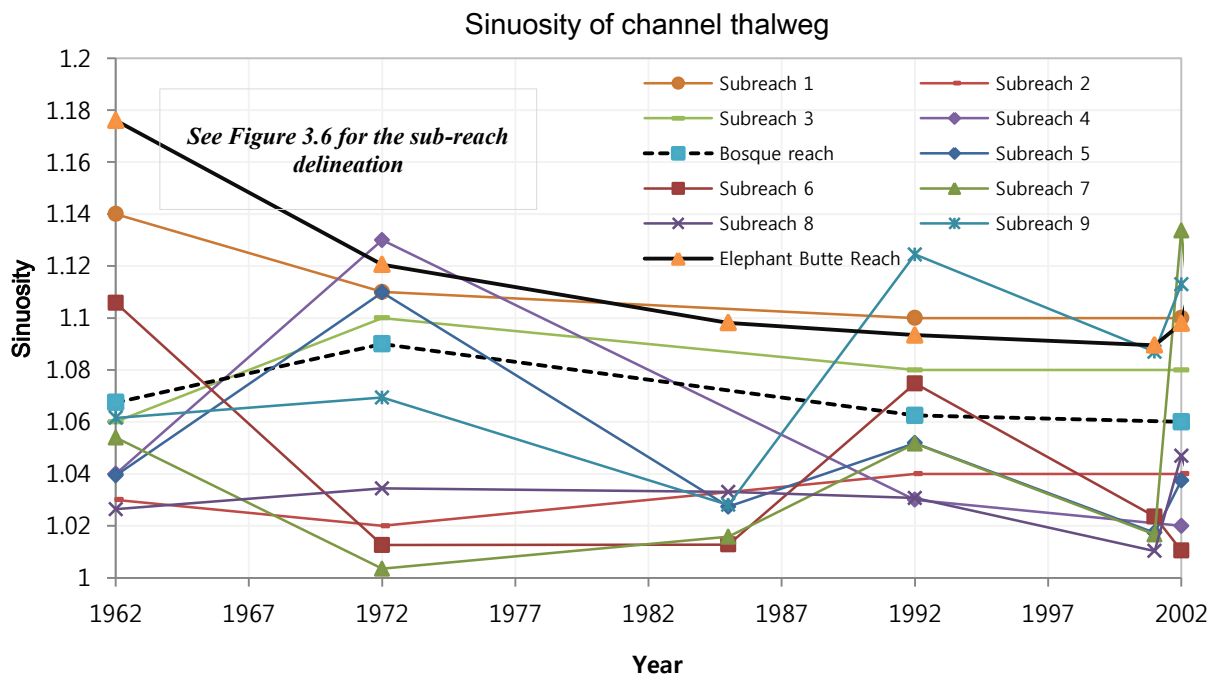


Figure 7.15. Sinuosity of channel thalweg (1962 – 2002)

7.3.2 Sharp bends

In contrast to the overall channel straightening, sharp bends, which were observed around the Bosque sediment plug at Agg/Deg 1555 ~ Agg/Deg 1557, have had higher sinuosity over time (Figure 7.16). In 1996, the channel was braided and no meandering was observed. The 2005 Google imagery shows one sharp bend of 90 degrees around Agg/Deg 1555 and lateral migration due to meandering caused the erosion of the east side bank and formed another bend at Agg/Deg 1557. The present channel has two 90 degree bends in sequence.

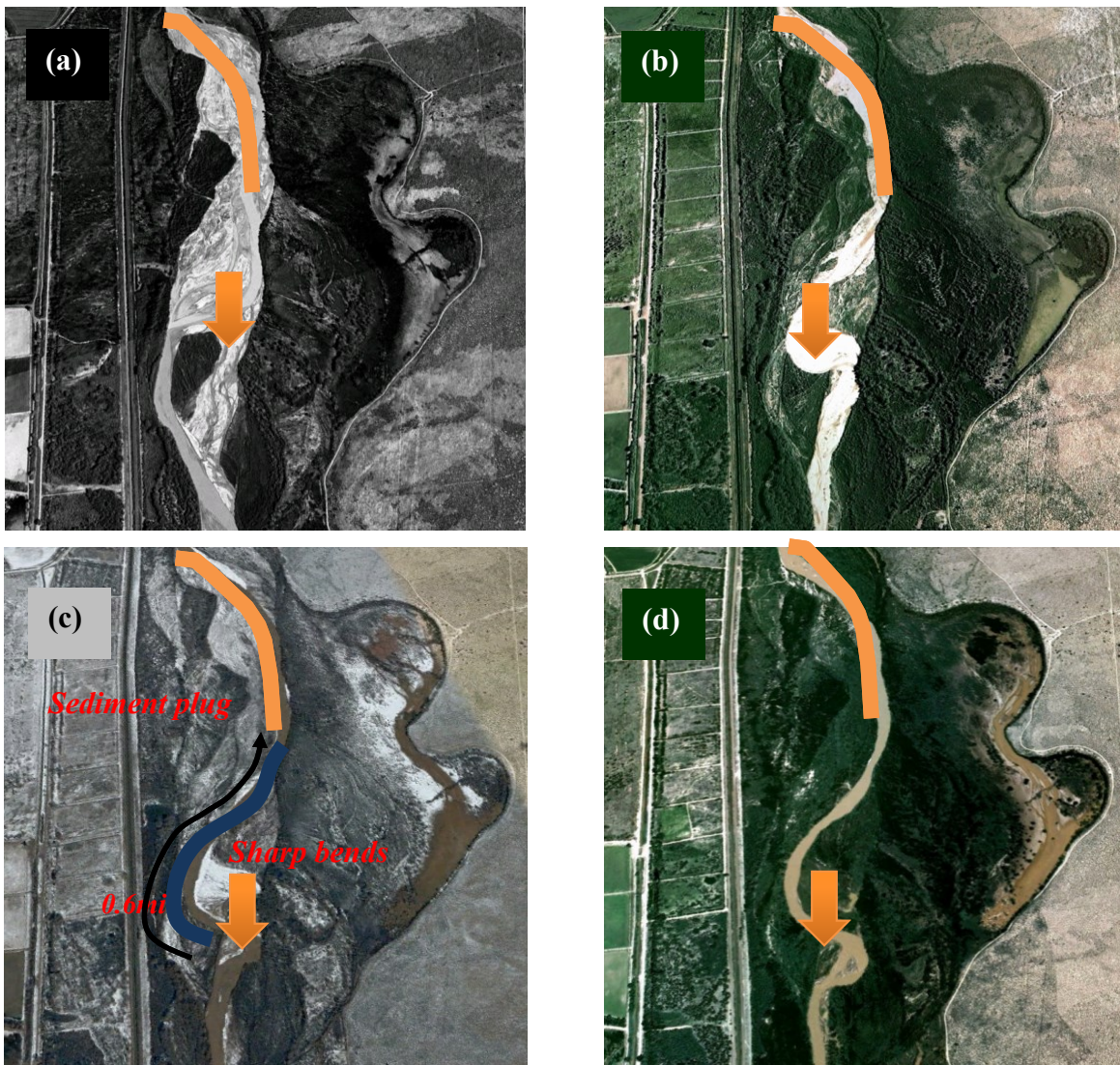


Figure 7.16. Progress of sinuosity (Agg/Deg 1555~1557) (a)1996, (b)2005, (c)2006, and (d)2009

7.3.3 Backwater effect on water depth

In order to consider the effect of channel sinuosity on backwater profile and sediment transport, the energy loss due to sinuosity can be determined by using the following equation.

$$\Delta E = K_b \frac{V^2}{2g} \quad (7.2)$$

where ΔE : energy loss due to bended channel thalweg, K_b : energy loss coefficient, V : flow velocity. Several authors proposed equations to estimate the energy loss coefficient K_b : (1) analytical equations based on variables associated with energy loss (Froude number, water depth, channel widths, radius of curvature, meandering angle); (2) Mockmore's (1944) empirical equation; (3) Scobey's (1933) increase of Manning coefficient and energy loss due to meandering; (4) Rozovskii's (1957) energy loss coefficient; and (5) Chang's (1983) energy loss coefficient. Among these, Rozovskii's method was used in this computation.

$$\Delta E = K_b \frac{V^2}{2g} = (24 \frac{\sqrt{g}}{C} + 60 \frac{g}{C^2}) (\frac{y}{r_c}) \theta \frac{V^2}{2g} \quad (7.3)$$

where, g : gravitational acceleration, C : Chezy coefficient (Conveyance), y : flow depth at downstream, r_c : radius of curvature, θ : meandering angle.

At a 5,000 cfs discharge, Table 5.1 shows an energy loss of 0.76 ft between sections 3 and 4, 0.56 ft between sections 2 and 3, and 0.31ft between sections 1 and 2 (Figure 7.17). The total energy loss is estimated at 1.6 ft. The average bed slope of the upstream reach was around 0.0003, thus the increased water depth might propagate roughly 1 mile upstream (1.6 ft / 0.0003 = 5,300 ft \approx 1 mile).

Table 5.1. Energy loss due to sharp bends

Sub-reaches	W(ft)	H(ft)	C	r(ft)	V(ft2/s)	Bend angle(degree)	Energy loss (ft)
3-4	205	5.8	100.0	290	4.18	90	0.8
2-3	360	4.2	94.5	340	3.33	160	0.6
1-2	195	6.0	100.5	810	4.3	95	0.3
Total							1.6

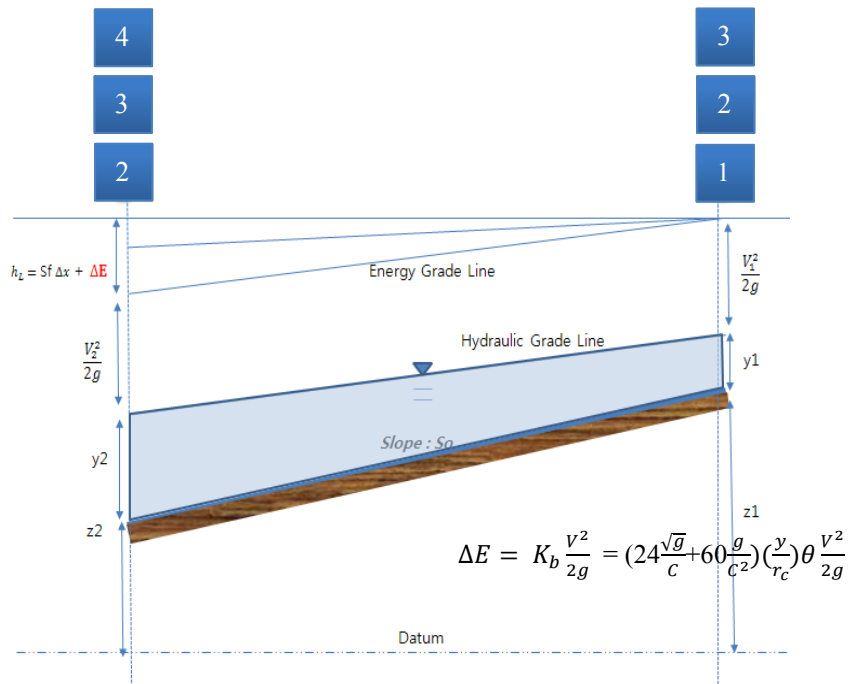
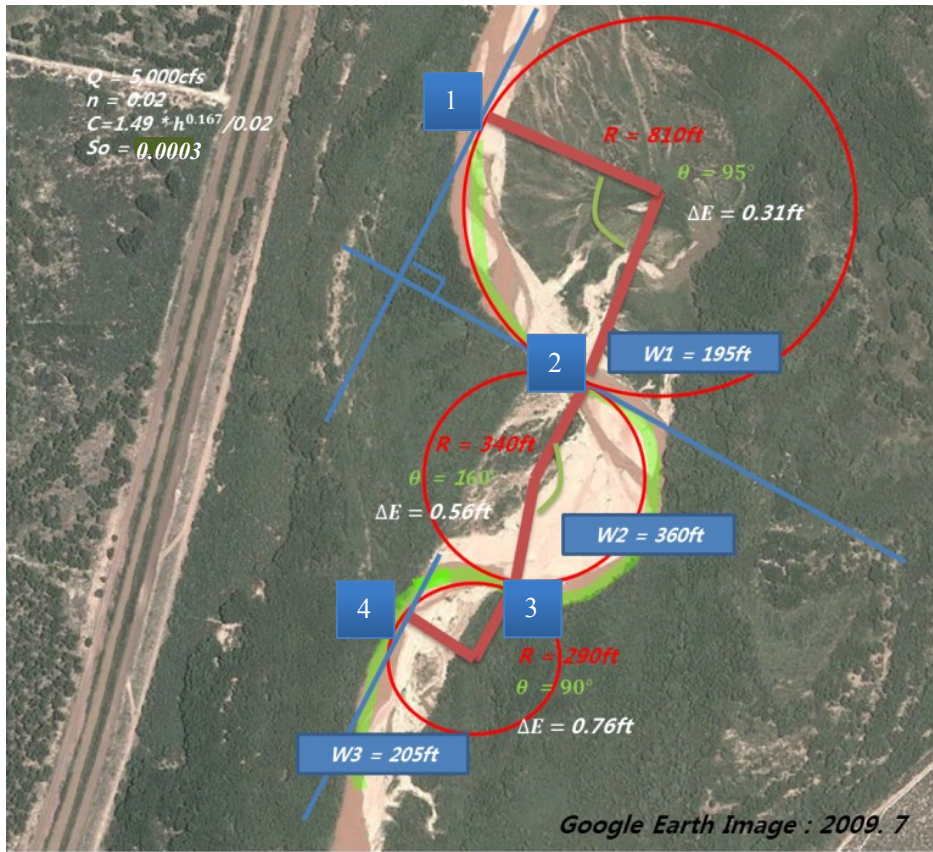


Figure 7.17. Sharp bends at Agg/Deg 1555 ~ 1557

7.3.4 Backwater effect on sediment deposits

The energy loss due to sharp bends caused the aggradation of the channel bed. From the Saint-Venant equation ($S_f = S_o - \frac{\partial h}{\partial x} - \frac{v}{g} \frac{\partial v}{\partial x}$), the energy loss can be described as $\frac{\Delta E}{\Delta x} = S_o - S_f$.

The loss of energy caused the decrease of sediment transport capacity as $Q_s =$

$18W \sqrt{gd_s^3} \left(\frac{hs_f}{(G-1)d_s} \right)^2$, leading to the channel bed aggradation (Figure 7.18). As the increase in water depth reached about 1 mile upstream and the historic sediment plug location was 0.6 miles upstream, the backwater effect accelerates the channel bed aggradation.

To quantify the magnitude of aggradation, the sediment filling time was determined by using the same procedures as the reservoir effect on sedimentation. Assuming that the inflowing sediment deposits within the backwater zone, the time to fill the main channel up to 2.85 ft, which was the channel depth at Agg/Deg 1550 in 2002, was estimated as approximately 17 days. This result shows that two sharp bends less than 1 mile downstream from the 2008 Bosque plug location were the primary causal factor during snowmelt floods. Although the time to fill depends on the flow discharge, the main channel can be filled within several weeks.

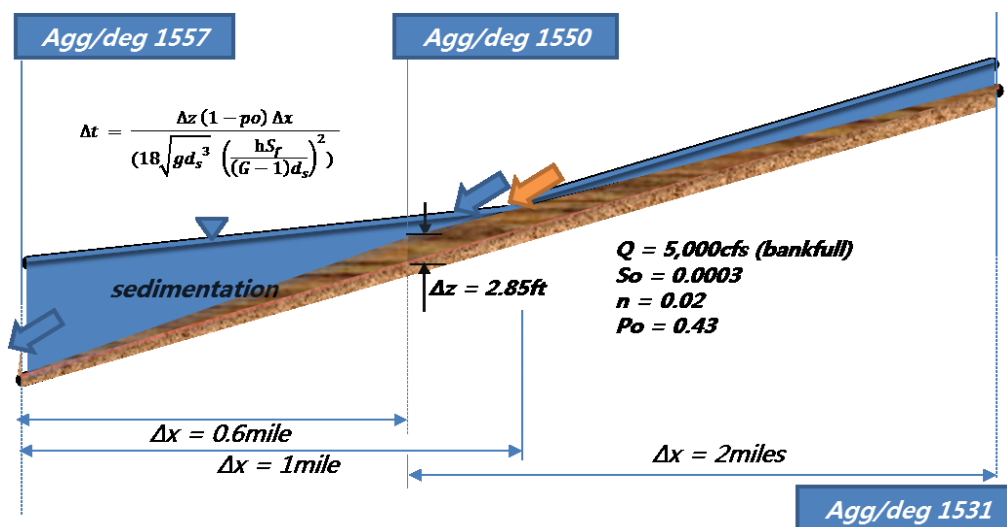


Figure 7.18. Time to fill active channel with sediments

CHAPTER 8 NUMERICAL SIMULATIONS

8.1 INTRODUCTION

A 1-D aggradation/degradation numerical model was developed to verify the seven criteria to reproduce the historic sediment plug formations: contraction and expansion of channel widths, roughness, perching and overbanking, vertical sediment concentration profile, and the change in backwater profile due to downstream reservoir and/or bridge piers, sharp bends.

Basically, the model is composed of hydrodynamic and sedimentation modules. In hydrodynamics, the water surface profile is computed considering energy loss, cross section variation, and reservoir stage. After the water depth for each cross section is calculated, the sediment transport capacity is calculated for each cross section. Finally, with Exner's bed change equation, the new channel bed elevation is determined and used for the next calculation of the water surface profile.

8.2 HYDRODYNAMICS

A water surface profile is determined by a standard step formation of the quasi-steady dynamic wave of the St-Venant equation ($S_f = S_o - \frac{dh}{dx} - \frac{V}{g} \frac{dV}{dx}$), which can be expressed as (Chow 1959, Abbott 1979):

$$\frac{dh}{dx} = \frac{S_o - S_f}{1 - F_r^2} \quad (8.1)$$

where S_o is the bed slope, S_f is the friction slope, F_r is the Froude number, h is the flow depth, and x is the distance along the channel. In order to compute the backwater profile by integrating the water profile equation, the trial-error approach was used (Cunge et al.1980).

A water depth for each cross section is determined by starting a trial value and iterating before the error approach to less than a given error tolerance. When the error between current and previous time steps is still greater than error tolerance, current flow depth is used to compute the flow depth of the next upstream cross section. Hydraulic geometry characteristics of the channel can be computed for trapezoidal or rectangular cross sections. The side slope, z , has to be specified in either case. If $z=0$, the cross section is rectangular. The component of the program that computes the backwater profile works for rectangular and/or trapezoidal cross sections.

As the model uses the VBA platform on Excel, data input, simulation run, and post-processing graphics are displayed on a GUI basis. Cross section data and HEC-RAS geometry are from Reclamation. The 1992 cross sections are used for the 1995 Tiffany plug simulation and the 2002 cross sections for the 2008 Bosque plug simulation. The Bosque and Elephant Butte cross sections are combined for an integrated HEC-RAS geometry. Through averaging and comparing with GIS maps, 67 wide-rectangular cross sections 1,000 m apart are used. The cross section data include distances, bed slopes, initial bed elevations, minimum bed elevations, bottom widths, bank crest elevations, and Manning n . These geometric data are obtained from the HEC-RAS geometry and processed to fit a new model.

Flow discharge, water temperature, and upstream bed elevation /downstream reservoir stage are also input on a daily basis as default. Values were interpolated for shorter than daily simulation time steps. Flow discharges at San Marcial are also used as inflow data. Flow discharges at San Acacia are used to determine the amount of overbank flow and water losses during delivery. The water temperatures at San Acacia determine the viscosity of sediment-laden flows. Since temperature observations are not available on a daily basis, missing temperature values are acquired by interpolating existing temperature data.

The upstream bed elevation and the reservoir stage are the boundary conditions. The upstream end is located at Arroyo de las Canas, where the bed elevation has been stable over time. Overbank flows above bank crest are computed by using the broad-crested weir equation (Mays 1999), which is a function of the weir length and overbank water depth. The weir length uses the distance between neighboring cross sections and the water depth above bank crest is used for the depth in the equation. The most important parameter, weir coefficient was computed by comparing flow discharge between San Acacia and San Marcial gauges. The loss of water in simulation should be the difference of water discharge between two flow gauges.

When the channel is perched, the loss of water from the active channel to floodplains does not return to the active channel, while the un-perched channel does. Accordingly, the model considers the flow to perched floodplains as water loss, while an un-perched channel deals with the loss of water as lateral inflow to the next cross section. In addition, there are 2 major locations where return flows occur, as forementioned. The location where return flows occurs are detected by the geometric data using LIDAR, DEM, HEC-RAS, and satellite imagery.

For computing backwater effects due to reservoir stages on channel sedimentation, reservoir stages in the simulation are set to E.L.4107 ft, which was the maximum reservoir level. Backwater profiles due to the railroad bridge were determined from: (1) the flow depth downstream of the bridge; (2) the Froude number; and (3) Yarnell's equation. During the numerical simulation, the water surface profile is calculated in the upstream direction. The energy loss due to channel meandering is determined by Rozovskii's equation.

8.3 SEDIMENTATION

Yang's (1973) total sediment transport equation and Julien's (2002) simplified sediment transport equation were used to compute the sediment discharge along the channel at each time step. Based on the given hydraulic variables, sediment discharge in terms of sediment concentration by volume can be determined. Figure 8.1 shows the procedure to compute the sediment transport capacity of a given cross section.

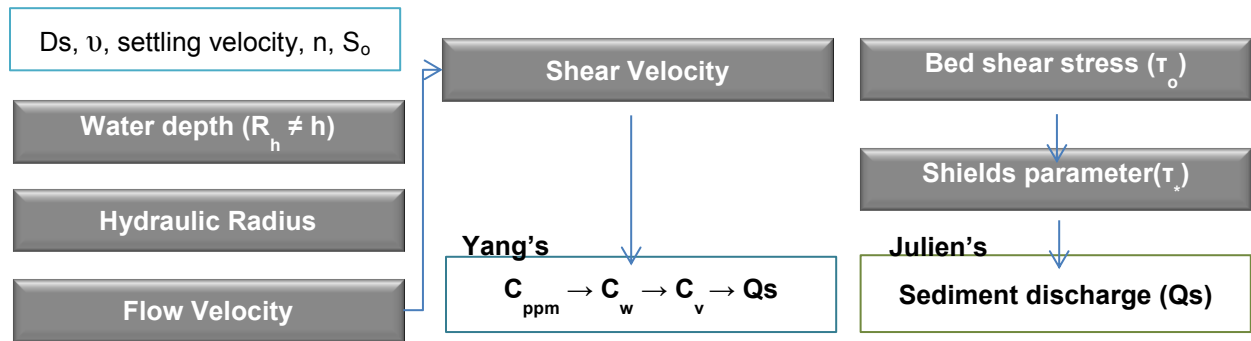


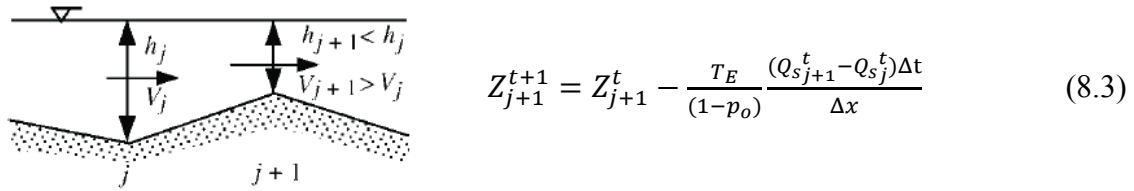
Figure 8.1. Procedure to compute the sediment discharge Q_s

The sediment concentration profile was determined by calculating the Rouse number and the shear stress at each cross section. A sediment diameter of 0.25 mm was used through the whole simulation. The summation of the distribution profile was done with Simpson's integration rule (Chapra 1990, Moin 2010). The amounts of sediment in the main channel and overbank areas were computed by using overbank flows and overbank sediment concentration. Changes in channel bed elevations were computed with the conservation equation of sediment without sediment source (Julien 1995) given by:

$$\frac{\Delta A}{\Delta t} + \frac{T_E}{(1-p_o)} \frac{\Delta Q_s}{\Delta x} = 0 \quad (8.2)$$

where A is the area of the bed layer, P_o is the porosity of the sediment, Q_s is the sediment discharge by volume, and T_E is the trap efficiency, defined as $T_E = 1 - e^{(-\frac{\Delta x \omega}{q})}$ (≈ 1), ω is the sediment fall velocity, q is the unit discharge, and x is the distance along the channel.

This equation can then be discretized in terms of the change of channel bed elevation as:



$$Z_{j+1}^{t+1} = Z_{j+1}^t - \frac{T_E}{(1-p_o)} \frac{(Q_{s_{j+1}}^t - Q_{s_j}^t) \Delta t}{\Delta x} \quad (8.3)$$

Figure 8.2 channel aggradation/degradation numerical model

The superscript, t, refers to a node in time and the subscript, j, refers to a node in space. The subscript, j, increases in the downstream direction. The median grain size, d_{50} , is used to compute the sediment load as ds. The grain size does not change along the main channel. It is assumed that the bed elevation at the first upstream node does not change with time as the upstream boundary condition. Due to the numerical scheme used (forward in time and backward in space), the change in elevation computed between the first upstream node j and the adjacent node downstream j + 1 will be assigned to the node j + 1. The slope at node j is the slope computed with the elevations of nodes j (upstream) and j + 1 (downstream).

8.4 STABILITY

The stability of the hydraulic model depends on the time step, Δt , and space intervals, Δx , specified. The stability of the model is checked at each node with the Courant-Friedrichs-Lewy condition. The Courant-Friedrichs-Lewy number can be expressed as $\frac{\Delta t}{\Delta x} \frac{5}{3} V$, when using Manning's resistance equation, where V is the mean flow velocity (Julien 2002). If C exceeds 1, the model produces a warning message to indicate that numerical instability is likely to occur. For stable sediment calculations, weighting factors for hydraulic parameters from the HEC-6 manual were used: (1) 1 at upstream point; (2) 0.5 at downstream point; (3) 0.25~0.5 at interior point; and (4) $\alpha = 0.6$ for the change in bed elevation ($\Delta Z_j = \alpha \Delta Z$, $\Delta Z_{j+1} = (1 - \alpha) \Delta Z$).

8.5 PROGRAM LIMITATIONS

The model was developed for subcritical flow. Therefore, the flow is controlled at the downstream end of the channel. The downstream flow depth must be provided to start the computation of the backwater profile. The program computes the normal depth at the first downstream node to start the backwater computation. If an adverse slope develops in the first downstream node, the model will stop because normal depth does not exist on adverse slopes. The model uses a fixed rectangular cross section, thus lateral migration and changes in width are not considered in this model. Bank erosion and bed surface armoring are out of the study scope. Channel patterns and in-stream features are not included. Cross sections are estimated as a single thread channel. The lateral flow velocity distribution and the lateral sedimentation distribution are also out of the simulation scope. Figure 8.3 shows the program structure and modeling procedure based on these limitations and assumptions.

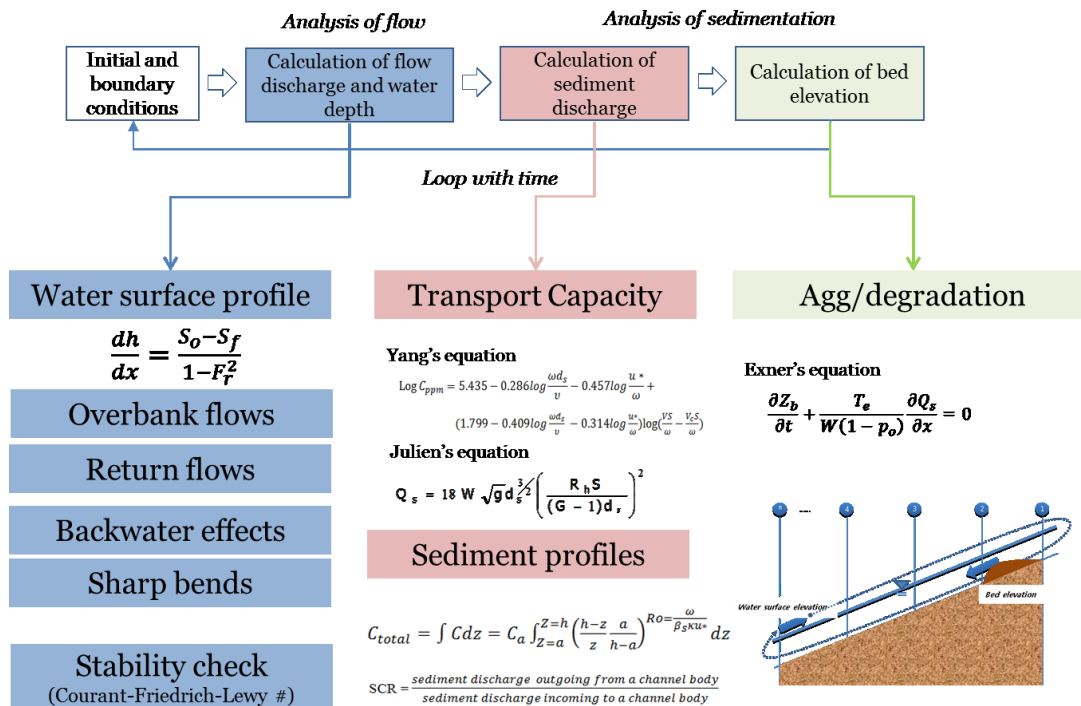


Figure 8.3. Program structure and modeling procedure

8.6 APPLICATION TO THE MIDDLE RIO GRANDE

Aggradation/degradation simulations are applied to the Rio Grande based on limited irregular surveys, thus, in some cases, quantitative and/or qualitative evaluations were carried out. For sediment plug simulations, the 1995 Tiffany plug was used for calibration and the 2008 Bosque plug for validation.

8.6.1 Geometric factors

Bender (2011) showed that the flow is subcritical in the entire reach. An expansion between cross sections yields a backwater M-1 type profile, while flow depths lower than normal depths lead to an M-2 curve (Figure 8.4). A channel bed elevation aggrades at expansion reaches, while contraction reaches degrade. The increase in roughness causes an increase of water depth and variability of friction slope. The decreased friction slope leads to the decrease of sediment transport capacity, which causes the channel sedimentation. The changes in channel widths itself have limited effects on channel sedimentation (Figure 8.5).

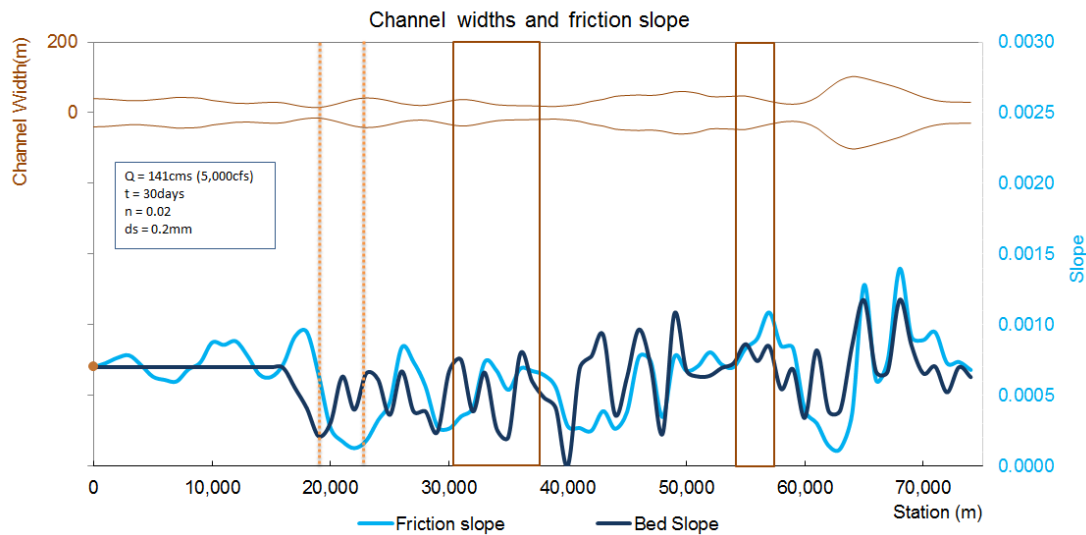


Figure 8.4. Distribution of friction slope and bed slope depending on channel widths

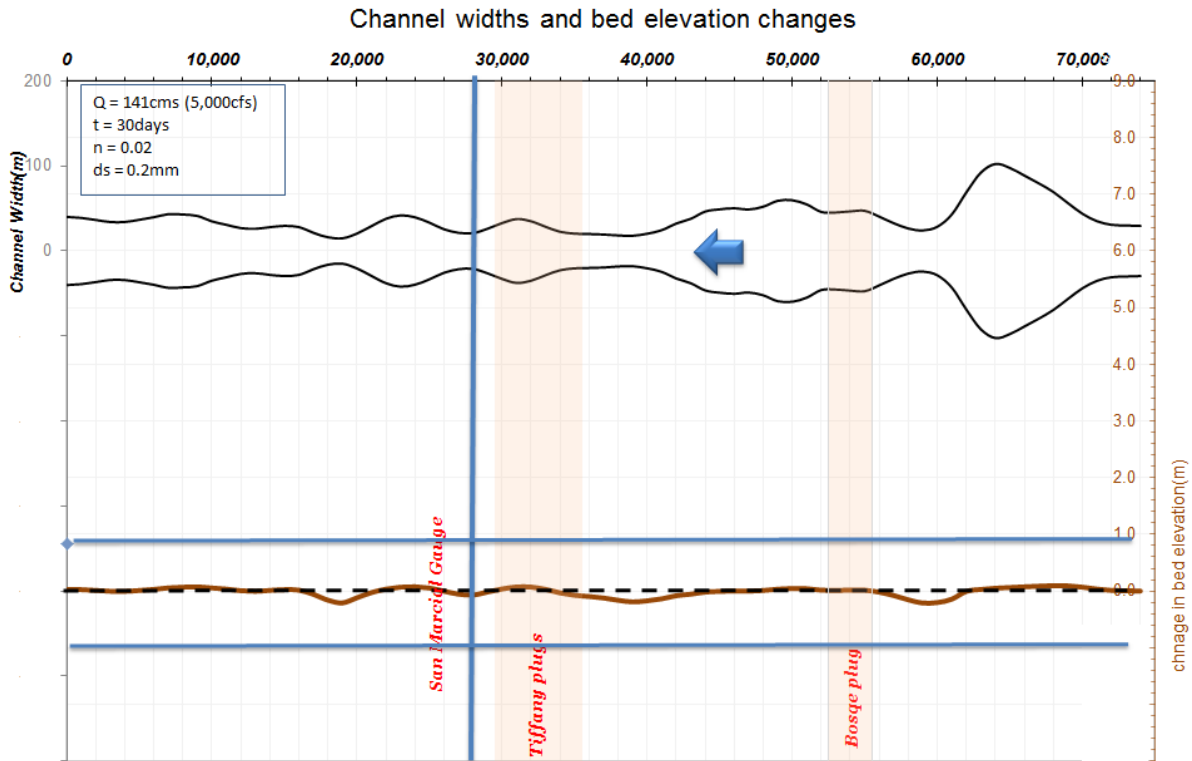


Figure 8.5. Bed elevation changes depending on channel widths

8.6.2 Overbank flows and concentration distribution profiles

The 2008 Bosque plug was simulated with uniformly distributed concentration profiles and non-uniform concentration profiles (Figures 8.6 and 8.7). The flow discharge above the bank crest was lost to overbank areas. The height of main channel aggradation, when a vertical concentration profile was considered, was greater than that of uniformly distributed sediment discharge. Rouse number ranged 0.4-7.6 and an average value was 1.1. Considering that the aggradation of the Bosque sediment was about 1 m, the simulation result was reasonable. Thus, overbank flow and concentration distribution accelerates channel sedimentation more than other factors in a short time of period.

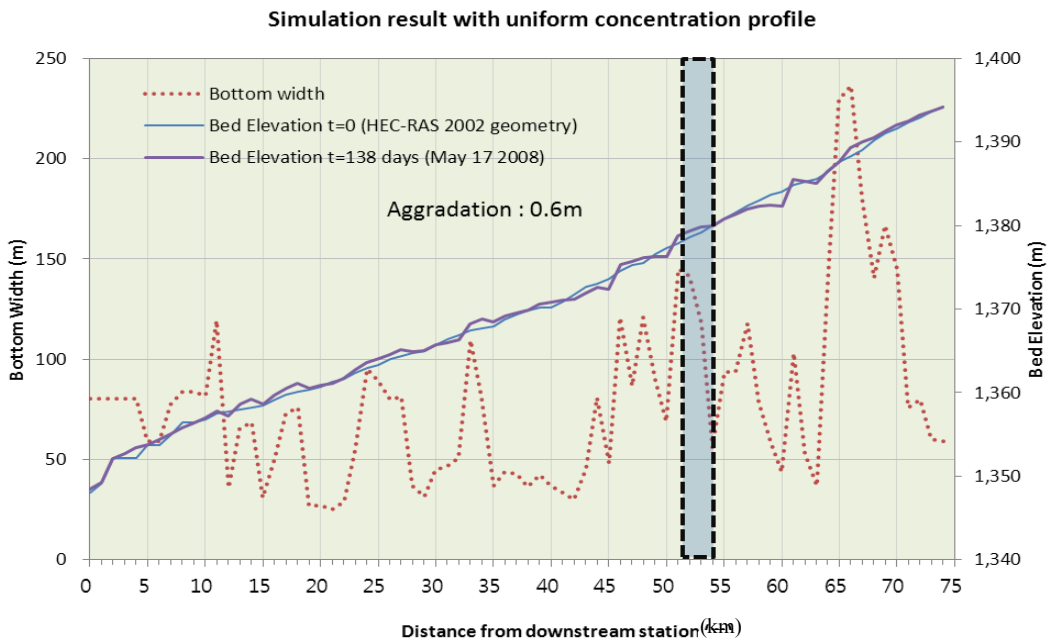


Figure 8.6. Simulation results with uniform concentration profile at Bosque plug location

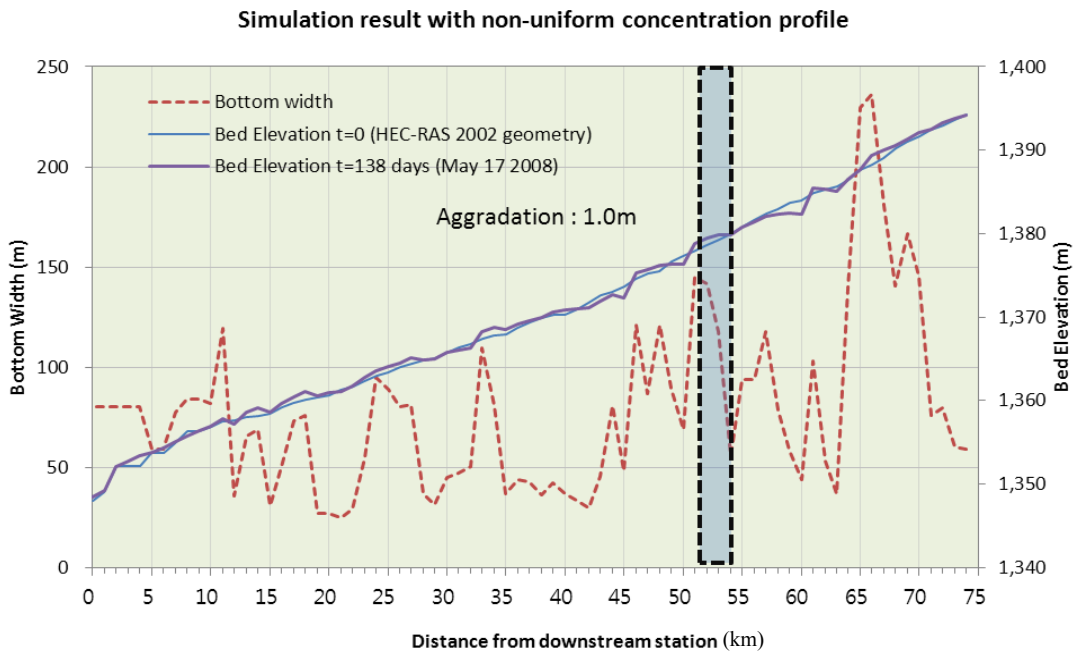


Figure 8.7. Simulation results with non-uniform concentration profile at Bosque plug location

8.6.3 Backwater effects from the reservoir, the bridge, and sharp bends

Backwater effect from the reservoir

When the reservoir stage remains constant at maximum water level (E.L.1343 m) through simulation, the reservoir effect on the Tiffany plug location would take over 10 years (Figure 8.8). The reservoir stage has a limited short-term influence on aggradation and degradation. But the long-term high bed elevation due to the reservoir stage provides the channel with feasible geometric conditions.

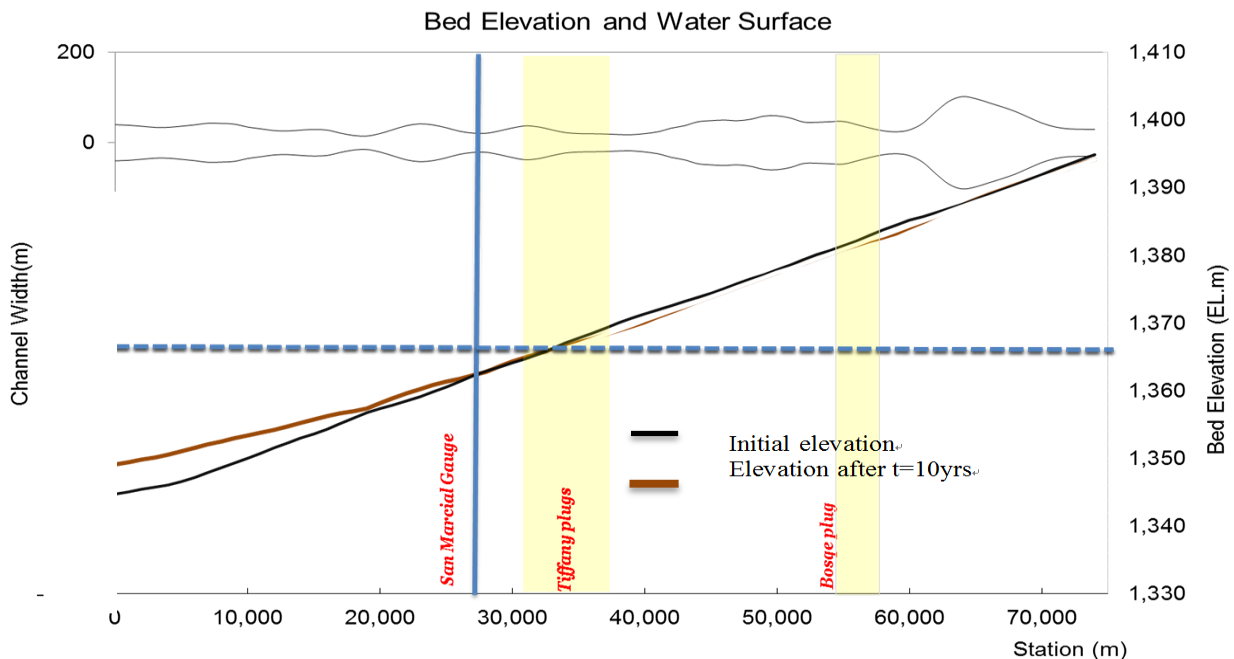


Figure 8.8. Channel bed aggradation due to reservoir backwater

Backwater effect from the bridge and sharp bends

Backwater from the San Marcial Railroad Bridge causes an increase in water depths in the upstream areas, which leads to more sedimentation at the Tiffany plug locations during floods (Figure 8.9).

The sharp bends between Agg/Deg 1554 and Agg/Deg 1558, observed just downstream of the Bosque sediment plug location, cause the loss of energy, which leads to the increase of water depths at the upstream reaches (Figure 8.10). Like the backwater effect from a bridge, the increase of water depth in the sharp bends induced backwater and sedimentation near the Tiffany plug area.

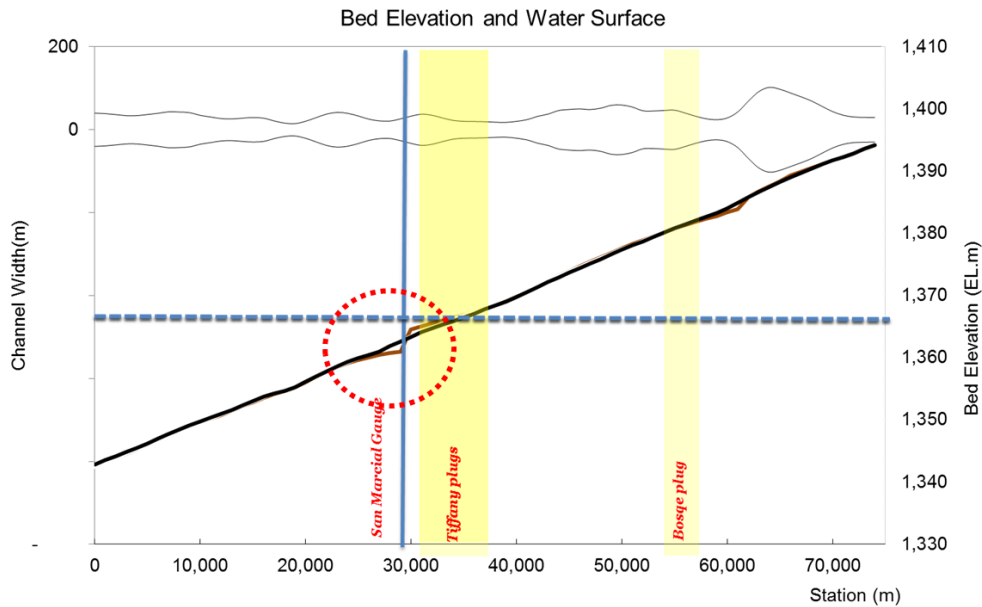


Figure 8.9. Backwater effect from the bridge on bed elevation

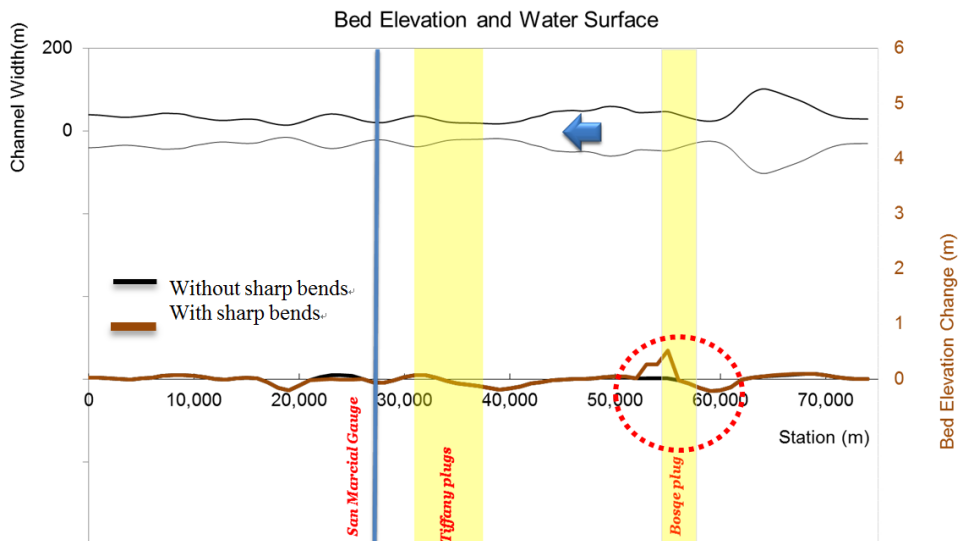


Figure 8.10. Backwater effect from sharp bends on bed elevation

8.6.4 Application to the Middle Rio Grande sediment plugs

Combining all seven causing factors affecting the mechanic of sediment plug formation, the 1-D aggradation-degradation model was applied to the historic sediment plugs. With monitored flow discharges and water temperature as well as geometric data, the numerical model results show that aggradation tendency at the historic plug locations is distinct compared with adjacent sub-reaches.

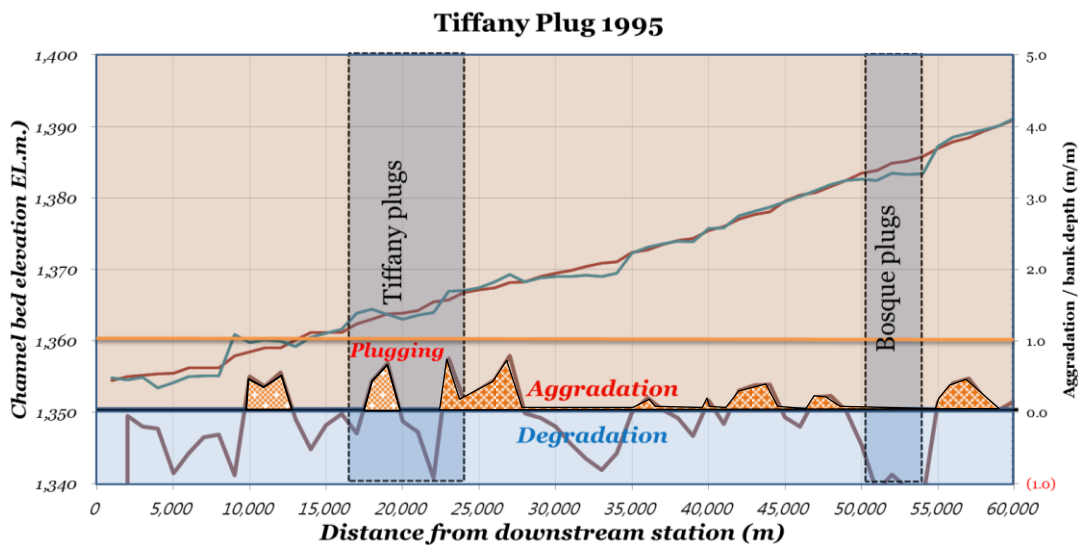


Figure 8.11. Simulation of 1995 Tiffany plug

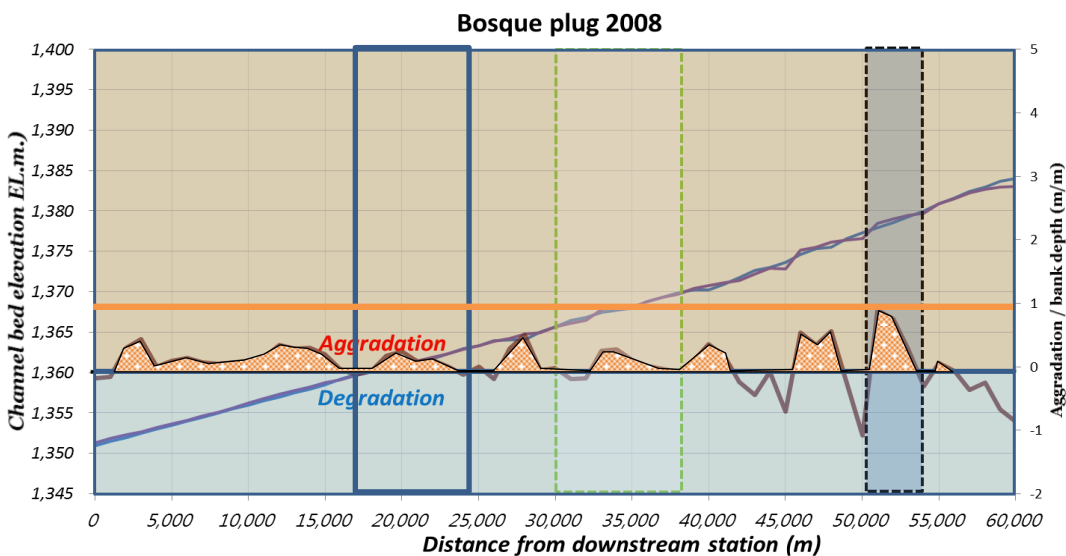


Figure 8.12. Simulation of 2008 Bosque plug

CHAPTER 9 SUMMARY AND CONCLUSIONS

Based on the historic flow and geometric characteristics of plug areas, seven parameters were identified as major causing factors of sediment plug formation in the Middle Rio Grande. These factors were divided into three categories and analyzed to assess the primary causing factors using analytical and numerical methods. Conclusions with respect to the mechanics of sediment plug formation are summarized as follows:

- ***Geometric factors: channel width and roughness***

The channel has narrowed 40% between 1962 and 2002 and channel capacity has decreased over time (77% at Bosque plug area). The channel narrowing and vegetation encroachment toward the main channel caused the 50 % increase of the representative composite roughness between 1992 and 2002 at 5,000 cfs discharge. Accordingly sediment transport capacity has decreased 45%. The historic sediment plugs occurred at the sub-reaches 3 and 6 had lower transport capacity compared with adjacent sub-reaches. The decrease of channel width (40% over 40 years) does not cause significant increase of sediment transport capacity ($0.6^{-0.2} = 1.1$, 10% increase over 40 years), while the increase of roughness (50%) causes considerable loss of sediment transport capacity (45%). Therefore geometric factors induce more overbank flows and channel bed aggradation.

- ***Sedimentation factors: overbank flows and sediment concentration profiles***

While the cross-section of the Bosque plug was wide with a relatively wide floodplain, the Tiffany plug cross-section was narrow and perched with a considerably wider floodplain,

causing significant loss of flow and sediment. The perching ratio has increased (13% → 87%) and bank depth has decreased 51% between 1992 and 2002. The perching and lower bank depth facilitated more overbank flows and 13 ~ 20% loss of water between the San Acacia gauge and the San Marcial gauge.

Sediment concentration profile can be determined by the Rouse equation. Over time, particle size has coarsened (0.2mm → 0.25mm) and the width/depth ratio has increased (129 → 229) between 1992 and 2002. Accordingly, the Rouse number has increased and sediment concentration profile became more concentrated near the bed. The Rouse number ranged from 0.6 to 1.7 from 1992 to 2002. The high Rouse number ($Ro > 1.4$) and near-bed sediment concentration profile accelerate the aggradation rates (4 ~ 7 times faster) than for uniform-concentration profiles. In order to fill the main channel, about 3 months is needed when the overbank flows is considered only. However, the high near-bed concentration shortens the plug formation time to 20 days. Since snowmelt floods more than bankfull discharges last less than 2 months, the acceleration factors are essential for sediment plug to form.

◦ ***Hydraulic factors: Backwater effects from reservoir, bridge, and sharp bends***

Stages at the Elephant Butte Reservoir influenced the upstream channel bed elevation over time. With an average flow discharge (1,550 cfs), the aggradation (up to 7 ft) time to fill the 25.5 mile long channel is roughly 10 years. And the historic Tiffany plug area has been influenced by the reservoir levels, but with some lag time. Although backwater effects from the reservoir on the channel bed elevation around the Tiffany area takes a matter of years, aggradation due to high reservoir stage provided a better condition for sediment plug to form. Low reservoir levels cause the increase of channel capacity and decrease of backwater effect from the railroad bridge, significantly reducing the likelihood of sediment plug formation.

The upstream channel bed around the San Marcial Railroad Bridge (Agg/deg 1702) has aggraded consistently (12ft increased between 1979 and 1987). The pier contraction and congested abutments generate about 1ft high backwater which propagates to the Tiffany plug area (1.6 miles upstream). Historic inundated areas shows the backwater effects from the bridge and explain why the Tiffany plug initiated at the location (Agg/deg 1683).

Sharp bends observed around the Bosque plug area cause a 1.6ft high backwater which propagates roughly 1 mile upstream. As the beginning point of the Bosque plug is located 0.6 mile upstream, backwater from the sharp bends might influence the channel aggradation Bosque plug. The time to fill the main channel up to 2.85ft (bank height in 2002) was estimated as approximately 17 days.

◦ *Analysis of the most important factors*

Backwater effects from the reservoir has influenced the upstream channel elevation on a long-term basis ($7 \text{ ft} / 10 \text{ years} = 0.06 \text{ cm} / \text{day}$), providing the basic condition for a sediment plug formation. Under the influence of low reservoir stage, the occurrence of a sediment plug is less likely. Channel narrowing and higher roughness promote overbank flows and induce loss of water to overbank areas, thus these two factors can be categorized as temporal factors (1% decrease per year). Owing to the increase of overbank flows, sediment concentration profiles speed up the main channel aggradation, causing a sediment plug to form within a matter of weeks, thus these two factors are the most significant factors ($1.3 \text{ ft} / 20 \text{ days} = 2 \text{ cm} / \text{day}$).

Two other factors, the backwater effect from the railroad bridge and sharp bends, explain why the historic sediment plugs formed at particular areas, therefore these two parameters can be classified as local triggering factors ($\sim 1.6 \text{ ft} / 20 \text{ days} = 2.5 \text{ cm} / \text{day}$).

In a view point of significance, perching/overbank flow and sediment concentration profile can be considered as the primary causing factors of sediment plugs, followed by the backwater effects from bridge and sharp bends. Without the temporal changes of channel widths and roughness, the occurrence probability of a sediment plug will decrease significantly. On the other hand, causal factors can be divided into two groups depending on the plug location. The Tiffany plugs have been more affected by the backwater effect from the reservoir and railroad bridge, while the Bosque plug was more influenced by the decrease of channel width/channel capacity, roughness, and sharp bends. Sediment concentration profiles and overbank flows were commonly significant at both plug locations. As shown in Table 9.1, when the reservoir level is high for a long period of time and a long and high snowmelt flood occurs, a new sediment plug may form around the historic sediment plug location (aggradation rate $\Delta z > 2 \sim 5\text{cm} / \text{day}$). Water temperature, coarsening of bed material, and tributary sediment inflows also can be categorized as possible factors, but there was no significant proof from the given data and documentation.

Table 9.1. Significance of causing factors

Possible causing factors		Significance	Location (Tiffany:T, Bosque:B)	Duration of Influence	Level of condition (Conditional: C, Accelerator : A)	Remarks (Aggradation rate ¹) (numerical simulation)
Geometric factors	Channel widths	Medium	B	Long	C	Less than 0.01cm/day
	Roughness	Medium	B	Long	C	Less than 0.1cm/day
Overbanking factors	Perching/overbank flows	High	T, B	Short	A	0.6cm/day (0.3cm/day)
	Concentration profiles	High	T, B	Short	A	2cm/day (1.5cm/day)
Backwater effect factors	reservoir	Medium	T, B	Long	C	0.06cm/day (0.06cm/day)
	bridge	High	T	Short	C, A	5cm/day (3cm/day)
	sharp bends	High	B	Short	C, A	4cm/day (1.3cm/day)
Other factors	Water temperature	Low	T, B	Long	A	-
	Particle coarsening	Low	T, B	Long	A	
	Tributary inflows	Low	T, B	Short	A	

* flow discharge : 44m³/s for backwater from reservoir, 141 m³/s for backwater from bridge and sharp bends,

57 m³/s for overbank flows /concentration profiles, 49 ~ 137 m³/s for numerical simulation

RECOMMENDATIONS FOR FUTURE STUDY

In addition to imagery comparison and HEC-RAS modeling in this study, regular field measurements are strongly recommended to determine the amounts of water loss to the overbank areas and return flow to the main channel. Understanding regarding the momentum exchange between the active channel and overbank areas can help to accurately estimate the overbank flow and sediment loss, improving the numerical modeling outcome. Although a subcritical flow condition was assumed in this study, local critical flow (e.g., overbank flows on top of ban crest) or supercritical flow (e.g., contraction flow under the San Marcial Railroad Bridge) need to be monitored.

Vegetation encroachment has been significant over time. In addition to the vegetation encroachment in terms of vegetation area, vegetation density also needs to be studied to accurately estimate the resistance to flow. Increase of roughness due to channel planform also deserve to investigate for obtaining accurate total roughness. Roughness coefficients in accordance with local vegetation conditions need to be studied in further research, since the overbank flow is a primary factor in sediment plug formation and roughness is a key factor that causes the overbank flow.

Since historic sediment plugs only occurred during snowmelt floods, further study to understand why a sediment plug did not occur during the monsoon season needs to proceed. The tributary sediment inflow in the previous years can be a clue for that. Data gathering from five arroyos in the study area will support the hypothesis.

Sediment concentration and profiles need to be monitored during snowmelt and monsoon rainfall seasons. In this study, lateral distribution of sedimentation was out of the scope. Concentration profiles measured in the main channel and floodplains as well as channel-

floodplain interaction zones may provide better information of the lateral profiles at cross sections. The monitoring also enhances the reliability of numerical simulations.

Backwater effects from reservoir were roughly simulated to estimate the time to influence upstream channel bed elevation. The relationship between reservoir levels and upstream channel aggradation / degradation is valuable to establish standard dam operating procedures to prevent the Tiffany plug formation. Investigation of how the backwater effect responds to the channel bed elevation through physical and (2-D or 3-D) numerical modeling will assist in the determination of the increase of water depth and its effect on the channel sedimentation. Since the existing bridge backwater equation was roughly developed based on a fixed-bed channel, a mobile-bed equation also needs to be investigated.

Physical modeling is also recommendable to deeply understand the mechanics of backwater and sedimentation behind the bridge piers. In addition to the bridge piers and abutments, bridge girders also augment the backwater effect at high flow discharge. The submerging effect due to bridge girders cause more extensive flooded areas. Sharp bends was observed after 2006. The reason why sharp bends formed at the location is not fully examined. Monitoring and understanding the process of sharp bend development also helps to understand the mechanics of the Bosque plug formation.

BIBLIOGRAPHY

- Abbott, M. B. (1979). *Computational Hydraulics*, Pitman Advanced Pub. Program, London.
- Baird, D. C. (1998). "Bank stabilization experience on the Middle Rio Grande." *Water Resources Engineering* 98, ASCE, New York, NY, 387-392.
- Bauer, T. R. (2000). "Morphology of the Middle Rio Grande from Bernalillo Bridge to the San Acacia Diversion Dam." M.S. Thesis, Colorado State University, Fort Collins, CO.
- Bauer, T. R. (2006). "Bed Material Data Collection Trip Report." U.S. Department of the Interior, Bureau of Reclamation, Technical Services Center, Sedimentation and River Hydraulics Group, Denver, CO.
- Belcher, R. C. (1975). "The geomorphic evolution of the Rio Grande." *Baylor Geologic Studies, Bulletin no. 29*, Baylor University, Waco, TX.
- Bender, T. R., and Julien, P. Y. (2011) "Overbank flow analysis." Tech. Report for Reclamation, Albuquerque, NM.
- Boroughs, C. B. (2005). "Criteria for the Formation of Sediment Plugs in Alluvial Rivers." Ph.D. Dissertation, Colorado State University, Fort Collins, CO.
- Boroughs, C. B., Padilla, R., and Abt, S. R. (2005). "Historical sediment plug formation along the Tiffany Junction Reach of the Middle Rio Grande." *Proc. of the 2005 New Mexico Water Research Symp.*, New Mexico Water Resources Research Institute, Las Cruces, NM.
- Boroughs, C.B., Abt, S.R., and Baird, D.C. (2011). "Criteria for the Formation of Sediment Plugs in Alluvial Rivers." *Journal of Hydraulic Engineering, ASCE*, V137, 569-576.
- Carson, M., and G. Griffiths (1987). "Gravel transport rates and yields related to channel width." *Journal of Hydrology (N.Z.)*, 26, 81-108.
- Carter, R. H. (1955). "Control of arroyo floods at Albuquerque, New Mexico." *Proceedings of the ASCE Waterways Division*, v. 81, Paper No. 801.
- Chang, H. H. (1979). "Minimum stream power and river channel patterns." *Journal of Hydrology*, 41, 303-327.
- Chapra, S. C., and Canale, R. P. (1990). *Numerical methods for engineers*, McGRAW-Hill, New York.

- Chitale, S. V. (2003). "Modeling for width reductions in alluvial rivers." *Journal of Hydraulic Engineering*, ASCE, V129, 404-407.
- Chow, V. T. (1959). *Open-Channel Hydraulics*, McGraw-Hill Book Company
- Culbertson, J. K., and Dawdy, D. R. (1964). "A study of fluvial characteristics and hydraulic variables Middle Rio Grande, New Mexico." U.S. Geological Survey Water Supply Paper 1498-F.
- Culbertson, J. K., Scott, C. H., and Bennett, J. P. (1972). "Summary of alluvial-channel data from Rio Grande conveyance channel, New Mexico, 1965-1969." U.S. Geological Survey Professional Paper 562-J.
- Cunge, J.A., F.M. Holly, and A. Verwey. (1980). *Practical Aspects of Computational River Hydraulics*. Pittman Publishing Limited, Boston.
- Dewey, J. D., Roybal, F. E., and Funderburg, D. E. (1979). "Hydrologic data on channel adjustments, 1970 to 1975, on the Rio Grande downstream from Cochiti Dam, New Mexico, Before and After Closure." U.S. Geol. Survey Water Resources Investigation 79-70.
- Diehl, T. H. (1994). "Causes and effects of valley plugs in west Tennessee." Proc. of the Symp. on Responses to Changing Multiple-Use Demands; New Directions for Water Resources Planning and Management, American Water Resources Association (AWRA), Nashville, TN, 97-100.
- Diehl, T. H. (2000). "Shoals and valley plugs in the Hatchie River watershed." Rep. 00-4279, U.S. Geological Survey Water-Resources Investigation, Denver, CO.
- Einstein, H. A., and Chien (1954). "Second approximation to the solution of the suspended load theory" California Univ., Inst. Engineering Research, Missouri River Div. sediment sev.3.
- Finch, D. M. (1995). "Ecology, diversity, and sustainability of the Middle Rio Grande Basin", USDA, Forest service, General Tech. Report, RM-GTR-268.
- Ferguson, R. (1986), "Hydraulics and hydraulic geometry." *Progress in Physical Geography*, 10.
- FLO Engineering, Inc. (1995). "Manning's n-value calibration for SO lines, 1993 runoff season." Prepared for the Bureau of Reclamation.
- FLO Engineering, Inc. (1995). "Manning's n-value calibration for SO lines, 1994 runoff season." Prepared for the Bureau of Reclamation.

- Gabin, V. L., and Lesperance, L. E. (1977). "New Mexico climatological data: Precipitation, temperature, evaporation and wind: Monthly and annual 24 mean, 1850-1975." W.K. Summers and Associates, Socorro, NM.
- Gergens, R. (2003). "Canyon lake flood emergency operations." Proc. From the Watershed System 2003 Conf., U.S. Army Corps of Engineers, Northwestern Division, Portland, OR.
- Gorbach, C. (1999). "History and Significance of the Low-Flow Conveyance Channel : What is the Future ?" WRRRI Conference Proceedings, Santa Fe, 1-5.
- Graf, W.L. (1994). *Plutonium and the Rio Grande: Environmental change and contamination in the nuclear age*. Oxford University Press, New York.
- Hay, A. E., and Sheng, J. (1992). "Vertical profiles of suspended sand concentration and size from multifrequency acoustic backscatter." J. of Geophysical Res., Vol. 97, No. C10, 661-15
- Henderson, F.M. (1966). *Open Channel Flow*. Macmillan Publishing Company, New York, NY
- Hickman, T. (2001). "The Fisheries Program Response to the Floods of the Mid-1990's." Unites States Department of Agriculture. Pacific Northwest Region Report.
- Holmes, R. R., and Garcia, M. H. (2002). "Velocity and sediment concentration measurements over bedforms in sand-bed Rivers." U.S. Geological Survey, Hydraulic Measurements and Experimental Methods 2002.
- Huang, H., and Nanson, G. (1995). "The multivariate controls of hydraulic geometry: A casual investigation in terms of boundary shear distribution." *Earth Surface Processes and Landforms*, V20, 115-130.
- Huang, H. Q., and Nanson, G. (2000), "Hydraulic geometry and maximum flow efficiency as products of the principle of least action." *Earth Surface Processes and Landforms* , V25, 1-16.
- Huang, J. V., Greimann, B., and Yang, C.T. (2003). "Numerical Simulation of Sediment Transport in Alluvial River with Floodplains." *International Journal of Sediment Research*. Vol. 18, No. 1. 50-59.
- Huang. J. V., Makar, P. W. (2010). " 2009 historical bed elevation trends and hydraulic modeling: San Antonio to Elephant Butte Reservoir." Technical Report for Reclamation.

- Huang, J. V., Makar, P. W. (2011). “Sediment modeling of the Middle Rio Grande with and without the temporary channel maintenance in the Delta: San Antonio to Elephant Butte Reservoir.” Technical Report for Reclamation.
- Ismail, H. M. (1952). “Turbulent Transfer Mechanism and Suspended Sediment in Closed Channels,” Trans. Am. SOC. Civil Engrs., 117, 409-446
- Julien, P. Y., and J. Wargadalam (1995). “Alluvial channel geometry: Theory and applications.” Journal of Hydraulics Engineering, 121, 312-325.
- Julien, P. Y. (1998). *Erosion and Sedimentation*, Cambridge University Press, New York.
- Julien, P. Y. (2010). *Erosion and Sedimentation*, Cambridge University Press, New York.
- Julien, P. Y. (2002). *River Mechanics*, Cambridge University Press, New York.
- Kammerer, J. C. (1990). “Largest rivers in the United States.” U.S. Geological survey.
- Kim, H. (2003). “Temporal variation of suspended sediment concentration for wave ripples.”, Int. J. of Sediment Research, Vol. 18, No. 3, 248-265
- Kirkby, M. (1977). “Maximum Sediment Efficiency as a Criterion for Alluvial Channels.” John Wiley & Sons, Ltd., Belfast, N. Ireland, chapter 27. 429-442.
- Knighton, D. (1998). *Fluvial Forms and Processes, a New Perspective*. John Wiley and Sons, Inc. New York, N.Y.
- Lagasse, P. F. (1980). “An Assessment of the response of the Rio Grande to dam construction-Cochiti to Isleta reach”, U.S. Army Corps of Engineers, Albuquerque, N.M.
- Lagasse, P. F. (1994). “Variable Response of the Rio Grande to Dam Construction. The Variability of Large Alluvial Rivers, ASCE Press, New York, N.Y.
- León, C. (1998). “Morphology of the Middle Rio Grande from Cochiti Dam to Bernalillo Bridge, New Mexico.” M.S. Thesis, Colorado State University, Fort Collins, CO.
- León C., Julien, P.Y, and Baird, D.C. (2009). “Case Study : Equivalent widths of the Middle Rio Grande, New Mexico.” Journal of Hydraulic Engineering, ASCE V135, 306-315.
- León C., (2003). “Analysis of equivalent widths of alluvial channels and application for instream habitat in the Rio Grande.” Colorado State University, Ph.D dissertation.

- Lai, Y.G. (2009). "Sediment Plug Prediction on the Rio Grande with SRH Model." Bureau of Reclamation, Technical Service Center, Denver, CO.
- Lai, Y. G. (2012). "Prediction of channel morphology upstream of Elephant Butte Reservoir on the Middle Rio Grande." Technical Report No.SRH-2011-04.
- Liu, Q. Q., Shu, A. P., Singh, V. P. (2007). "Analysis of the vertical profile of concentration in sediment-Laden flows." J of Eng. Mechanics, V133, No.6, 601-607.
- Mays, L. W. (1999). *Hydraulic Design Handbook*, McGrawHill, New York, NY.
- Makar, P. W., Padilla, R. S., and Baird, D. C. (2012). "Middle Rio Grande assessment for maintenance planning." World Environmental and Water Resources Congress 2012, ASCE, 2627-2636
- Mofjeld, H. O., and Lavelle, J. W. (1988). "Formulas for velocity, sediment concentration and suspended sediment flux for steady uni-directional pressure-driven flow.", NOAA Tech. Memo. ERL PMEL-83.
- Moin, P. (2010). *Fundamentals of Engineering Numerical Analysis*, Cambridge, New York, NY.
- Mussetter Engineering, Inc. (MEI). (2002). "Geomorphic and Sedimentologic Investigations of the Middle Rio Grande between Cochiti Dam and Elephant Butte Reservoir." technical report for the New Mexico Interstate Stream Commission, 1.1-5.8
- Nordin. C. F., Dempster, G.R. (1963). "Vertical distribution of velocity and suspended sediment Middle Rio Grande New Mexico." Geological survey professional paper 462-B.
- Owen, T. E., and Julien, P. Y. (2011). "Elephant Butte Reach report: Hydraulic Modeling Analysis." Tech. Report for Reclamation, Albuquerque, NM.
- Padilla, R., and Baird, D.C.(2010). "Channel changes and maintenance on the San Acacia Reach of the Middle Rio Grande." 2nd Joint Federal Interagency Conferences, Las Vegas, NV. 1-11.
- Paris, A., Anderson, K., Shah-Fairbank, S. C., and Julien, P.Y. (2011). "Bosque del Apache Reach Hydraulic Modeling Analysis." Tech. Report for Reclamation, Albuquerque, NM.
- Park, K., and Julien, P.Y. (2011). "Sustainable width analysis for Bosque Reach." Tech. Report for Reclamation, Albuquerque, NM.
- Park, K., Bender, T. R., and Julien, P.Y. (2011). "Literature review and conceptual assessment." Tech. Report for Reclamation, Albuquerque, NM.

- Park, K., and Julien, P.Y. (2012). "Mechanics of sediment plug formation in the Middle Rio Grande." Tech. Report for Reclamation, Albuquerque, NM.
- Reclamation (1998). "Rio Grande geomorphology study 1918–1992." U.S. Bureau of Reclamation, Remote Sensing and Geographic Information Group, Denver, CO.
- Reclamation (2000). "Rio Grande and low flow conveyance channel modifications. Environmental impact statement." Technical Rep., Albuquerque Area Office, Albuquerque, N.M.
- Reclamation (2001). "Water Measurement Manual, Chapter 2 – Basic Concepts related to flowing water and measurement." Water Resources Research Laboratory, Water Resources Technical Publication, Washington, DC.
- Reclamation (2005). "Sediment plug computer modeling study, Tiffany Junction Reach." U.S. Department of the Interior Bureau of Reclamation, Albuquerque, N.M.
- Reclamation (2006). "Erosion and Sedimentation Manual." U.S. Department of the Interior Bureau of Reclamation, Technical Service Center, Denver, CO
- Reclamation (2007). "Middle Rio Grande River Maintenance Plan." Technical Rep. for U.S. Department of the Interior Bureau of Reclamation, Albuquerque, N.M.
- Reclamation (2008). "Sediment Plug Removal at Bosque del Apache National Wildlife Refuge Middle Rio Grande Project, New Mexico." U.S. Department of the Interior Bureau of Reclamation, Albuquerque, N.M.
- Reclamation (2011). "Bosque del Apache Sediment Plug Management : alternative analysis." U.S. Department of the Interior Bureau of Reclamation, Albuquerque, N.M.
- Reclamation (2011). "Bosque del Apache Sediment Plug Baseline Studies." Annual Report 2010, Technical Service Center, Denver, CO
- Reclamation (2012). "Bosque del Apache Sediment Plug Baseline Studies." Annual Report 2011, Technical Service Center, Denver, CO
- Reclamation (2012). "Prediction of Channel Morphology : upstream of Elephant Butte Reservoir on the Middle Rio Grande." Tech. Report No. SRH-2011-4.
- Richard, G. A. (2001). "Quantification and prediction of lateral channel adjustments downstream from Cochiti Dam, Rio Grande, New Mexico." Ph.D. dissertation, Colorado State University, Fort Collins, CO.

- Rittenhouse, G. (1944). "Sources of modern sands in the Middle Rio Grande valley, New Mexico." *Jour. of Geology*, V52, 145-183.
- Rouse, H. (1938). *Fluid mechanics for hydraulic engineers*, McGRAW-HILL Book Com., New York. 327-350
- Schumm, S. (1977). *The Fluvial System*, Wiley, New York.
- Shields, F. D., Jr., Knight, S. S., and Cooper, C. M. (2000). "Cyclic perturbation of lowland river channels and ecological response." *Regul. Rivers Res. Manage.*, 16, 307–325.
- Shrimpton, C., and Julien, P.Y. (2012). "Hypotheses of sediment plug formation" M.S. Thesis, Colorado State University, Fort Collins, CO.
- Simoes, F. J.M, Yang, C.T. (2006). "Erosion and sedimentation manual; chapter 5. Sedimentation Modeling for Rivers and Reservoirs." *Reclamation*, 5-1~5-34.
- Smith, K. I., Makar, P. W., and Baird, D. C. (2001). "No action alternative future scenarios for the Elephant Butte, New Mexico headwater area." *Proc. of Seventh Federal Interagency Sedimentation Conference*, Reno, Nevada, March 25-29, II-107 ~ II-114.
- Tetra Tech, Inc. (2003). "Conceptual Restoration Plan Active Floodplain of the Rio Grande (San Acacia to San Marcial, NM) Phase 3. Concepts and Strategies for River Restoration Activities." Tech. Report for Reclamation, Albuquerque, NM.
- Tetra Tech, Inc. (2010). "River mile 80 to river mile 89 : Geomorphic Assessment and Hydraulic and Sediment-continuity Analyses." Tech. Report for Reclamation, Albuquerque, NM.
- Tuan, Yi-Fu., Everard, C. E., Widdison, J. G., and Bennett, I. (1973). "The Climate of New Mexico." New Mexico State Planning Office, Santa Fe, NM.
- U.S. Army Corps of Engineers (1989). "Engineering and Design : Sedimentation investigation of rivers and reservoirs" EM1110-4000, 5.5-5.6.
- U.S. Army Corps of Engineers Albuquerque District. (2010). "Report of Civil Works Activities 2010 : Rio Grande Basin"
- U.S. Army Corps of Engineers (USACE), Hydrologic Engineering Center (HEC). (2010). *HEC-RAS, River Analysis System, Hydraulic Reference manual, Version 4.1*, Davis, CA
- Vanoni, V. A. (1946). "Transportation of suspended sediment by water." *American Society of Civil Engineers*, paper 2267, V111, 67-102.

- Vanoni, V. A, and Brooks, N.H. (1957). "Laboratory studies of the roughness and suspended load of alluvial streams" California Inst. Technology, sediment lab., Rept. E-68.
- Vanoni et al. (1975). *Sedimentation Engineering*, American Society of Civil Engineers
- White, W., R. Bettess, and E. Paris. (1982). "Analytical approach to river regime". Journal of the Hydraulics Division, ASCE, 108, 179-1193.
- Williams, G. P. (1989). "Sediment concentration versus water discharge during single hydrologic events in rivers." J of Hydrology, 111 (1989) 89-106.
- Woo, H. S., Julien, P.Y., and Richardson, E.V. (1988). "Suspension of large concentrations of sands." J. of Hydraulic Eng. Vol. 114, No. 8, 888-898
- Woo, H. (2001). *River Hydraulics*, Cheongmungak pub., seoul, chapter II. 321-708
- Yang, C. T. (2007). *Sediment Transport: theory and practice*, Cheongmungak pub, Seoul.
- Yang, C. T., Huang, J. V., and Greimann, B. (2005). "User's Manual for GSTAR-1D 1.0 (Generalized Sediment Transport for Alluvial Rivers – One Dimension, Version 1.0)." Technical Service Center, U.S. Bureau of Reclamation, Denver, Colorado.

APPENDIX A. Summary of Reclamation’s river maintenance plan (Park 2011)

Sub-reach	Geomorphology	Maintenance Activities	Maintenance Needs and Strategies
<p>San Acacia to Arroyo Canas (RM 116.2 to 95, 21miles)</p>	<ul style="list-style-type: none"> Channel incision downstream of San Acacia Diversion Dam has been rapid (12 feet/60yrs), 8-10 ft after 1988 The banks are susceptible to riverine erosion Channel location is moving, but channel area and width appear to be remaining fairly constant Bankful discharge is at least 10,000 cfs 	<ul style="list-style-type: none"> The dam was constructed in 1934 to divert a maximum 283 cfs for irrigation, rehabilitated in 1957 LFCC which was constructed in the 1950s begins at this dam <ul style="list-style-type: none"> Operation from 1959 Conveying up to 2000 cfs Since 1981, it has been used as a drain and to return irrigation flows to the river Large-scale channelization took place in the early 1950s 	<ul style="list-style-type: none"> Degradation is progressing downstream Bend series migrate both downstream and laterally. Meander bends can develop and migrate into the LFCC levee A large levee setback project has been performed Possible levee protections : moving the river to the east, levee setbacks, bend-way weirs, and lowering east-side terraces
<p>Canas to San Antonio (Highway 380 Bridge) (RM 95 to 87.1, 8miles)</p>	<ul style="list-style-type: none"> The channel alignment, the bank-line, and bed are mostly stable For in-channel habitat, this reach may continue to narrow and possibly incise as the thalweg becomes more concentrated into an ever smaller active channel, reducing space for aquatic habitat 	<ul style="list-style-type: none"> During construction of the LFCC, a spoil levee was built between the LFCC and the river The area was channelized in the 1950s. The channel was straightened and deepened, vegetation was cleared, and Kellner jetty jacks were placed. The channel is relatively wide and the channel alignment and bed elevation has been stable 	<ul style="list-style-type: none"> The bed elevation has been stable since the 1930s and is expected to remain stable Lessons learned from other reaches should be considered in evaluating conditions of this reach
<p>San Antonio to RM78 (RM 87.1 to 78, 9miles)</p>	<ul style="list-style-type: none"> This reach is and has been gradually aggrading since the 1930s Bank heights are low and the floodplain along with recently formed islands are flood prone at relatively low flow (3,000 cfs) The amount of aggradation increases in the downstream direction This section of river has always been among the widest Channel slope lessens slightly This reach receives water and sediment from numerous tributaries that are not controlled for flood or sediment production There has been less channel maintenance work in this reach because it is not as directly influenced by Elephant Butte Reservoir. 	<ul style="list-style-type: none"> The North Boundary Pump Site, located at BDANWR’s north boundary, pumps water from the LFCC to the floodway during dry years. This is intended to keep water flowing in the river to help protect the endangered RGSM There is one priority site in this reach, which addresses levee capacity in the downstream portion of the reach, where the river has aggraded and is often perched above the adjacent floodplain. The width constriction and slope changes near RM 78 may be acting to limit sediment transport In locations, where the channel was straightened by cutting pilot channel through the floodplains, the channel width is significant narrower The likely evolution of this reach is that a single dominant channel will emerge, with the rest of the current active channel becoming vegetated floodplain 	<ul style="list-style-type: none"> Bed elevation is fairly stable, connection to the floodplain begins at 2,000-3,000 cfs. Channel plan-form is narrowing rapidly with vegetation encroachment There is some concerns about a head-cut moving upstream through the reach due to base level lowering resulting from the drop in pool elevation of Elephant Butte Reservoir Lowering of the water table, which potentially could occur through upstream migration of head-cut or avulsion of the river into a lower elevation portion of the valley, could have an immediate harmful effect on SWFL habitat by drying currently used nesting area. Bank erosion and lateral migration may also be beginning; however, there are currently no sites in this reach where river maintenance is planned

Sub-reach	Geomorphology	Maintenance Activities	Maintenance Needs and Strategies
RM 78 to Elephant Butte (RM 78 to 50, variable)	<ul style="list-style-type: none"> Reclamation's maintenance reach may be 19 to 28 miles long. Much of the reach has been channelized through cohesive materials Prior to 2005, the river channel was rapidly aggrading by influenced by reservoir stage. In 2005 the head-cut migrate upstream with spring runoff. The most upstream portion of the head-cut has tapered out in the upstream portion of this reach near Tiffany. Subsequent bed degradation in 2005 from the head-cut caused significant bed elevation lowering (degradation) which adversely affects aquatic and riparian species alike. Regardless of the exact amount, degradation has resulted in abandonment of most of the floodplain in this reach. The main portion of the Temporary Channel (upstream of the Narrows) has started to evolve since it was first constructed in 2001-2004. <ul style="list-style-type: none"> The head-cut will increase channel capacity within the constructed channel, while lowering the water table. 	<ul style="list-style-type: none"> Storage for the reservoir began in 1915; the full pool elevation of 4407 feet extends to RM 62 There was extensive channelization and floodway clearing in the 1950s. During the LFCC construction, the floodway was moved to the east side of the river valley Sediment plug formed in the area between RM 74 and RM 70 in 1991, 1995, and 2005. The San Marcial Railroad Bridge constructed in 1930 is located at RM 68.6. Attesting to the aggradational trend in the reach, the tracks are now more than 20 feet higher than they were on the original bridge in 1920. The limited channel capacity under the bridge often controls flood releases from Cochiti Dam Since 1991, three Temporary Channels have been constructed to re-connect the river and the reservoir pool to maintain water delivery to the reservoir 4 different river maintenance problems <ul style="list-style-type: none"> Levee capacity Bank erosion / migration Sediment plug formation channel connection to the reservoir pool 	<ul style="list-style-type: none"> Rapid aggradation can occur during high flow periods, with the location of aggradation greatly influenced by reservoir stage The condition of this reach is dynamic, but long term aggradation will continue to occur Levees are periodically raised but have reached elevations whether further raising has become impractical in many locations. The existing practice of levee raising is not sustainable over the long term. A head-cut has recently progressed upstream, and has lowered channel elevations, temporarily reducing the urgency of the levee elevation and flood capacity issue. The continual aggradation causes several maintenance problems <ul style="list-style-type: none"> Without continual excavation, sediment will deposit at the upstream end of the reservoir, and the channel will not flow all the way to the reservoir pool. Reclamation has excavated pilot channels through the sediment plugs to reestablish the channel, but nothing has been done to prevent the problem from recurring.
Low Flow Conveyance Channel (RM 116.2 to 61.4, 56 miles)	<ul style="list-style-type: none"> LFCC was constructed from 1951 to 1959 to aid the State of New Mexico in delivering waters obligated to Texas under the Rio Grande Compact The channel also served to improve agricultural drainage and to supplement irrigation water supplies to both the BDANWR as well as irrigators of the MRGCD LFCC conveyed up to 2,000 cfs to Elephant Butte Reservoir The LFCC currently functions only as a passive drain for seepage and irrigation return flows 	<ul style="list-style-type: none"> The LFCC was shortened to a length of 54.7 miles to the outfall location at about RM 60. During the high reservoir storage period from 1979 to the late 1990s, sediment deposited upstream of the reservoir pool and elevated the river channel bed. The levee has been raised significantly to maintain flow capacity in the river channel. Outfall channels and associated infrastructure into the river could be constructed at different locations including For Craig, RM 60, Elephant Butte Range Line (RL) 32, or the Narrows. Currently the location of the outfall is near RM 55 	<ul style="list-style-type: none"> This reach is in a continual dynamic state depending upon Elephant Butte Reservoir stage and the location of the delta sediment deposits There will be long term sediment deposition in the reservoir delta The channel is not self-maintaining in the delta of Elephant Butte Reservoir, because the sediment load is too large for the hydrology and valley slope. Changing the operations of the LFCC from the current operations is difficult, and requires a lot of political will and additional funding beyond the current annual river maintenance appropriations

APPENDIX B. Computation of sediment transport capacity for various channel widths

Sediment Diameter 0.25 mm

d* 6.3

Manning n 0.026

Slope 0.0007 m/m

Calculate !!

Width	HR	HD	W/h
0.1	10209.35	76.73	0.00
0.4	1013.03	33.40	0.00
0.8	319.31	22.04	0.00
1	220.29	19.27	0.00
4	23.07	8.39	0.17
10	6.83	4.84	1.46
50	1.90	1.84	26.34
100	1.23	1.22	81.43
200	0.80	0.80	248.47
400	0.53	0.53	754.83
800	0.35	0.35	2289.85
1000	0.31	0.31	3272.71
2000	0.20	0.20	9922.63
3000	0.16	0.16	18984.08

rouoff error	HR	HD
0.00001000	-0.00002689	-0.00003688
-0.00000249	-0.00003688	-0.00003688
-0.00009926	-0.00003688	-0.00003688
-0.00032178	-0.00003688	-0.00003688
0.00027901	-0.00003688	-0.00003688
0.00000192	-0.00003688	-0.00003688
-0.00002391	-0.00003688	-0.00003688
-0.00003203	-0.00003688	-0.00003688
-0.00003521	-0.00003688	-0.00003688
-0.00003632	-0.00003688	-0.00003688
-0.00003670	-0.00003688	-0.00003688
-0.00003675	-0.00003688	-0.00003688
-0.00003684	-0.00003688	-0.00003688
-0.00003686	-0.00003688	-0.00003688

cases	HR	HD
0.1	0.05	0.05
0.4	0.20	0.20
0.8	0.40	0.39
1	0.50	0.49
4	1.84	1.62
10	2.89	2.46
50	1.76	1.72
100	1.20	1.19
200	0.80	0.80
400	0.53	0.53
800	0.35	0.35
1000	0.31	0.31
2000	0.20	0.20
3000	0.16	0.16

Depth (m)	Width	HR	HD
0.1	0.1	0.14	18.38
0.4	0.4	0.35	10.55
0.8	0.8	0.55	8.00
1	1	0.64	7.32
4	4	1.53	4.20
10	10	2.06	2.91
50	50	1.49	1.53
100	100	1.15	1.16
200	200	0.88	0.88
400	400	0.67	0.67
800	800	0.50	0.50
1000	1000	0.46	0.46
2000	2000	0.35	0.35
3000	3000	0.30	0.30

Flow Velocity (m/s)	Width	HR	HD
0.1	0.1	0.02	0.02
0.4	0.4	0.04	0.04
0.8	0.8	0.05	0.05
1	1	0.06	0.06
4	4	0.11	0.11
10	10	0.14	0.13
50	50	0.11	0.11
100	100	0.09	0.09
200	200	0.07	0.07
400	400	0.06	0.06
800	800	0.05	0.05
1000	1000	0.05	0.05
2000	2000	0.04	0.04
3000	3000	0.03	0.03

Shear Velocity (m/s)	Width	HR	HD
0.1	0.1	0.00000	3.77866
0.4	0.4	0.00003	0.71592
1	1	0.00010	0.31162
4	4	0.00016	0.23842
10	10	0.00217	0.04517
50	50	0.00535	0.01504
100	100	0.00200	0.00218
200	200	0.00092	0.00095
400	400	0.00041	0.00041
800	800	0.00018	0.00018
1000	1000	0.00008	0.00008
2000	2000	0.00006	0.00006
3000	3000	0.00003	0.00003

Hydraulic Radius	Width	HR	HD
0.1	0.1	0.1	130.2
0.4	0.4	0.3	56.7
0.8	0.8	0.7	37.4
1	1	0.8	32.7
4	4	3.1	14.2
10	10	4.9	8.2
50	50	3.0	3.1
100	100	2.0	2.1
200	200	1.4	1.4
400	400	0.9	0.9
800	800	0.6	0.6
1000	1000	0.5	0.5
2000	2000	0.3	0.3
3000	3000	0.3	0.3

q _{bw} (tons/day)	Width	STC per day,width	HD
0.1	0.1	4	8487231
0.4	0.4	58	1608030
1	1	230	699936
4	4	359	535508
10	10	4882	101460
50	50	12017	33788
100	100	4486	4898
200	200	2071	2132
400	400	919	928
800	800	403	404
1000	1000	176	176
2000	2000	134	135
3000	3000	59	59
3000	3000	36	36

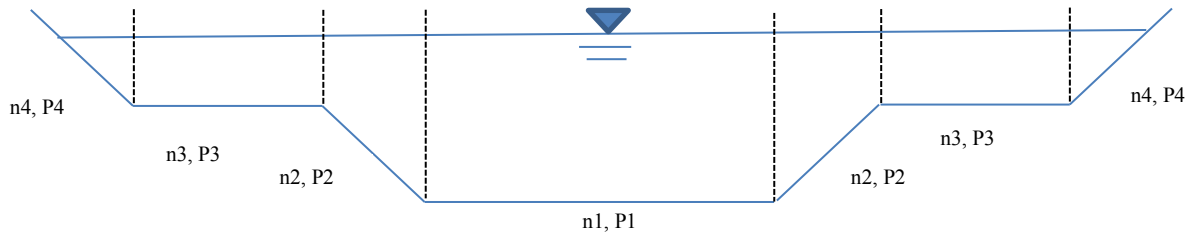
q _{bw}	Width	HR	HD
0.1	0.1	0.00000	3.77866
0.4	0.4	0.00003	0.71592
1	1	0.00010	0.31162
4	4	0.00016	0.23842
10	10	0.00217	0.04517
50	50	0.00535	0.01504
100	100	0.00200	0.00218
200	200	0.00092	0.00095
400	400	0.00041	0.00041
800	800	0.00018	0.00018
1000	1000	0.00008	0.00008
2000	2000	0.00006	0.00006
3000	3000	0.00003	0.00003

τ*	Width	HR	HD
0.1	0.1	0.1	130.2
0.4	0.4	0.3	56.7
0.8	0.8	0.7	37.4
1	1	0.8	32.7
4	4	3.1	14.2
10	10	4.9	8.2
50	50	3.0	3.1
100	100	2.0	2.1
200	200	1.4	1.4
400	400	0.9	0.9
800	800	0.6	0.6
1000	1000	0.5	0.5
2000	2000	0.3	0.3
3000	3000	0.3	0.3

APPENDIX C. Computation of composite roughness

Composite roughness coefficient which represents the cross section was determined using the HEC-RAS modeling results and Horton equation (1933).

$$n_e = \left[\frac{\sum_{i=0}^N (P_i n_i^{\frac{3}{2}})}{P} \right]^{\frac{2}{3}}$$



Station. No	Channel length (ft)	Perimeter			Manning n			Composite Manning n
		Channel	left bank	right bank	Channel	left bank	right bank	
1	520	228	927.7	127.22	0.02	0.1	0.1	0.088
2	573	796.6		189.82	0.02		0.1	0.041
3	514	781.01		4.11	0.02		0.1	0.020
4	556	916	0.63	72.55	0.02	0.1	0.1	0.029
5	538	972.22			0.02			0.019
6	500	792	5.88	2.57	0.02	0.1	0.1	0.021
7	494	649.51		1.75	0.02		0.1	0.020
8	417	660	158.27	99.84	0.02	0.1	0.1	0.049
9	343	839	0.39	3.07	0.02	0.1	0.1	0.020
10	465	753	175.98	154.49	0.02	0.1	0.1	0.051
11	538	424	10.72	1.18	0.02	0.1	0.1	0.023
.....								
146	454	163	11.76	22.93	0.024	0.1	0.1	0.042294
145	482	186	1194.25	468.83	0.024	0.1	0.1	0.093656
251	570	190	1506.02	274.62	0.024	0.1	0.1	0.094008
252	555	155	1499.51	328.83	0.024	0.1	0.1	0.095156
253	495	156	1337.13	388.51	0.024	0.1	0.1	0.094831
254	475	122	10.95	16.13	0.024	0.1	0.1	0.042112

APPENDIX D. Relationships between flow discharge and sediment discharge

Basic equations :

$$\text{Flow discharge } Q = \frac{\varphi W}{n} h^{\frac{5}{3}} S_o^{\frac{1}{2}}$$

$$\text{Sediment discharge } Q_s = 18W \sqrt{g d_s^3} \left(\frac{h S_f}{(G-1)d_s} \right)^2$$

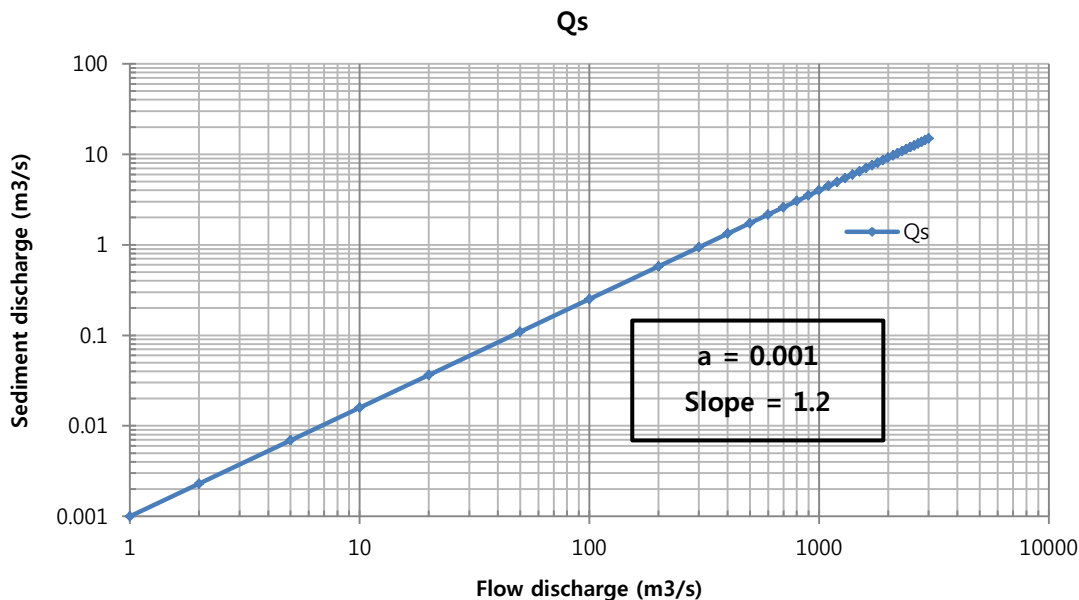
From the sediment discharge equation, all parameters which have constant values during computation can be separated from flow discharge terms:

$$Q_s = 18W \sqrt{g d_s^3} \left(\frac{h S_f}{(G-1)d_s} \right)^2 = \left(\frac{\varphi W}{n} h^{\frac{5}{3}} S_o^{\frac{1}{2}} \right)^{6/5} \frac{18\sqrt{g} W h^2 S_f^2}{(G-1)^2 \sqrt{d_s}} \frac{\varphi^{6/5} W}{n^{6/5} h^2 S_o^{\frac{3}{5}}}$$

$$= \alpha Q^{1.2}$$

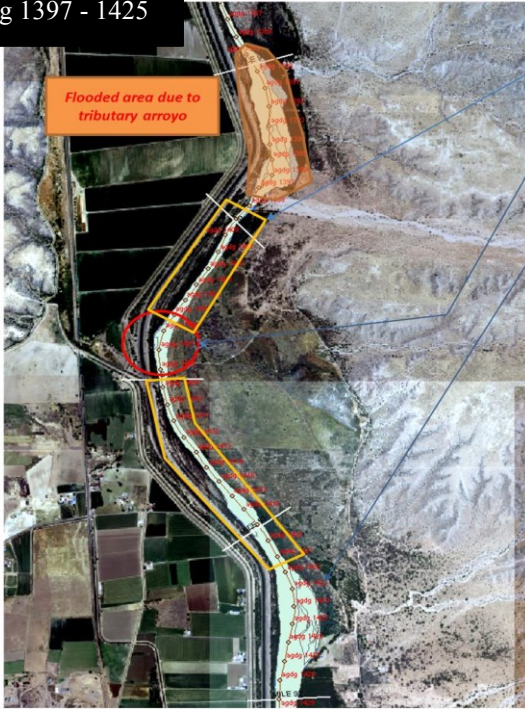
$$\text{where } \alpha = \left[\frac{18\sqrt{g} n^{6/5} S_f^{7/5}}{(G-1)^2 \varphi^{6/5} \sqrt{d_s}} \right]$$

Therefore, water loss due to perching/ overbank flows causes ore decrease of sediment transport capacity as $Q_s = \alpha Q^{1.2}$.



APPENDIX E. Flooding area analysis (USGS satellite imagery and USBR flood database)

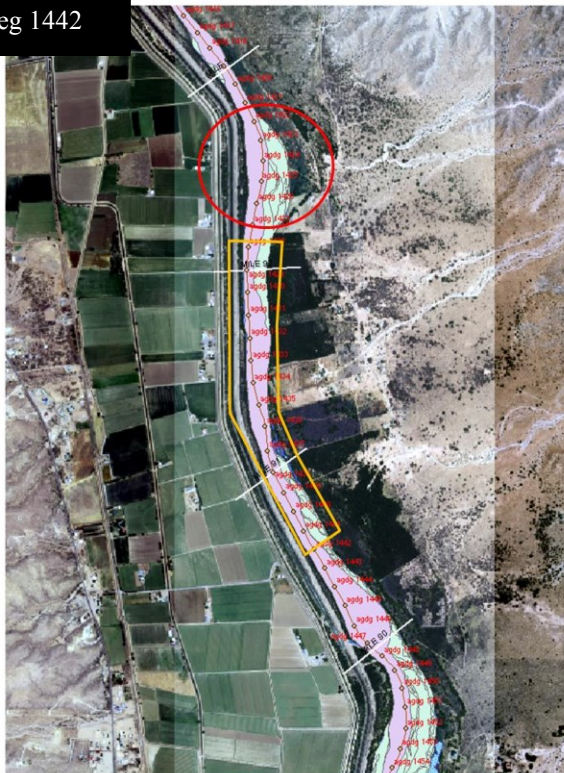
Agg/deg 1397 - 1425



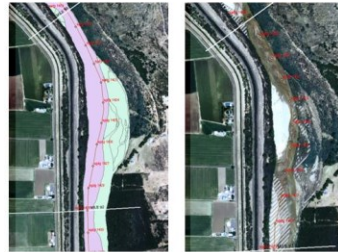
- From starting station to 1405 (straight channel)
 - no change in geometry
- Agg/deg 1406, 1407, 1408
 - curved, 2-3 times of channel widths
- Agg/deg 1409 ~ Agg/deg 1421
 - no change in channel widths
 - 1418 : wider section due to bars
- Agg/deg 1422 ~ Agg/deg 1425
 - width increases (channel meandering)



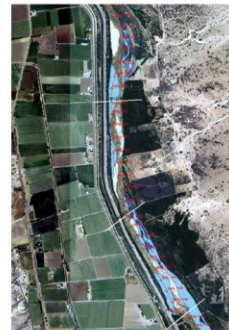
~ Agg/deg 1442



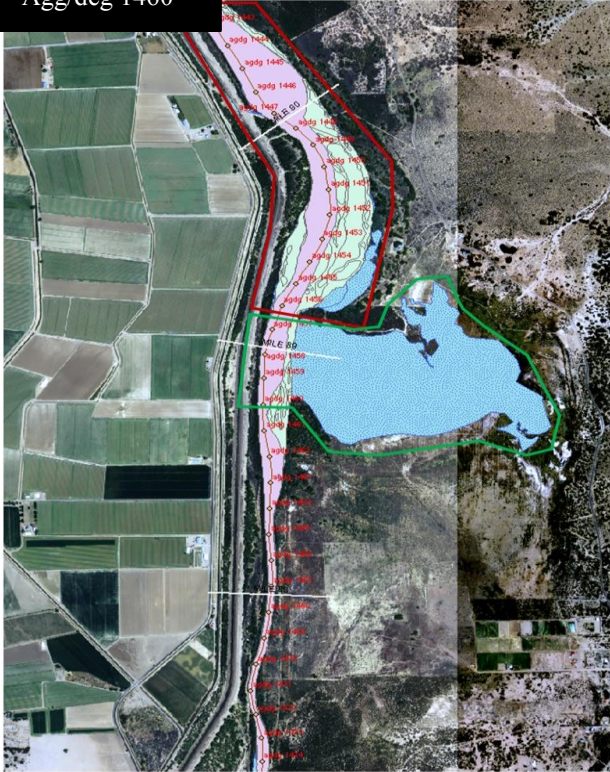
- Agg/deg 1422 ~ Agg/deg 1428
 - 3-5 times of channel widths
 - traverse bars



- Agg/deg 1428 ~ Agg/deg 1442
 - between curved sections
 - traverse bars



~ Agg/deg 1460



- Agg/deg 1442 ~ Agg/deg 1448
- wider sections compared with agg/deg 1449 & downstream
- Agg/deg 1449 ~ Agg/deg 1456
- curved
- narrow at low flow and wide at high flows



- Agg/deg 1457 ~ Agg/deg 1460
- significant amount of overbank flows



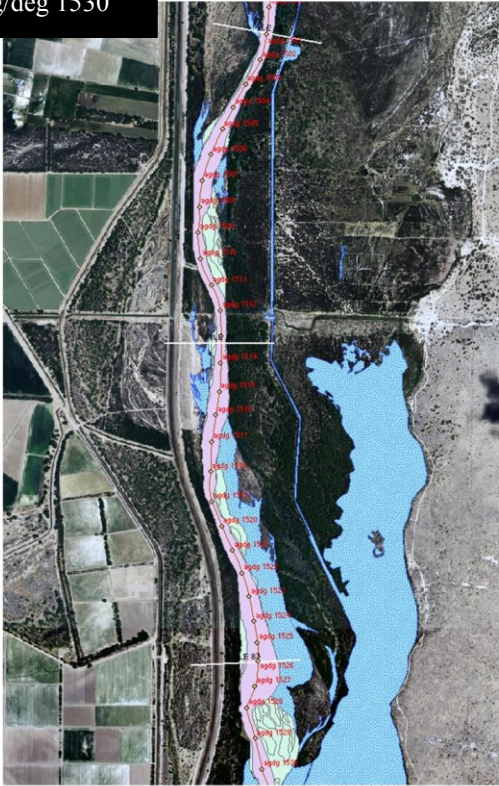
- Agg/deg 1461 ~ Agg/deg 1474 (straight and having high banks)

~ Agg/deg 1500

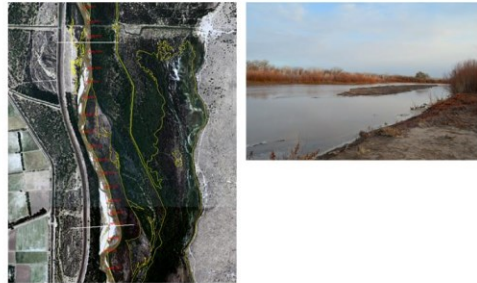


- Agg/deg 1476 ~ Agg/deg 1500
- straight and high banks

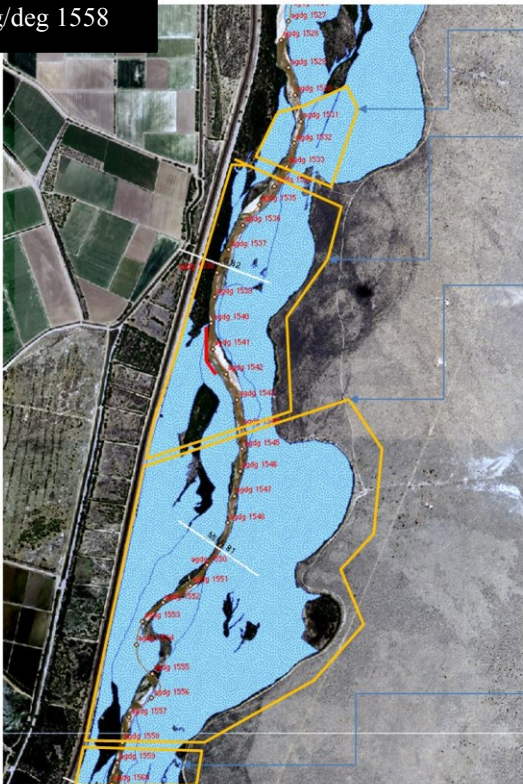
~ Agg/deg 1530



- Agg/deg 1501 ~ Agg/deg 1504
- straight and having high banks & no overbank flows
- Agg/deg 1505 ~ 1511
- sinuous
- bars at concave
- Agg/deg 1512 ~ 1514
- straight without overbanks
- Agg/deg 1515 ~ 1530
- significant overbank flows to left floodplains

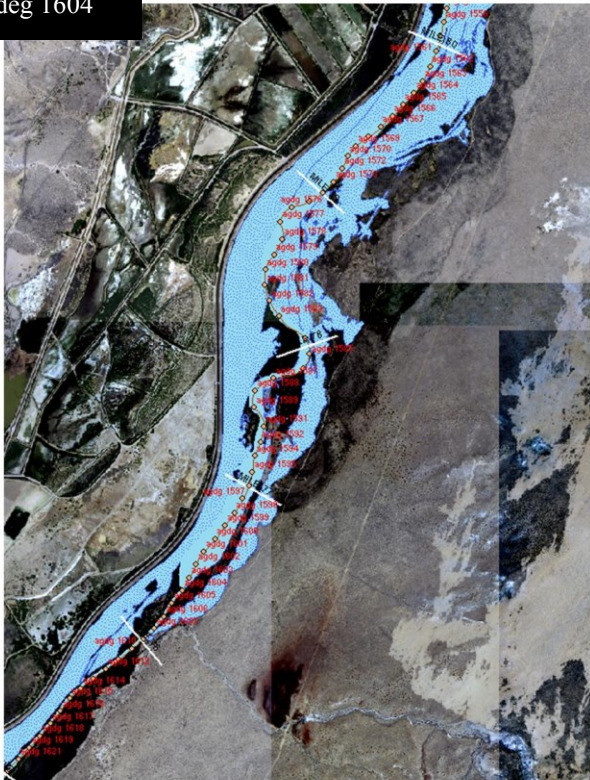


~ Agg/deg 1558



- Agg/deg 1531 ~ Agg/deg 1533
- Overbank flows with perching
- Agg/deg 1534 ~ 1544
- No significant changes in channel widths
- 1540 ~ 1542 : overbank flows with perching
- flow returns to 1564
- Agg/deg 1545 ~ 1558
- 2-3 times of channel widths
- with significant overbank flows
- 1553 ~ 1557 : sharp bends
- Agg/deg 1559 ~ downstream
- narrow channel

~ Agg/deg 1604



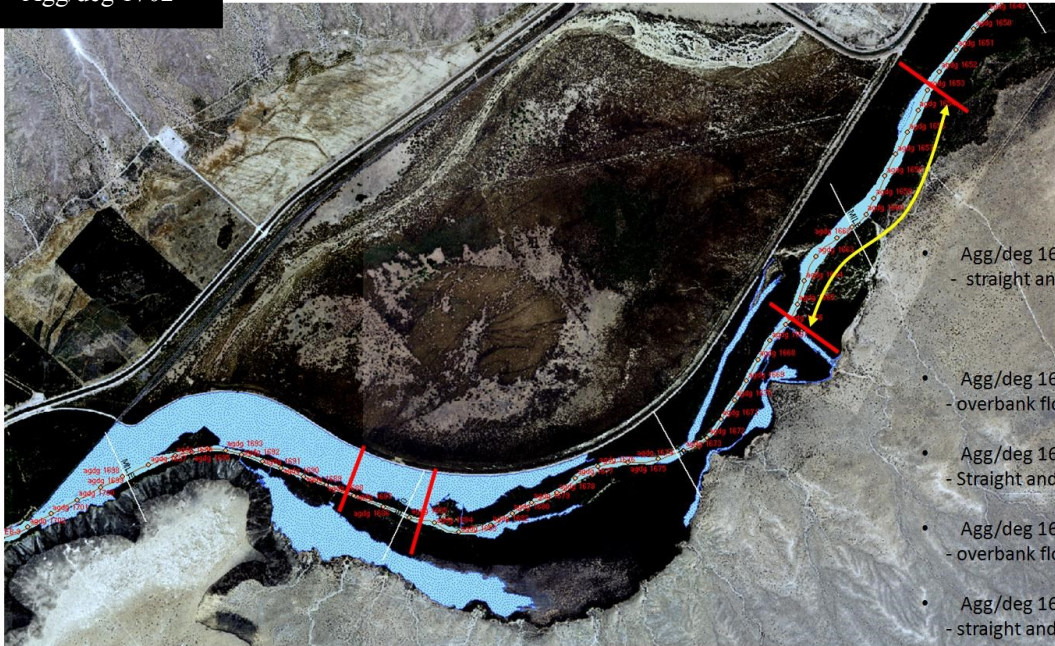
- Agg/deg 1559~ Agg/deg 1597
 - right banks with overbank flows 1559-1582
 - from 1585 to 1610 : return flows
 - 1582-1594 : without overbanking at right side
 - 1587-1610 : without overbanking at left side
- Agg/deg 1594-1604 : right banks with overbanking flows
 - returns to 1638

~ Agg/deg 1638



- Agg/deg 1621– 1638
 - straight and main channel flows
- Agg/deg 1638
 - return flow from 1559-1604 (except 1582-1594)
- Agg/deg 1638-1654
 - straight and narrow/deep channel

~ Agg/deg 1702



- Agg/deg 1654~1667
- straight and deep channel
- Agg/deg 1667
- overbank flows with perching
- Agg/deg 1668~1672
- Straight and deep channel
- Agg/deg 1673
- overbank flows with perching
- Agg/deg 1674-1682
- straight and narrow without perching
- Agg/deg 1683-1685
- right side with overbank flows and perching
- Agg/deg 1686-1687
- main channel flows
- Agg/deg 1688, 1692, 1693
- overbank flows with perching
- Agg/deg 1697-1702
- right side with overbank flows

APPENDIX F. Program Source Code

Main program

```
Public Sub MainProgram()  
Dim t0 As Double  
' time to begin simulation  
t0 = Timer()  
  
'Set the system of units : SI or English  
If IsEmpty(gravity) Or IsEmpty(phi) _  
    Or gravity = 0 Or phi = 0 Then  
    SetUnits SI  
End If  
  
"*****" Get input data "*****"  
Dim BR_projectbook As Workbook  
Dim dt As Double  
Dim n As Double  
Dim ds As Double  
Dim vis As Double  
Dim po As Double  
Dim z As Double  
Dim ttime As Double  
Dim tt As Long  
Dim nxsections As Long  
Dim ntimesteps As Long  
Dim tsteps() As timestep  
Dim timestepinputsheet As Worksheet  
Dim flowinputfile As String  
Dim xsectioninputsheet As Worksheet  
Dim xsectinputfile As String  
Dim outputsheet As Worksheet  
Dim outputfile As String  
Dim datainputsheet As Worksheet  
  
Set BR_projectbook = ThisWorkbook  
Set datainputsheet = BR_projectbook.Worksheets("BR_Data")  
Set timestepinputsheet = BR_projectbook.Worksheets("BR_QandElevInput")  
Set xsectioninputsheet = BR_projectbook.Worksheets("BR_NodeInput")  
Set outputsheet = BR_projectbook.Worksheets("BR_Out")  
'input data used commonly through whole simulation
```

```

mto_IO.initialinput datainputsheet, _
    dt, ds, vis, po, n, TOL_NORMALDEPTH, TOL_BACKWATER, _
    MAX_NORMALDEPTH, MAX_ITERATIONS, _
    flowinputfile, xsectinputfile, outputfile

```

```

Set fs = CreateObject("Scripting.FileSystemObject")
fs.CreateTextFile outputfile

```

```

' Timestep data

```

```

mto_IO.gettimesteps tsteps, ntimesteps, dt, timestepinputsheet

```

```

' Cross section data : station, bed slope, bed elevation, bottom width, _

```

```

'   minimum bed elevation, bank elevation, Manning n, options

```

```

mto_IO.getxsections tsteps(1).xsect(), nxsections, xsectioninputsheet

```

```

' Reach data based on cross sectional data

```

```

mto_IO.getreaches tsteps(1).rch(), tsteps(1).xsect(), nxsections

```

```

For tt = 1 To ntimesteps

```

```

    tsteps(tt).ds = ds

```

```

    tsteps(tt).epsilon = TOL_BACKWATER

```

```

    tsteps(tt).po = po

```

```

    tsteps(tt).dt = dt

```

```

' Computing viscosity and falling velocity

```

```

ViscosityfromTemp tsteps(tt)

```

```

fallv tsteps(tt)

```

```

' Computing backwater profiles and hydraulic parameters

```

```

mtb_Backwater.BackwaterLoop tsteps(tt), nxsections

```

```

' Computing representative hydraulic parameters with weighting factors

```

```

mtz_Rephyd.hyd tsteps(tt), nxsections

```

```

' Computing channel bed elevation

```

```

mtb_SedTrans.SedLoop tsteps(tt), tsteps(tt + 1), nxsections, dt

```

```

' Writing hydraulic and sedimentation results to a designated file

```

```

mto_FileIO.writexsectionarraytofile_csv tsteps(tt).xsect, _
    tsteps(tt).day, tsteps(tt).omega, outputfile, fs, nxsections

```

```

Next tt

```

```

' time to end simulation

```

```

tf = Timer

```

```

MsgBox ((tf - t0) & " seconds elapsed during calculation")

```

```

End Sub

```

Backwater profile computation

```
Public Sub BackwaterLoop(ByRef tstp As timestep, _  
    ByRef nx As Long)
```

```
Dim sta As Long ' sta is the counter for cross sections.
```

```
Dim hnmax As Double
```

```
' Checking for zero discharge.
```

```
' If  $Q = 0$ , everything else is 0
```

```
If tstp.Q = 0 Then
```

```
    For sta = 1 To nxsections
```

```
        tstp.xsect(sta).h = 0
```

```
        hnmax = MAX_NORMALDEPTH
```

```
        mtf_Normal.normaldepth tstp.xsect(sta), tstp.Q, _  
            hnmax, 0, TOL_NORMALDEPTH
```

```
        mtf_Critical.criticaldepth tstp.xsect(sta), tstp.Q
```

```
        mtf_Geometry.AllGeom tstp.xsect(sta), tstp.Q
```

```
        mtf_Hydraulics.AllHydr tstp.xsect(sta)
```

```
    Next sta
```

```
Else
```

```
    ' Compute the normal depth and the critical depth at station 1
```

```
    hnmax = MAX_NORMALDEPTH
```

```
    mtf_Normal.normaldepth tstp.xsect(nx), tstp.Q, _  
        hnmax, 0, TOL_NORMALDEPTH
```

```
    mtf_Critical.criticaldepth tstp.xsect(nx), tstp.Q
```

```
    ' Assume downstream depth (sta 1) = normal depth.
```

```
    ' If the normal depth is less than the critical depth,
```

```
    ' the critical depth is used as a downstream boundary condition.
```

```
If tstp.xsect(nx).yn > tstp.xsect(nx).yc Then
```

```
    tstp.xsect(nx).h = tstp.xsect(nx).yn
```

```
Else: tstp.xsect(nx).h = yc
```

```
End If
```

```
' Compute basic hydraulic properties : perimeter, hydraulic radius, velocity,
```

```
' velocity head, total energy and friction, slope at downstream end station
```

```
mtf_Geometry.AllGeom tstp.xsect(nx), tstp.Q
```

```
mtf_Hydraulics.AllHydr tstp.xsect(nx)
```

```

' ***** Standard Step Loop *****
' sta : unknown upstream node
' sta + 1 : known downstream node
' compute the upstream water depth with standard step formation
' Loop continues to nx-1 reaches

For sta = nx - 1 To 1 Step -1

    ' Compute the normal depth and the critical depth at station 1

    hnmax = MAX_NORMALDEPTH
    mtf_Normal.normaldepth tstp.xsect(sta), tstp.Q, hnmax, 0, TOL_NORMALDEPTH
    mtf_Critical.criticaldepth tstp.xsect(sta), tstp.Q

    ' Compute a backwater profile at each reach

    BackwaterReach tstp.xsect(sta), _
                    tstp.xsect(sta + 1), _
                    tstp.rch(sta), _
                    tstp.Q, tstp.epsilon, tstp.options, CInt(errorcode)

    ' Standard Step Loop Error Checking
    ' If computed water depth less than critical depth,
    '     critical water depth is assumed to be the water depth at the station

    If tstp.xsect(sta).h < tstp.xsect(sta).yc Then
        tstp.xsect(sta).h = tstp.xsect(sta).yc
    End If

    ' If the Upstream width is greater than the downstream width,
    ' there is a contraction

    If tstp.xsect(sta).Tw > tstp.xsect(sta + 1).Tw Then

        ' check if the specific energy at the upstream station
        ' is less than the critical energy at the constriction downstream.
        tstp.xsect(sta).senergy = tstp.xsect(sta).velhead + tstp.xsect(sta).h
        mtf_Critical.criticalenergy tstp.xsect(sta + 1), tstp.Q

        ' If energy < critical energy, the water has to backup
        ' until it gets sufficient energy to pass.

```

```

If tstp.xsect(sta).senergy < tstp.xsect(sta + 1).cenergy Then

    Dim hmin As Double ' minimum upstream head
    Dim hmax As Double ' maximum upstream head
                        ' hmax is arbitrarily set to 1.5x solved depth.

    Dim k As Integer
    Dim dscenergy As Double ' downstream critical energy
    Dim ussenergy As Double ' upstream specific energy
                        ' Declaring these two variables
                        ' saves time in the loop.

    hmin = tstp.xsect(sta).yc
    hmax = 5 * tstp.xsect(sta).h
    k = 1
    dscenergy = tstp.xsect(sta + 1).cenergy
    ussenergy = tstp.xsect(sta).senergy

    Do Until Abs(ussenergy - dscenergy) < 0.00000001 _
        Or k = MAX_ITERATIONS
        mtf_Hydraulics.VelocityHead tstp.xsect(sta)
        ussenergy = tstp.xsect(sta).velhead + tstp.xsect(sta).h

        ' If specific energy is still too low,
        ' then the head is adjusted upward and vice versa.

        bisection (ussenergy - dscenergy), _
            tstp.xsect(sta).h, _
            hmax, _
            hmin, _
            tstp.rch(sta).epsilon

        k = k + 1
    Loop
End If

mtf_Geometry.AllGeom tstp.xsect(sta), tstp.Q
mtf_Hydraulics.AllHydr tstp.xsect(sta)

' ***** Compute Courant Condition *****
' Compute the Courant-Friedrich-Levy number and check stability
tstp.rch(sta).courant = dt * 5 _
    * tstp.xsect(sta).ubar / (3 * tstp.rch(sta).deltax) ' ;
If tstp.rch(sta).courant > 1 Then

```

```

        MsgBox ("the model is unstable")
    End If
Next sta
End If
End Sub

Public Sub BackwaterReach(ByRef usxsct As xsection, _
    ByRef dsxsct As xsection, _
    ByRef rch As reach, _
    ByRef Q As Double, _
    ByRef epsilon As Double, _
    ByRef options As Integer, _
    ByRef errorcode As Integer)

    Dim mindeltaH As Double
    Dim h_at_mindeltaH As Double

    Dim k As Long
    Dim Qtrial As Long

    ' Assume upstream depth = downstream depth
    usxsct.h = dsxsct.h

    ' Initializing
    h_at_mindeltaH = usxsct.h
    rch.epsilon = epsilon
    rch.DeltaHe = 0
    ' reach length
    rch.deltax = Abs(usxsct.x - dsxsct.x)

    ' solve h1 from h2 with trial-error approach
    k = 0
    rch.numiterations = 0
    Do
        k = k + 1
        ' lateralQ is recalculated within the loop
        ' because it could theoretically depend on head.

        ' If the water stage exceeds the crest of bank, overbank flow begins.
        If (usxsct.h + usxsct.z) > usxsct.bankelev Then
            rch.ql = 0.0005 * (Abs(usxsct.h + usxsct.z - usxsct.bankelev)) ^ (2 / 3)
        ElseIf (usxsct.h + usxsct.z) <= usxsct.bankelev Then
            rch.ql = 0
        End If
    Loop

```

End If

lateralQ = rch.q1 * rch.deltax

'Depending on given options,

'overbank flows are assumed as complete loss or return flow to the next reache.

'option 0 : perching (water loss)

'option 1 : return flow

'option 2 : energy loss due to backwater from bridge (no water loss)

'option 3 : energy loss due to backwater from sharp bends (no water loss)

If usxsct.options = 0 Then

 Qtrial = Q - lateralQ

Else: Qtrial = Q

End If

rch.numiterations = rch.numiterations + 1

mtf_Geometry.AllGeom usxsct, Q

mtf_Hydraulics.AllHydr usxsct

' Compute the average friction slope between stations sta and sta-1

rch.sfbar = (usxsct.sf + dsxsct.sf) / 2

'options 3 : energy loss due to sharp bends

If usxsct.options = 3 Then

 c = (dsxsct.hyradius) ^ (1 / 6) / dsxsct.n

 rch.Cb = (24 * (9.81) ^ 0.5 / c + 60 * 9.81 / c ^ 2) * (dsxsct.h / 88 * 90 + dsxsct.h / 104 * 160 + dsxsct.h / 247 * 95)

Else: rch.Cb = 0

End If

'options 2 : water depth increase due to bridge contraction

If usxsct.options = 2 Then

 rch.DeltaB = 1.25 * dsxsct.Fr2 * (1.25 + 5 * dsxsct.Fr2 - 0.6) * (0.13 + 15 * 0.13 ^ 4) * dsxsct.h

Else: rch.Cb = 0

End If

' Minor losses for contraction or expansion

' 0.1 for contraction and 0.3 for expansion (HEC-RAS manual)

If dsxsct.ubar > usxsct.ubar Then

 rch.CeCc = 0.1

```

ElseIf dsxsct.ubar < usxsct.ubar Then
    rch.CeCc = 0.3
Else
    rch.CeCc = 0
End If
'DeltaHe = Head loss due to contractions, expansions, and bends.
'DeltaCecC : energy loss due to contraction/expansion
'DeltaCb : energy loss due to bends

rch.DeltaCeCc = rch.CeCc * _
    Abs((usxsct.alpha * usxsct.ubar ^ 2) _
    - (dsxsct.alpha * dsxsct.ubar ^ 2)) _
    / (2 * gravity)
rch.DeltaCb = rch.Cb * ((usxsct.alpha * usxsct.ubar ^ 2) / (2 * gravity))
rch.DeltaHe = rch.DeltaCeCc + rch.DeltaCb

'Compute the total energy at the u/s station (sta)
'= the total energy d/s + the head lost between both stations
'Head loss = mean friction slope * dx + bend and geometry head loss

rch.head1starprime = dsxsct.Tenergy + rch.sfbar _
    * rch.deltax + rch.DeltaHe

'Compute the difference in total energy in station sta
'by subtracting the total energy start (etstart) and
'the total energy computed with the function geometry energyt

rch.deltaH = rch.head1starprime - usxsct.Tenergy

'Comparing to the minimum from previous iterations.
'If the current error is smaller, it replaces the stored value.
'The corresponding depth also replaces the stored value for that parameter.
If k = 1 Then
    mindeltaH = rch.deltaH
ElseIf Abs(rch.deltaH) < Abs(mindeltaH) Then
    mindeltaH = rch.deltaH
    h_at_mindeltaH = usxsct.h
End If

'Check if rch.deltaH (denenergy) is less than a specified error.
'If yes, we can proceed to the next u/s station.
'If not, a new value will be assumed.
'dhstart is added to the previous assumed depth to compute the new assumed depth.

```

' dhstart equation comes from Henderson (1966) book pp.143

```
If Abs(rch.deltaH) > rch.epsilon Then
    usxsct.h = usxsct.h + Deltah1star_c(rch.deltaH, usxsct.Fr, _
        rch.CeCc, usxsct.sf, rch.deltax, usxsct.hyradius)
End If
```

*' If the convergence function "Deltah1star_c" creates an upstream depth
' which is negative, the solution will be set to depth of the previous iteration*

*' If the guessed head is negative then the iteration will not converge.
' The counter is set to the maximum and the loop terminates.
' After exiting the loop, the head will be set to the minimum error head.*

```
If usxsct.h < 0 Then
    k = MAX_ITERATIONS
End If
```

```
Loop Until (Abs(rch.deltaH) < rch.epsilon) Or (k = MAX_ITERATIONS)
```

```
If k = MAX_ITERATIONS Then
    usxsct.h = h_at_mindeltaH
    rch.mindeltaH_used = True
End If
```

```
rch.numiterations = k
End Sub
```

*' If the convergence criteria is not met, this function is called
' to generate a new guess for the downstream depth.*

```
Private Function Deltah1star_c(ByRef deltacaph As Double, _
    ByRef froude1star As Double, _
    ByRef c1star As Double, _
    ByRef sf1star As Double, _
    ByRef deltax As Double, ByRef r1star As Double)
Deltah1star_c = deltacaph / (1 - froude1star ^ 2 * _
    (3 * sf1star * deltax / 2 / r1star))
End Function
```

Sedimentation computation

'''''''''' - SEDIMENT TRANSPORT - AGGRADATION/DEGRADATION - ''''''''''

```
Public Sub SedLoop(ByRef tstp1 As timestep, _  
    ByRef tstp2 As timestep, _  
    ByRef nx As Long, _  
    ByRef dt As Double)
```

```
Dim sta As Long  
tstp2.xsect = tstp1.xsect  
tstp2.rch = tstp1.rch
```

'initialize the available volume

```
If tstp1.day = 1 Then  
    mtf_SedFunc.InitializeAvailableVolume tstp1, nx  
End If
```

' If discharge is zero, then the bed elevation and slope do not change

```
If tstp1.Q = 0 Then  
    For sta = 1 To nx  
        tstp2.xsect(sta).z = tstp1.xsect(sta).z  
        tstp2.xsect(sta).s0 = tstp1.xsect(sta).s0  
        tstp1.xsect(sta).qst = 0  
    Next sta  
    tstp2.rch = tstp1.rch
```

*' If discharge is not zero, sediment discharge is computed by
' (1) Yang's equation or (2) Julien's equation*

Else

```
If Sheet1.optbtn_Yang Then  
    mtf_SedFunc.AllSed_Yangs tstp1, nx, dt  
ElseIf Sheet1.optbtn_Julien Then  
    mtf_SedFunc.AllSed_Julien tstp1, nx, dt  
End If
```

' Elevation at upstream end is given as a boundary condition
tstp2.xsect(1).z = tstp2.uselev
' Bed slope at last downstream section assumed to be constant.
tstp2.xsect(nx).s0 = tstp1.xsect(nx).s0

```

For sta = 1 To nx - 1
    SedReach tstp1.rch(sta), tstp2.rch(sta), _
        tstp1.xsect(sta), tstp1.xsect(sta + 1), _
        tstp2.xsect(sta), tstp2.xsect(sta + 1), _
        tstp1.omega, _
        tstp1.po, _
        tstp1.dt, _
        errorcode

    Next sta
End If
End Sub

Public Sub SedReach(ByRef rch1 As reach, _
    ByRef rch2 As reach, _
    ByRef usxsct1 As xsection, _
    ByRef dsxsct1 As xsection, _
    ByRef usxsct2 As xsection, _
    ByRef dsxsct2 As xsection, _
    ByRef omega As Double, _
    ByRef po As Double, _
    ByRef dt As Double, _
    ByRef errorcode As Integer, _
    Optional ByRef deltac As Double)

Dim CR As Double
Dim delhh As Double
Dim Rouse As Double

    ' Average top width in a reach
    rch1.aveTw = 0.5 * (usxsct1.Tw + dsxsct1.Tw)
    ' Active channel depth : bank crest elevation – active channel bottom elevation
    delhh = usxsct1.bankelev - usxsct1.z
    ' Calculate the Rouse number
    Rouse = 2.5 * omega / (9.81 * dsxsct1.h * dsxsct1.sf) ^ 0.5
    ' Determine the sediment concentration profiles
    If delhh > 0 Then
        Module2.Simpson CR, 0.0005, dsxsct1.h, 20, Rouse, delhh
    Else: Module2.Simpson CR, 0.0005, dsxsct1.h, 20, Rouse, 0.01
    End If

    ' If WSE is below the bank crest elevation, no sediment loss

```

If dsxsct1.WSE <= dsxsct1.bankelev Then

deltac = 1# 'SSUM2 / SSUM1

Else: deltac = CR

End If

' Change in sediment discharge between 2 adjacent stations

' Out - in

rch1.deltaqst = dsxsct1.qst - usxsct1.qst

rch1.balance = rch1.deltaqst - rch1.ql * rch1.deltax * 86400 * dt * _

(usxsct1.qst / (usxsct1.hydepth ^ (5 / 3) * usxsct1.sf ^ 0.5 / usxsct1.n * 86400)) * deltac

dsxsct2.z = dsxsct1.z

' << degradation >>

If rch1.deltaqst > 0 Then

' If the balance is >= available volume, everything will move downstream.

' The new elevation is equal to the minimum elevation.

If rch1.balance >= rch1.avolume Then

dsxsct2.z = dsxsct2.zmin

' Amount of sediment that goes into the next node

' = what comes into the previous one + the available volume.

rch1.ehqst = usxsct1.qst + rch1.avolume

' the new available volume is zero, because

' everything was moved out downstream

rch2.avolume = 0

Else

' If available volume is > balance, then only a part of

' the available sediment is moved downstream

rch2.avolume = rch1.avolume - rch1.balance

' compute new elevation at downstream station

' node due to the volume remaining

dsxsct2.z = dsxsct1.zmin + _

*rch2.avolume / ((1 - po) * _*

```

                rch2.deltax * (rch1.aveTw))
    End If

    If dsxsct2.z < 0 Then
        'error(' unstable' )
    End If

    '<< aggradation >>

    Else 'there is aggradation
        'Trap efficiency at time t+1 based on h and
        'velocity computed at time = t

        dsxsct1.trapeff = 1 - Exp(-rch1.deltax * _
            omega / (dsxsct1.h * dsxsct1.ubar))

        'Theoretical change in bed elevation at time t+1

        dsxsct1.deltaz = -dsxsct1.trapeff * _
            rch1.deltaqst / ((1 - po) * _
            rch1.deltax * rch1.aveTw) * dt

        usxsct2.z = usxsct1.z + 0.4 * dsxsct1.deltaz
        dsxsct2.z = dsxsct1.z + 0.6 * dsxsct1.deltaz

        'Compute the available volume
        'balance is <0,when aggradation
        rch2.avolume = rch1.avolume - rch1.balance

    End If

    'Calculate the new bed channel slope
    rch2.deltaz = usxsct2.z - dsxsct2.z
    rch2.S0bar = rch2.deltaz / rch2.deltax

    'For use in calculation, the upstream cross section is
    'assumed to have the bed slope of the adjacent reach
    usxsct2.s0 = rch2.S0bar

End Sub

```

Critical depth and energy

```
Public Sub criticaldepth(ByRef xsct As xsection, _  
    ByRef Q As Double, _  
    Optional ByRef hmax As Double, _  
    Optional ByRef hmin As Double, _  
    Optional ByRef epsilon As Double, _  
    Optional ByRef gravity As Double = 9.81, _  
    Optional ByRef rho As Double = 1000)
```

```
    If Q = 0 Then  
        xsct.yc = 0  
    Else  
        Select Case xsct.gamma.channeltype  
            Case Is = 1      'For Rectangular chanel  
                xsct.yc = ((Q / xsct.gamma.g1) ^ (2) / gravity) ^ (1 / 3)  
            Case Is = 2      'Trapezoidal Channel  
        End Select  
    End If  
End Sub
```

```
Public Sub criticalenergy(ByRef xsct As xsection, _  
    ByRef Q As Double, _  
    Optional ByRef hmax As Double, _  
    Optional ByRef hmin As Double, _  
    Optional ByRef epsilon As Double, _  
    Optional ByRef gravity As Double = 9.81, _  
    Optional ByRef rho As Double = 1000)
```

```
    Dim yc As Double  
    If Q = 0 Then  
        xsct.cenergy = 0  
    Else  
        yc = xsct.yc  
        Select Case xsct.gamma.channeltype  
            'Rectangular Channel  
            Case Is = 1      xsct.cenergy = 3 * yc / 2  
            'Trapezoidal Channel  
            Case Is = 2  
        End Select  
    End If  
End Sub
```

Hydraulic parameters 1

*' Calculates Hydraulic Geometry Parameters
' main subroutine for hydraulic parameter computation*

```
Public Sub AllGeom(ByRef xsct As xsection, _  
    ByRef Q As Double)  
If Q = 0 Then  
    xsct.area = 0  
    xsct.Pw = xsct.gamma.g1  
    xsct.Tw = xsct.gamma.g1  
    xsct.WSE = xsct.z  
    xsct.ubar = 0  
    xsct.hyradius = 0  
    xsct.hydepth = 0  
Else  
    mtf_Geometry.AreaFromDepth xsct  
    mtf_Geometry.WettedPerimeterFromDepth xsct  
    mtf_Geometry.TopWidthFromDepth xsct  
    xsct.WSE = xsct.h + xsct.z  
    xsct.ubar = Q / xsct.area  
    xsct.hyradius = xsct.area / xsct.Pw  
    xsct.hydepth = xsct.area / xsct.Tw  
End If  
End Sub
```

*' For a given depth and channel geometry, this function
' calculates the area of flow.*

```
Public Sub AreaFromDepth(ByRef xsct As xsection)
```

```
Dim b As Double  
Dim z As Double  
Dim depth As Double  
depth = xsct.h  
If depth = 0 Then  
    xsct.area = 0  
Else  
    Select Case xsct.gamma.channeltype  
        ' Rectangular Channel  
    Case Is = 1  
        b = xsct.gamma.g1  
        xsct.area = b * depth
```

```

    ' Trapezoidal Channel
    Case Is = 2
        b = xsct.gamma.g1
        z = xsct.gamma.g2
        xsct.area = (b + b + z * 2 * depth) / 2 * depth
    End Select
End If
End Sub

' For a given depth and channel geometry, this function
' calculates the wetted Perimeter of flow.
Public Sub WettedPerimeterFromDepth(ByRef xsct As xsection)

Dim depth As Double
Dim b As Double
Dim z As Double
depth = xsct.h
If depth = 0 Then
    xsct.Pw = xsct.gamma.g1
Else
    Select Case xsct.gamma.channeltype
        ' Rectangular Channel
        Case Is = 1
            b = xsct.gamma.g1
            xsct.Pw = b + 2 * depth

            ' Trapezoidal Channel
            Case Is = 2
                b = xsct.gamma.g1
                z = xsct.gamma.g2
                xsct.Pw = b + 2 * ((depth * z) ^ 2 + depth ^ 2) ^ (1 / 2)
            End Select
    End If
End Sub

' For a given depth and channel geometry, this function
' calculates the Top Width of flow.
Public Sub TopWidthFromDepth(ByRef xsct As xsection)

Dim depth As Double
Dim b As Double
Dim z As Double

```

```

depth = xsct.h
If depth = 0 Then
    xsct.Tw = xsct.gamma.g1
Else
    Select Case xsct.gamma.channeltype
    'Rectangular Channel
    Case Is = 1
        b = xsct.gamma.g1
        xsct.Tw = b

    'Trapezoidal Channel
    Case Is = 2
        b = xsct.gamma.g1
        z = xsct.gamma.g2
        xsct.Tw = b + 2 * z * depth
    End Select
End If
End Sub

' For a given depth and channel geometry, this function
' calculates the Bed Slope.
Public Sub BedslopefromStationElevation(ByRef usxsct As xsection, _
    ByRef dsxsct As xsection, _
    ByRef rch As reach)

rch.S0bar = (usxsct.z - dsxsct.z) / _
    (dsxsct.x - usxsct.x)

End Sub

```

Hydraulic parameters 2

```
Public Sub AllHydr(ByRef xsct As xsection)
    mtf_Hydraulics.froude xsct
    mtf_Hydraulics.TotalMechanicalEnergyHead xsct
    mtf_Hydraulics.VelocityHead xsct
    mtf_Hydraulics.ManningSlope xsct
End Sub
```

' Calculates Froude number

```
Public Sub froude(ByRef node As xsection, _
    Optional ByRef gravity As Double = 9.81)
node.Fr2 = node.ubar ^ 2 / gravity / node.hydepth
node.Fr = Sqr(node.Fr2)
End Sub
```

' Calculates total mechanical energy from the bernoulli equation

```
Public Sub TotalMechanicalEnergyHead(ByRef node As xsection, _
    Optional ByRef includez As Integer = 1, _
    Optional ByRef gravity As Double = 9.81)
node.Tenergy = node.z * includez + node.h + _
    node.alpha * node.ubar ^ 2 / 2 / gravity
End Sub
```

' Calculates total mechanical energy from the bernoulli equation

```
Public Sub VelocityHead(ByRef node As xsection, _
    Optional ByRef gravity As Double = 9.81)
node.velhead = node.alpha * node.ubar ^ 2 / 2 / gravity
End Sub
```

' Calculates Friction Slope using mannings equation

```
Public Sub ManningSlope(ByRef node As xsection, _
    Optional ByRef gravity As Double = 9.81, _
    Optional ByRef phi As Double = 1#)
node.sf = node.n ^ 2 * node.ubar ^ 2 / (phi ^ 2) / (node.hyradius ^ (4 / 3))
End Sub
Public Sub ViscosityfromTemp(ByRef tstep As timestep)
```

' Calculate the kinematic viscosity of water as a function of temperature

```
Dim t As Double
t = tstep.temp
tstep.vis = 4.496729E-10 * t ^ 2 - 0.000000046205 * t + 0.000001762786 '
End Sub
```

Normal depth

' Calculate normal depths

```
Public Sub normaldepth(ByRef xsct As xsection, _
    ByRef Q As Double, _
    ByRef hnmax As Double, _
    ByRef hnmin As Double, _
    ByRef epsilon As Double, _
    Optional ByRef gravity As Double = 9.81, _
    Optional ByRef rho As Double = 1000, _
    Optional ByRef phi As Double = 1#)

    Dim C1 As Double
    Dim xscttrial As xsection
    Dim C1trial As Double
    Dim k As Long

    If Q = 0 Then
        xscttrial.yn = 0
    ElseIf xsct.s0 <= 0 Then
        xscttrial.yn = 0
    Else
        xscttrial = xsct
        ' Compute constant c1
        C1 = (Q * xsct.n) / (Sqr(xsct.s0) * phi)
        ' Compute function of hn (normal depth)
        xscttrial.h = (hnmin + hnmax) / 2
        k = 1
        Do Until Abs(C1 - C1trial) < epsilon Or k > MAX_ITERATIONS
            mtf_Geometry.AreaFromDepth xscttrial
            mtf_Geometry.WettedPerimeterFromDepth xscttrial
            ' If trial flow is greater than actual flow,
            ' then the change in elevation is too small.
            C1trial = xscttrial.area ^ (5 / 3) / xscttrial.Pw ^ (2 / 3)
            bisection (C1trial - C1), _
                xscttrial.h, _
                hnmax, hnmin, epsilon
            k = k + 1
        Loop
        xsct.yn = xscttrial.h
    End If
End Sub
```

Sediment Transport Capacity

' Calculate sediment discharge with Julien's equation

Public Sub AllSed_Julien(tstp1 As timestep, nx, dt)

Dim sta As Long

For sta = 1 To nx

' Calculate bed shear

bedshear tstp1.xsect(sta)

' Unit sediment discharge

julien tstp1.xsect(sta).qbv, tstp1.ds, tstp1.xsect(sta).taubed

' Sediment discharge in m3/day

tstp1.xsect(sta).qst = tstp1.xsect(sta).qbv * tstp1.xsect(sta).Tw * 86400 * dt

Next sta

End Sub

' Calculate sediment discharge with Yang's equation

Public Sub AllSed_Yangs(tstp1 As timestep, nx, dt)

Dim sta As Long

Dim cmgl As Double

Dim ckgm3 As Double

For sta = 1 To nx

' Calculate bed shear

bedshear tstp1.xsect(sta)

' Sediment concentration

yangs cmgl, tstp1.vis, tstp1.ds, _
tstp1.xsect(sta).taubed, tstp1.xsect(sta).ubar, _
tstp1.xsect(sta).sf, tstp1.omega

' Unit sediment discharge

' qbv -- unit sediment discharge by volume in m²/s

' First convert Concentration in mg/Liter to kg / m²

*' ckgm3 = cmgl * 1000# / 1000000#*

' Then compute unit discharge by dividing by top width and sediment density.

tstp1.xsect(sta).qbv = ckgm3 / (2.65 * 1000#) * tstp1.Q / tstp1.xsect(sta).Tw

' Sediment discharge in m3/day

tstp1.xsect(sta).qst = tstp1.xsect(sta).qbv * tstp1.xsect(sta).Tw * 86400 * dt

Next sta

End Sub

```

' Calculate bed shear
Public Sub bedshear(ByRef node As xsection, _
    Optional ByRef rho As Double = 1000, _
    Optional ByRef gravity As Double = 9.81)

node.taubed = rho * gravity * node.hyradius * node.sf
End Sub

' Calculate falling velocity
Public Sub fallv(ByRef timestep As timestep, _
    Optional ByRef gravity As Double = 9.81, _
    Optional ByRef Gsed As Double = 2.65)

Dim a As Double
Dim b As Double
Dim ds As Double
Dim vis As Double

ds = timestep.ds
vis = timestep.vis

a = (Gsed - 1) * gravity * ds ^ 3 ' ;
b = (Gsed - 1) * gravity * ds ' ;

timestep.omega = (Sqr((2 / 3) + (36 * vis ^ 2) / a) - _
    Sqr((36 * vis ^ 2) / a)) * Sqr(b)

End Sub

' Calculate sediment transport capacity with Julien's equation
Public Sub julien(ByRef qbv As Double, _
    ByRef d As Double, _
    ByRef taubed As Double, _
    Optional ByRef gravity As Double = 9.81, _
    Optional ByRef rho As Double = 1000, _
    Optional ByRef Gsed As Double = 2.65)

Dim taustart As Double
' Calculation of Shields parameter
' taustart = (taubed/9810)/(1.65*d);
taustart = (taubed / (rho * gravity)) / ((Gsed - 1) * d)

End Sub

```

```

' Calculate the available volume
Public Sub InitializeAvailableVolume(ByRef tstp1 As timestep, _
    ByRef nx As Long)
    Dim sta As Long
    ' Initialize the accumulated volume of sediment in the channel at time 1
    For sta = 1 To nx - 1
        tstp1.rch(sta).avedD = 0.5 * ((tstp1.xsect(sta).z - _
            tstp1.xsect(sta).zmin) + _
            (tstp1.xsect(sta + 1).z - tstp1.xsect(sta + 1).zmin))
        tstp1.rch(sta).aveTw = 0.5 * (tstp1.xsect(sta + 1).Tw _
            + tstp1.xsect(sta).Tw)
        tstp1.rch(sta).avolume = tstp1.rch(sta).avedD * _
            tstp1.rch(sta).aveTw
        tstp1.rch(sta).avolume = tstp1.rch(sta).avolume * _
            (1 - tstp1.po) * tstp1.rch(sta).deltax
    Next sta
End Sub

```

```

' Calculate sediment transport capacity with Julien's equation

```

```

Public Sub yangs(ByRef cmgl As Double, _
    ByRef vis As Double, _
    ByRef ds As Double, _
    ByRef taubed As Double, _
    ByRef v As Double, _
    ByRef sf As Double, _
    ByRef omega As Double, _
    Optional ByRef gravity As Double = 9.81, _
    Optional ByRef rho As Double = 1000, _
    Optional ByRef Gsed As Double = 2.65)

```

```

Dim ustar As Double
    Dim restar As Double
    Dim vcomega As Double
    Dim a As Double
    Dim b As Double
    Dim c As Double
    Dim d As Double
    Dim logcppm As Double
    Dim cppm As Double
    '% Calculate shear velocity %ustar = sqrt(taubed);
    ustar = (taubed) ^ 0.5
    '% Calculate Grain shear Reynolds number : restar = ustar*ds/vis;
    restar = ds * ustar / vis

```

```

% Calculate dimensionless critical velocity
If restar > 0 And restar < 70 Then
    vcomega = (2.5 / (Log10(restar) - 0.06)) + 0.66
ElseIf restar >= 70 Then
    vcomega = 2.05
End If
% Calculate the ratio of shear velocity to fall velocity
a = ustar / omega
% Calculate the product of fall velocity times diameter, and divide it by viscosity
b = omega * ds / vis
% Calculate the product of vcw and sf
c = vcomega * sf
% Calculate the product of v and sf and divide it by omega;
d = v * sf / omega
% Compare c and d. If c > d, the sediment does not move
If c >= d Then
    cmgl = 0
ElseIf c < d Then
    ' % Calculate the logarithm (base 10) of the sediment concentration
    ' in ppm according to Yang's equation
    logcppm = 5.435 - 0.286 * Log10(b) - _
        0.457 * Log10(a) + (1.799 - 0.409 * Log10(b) - _
        0.314 * Log10(a)) * Log10(d - c)
    '
    ' % Convert the concentration in ppm to concentration in mg/l
    cppm = 10 ^ logcppm
    ' %cmgl = 2.65*cppm/(2.65 + (1-2.65)*0.000001*cppm);
    cmgl = 2.65 * cppm / (2.65 + (1 - 2.65) * 0.000001 * cppm)
End If

End Sub

```

Data Input and Output

```
' Data Input
Public Sub getxsectionsfromfile(ByRef xsectionarray() As xsection, _
    ByRef nxsections As Long, ByRef xsectionsheets As Worksheet)
Dim k As Integer
k = 1
Do
ReDim Preserve xsectionarray(k)
xsectionarray(k).ID = xsectionsheets.Cells(k + 1, 1)
xsectionarray(k).x = xsectionsheets.Cells(k + 1, 2)
xsectionarray(k).s0 = xsectionsheets.Cells(k + 1, 3)
xsectionarray(k).z = xsectionsheets.Cells(k + 1, 4)
xsectionarray(k).zmin = xsectionsheets.Cells(k + 1, 5)
xsectionarray(k).alpha = 1
' xsectionarray(k).dxdown = xsectionarray(k).x - xsectionarray(k - 1).x
xsectionarray(k).gamma.channeltype = xsectionsheets.Cells(k + 1, 6)
xsectionarray(k).gamma.g1 = xsectionsheets.Cells(k + 1, 7)
xsectionarray(k).gamma.g2 = xsectionsheets.Cells(k + 1, 8)
xsectionarray(k).gamma.g3 = xsectionsheets.Cells(k + 1, 9)
xsectionarray(k).gamma.g4 = xsectionsheets.Cells(k + 1, 10)
k = k + 1
Loop While xsectionsheets.Cells(k + 1, 1).Value > 0
nxsections = k - 1 ' k - 1 accounts for top row of worksheet with headers.
End Sub

' Data Output
Public Sub writexsectionarraytofile(ByRef nodes() As xsection, _
    ByRef iteration As Long, ByRef Filename As String, ByRef fs As Variant, _
    ByRef outf As Variant, ByRef nx As Long)
Dim f As Variant
Set f = fs.OpenTextFile(Filename, 8, -2)
If iteration = 1 Then
    f.write ("iteration" & vbTab)
    f.write ("nodes(k).ID" & vbTab)
    f.write ("nodes(k).x" & vbTab)
    f.write ("nodes(k).s0" & vbTab)
    f.write ("nodes(k).z" & vbTab)
    f.write ("nodes(k).Tw" & vbTab)
    f.write ("nodes(k).ubar" & vbTab)
    f.write ("nodes(k).area" & vbTab)
    f.write ("Q" & vbTab)
    f.write ("nodes(k).h" & vbTab)
    f.write ("nodes(k).SF" & vbTab)
```

```

        f.write ("nodes(k).Fr2" & vbTab)
        f.write ("nodes(k).yn" & vbTab)
        f.write ("nodes(k).qst" & vbTab)
        f.write ("nodes(k).SDR" & taubed)
        f.write ("nodes(k).n")
        f.writeline
    End If
    ' Write out Node Related Data
    Dim k As Long
    Dim j As Long
    For k = 1 To nx Step 1
        f.write (iteration & vbTab)
        f.write (nodes(k).ID & vbTab)
        f.write (nodes(k).x & vbTab)
        f.write (nodes(k).s0 & vbTab)
        f.write (nodes(k).z & vbTab)
        f.write (nodes(k).Tw & vbTab)
        f.write (nodes(k).ubar & vbTab)
        f.write (nodes(k).area & vbTab)
        f.write (nodes(k).area * nodes(k).ubar & vbTab)
        f.write (nodes(k).h & vbTab)
        f.write (nodes(k).sf & vbTab)
        f.write (nodes(k).Fr2 & vbTab)
        f.write (nodes(k).yn & vbTab)
        f.write (nodes(k).qst) & vbTab
        f.write (nodes(k).SDR) & taubed
        f.write (nodes(k).n)
        f.writeline
    Next k
    f.Close
End Sub

' Data Output (Excel CSU file)

Public Sub writexsectionarraytofile_csv(ByRef nodes() As xsection, _
    ByRef iteration As Long, ByRef omega As Double, ByRef Filename As String, _
    ByRef fs As Variant, ByRef nx As Long)

    Dim f As Variant
    Set f = fs.OpenTextFile(Filename, 8, -2)
    If iteration = 1 Then
        f.write ("iteration,")
        f.write ("nodes_ID,")

```

```

f.write ("nodes_x,")
f.write ("nodes_s0,")
f.write ("nodes_z,")
f.write ("nodes_Tw,")
f.write ("nodes_ubar,")
f.write ("nodes_area,")
f.write ("Q,")
f.write ("nodes_h,")
f.write ("nodes_Sf,")
f.write ("nodes_Fr2,")
f.write ("nodes_yn,")
f.write ("nodes_SDR,")
f.write ("nodes_Elyn,")
f.write ("nodes_Ro")
f.writeline
End If
' Write out Node Related Data
Dim k As Long
Dim j As Long
For k = 1 To nx Step 1
f.write (iteration & ", ")
f.write (nodes(k).ID & ", ")
f.write (nodes(k).x & ", ")
f.write (nodes(k).s0 & ", ")
f.write (nodes(k).z & ", ")
f.write (nodes(k).Tw & ", ")
f.write (nodes(k).ubar & ", ")
f.write (nodes(k).area & ", ")
f.write (nodes(k).area * nodes(k).ubar & ", ")
f.write (nodes(k).h & ", ")
f.write (nodes(k).sf & ", ")
f.write (nodes(k).Fr2 & ", ")
f.write (nodes(k).yn & ", ")
f.write (nodes(k).SDR & ", ")
f.write (nodes(k).z + nodes(k).yn & ", ")
f.write (2.5 * omega / (9.8 * nodes(k).h * nodes(k).sf) ^ 0.5)
f.writeline
Next k
f.Close
End Sub

```

Creating a chart on Excel workbook

```
Public Sub createchart(ByRef dataChart As Chart, _
    ByRef outsheet As Worksheet, _
    ByRef nodeSheet As Worksheet, _
    ByRef usstation As Long, _
    ByRef dsstation As Long)

    Dim chartlines As SeriesCollection
    Dim i As Integer
    Dim a As Variant
    Dim xstr As String
    Dim ystr As String
    Set chartlines = dataChart.SeriesCollection

    dataChart.ChartType = xlXYScatter

    For i = 8 To chartlines.Count Step -1
        a = chartlines.ADD(Source:=outsheet.Range(outsheet.Cells(2, 2), outsheet.Cells(2, 3)))
    Next i

    ' loading input data for plotting on a output chart
    Dim rowadjust As Integer
    rowadjust = 2
    For i = 0 To 2
        chartlines(2 * i + 1).XValues = outsheet.Range( _
            outsheet.Cells(rowadjust, 3 * i + 1), _
            outsheet.Cells(dsstation - usstation + rowadjust, 3 * i + 1))
        chartlines(2 * i + 1).Values = outsheet.Range( _
            outsheet.Cells(rowadjust, 3 * i + 2), _
            outsheet.Cells(dsstation - usstation + rowadjust, 3 * i + 2))

        chartlines(2 * i + 2).XValues = outsheet.Range( _
            outsheet.Cells(rowadjust, 3 * i + 1), _
            outsheet.Cells(dsstation - usstation + rowadjust, 3 * i + 1))
        chartlines(2 * i + 2).Values = outsheet.Range( _
            outsheet.Cells(rowadjust, 3 * i + 3), _
            outsheet.Cells(dsstation - usstation + rowadjust, 3 * i + 3))
    Next i

    chartlines(6).XValues = outsheet.Range( _
        outsheet.Cells(rowadjust, 1), _
        outsheet.Cells(dsstation - usstation + rowadjust, 1))
```

```

chartlines(6).Values = outsheet.Range( _
    outsheet.Cells(rowadjust, 10), _
    outsheet.Cells(dsstation - usstation + rowadjust, 10))

chartlines(1).XValues = outsheet.Range( _
    outsheet.Cells(rowadjust, 1), _
    outsheet.Cells(dsstation - usstation + rowadjust, 1))
chartlines(1).Values = outsheet.Range( _
    outsheet.Cells(rowadjust, 11), _
    outsheet.Cells(dsstation - usstation + rowadjust, 11))

xstr = "{ "
For i = 0 To dsstation - usstation
    xstr = xstr & outsheet.Cells(dsstation - usstation - i + rowadjust, 1)
    xstr = xstr & ", "
Next i
xstr = Left(xstr, Len(xstr) - 1)
xstr = xstr & "}"
chartlines(7).XValues = xstr
chartlines(7).Values = nodeSheet.Range( _
    nodeSheet.Cells(rowadjust, 6), _
    nodeSheet.Cells(dsstation - usstation + rowadjust, 6))

chartlines(8).XValues = xstr
ystr = "{ "
For i = rowadjust To dsstation - usstation + rowadjust
    ystr = ystr & nodeSheet.Cells(i, 5) / 2
    ystr = ystr & ", "
Next i
ystr = Left(ystr, Len(ystr) - 1)
ystr = ystr & "}"
chartlines(8).Values = ystr
chartlines(9).XValues = xstr
ystr = "{ "
For i = rowadjust To dsstation - usstation + rowadjust
    ystr = ystr & nodeSheet.Cells(i, 5) / -2
    ystr = ystr & ", "
Next i
ystr = Left(ystr, Len(ystr) - 1)
ystr = ystr & "}"
chartlines(9).Values = ystr
chartlines(9).Values = nodeSheet.Range( _
    nodeSheet.Cells(rowadjust, 5), _

```

nodeSheet.Cells(dsstation - usstation + rowadjust, 5))

```
If dataChart.Legend.LegendEntries.Count > 8 Then  
    dataChart.Legend.LegendEntries(9).Delete  
End If
```

' Chart Legend

```
chartlines(1).Name = ""Water depth""  
chartlines(2).Name = ""Current Bed Elevation""  
chartlines(3).Name = ""Initial Water Surface""  
chartlines(4).Name = ""Initial Bed Elevation""  
chartlines(5).Name = ""Final Water Surface""  
chartlines(6).Name = ""Final Bed Elevation""  
chartlines(7).Name = ""Minimum Bed Elevation""  
chartlines(8).Name = ""Channel Width""
```

```
chartlines(6).AxisGroup = 1  
chartlines(8).AxisGroup = 2  
chartlines(9).AxisGroup = 2
```

' set the chart line properties

```
With chartlines(1).Border  
    .ColorIndex = 34  
    .Weight = xlThick  
    .LineStyle = xlContinuous
```

End With

```
With chartlines(1)  
    .MarkerBackgroundColorIndex = xlNone  
    .MarkerForegroundColorIndex = xlNone  
    .MarkerStyle = xlNone  
    .Smooth = True  
    .MarkerSize = 7  
    .Shadow = False
```

End With

```
With chartlines(2).Border  
    .ColorIndex = 6  
    .Weight = xlThick  
    .LineStyle = xlContinuous
```

End With

```
With chartlines(2)
    .MarkerBackgroundColorIndex = xlNone
    .MarkerForegroundColorIndex = 35
    .MarkerStyle = xlNone
    .Smooth = True
    .MarkerSize = 7
    .Shadow = False
End With
```

```
With chartlines(3).Border
    .ColorIndex = 41
    .Weight = xlThin
    .LineStyle = xlDot
End With
```

```
With chartlines(3)
    .MarkerBackgroundColorIndex = xlNone
    .MarkerForegroundColorIndex = xlNone
    .MarkerStyle = xlNone
    .Smooth = False
    .MarkerSize = 5
    .Shadow = False
End With
```

```
With chartlines(4).Border
    .ColorIndex = 2
    .Weight = xlThick
    .LineStyle = xlContinuous
End With
```

```
With chartlines(4)
    .MarkerBackgroundColorIndex = 12
    .MarkerForegroundColorIndex = 12
    .MarkerStyle = xlNone
    .Smooth = True
    .MarkerSize = 5
    .Shadow = False
End With
```

```
With chartlines(5).Border
    .ColorIndex = 54
    .Weight = xlThin
    .LineStyle = xlDot
End With
```

```
With chartlines(5)
    .MarkerBackgroundColorIndex = xlNone
```

```
.MarkerForegroundColorIndex = xlNone
.MarkerStyle = xlAutomatic
.Smooth = True
.MarkerSize = 5
.Shadow = False
End With
```

```
With chartlines(6).Border
.ColorIndex = 6
.Weight = xlThick
.LineStyle = xlContinuous
End With '
```

```
With chartlines(6)
.MarkerBackgroundColorIndex = xlNone
.MarkerForegroundColorIndex = 35
.MarkerStyle = xlNone
.Smooth = True
.MarkerSize = 7
.Shadow = False
End With
```

```
With chartlines(7).Border
.ColorIndex = 3
.Weight = xlHairline
.LineStyle = xlDashDotDot
End With
```

```
With chartlines(7)
.MarkerBackgroundColorIndex = xlNone
.MarkerForegroundColorIndex = xlNone
.MarkerStyle = xlNone
.Smooth = True
.MarkerSize = 3
.Shadow = False
End With
```

'chartlines(8), chartline(9) : attributes of channel width

```
With chartlines(8).Border
.ColorIndex = 2
.Weight = xlMedium
.LineStyle = xlContinuous
End With
```

```
With chartlines(8)
    .MarkerBackgroundColorIndex = xlNone
    .MarkerForegroundColorIndex = xlNone
    .MarkerStyle = xlDot
    .Smooth = True
    .MarkerSize = 8
    .Shadow = False
```

End With

```
With chartlines(9).Border
    .ColorIndex = 2
    .Weight = xlMedium
    .LineStyle = xlContinuous
```

End With

```
With chartlines(9)
    .MarkerBackgroundColorIndex = xlNone
    .MarkerForegroundColorIndex = xlNone
    .MarkerStyle = xlDot
    .Smooth = True
    .MarkerSize = 5
    .Shadow = False
```

End With

'Set the Horizontal Axis Properties

```
With dataChart.Axes(xlCategory)
    .MaximumScale = 75000
    .MinimumScale = 0
    .MinorUnitIsAuto = True
    .MajorUnitIsAuto = True
    .Crosses = xlMaximum
    .ReversePlotOrder = False
    .DisplayUnit = xlNone
```

End With

```
With dataChart.Axes(xlValue)
    .MaximumScale = 8
    .MinimumScale = -2
    .MajorTickMark = xlOutside
    .MinorTickMark = xlInside
    .TickLabelPosition = xlNextToAxis
```

End With

```
With dataChart.Axes(xlValue, xlSecondary)
    .HasTitle = True
```

```

.AxisTitle.Characters.Text = "Channel Width(m)"
'Make the Secondary Title and Axis Labels Gray
.MaximumScale = 400
.MinimumScale = -800
.AxisTitle.Font.ColorIndex = 0
.TickLabels.Font.ColorIndex = 16
.AxisTitle.Font.Italic = msoTrue
.AxisTitle.Font.Bold = msoTrue
.AxisTitle.Top = 50
.AxisTitle.Left = 5
.TickLabels.NumberFormatLocal = "#,##0;[Red](#,##0.)"
.MajorTickMark = xlInside
.MajorUnit = 100
End With

With dataChart.Axes(xlValue)
    .TickLabels.NumberFormatLocal = "#,##0;[Red](#,##0.)"
End With

With dataChart
    .HasTitle = True
    .ChartTitle.Characters.Text = "Bed Elevation and Water Surface: DAY 0"
End With
dataChart.Refresh
End Sub

' update chart using new data
Public Sub updatechart(ByRef dataSheet As Worksheet, _
    ByRef dataChart As Chart, _
    ByRef itnum As Long, _
    ByRef SQLstr As String, _
    ByRef queryrange As String, _
    ByRef fieldcase As Long, _
    ByRef datafilename As String, _
    ByRef fileprefix As String, _
    ByRef outpath As String, _
    ByRef graphicsfileformat As String, _
    ByRef usstation As Long, _
    ByRef dsstation As Long, _
    Optional ByRef fieldnames As Variant)
On Error GoTo Err_updatechart
Dim framefile As Variant
Dim magickmsgs As Variant

```

```
Dim ppmimg As MagickImage
Set ppmimg = New MagickImage
Dim dt As Double
```

```
mto_VideoFrames.buildSQL SQLstr, _
    fieldcase, _
    datafilename, _
    itnum, _
    usstation, _
    dsstation
```

```
With dataSheet.Range(queryrange).QueryTable
    .CommandText = SQLstr
    .Refresh
End With
```

' Edit the title to reflect the day of the particular simulation.

```
With dataChart
    .HasTitle = True
    .ChartTitle.Characters.Text = "Bed Elevation and Water Surface: DAY " & Int(itnum * 0.1)
End With
dataChart.Refresh
framefile = outpath & fileprefix & "frame." & Format(itnum, "0000") & "." & graphicsfileformat
dataChart.Export Filename:=framefile, _
    Filtername:=graphicsfileformat
magickmsgs = Left(framefile, Len(framefile) - 3)
magickmsgs = magickmsgs & "ppm"
```

```
Exit_updatechart:
    Exit Sub
```

```
Err_updatechart:
    MsgBox Err.Description
    Resume Exit_updatechart
End Sub
```

Data loading from workbook in Excel

' Get the time step data

```
Public Sub gettimesteps(ByRef timesteparray() As timestep, _
    ByRef ntimesteps As Long, _
    ByRef dt As Double, _
    ByRef timestepssheet As Worksheet)
Dim k As Integer
k = 1
Do
ReDim Preserve timesteparray(k)
timesteparray(k).day = timestepssheet.Cells(k + 1, 1)
timesteparray(k).Q = timestepssheet.Cells(k + 1, 2)
timesteparray(k).temp = timestepssheet.Cells(k + 1, 3)
timesteparray(k).uselev = timestepssheet.Cells(k + 1, 4)
k = k + 1
Loop While timestepssheet.Cells(k, 1).Value > 0
' One additional timestep has been created for the
' last iteration.
ntimesteps = k - 2
End Sub
```

' Get the cross section data

```
Public Sub getxsections(ByRef xsectionarray() As xsection, _
    ByRef nxsections As Long, ByRef xsectionsheet As Worksheet)
Dim k As Integer
k = 1
Do
ReDim Preserve xsectionarray(k)
xsectionarray(k).ID = xsectionsheet.Cells(k + 1, 1)
xsectionarray(k).x = xsectionsheet.Cells(k + 1, 2)
xsectionarray(k).s0 = xsectionsheet.Cells(k + 1, 3)
xsectionarray(k).z = xsectionsheet.Cells(k + 1, 4)
xsectionarray(k).alpha = 1
' xsectionarray(k).dxdown = xsectionarray(k).x - xsectionarray(k - 1).x
xsectionarray(k).gamma.channeltype = 1
xsectionarray(k).gamma.g1 = xsectionsheet.Cells(k + 1, 5)
xsectionarray(k).zmin = xsectionsheet.Cells(k + 1, 6)
xsectionarray(k).bankelev = xsectionsheet.Cells(k + 1, 7)
xsectionarray(k).n = xsectionsheet.Cells(k + 1, 8)
xsectionarray(k).options = xsectionsheet.Cells(k + 1, 9)
'xsectionarray(k).gamma.g4 = xsectionsheet.Cells(k + 1, 10)
k = k + 1
Loop While xsectionsheet.Cells(k + 1, 1).Value > 0
```

nxsections = k - 1 ' k - 1 accounts for top row of worksheet with headers.
End Sub

' Get the reach data

```
Public Sub getreaches(ByRef reacharray() As reach, _
    ByRef xsectionarray() As xsection, _
    ByRef nxsections As Long)
Dim k As Integer
ReDim reacharray(nxsections - 1)
For k = 1 To nxsections - 1
'reacharray(k).nodeup = k
'reacharray(k).nodedn = k + 1
reacharray(k).deltax = Abs(xsectionarray(k).x - _
    xsectionarray(k + 1).x)
reacharray(k).deltaz = Abs(xsectionarray(k).z - _
    xsectionarray(k + 1).z)
reacharray(k).S0bar = reacharray(k).deltaz / _
    reacharray(k).deltax
reacharray(k).n = xsectionarray(k).n
reacharray(k).options = xsectionarray(k).options
Next k
ntimesteps = k - 1
End Sub
```

' Get the initial input data

```
Public Sub initialinput(ByRef dataSheet As Worksheet, _
    ByRef dt As Double, _
    ByRef ds As Double, _
    ByRef vis As Double, _
    ByRef po As Double, _
    ByRef n As Double, _
    ByRef epsilon_normal As Double, _
    ByRef epsilon_backwater As Double, _
    ByRef dsh_max As Double, _
    ByRef it_max As Long, _
    ByRef flowinputfile As String, _
    ByRef xsectinputfile As String, _
    ByRef outputfile As String)
dt = dataSheet.Range("b3")
ds = dataSheet.Range("b4")
vis = dataSheet.Range("b5")
po = dataSheet.Range("b6")
n = dataSheet.Range("b7")
```

```

epsilon_normal = dataSheet.Range("b8")
epsilon_backwater = dataSheet.Range("b9")
dsh_max = dataSheet.Range("b10")
it_max = dataSheet.Range("b11")
flowinputfile = dataSheet.Range("b13")
xsectinputfile = dataSheet.Range("b14")
outputfile = dataSheet.Range("b15")
End Sub

```

' Write result data to Excel sheet

```

Public Sub writexsectionarray(ByRef nodes() As xsection, _
    ByRef iteration As Long, _
    ByRef nodeoutsheet As Worksheet, _
    ByRef nx As Long)
nodeoutsheet.Cells(1, 1) = "nodes(k).ID"
nodeoutsheet.Cells(1, 2) = "nodes(k).z"
nodeoutsheet.Cells(1, 3) = "nodes(k).x"
nodeoutsheet.Cells(1, 4) = "nodes(k).Sf"
nodeoutsheet.Cells(1, 5) = "nodes(k).h"
nodeoutsheet.Cells(1, 6) = "nodes(k).ubar"
nodeoutsheet.Cells(1, 7) = "nodes(k).area"
nodeoutsheet.Cells(1, 8) = "nodes(k).Tenergy"
nodeoutsheet.Cells(1, 9) = "nodes(k).hyradius"
nodeoutsheet.Cells(1, 10) = "nodes(k).hydepth"
nodeoutsheet.Cells(1, 11) = "nodes(k).Fr"
nodeoutsheet.Cells(1, 12) = "nodes(k).WSE"
nodeoutsheet.Cells(1, 13) = "nodes(k).Pw"
nodeoutsheet.Cells(1, 14) = "iteration"
Dim k As Long
Dim j As Long
For k = 1 To nx
j = k + nx * (iteration - 1) + 1
nodeoutsheet.Cells(j, 1) = nodes(k).ID
nodeoutsheet.Cells(j, 2) = nodes(k).z
nodeoutsheet.Cells(j, 3) = nodes(k).x
nodeoutsheet.Cells(j, 4) = nodes(k).sf
nodeoutsheet.Cells(j, 5) = nodes(k).h
nodeoutsheet.Cells(j, 6) = nodes(k).ubar
nodeoutsheet.Cells(j, 7) = nodes(k).area
nodeoutsheet.Cells(j, 8) = nodes(k).Tenergy
nodeoutsheet.Cells(j, 9) = nodes(k).hyradius
nodeoutsheet.Cells(j, 10) = nodes(k).hydepth
nodeoutsheet.Cells(j, 11) = nodes(k).Fr

```

```

nodeoutsheet.Cells(j, 12) = nodes(k).WSE
nodeoutsheet.Cells(j, 13) = nodes(k).Pw
nodeoutsheet.Cells(j, 14) = iteration
Next k

```

```
End Sub
```

' Get the graphic data

```

Public Sub getgraphicsdata(ByRef datafilename As String, _
    ByRef MPEGtime As Double, _
    ByRef firstframe As Long, _
    ByRef lastframe As Long, _
    ByRef frameinterval As Long, _
    ByRef usstation As Long, _
    ByRef dsstation As Long)
datafilename = ThisWorkbook.Worksheets("BR_Data").Range("b15")
MPEGtime = ThisWorkbook.Worksheets("BR_Data").Range("b17")
firstframe = ThisWorkbook.Worksheets("BR_Data").Range("b18")
lastframe = ThisWorkbook.Worksheets("BR_Data").Range("b19")
frameinterval = ThisWorkbook.Worksheets("BR_Data").Range("b20")
usstation = ThisWorkbook.Worksheets("BR_Data").Range("b21")
dsstation = ThisWorkbook.Worksheets("BR_Data").Range("b22")

```

```
End Sub
```

' Write the results data

```

Public Sub writeiterationarray(ByRef iterations() As Double, _
    ByRef itoutsheet As Worksheet, _
    ByRef itnum As Integer)

```

```

If itnum = 1 Then
    itoutsheet.Range("A" & numits + 2 & ":IV65536").Clear
End If

```

```

itoutsheet.Cells(itnum + 1, 1) = iterations(1, itnum)
itoutsheet.Cells(itnum + 1, 2) = iterations(2, itnum)
itoutsheet.Cells(itnum + 1, 3) = iterations(3, itnum)
itoutsheet.Cells(itnum + 1, 4) = iterations(4, itnum)
End Sub

```

Definition of data types

```
'Public Const MAX_ITERATIONS As Long = 50
'Public Const MAX_NORMALDEPTH As Double = 10#
'Public Const TOL_NORMALDEPTH As Double = 0.00001
Public TOL_NORMALDEPTH As Double
Public TOL_BACKWATER As Double
Public errorcode As Integer
Public MAX_NORMALDEPTH As Double
Public MAX_ITERATIONS As Long

Public Type geometry
    channeltype As Integer
    g1 As Double
    g2 As Double
    g3 As Double
    g4 As Double
End Type

' Define the data type for cross sections
Public Type xsection
ID As String
    x As Double
    s0 As Double
    z As Double
    zmin As Double
    bankelev As Double
    deltaz As Double ' change in elevation from previous condition
    po As Double ' Sediment Porosity
    n As Double ' Manning n
    ds As Double ' Mean Sediment particle diameter
    options As Integer
    gamma As geometry
    h As Double
    area As Double
    ubar As Double
    Q As Double
    Qtrial As Double
    velhead As Double ' Velocity Head = alpha * ubar ^ 2 / 2 / g
    Tenergy As Double ' Total Mechanical Energy Head
    senergy As Double ' Specific Energy = velocity head + depth
    cenergy As Double
    Pw As Double
```

```

Tw As Double
hyradius As Double
taubed As Double ' Shear at the bed surface
trapeff As Double
alpha As Double ' Kinetic Energy Correction Factor
sf As Double
Fr As Double ' Hydraulic Froude number =
Fr2 As Double ' True Froude number = .Fr ^ 2
hydepth As Double
WSE As Double
yc As Double
yn As Double
' Sediment Related Parameters
qst As Double
qbv As Double
SDR As Double
End Type

```

' Define the data type for reaches

```

Public Type reach
  nodeup As Integer
  nodedn As Integer
  n As Double
  avolume As Double
  balance As Double
  ehqst As Double
  courant As Double
  mindeltaH_used As Boolean
  CeCc As Double
  Cb As Double
  ql As Double
  Qtrial As Double
  S0bar As Double
  sfbar As Double
  headIstarprime As Double
  aveTw As Double
  aveseD As Double
  deltaz As Double
  deltaH As Double
  epsilon As Double
  deltax As Double
  deltaqst As Double
  DeltaHe As Double

```

```
DeltaCeCc As Double
DeltaCb As Double
deltac As Integer
SDR As Double
numiterations As Integer
options As Integer
End Type
```

```
Public Type timestep
  xsect() As xsection
  rch() As reach
  omega As Double
  vis As Double
  dt As Double
  n As Double
  ds As Double
  po As Double
  day As Long
  Q As Double
  Qtrial As Double
  temp As Double
  uselev As Double
  epsilon As Double
  options As Integer
End Type
```

```
Static Function Log10(x)
  Log10 = Log(x) / Log(10#)
End Function
```

Bisection method

```
Public Sub bisection(ByRef testvalue As Double, ByRef trialvalue As Double, _  
    UBnd As Double, LBnd As Double, epsilon As Double)
```

```
    If testvalue < 0 Then
```

```
        LBnd = trialvalue
```

```
        trialvalue = (trialvalue + UBnd) * 1 / 2
```

```
    Else
```

```
        UBnd = trialvalue
```

```
        trialvalue = (trialvalue + LBnd) * 1 / 2
```

```
    End If
```

```
End Sub
```

Computing representative hydraulic parameters (h, W, V, S)

Public Sub hyd(ByRef tstp As timestep, _

ByRef nx As Long)

For sta = nx - 5 To 5 Step -1

If sta = nx - 1 Then

tstp.xsect(sta).h = (tstp.xsect(sta + 1).h + tstp.xsect(sta).h) * 0.5

tstp.xsect(sta).Tw = (tstp.xsect(sta + 1).Tw + tstp.xsect(sta).Tw) * 0.5

tstp.xsect(sta).ubar = (tstp.xsect(sta + 1).ubar + tstp.xsect(sta).ubar) * 0.5

tstp.xsect(sta).s0 = (tstp.xsect(sta + 1).s0 + tstp.xsect(sta).s0) * 0.5

ElseIf sta = 2 Then

tstp.xsect(sta).h = tstp.xsect(sta + 1).h

tstp.xsect(sta).Tw = tstp.xsect(sta + 1).Tw

tstp.xsect(sta).ubar = tstp.xsect(sta + 1).ubar

tstp.xsect(sta).s0 = tstp.xsect(sta + 1).s0

ElseIf sta = 1 Then

tstp.xsect(sta).h = tstp.xsect(sta + 1).h

tstp.xsect(sta).Tw = tstp.xsect(sta + 1).Tw

tstp.xsect(sta).ubar = tstp.xsect(sta + 1).ubar

tstp.xsect(sta).s0 = tstp.xsect(sta + 1).s0

Else

tstp.xsect(sta).h = 0.25 * tstp.xsect(sta + 1).h + 0.5 * tstp.xsect(sta).h + 0.25 * tstp.xsect(sta - 1).h

tstp.xsect(sta).Tw = 0.25 * tstp.xsect(sta + 1).Tw + 0.5 * tstp.xsect(sta).Tw + 0.25 * tstp.xsect(sta -

1).Tw

tstp.xsect(sta).ubar = 0.25 * tstp.xsect(sta + 1).ubar + 0.5 * tstp.xsect(sta).ubar + 0.25 * tstp.xsect(sta -

1).ubar

tstp.xsect(sta).s0 = tstp.xsect(sta).s0

End If

Next sta

End Sub

Set the units for calculation

Option Explicit

' Public Const GRAVITY As Double = 9.81

' Public Const phi As Double = 1#

Public Const SI = 0

Public Const US = 1

Public gravity As Double

Public phi As Double

Public rho As Double

Public Gsed As Double

Public Sub SetUnits(unitsystem As Integer)

Select Case unitsystem

Case Is = 0

gravity = 9.81

phi = 1#

Case Is = 1

gravity = 32.2

phi = 1.486

End Select

End Sub

Integrating sediment concentration distribution and determining CR

Public Sub Simpson(CR As Double, alpha As Double, depth As Double, PanNum As Integer, Rouse As Double, obnkEl As Double)

'This function calculates the area under the curve y(x) from x=a to x=b using Simpson's ' rule with n intervals Note (n must be even)

Dim sum As Double, term As Double

Dim depthx As Double

Dim i As Integer

Dim Simpson As Double

'Do error checking

If PanNum = 0 Or PanNum Mod 2 = 1 Then

Simpson = 0#

MsgBox "Sorry # of intervals has to be > 0 and even"

Exit Sub

End If

sum = 0

If depth < obnkEl Then CR = 1#

ElseIf obnkEl <= depth Then

For n = 1 To PanNum - 1

z1 = alpha + (depth - alpha) / PanNum * n

sum1 = sum1 + ((alpha / (depth - alpha)) ^ Rouse) * ((depth / z1 - 1) ^ Rouse)

Z2 = alpha + (obnkEl - alpha) / PanNum * n

sum2 = sum2 + ((alpha / (depth - alpha)) ^ Rouse) * ((depth / Z2 - 1) ^ Rouse)

Next n

SSUM1 = (0.5 * ((alpha / (depth - alpha)) ^ Rouse) * ((depth / alpha - 1) ^ Rouse) _
+ 0.5 * ((alpha / (depth - alpha)) ^ Rouse) * ((depth / depth - 1) ^ Rouse) _
+ sum1) * (depth - alpha) / PanNum

SSUM2 = (0.5 * ((alpha / (depth - alpha)) ^ Rouse) * ((depth / alpha - 1) ^ Rouse) _
+ 0.5 * ((alpha / (depth - alpha)) ^ Rouse) * ((depth / obnkEl - 1) ^ Rouse) _
+ sum2) * (obnkEl - alpha) / PanNum

CR = SSUM2 / SSUM1

End If

End Sub

Program development history

- 08/31/01 Claudia Leon Original code
- 11/28/01 Claudia Leon Update
- 08/06/05 James Halgren Convert to VBA
- August/11 Kiyoung Park Update Sedimentatin model
- August/12 Kiyoung Park Update sediment concentration profile model
- July/13 Kiyoung Park Update Sediment plug parameters